Unmasking the *in vivo* importance of STAT3 in multiple myeloma using three-dimensional culture and nanoparticle drug delivery system

by

Yung-Hsing Huang

A thesis submitted in partial fulfillment of the requirements for the degree of

Doctor of Philosophy

in

Molecular Pathology

Department of Laboratory Medicine and Pathology
University of Alberta

ABSTRACT

Multiple myeloma (MM) is a hematological malignancy which is caused by aberrant accumulation of monoclonal plasma cells (PCs) within the bone marrow. The oncogenesis of MM is mediated by chromosomal aberrations as well as the tumor microenvironment in the bone marrow. Signal transducer and activator of transcription 3 (STAT3) is active in more than 50% of MM patients, and it is known to induce cell growth, survival and drug resistance in MM cells. However, activation of STAT3 in MM cells is largely dependent on exogenous soluble factors and cell adhesion. Conventional culture method is therefore not an ideal model to recapitulate the *in vivo* STAT3 activity of MM cells. In this thesis, I explored the importance of STAT3 in MM cells with the consideration of MM tumor microenvironment using a 3D culture model. Moreover, I aimed to develop a method for better delivery and efficacy of STAT3 inhibitor *in vivo* as a therapy for MM. I hypothesize that STAT3 activity in MM cells is more pronounced in close-to-*in vivo* tumor microenvironment, hence improvement of STAT3 inhibitor delivery by nanoparticle conjugation and anti-CD38 conjugation is a valid therapy for MM.

A 3D scaffold culture model for MM cells was established for long-term culture of primary MM cells by Kirshner *et al*. However, the biochemical and biological effects on MM cells in this 3D model is not known. Two MM cell lines were found to have a higher level of active STAT3 (by means of phosphorylated STAT3 or pSTAT3) in the 3D culture model were compared with their counterparts in conventional culture. This elevated pSTAT3 level was dependent on the 3D environment since it decreased soon after transferring to conventional culture. STAT3 inhibition using a pharmacological agent, Stattic, significantly decreased the cell viability of MM cells and sensitized them to bortezomib in 3D culture but not in conventional culture. Using an

oligonucleotide array, 3D cultured MM cells showed increased expression of several known STAT3 downstream genes implicated in oncogenesis.

Primary multiple myeloma (PMM) cells harvested from patients are highly valuable resources for studying the biology of the disease and drug resistance. However, the use of these cells is limited by the fact that PMM cells are short-lived in conventional culture. The role of STAT3 and 3D culture system on prolonging the longevity of PMM cells was evaluated. Using PMM cells from patients, a significantly higher total viable PMM cell number in 3D compared to conventional culture was observed. However, the MM cell proliferation rate in the two culture systems was similar. Correlating with the high MM cell viability, higher pSTAT3 level was also observed in 3D culture. After treatment of IL6, the PMM cell viability in 3D culture was further improved. Treatment of Stattic on 3D cultured PMM cells significantly ablated their viability. On the other hand, treatment of IL6 or Stattic did not change the cell viability of conventionally cultured PMM cells.

Many STAT3 inhibitors have been developed, but none of them has been approved as a cancer therapy due to their hydrophobicity and severe off-target toxicity. Lavasanifar Lab has developed a nanoparticular formation of a STAT3 inhibitor, S3I-1757 (Null-S3I-NP) for better delivery and *in vivo* efficacy. This nanoparticular formulation was conjugated with CD38 monoclonal antibody (denoted as CD38-S3I-NP) to further increase its MM cell targeting ability and anti-MM efficacy. CD38-S3I-NP is slightly less stable than Null-NP with a higher S3I-1757 release rate within a short time. However, CD38-conjuagred nanoparticles showed significantly higher MM cellular uptake than compared to plain nanoparticles. In keeping with this, CD38-S3I-NP resulted in a

significantly lower IC_{50} value in two IL6-stimulated MM cell lines compared to Null-S3I-NP. CD38-S3I-NP suppressed MM tumor growth more effectively compared to Null-S3I-NP *in vivo*. The pSTAT3 level in the bone marrow mononuclear cells was significantly reduced in MM-bearing mice after CD38-S3I-NP treatment compared to Null-S3I-NP. These findings suggest that CD38-S3I-NP is potent anti-STAT3 agent with MM cell-targeting ability.

In conclusion, this thesis reveals the essential role of STAT3 activity in maintaining the viability of MM cells in the context of 3D microenvironment. Therefore, MM cell-targeting nanoparticles with STAT3 inhibitor is believed to be a promising therapy for MM.

PREFACE

This thesis is an original work by Yung-Hsing Huang ("I" in the main text), under supervision of Dr. Raymond Lai at the University of Alberta. All procedures on MM patient samples, in the form of bone marrow aspirates, were approved by Human Research Ethics Board of Alberta. (Interaction between malignant cells and stromal cells in bone marrow, protocol #: HREBA.CC-16-0346 and HREBA.CC-17-0591, expired date: 2018/11/22). All procedures involved animals in this thesis were approved by the Animal Care and Use Committee (ACUC) at University of Alberta (Nanotechnology for cancer therapy, protocol #: AUP00000282, expired date: 2019/01/20).

A modified version of **Chapter 2** has been published as "Huang, YH.; Molavi, O.; Alshareef, A.; Haque, M.; Wang, Q.; Chu, M.P.; Venner, C.P.; Sandhu, I.; Peters, A.C.; Lavasanifar, A.; Lai, R. Constitutive Activation of STAT3 in Myeloma Cells Cultured in a Three-Dimensional, Reconstructed Bone Marrow Model" in *Cancers* 2016;10(6):206. I was the first author of this paper who wrote the manuscript and conducted all the experiments. RL and OM edited the manuscript. OM, AL, RL and I designed experiments. MPC, CPV, IS and ACP provided patient bone marrow samples with patient consent. AA, MH and QW performed portions of the experiments, data analysis and intellectual input. All authors read and approved the manuscript.

ACKNOWLEDGEMENT

I would like to express my most sincere gratitude to the following individuals for their assistance and support during my PhD program, without whom this thesis would not be possible.

First, I would like to thank my supervisor, Dr. Raymond Lai for his teaching from experiment planning, data organization, scientific writing to critical thinking. His hard work, self-discipline and enthusiasm in research has been an extraordinary example for me.

I would like to thank Dr. Afsaneh Lavasanifar for being my co-supervisor who provided me a great amount of help in the pharmacology, pharmacokinetics and *in vivo* model aspects of my study. I would like to thank Dr. Ing Swie Goping for being my supervisory committee member. She provided valuable insights and constructive criticism on my project to make it better and better every time.

I would like to thank Dr. Monika Keelan for chairing my PhD candidacy exam and doctoral defense. As the graduate program coordinator of Department of Lab Medicine and Pathology, she also provided me guidance for PhD proposal/thesis writing and candidacy exam preparation. I am grateful to Dr. Michael Chu and Dr. Yangxin Fu for being the examiners for my candidacy exam. I would like to thank Dr. Anthony Reiman and Dr. Yangxin Fu for being the external examiners for my doctoral defense. Your thoughtful input on my proposal or thesis helped me a lot.

I would like to thank all the past and current lab members in Lai Lab and Lavasanifar Lab for their guidance, support and encouragement during my graduate training. I am especially grateful to Dr.

Haifeng Zhang, Dr. Abdulraheem Alshareef , Dr. Chengsheng Wu, Dr. Shyam Garg, Dr. Nidhi Gupta, Dr. Keshav Gopal, Dr. Ying Zhang, Dr. Hoda Soleymani, Dr. Mohammad Reza Vakili, Dr. Ommoleila Molavi for their mentorship during the early stage of my graduate program. I also want to thank Mr. Moinul Haque, Dr. Jing Li, Ms. Meaad Almowaled, Ms. Yuen Morrissey, Mr. Igor Paiva and Mr. Amir Soleimani for their assistance on experimental procedures during my study.

I would like to thank the clinical collaborators at University of Alberta Hospital and Cross Cancer Institute: Dr. Christopher Venner, Dr. Irwindeep Sandhu and Dr. Anthea Peters for providing patient samples and patient information for my study.

I would like thank Dr. Aja Rieger, Ms. Janice Cotton-McKay and Ms. Geraldine Barron for providing me training on flow cytometric analysis, animal anesthesia/euthanasia and Axioskop color microscopy, respectively. Special thanks to Ms. Aricy Pan for her excellent tissue sectioning skills for my immunocytochemistry studies.

I want to acknowledge the financial support from Alberta Innovative Health Solutions from 2014 to 2017. I want to thank Faculty of Graduate Studies and Research and Alberta Cancer Foundation for providing travel funds for Canadian Cancer Research Conferences in Montreal (2015) and Vancouver (2017), respectively.

Finally, I would like to thank my dearest family members, especially my parents, Dr. Zhou-Hui Huang and Ms. Tsai-Yu Lee, and my beloved wife Ms. Yongshan Jing for their consistent care, support and encouragement.

TABLE OF CONTENTS

LIST OF ABBREVIATIONS

2D – Two-dimensional

3D – Three-dimensional

ABCG2 - ATP-binding cassette subfamily G member 2

ACN – Antibody-conjugated nanoparticles

aka. – As known as

Akt – Protein kinase B

ALCL – Anaplastic large cell lymphoma

ALK – Anaplastic lymphoma kinase

ANGPT2 – Angiopoietin-2

ANOVA – Analysis of variance

ATCC – American tissue culture collection

β2M – β2-microglobulin

BAD - Bcl-2-associated death promoter

BCA – BSA colorimetric assay

Bcl-2 – B-cell lymphoma 2

Bcl-xL – B-cell lymphoma-extra large

Blimp1 – B-lymphocyte-induced maturation protein 1

BMMC – Bone marrow mononuclear cells

BSA – Bovine serum albumin

BTB – bortezomib

CA9 – Carbonic anhydrase 9

CAR-T – Chimeric antigen receptor T cell

CBP/p300 – 300 kDa CREB-binding protein

CCND – Cyclin D

CCL2 – C-C motif chemokine ligand 2

CETSA – Cellular thermal shift assay

CFSE – Carboxyfluorescein succinimidyl ester

c-Myc – Myelocytomatosis cellular oncogene

CNTF – Ciliary neurotrophic factor

CO_2 – Carbon dioxide

CRAB – hypercalcemia, renal failure, anemia and bone lesions

CSK1B – CDC28 protein kinase regulatory subunit 1B

CT – Computed tomography

CTLA4 – cytotoxic T-lymphocyte-associated protein 4

CXCR4 - C-X-C motif chemokine receptor 4

DDIT3 – DNA damage-inducible transcript 3

Dkk-1 – Dickkopf 1

DLL – Delta-like ligand

DMSO – Dimethyl sulfoxide

DNA – Deoxyribonucleic acid

DPBS – Dulbecco's Phosphate-Buffered Saline

e.g. – For example

ECL – Enhanced chemiluminescence

ECM – Extracellular matrix

EDC – 1-ethyl-3-(3-dimethylaminopropyl) carbodiimide hydrochloride

EDTA – Ethylenediaminetetraacetic acid

EGF(R) – Epidermal growth factor (receptor)

EPR – Enhanced permeability and retention

FBS – Fetal bovine serum

FCIP – Flow cytometry immunotyping

FGF(R) – Fibroblast growth factor (receptor)

FOXP3 - Forkhead box P3

FITC – Fluorescein isothiocyanate

GAS – γ-activated sequence

GAPDH – Glyceraldehyde 3-phosphate dehydrogenase

gp130 – Glycoprotein 130

HER2 – Human epidermal receptor 2

HLA-A – Human leukocyte antigens A

HPLC – High performance liquid chromatography

HREBA – Health Research Ethics Board of Alberta Cancer Committee

HRP – Horseradish peroxidase

Hsp70/90 – 70/90 kilodalton heat shock protein

i.e. – In other words

ICAM-1 – Intracellular adhesion molecule 1

IFN – Interferon

IGF1(R) – Insulin-like growth factor 1 receptor

Ig – Immunoglobulin

IKB – NF-κB inhibitor

IκK - Inhibitor of NF-κB kinase

IL# – Interleukin-# (# - any number)

IL#R – Interleukin-# receptor (# - any number)

iNKT – Invariant natural killer T cell

ISS – International staging system

JAK – Janus kinase

JNK – c-Jun N-terminus kinase

kDa – Kilodalton

LFA-1 - Lymphocyte function-associated antigen 1

LIF – Leukemia inhibitory factor

LIFR – Leukemia inhibitory factor receptor

LMP# - Latent membrane protein #

LPL – Lipoprotein lipase

LRP1 – Lipoprotein related protein 1

MAPK – Mitogen-activated protein kinase

MAF – Avian musculoaponeurotic fibrosarcoma oncogene homolog

Mcl-1 – Induced myeloid leukemia cell differentiation protein

MGUS – Monoclonal gammopathy of undetermined significance

MM – Multiple myeloma

MMP – Matrix metalloproteinase

MRI – Magnetic resonance imaging

mRNA – Messenger RNA

mTOR – Mammalian target of rapamycin

MTS - 3-(4,5-dimethylthiazol-2-yl)-5-(3-carboxymethoxyphenyl)-2-(4-sulfophenyl)-2H-tetrazolium

MUC-1 – Mucin-1

Myc – Myelocytomatosis oncogene

NF-κB – Nuclear factor kappa-light-chain-enhancer of activated B cells

NHS – N-hydroxysuccinimide

OPG – Osteoprotegerin

OSM(R) – Oncostatin M (receptor)

PARP - Poly (ADP-ribose) polymerase

PAX5 – Paired box 5

PBS – Phosphor buffered saline

PC – Plasma cell

PD-1 – Programmed cell death protein 1

PD-L1 – Programmed death ligand 1

PE – Phycoerythrin

PEO-*b*-PBCL - Poly(ethylene oxide)-block-poly(α-benzyl carboxylate-ε-caprolactone)

PET – Positron-emission tomography

PIAS3 – Protein inhibitor of activated STAT3

PI3K – Phosphatidylinositol-4,5-bisphosphate 3-kinase

PKC – Protein kinase C

PLGA – Poly(lactic-co-glycolic acid)

PMM – Primary multiple myeloma

PPARα/γ – Peroxisome proliferator-activated receptors alpha or gamma

PSMD4 – Proteasome 26S subunit, non-ATPase 4

PTEN - Phosphatase and tensin homolog

RANK(L) – Receptor activator of NF-κB (ligand)

RB – Retinoblastoma

RIPA – Radioimmunoprecipitation assay

RNA – Ribonucleic acid

(q)RT-PCR – (Quantitative) reverse transcription polymerase chain reaction

S6K – Ribosomal protein S6 kinase

SCID – Severe combined immunodeficient

SDS(-PAGE) – Sodium dodecyl sulfate (polyacrylamide gel electrophoresis)

SERPINB2 – Ovalbumin

sFRP-2 - Secreted frizzled-related protein 2

SGK – Serum- and glucocorticoid-induced protein kinase

SH2 – Src homology 2

SHIP1/2 – SH2 Domain-Containing Inositol 5-Phosphatase 1/2

SHP1/2 – Protein tyrosine phosphatase, non-receptor type 6/11

siRNA – Small interfering RNA

SMM – Smoldering multiple myeloma

SNAI3 – Snail homolog 3

SOCS3 – Suppressor of cytokine signaling 3

Src – Rous sarcoma oncogene

STAT(#) – Signal transducer and activator of transcription (#)

TBS – Tris-buffered saline

TGFβ – Transforming growth factor beta

Th17 – T helper 17 cells

TJP1 – Tight junction protein 1

TNFR1 – Type 1 tumor necrotic factor receptor

TPA – 12-O-Tetradecanoylphorbol-13-acetate

TRAIL – TNF-related apoptosis-inducing ligand

Treg – Regulatory T cells

VCAM-1 – Vascular cell adhesion molecule-1

VEGF(R) – Vascular endothelial growth factor (receptor)

VPA – Valproic acid

VLA-4 – Very late antigen-4

XBP1 – X-box binding protein 1

LIST OF TABLES

LIST OF FIGURES

CHAPTER 1

Introduction

1.1. Summary

Multiple myeloma (MM) is an incurable disease caused by accumulation of monoclonal plasma cells (PC) in the bone marrow (1). It accounts for 1.4% of incidences and 1.8% of deaths among all cancers in Canada in 2017 (2). The major symptoms of MM include hypercalcemia, renal failure, anemia and bone lesion (CRAB). The two common staging systems used in MM diagnosis are international staging system or Durie-Salmon staging system (3). The mainstream treatment of MM is autologous stem cell transplantation combined with anti-MM regimens (4). The oncogenesis of MM is resulted from aberrant chromosomal structures, extracellular stimulations and tumor microenvironment. Chromosomal aberrations in MM cells can be structural (i.e. translocation, amplification or deletion) or numerical (i.e. change in the total chromosome number). Additionally, myelomagenesis is supported by both extracellular soluble ligands such as interleukin-6 (IL6), insulin-like growth factor-1 (IGF1), B cell activating factor (BAFF)/ proliferation-inducing ligand (APRIL), and Notch receptor ligands. Other cell types and extracellular matrix proteins also support oncogenesis of MM. Therefore, three-dimensional (3D) culture models which precisely recapitulate the bone marrow microenvironment in MM provide better understanding of MM biology. Signal transducer and activator of transcription 3 (STAT3) is an oncoprotein which exerts its function by canonical and non-canonical pathways. The Y705 residue within the Src homology 2 (SH2) domain is the most important residue which dictate the activity of STAT3. STAT3 is found to be activated in over 50% of MM patients (5). STAT3 SH2 domain inhibitors targeting the Y705 residue have been reported (6), but the low water solubility and adverse side effects hinder them from clinical applications. Nanoparticle drug delivery system have shown improved safety and anti-tumor efficacy (7), hence an approach to improve STAT3 inhibitor therapy.

1.2. Multiple myeloma

1.2.1 Normal plasma cells

Plasma cells (PCs) are a relatively rare population within the bone marrow, occupying roughly 0.25% of the total bone marrow mononuclear cells (BMMCs) (8). PCs are responsible for secretion of antibody and are characterized by their large cell volume and abundant distribution of cytosolic Golgi apparatus and rough endoplasmic reticulum (9). PCs are differentiated from plasmablasts (i.e. immature plasma cells) in the bone marrow. After encountering an antigen, B cells undergo differentiation process to pre-plasmablasts, plasmablasts and eventually PCs. During this process, the cells lose the B cell identity via downregulation of *PAX5* and upregulation of *XBP1* and *Blimp1* (10). As a result, the cells lose B cell surface markers (e.g. CD20) and gain plasma surface markers (e.g. CD38 and CD138) (11). Due to limited PC niches in bone marrow, the newly differentiated PCs will replace the old ones. PCs are characterized as non-proliferating cells with a lifespan ranging from several days to several months depending on the antigen which activate them during the B-cell phases (12).

1.2.2 Statistics, epidemiology and symptoms of MM

Multiple myeloma (MM) is a type of hematologic malignancies that is caused by dysfunctional and clonogenic PCs (1). MM is usually derived from multiple niches within the bone marrow cavity instead of one tumor, hence earns its name. According to *2017 Canadian Cancer Statistics* published, it is predicted to have 2900 cases of newly diagnosed MM (1.4% of all cases) and 1450 deaths due to MM (1.8% of all cancer deaths) next year in Canada (2). MM occurs predominantly in seniors, with a median age of 65, and more often in American Africans compared to other ethnicities (13). Due to the advances in MM therapy, the 5-year survival of MM has increased

from 10-15% to nearly 50% (13,14). However, nearly all MM patients develop relapse after therapy, making it an incurable disease. MM cells typically have a slow proliferation rate, with an average of 3.0%, 6.0% and 6.5% Ki-67 (a cell proliferation marker) positivity in Stage I, II and III MM patients, respectively (15). However, they produce a large amount of monoclonal immunoglobulin fragments referred as "M components" or "M proteins". A high serum concentration of M protein eventually overwhelms the renal filtration system, leading to renal failure. Accumulation of MM cells in the bone marrow disturbs the hematopoiesis of normal red blood cells in the bone marrow, resulting in anemia. Lastly, MM cells facilitate bone resorption by inducing the differentiation and maturation of osteoclasts (bone-digesting cells), leading to occurrence of bone lesions. Collectively, hyper**c**alcemia, **r**enal failure, **a**nemia and **b**one lesions (**CRAB**) are the major symptoms of MM.

1.2.3. Diagnosis of MM and pre-MM disorders

According to World Health Organization MM staging standards, the minimum diagnostic criteria of MM is the presence of more than 10% neoplastic plasma cells in bone marrow biopsy (16). Quantification of plasma cells is therefore required for diagnosis of MM. The common methods for quantification of bone marrow plasma cell numbers are flow cytometry immunophenotyping (FCIP) and immunohistochemistry staining of MM patient bone marrow biopsy. Neoplastic plasma cells have some signatures different from normal plasma cells such as low CD19 and CD45 expressions and high CD56, CD38 and CD138 expressions (17). Some pathological parameters of MM including abundant secretion of M proteins and the presence of bone lytic lesions are also used for diagnosis of MM (16). Serum and urine concentrations of M proteins provides an estimation of the number of malignant PCs within in the bone marrow. Magnetic resonance

imaging (MRI), computed tomography (CT) scans and positron-emission tomography (PET) scans provide visualization of MM-induced bone lytic lesions.

Clinical criteria for MM and pre-MM disorders have been established according to the Clinical Practice Guidelines for MM published by Alberta Health System (18):

- Monoclonal gammopathy of undetermined significance (MGUS): <3g/dL M-protein, <10% monoclonal plasma cells in BM, no end-organ damage. In this stage, the concentration of serum M protein and the percentage of monoclonal PCs in BM is higher than healthy individuals, but no associated symptoms were observed. The rate of malignant transformation from MGUS to MM is 1% per year (19).
- Smoldering MM: >3g/dL M-protein, >10% monoclonal plasma cells in BM, no end-organ damage.
- Symptomatic MM: >3g/dL M-protein, >60% monoclonal plasma cells in the bone marrow, CRAB is usually seen and at least one bone lesion is observed.
- Extramedullary MM: above criteria plus if metastasis of MM cells outside of bone marrow is seen and/or secondary plasma cell leukemia is found.

Refractory MM refers to cases which did not show minimal response (i.e. 25-49% reduction of serum M proteins and 50-89% reduction of urine M protein within 24 hours according to the European Group for Blood and Marrow Transplantation criteria) to MM therapy (20). Refractory MM can be classified as “primary refractory MM” and “relapsed and refractory MM”. Patients with primary refractory MM never show minimal response or better to any initial MM therapy.

Relapsed and refractory MM patients are those who minimally respond to initial therapy, but not the following therapy, or progression of disease is observed 60 days after the initial therapy.

1.2.4. Common staging systems for MM

Within symptomatic MM, the patients can be classified into three stages. There are two common staging systems used in MM, International Staging System and Durie-Salmon Staging System.

1.2.4.1. International staging system

International staging system is the most commonly used for MM in Canada. It is determined by two parameters: serum β2-microglobulin and albumin levels. β2-microglobulin (β2M) indicates renal malfunction whereas albumin is the normal protein which is abundantly present in the serum of healthy individuals. In ISS, Stage I is defined as serum β2M concentration is less than 3.5 mg/L and serum albumin level is greater or equal to 3.5 g/dL. Stage III is defined as serum β2M level greater than 5.5 mg/L. Any concentration in between will be defined as Stage II (21). Although commonly employed, the ISS staging system does not always precisely predict the prognosis of MM. In a cohort study, a normal seral concentration of β2M was found in 9% of MM cases from diagnosis to death (15). Currently, a revised international staging system has been postulated with additional considerations on patients chromosomal abnormality which is linked to high-risk (i.e. deletion of chromosome 17p, translocation between chromosome 4 or 16 with chromosome 14) genomic alterations and lactate dehydrogenase levels (22).

1.2.4.2. Durie-Salmon staging system

Durie-Salmon staging system was proposed by two clinicians in 1975 (3). This system stratify MM patients based on the parameters that are directly linked to CRAB including hemoglobin level,

serum calcium concentration, serum and urinal monoclonal components and detectable bone lesions. The following features have to be met to be classified as Stage I: hemoglobin level higher than 100 g/L, blood calcium level ≤ 2.8 mmol/L, IgG/IgA levels less than 50 and 30 g/L, respectively and less than 4 g of M proteins in urine. Additionally, no detectable bone lesion or only single myeloma is seen in Stage I. To be diagnosed as Stage III, the hemoglobin level should be less than 85 g/L, blood calcium level should be more than 2.8 mmol/L, IgG/IgA levels should be higher than 70 and 50 g/L, respectively and urine M protein should be more than 12 g. In this stage, it is expected to see severe bone damage. Any feature which falls between Stage I and III will be diagnosed as Stage II.

1.2.5. Current therapy for MM

The two major approaches for MM treatment are autologous stem cell transplantation and anti-MM regimens, and both are used for most of the time. The eligibility of MM patients for autologous stem cell transplantation is determined by multiple factors such as age (typically ≤65 years old) and organ functionality. A complete course of autologous stem cell transplantation consists of 4 regimens for induction, conditioning, consolidation and maintenance as outlined in **Figure 1.1.** For induction regimen, it was reported that a triplet-based induction regimen (i.e. simultaneous treatment with three anti-MM compounds) resulted in best overall response rate compared to doublet-based regimens based on four Phase III clinical trials (23–26). Additionally, inclusion of at least one novel therapeutic (bortezomib, which is a proteasome inhibitor; lenalidomide or thalidomide, which are immunomodulatory drugs) in the triplet-based induction regimen is recommended. For example, the induction regimen containing bortezomib, doxorubicin and dexamethasone was found significantly increased the overall response rate compared to that

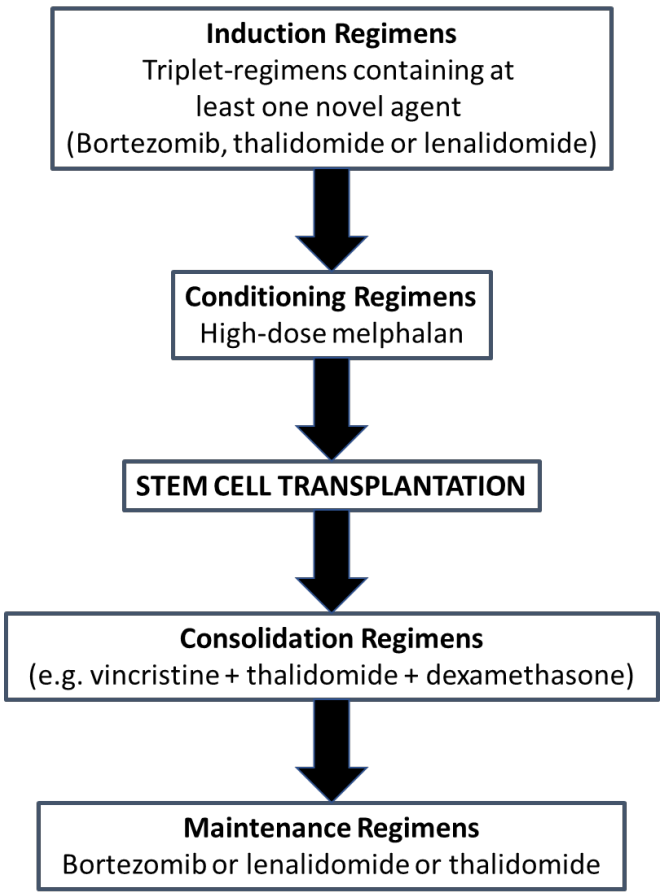

Figure 1.1. Scheme of autologous stem cell transplantation. Induction regimens consist of triplet-regimen including at least one of bortezomib, thalidomide or lenalidomide. Conditioning regimens contains high-dose melphalan. After transplantation, a consolidation regimen is followed. Single-agent maintenance regimens will be administered at last.

containing vincristine, doxorubicin and dexamethasone in a Phase III clinical trial (27). The common conditioning regimen before transplantation is high-dose melphalan 200 mg/kg^2 (28). After transplantation, a consolidation regimen is administered to improve the transplantation efficacy. For example, autologous stem cell transplantation followed by the treatment of vincristine, thalidomide and dexamethasone significantly resulted in increased complete response rate, very good partial response rate and partial response rate compared to transplantation alone in a clinical trial study (29). Finally, a maintenance regimen serves for prolonged response after

transplantation is required. Usually, a maintenance regimen contains a single agent (bortezomib, lenalidomide or thalidomide). For transplantation ineligible MM patients, a regimen containing cyclophosphamide, bortezomib and dexamethasone is used, followed by a maintenance regimen containing bortezomib (30). For relapsed and refractory MM patients, participation in clinical trials of novel agents is usually recommended (18). For example, it was shown that daratumumab, a monoclonal antibody against CD38, was able to induce cell lysis in lenalidomide- or bortezomib-resistant PMM cells (31).

1.2.6. Chromosomal aberrations in MM

Chromosomal aberrations found in MM patient samples can be categorized into two non-exclusive groups, structural and numerical aberrations. Structural aberrations are resulted from change of chromosome integrity by translocation, amplification (gain) or deletion (loss). The *IgH* gene locus on chromosome 14 is the most frequent spot of translocation, which account for approximately 70% of MM cases (32). Due to abundant expression of IgH in plasma/MM cells, the IgH translocation often lead to overexpression of the oncogenes integrated downstream of the *IgH* enhancer element including *Myc* (t(8;14)), *MAF* (t(14;16)), *CCND1* (t(11;14)) *CCND3* (t(6;14)) and *FGFR* (t(4;14)) (33). Common IgH translocations in MM patients include t(11;14) and t(4;14) which account for 12-14% and 15-21% of MM patients in three different cohort studies (34–36). The most common deletion in MM patients is at del13q14 (9-11%) and del17p13 (45-48%), where two well-known tumor suppressor genes, *RB1* and *p53* (34–36) locate. A common chromosome amplification in MM is $1q21^{+}$ which encodes oncogenes *PSMD4* and *CKS1B*, which contribute to bortezomib-resistance and cell-cycle progression in MM cells, respectively (37,38). Numerical aberrations are caused by changes in the total chromosome number and can be subdivided into

hyperdiploidy (when total chromosome number is between 48-74) and non-hyperdiploidy (any chromosome number other than 48-74). Numerical aberrations often occur in odd chromosomes as trisomy such as chromosomes 3, 5, 7, 9, 11, 15 and 19 (39). The frequencies of multiple chromosome aberrations within the MM cell population in a patient vary over time, suggesting the occurrence of MM clonal evolution. While IgH translocations and hyperdiploidy/non-hyperdiploidy are observed in the majority of MM cells, two studied have reported the appearance of minor chromosomal aberrations such as del13q14, del17p13 and $1q21^{+}$, suggesting the existence of MM subclones and clonal evolution (40,41). The prevalence of some chromosomal aberrations in MM patients were found positively correlated with disease progression, resistance to chemotherapy and poor prognosis. For example, $1q21^{+}$ was found in 43% newly diagnosed MM patients, but was found in 72% of relapsed MM patients (42). Another study showed that MM patients carrying $1q21^{+}$ or del17p13 resulted in significant short overall survival after lenalidomide and dexamethasone treatment (43). According to the *Clinical Practice Guidelines* published by Alberta Health System, MM patients carrying del17p13, t(4;14) or t(14;16) are classified as "high risk" and are expected to have a worse outcome after autologous stem cell transplantation (18).

The global-scale changes in chromosomes always lead to dramatic alteration in gene expression. Multiple changes in gene expression results in a broad range of survival in MM patients ranging from months to decades. Normal PCs are non-proliferative due to expression of cell cycle arrest proteins such as p21, p27 that prevents the progression of cell cycle. This regulation of cell is defected in myeloma cells. Aberrant chromosomal structures and/or signaling transduction lead to overexpression of cyclin D. In MM, the most overexpressed isoforms are cyclin D1 (CCND1) and cyclin D2 (CCND2). High expression of *CCND1* is caused by translocation of *CCND1* locus to the downstream of heavy chain IgH locus. Due to that IgH is highly expressed in PCs, the

translocated genes will be overexpressed as well. *CCND2*, on the other hand, is overexpressed due to aberrant signal transduction (e.g. cMyc or FGFR3). Overexpression of different CCNDs in MM cells can respond differently to different extracellular stimuli. It has been reported that APRIL and BAFF stimulated the cell-cycle progression and improved cell viability of primary MM cells (PMM) with *CCND2* but not *CCND1* or *CCND3* overexpression (44).

1.2.7. Extracellular signaling of MM

MM cells are stimulated by multiple extracellular ligands within the bone marrow as outlined in **Figure 1.2.** In this section, major extracellular signaling including IL6/IL6R, IGF1/IGF1R, BAFF/APRIL and Notch on MM cells will be discussed.

1.2.7.1. IL6/IL6R

IL6 is a cytokine which is required for B cell differentiation and plasmacytoma cell survival and proliferation (45,46). It was first found that IL6 induced proliferation of PMM cells in 6 out 10 patients in 1989 (47). IL6 is the most studied upstream stimulator of STAT3 signaling pathway in MM cells, despite that other members of IL6 family are also reported to activate STAT3 such as IL11, LIF, CNTF, OSM and cardiotrophin-1 (48–52). Upon binding, IL6 forms a complex with its receptor (IL6R) and a common receptor, glycoprotein 130 (gp130) which recruits intracellular Janus kinase (JAK) for downstream signal transduction. While gp130 is ubiquitously expressed, IL6R expression is tightly regulated and the limiting factor of IL6 signaling in normal cells. It is found that IL6R is significantly more expressed in MM cells or MGUS PCs compared to normal PCs (53). IL6R and gp130 can be soluble if its transmembrane domain is cleaved by proteolysis or by alternative mRNA splicing (54). Soluble IL6R is able to bind to IL6 and gp130 on cell

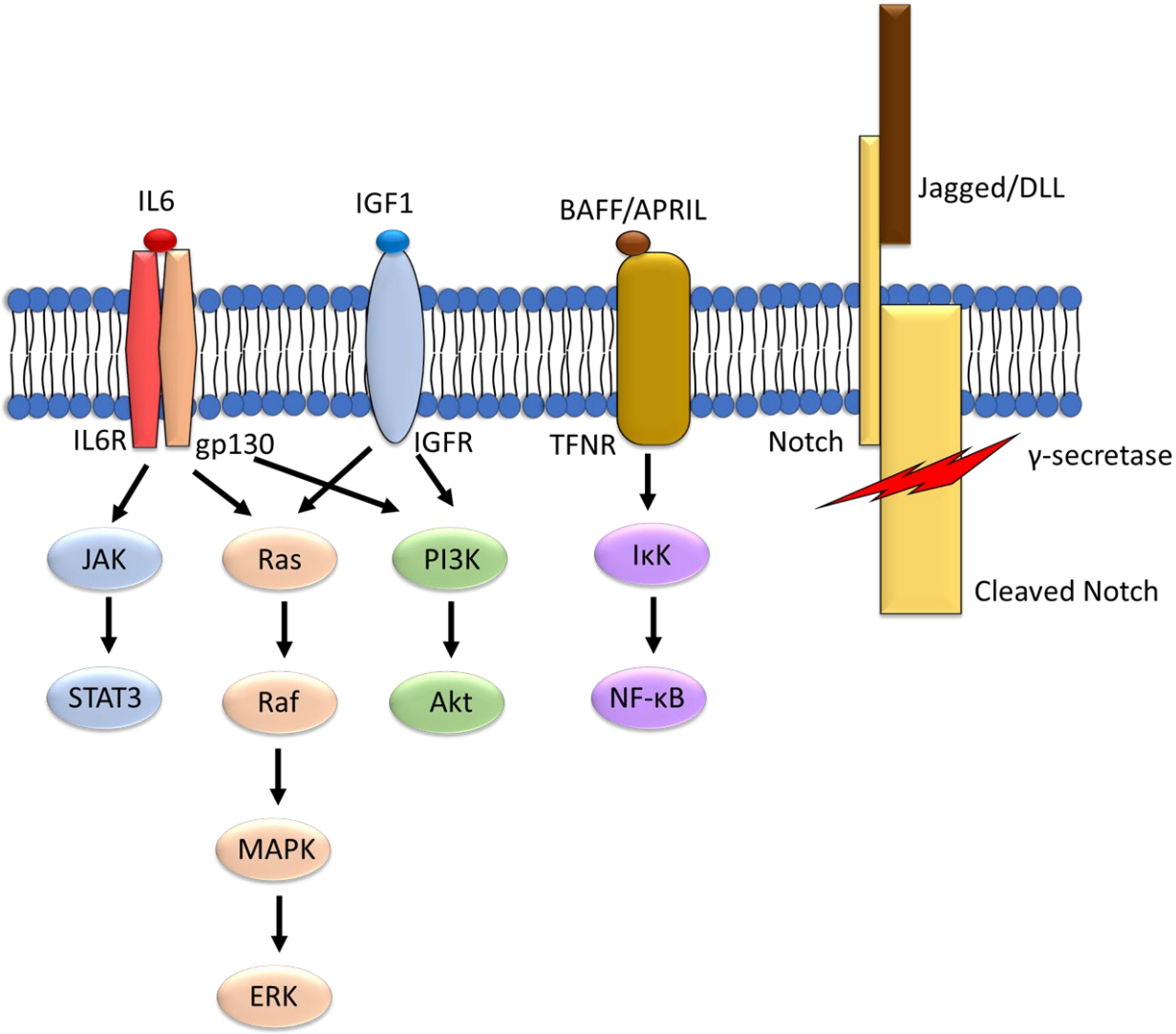

Figure 1.2. Extracellular signaling of MM cells. MM cells can be stimulated by extracellular ligands such as IL6, IGF1, BAFF/APRIL and Notch. These stimulations can trigger different signaling pathways. IL6/IL6R activates JAK/STAT3, MAPK/ERK and PI3K/Akt pathways. IGF1/IGF1R activates MAPK/ERK and PI3K/Akt pathways. BAFF/APRIL activates NF-κB pathway. Notch receptor can be cleaved upon binding of Jagged or DLL, and cleaved Notch can itself regulate gene expression.

membrane as an alternative source of IL6R (55). Soluble gp130, on the other hand, acts as an antagonist which sequester soluble IL6R and IL6 from binding to cell membrane.

It was found that the serum concentration of IL6 was higher in MM patients than in healthy donors (56). RT-PCR also revealed that the IL6 mRNA level in BMMCs from MM patients is higher compared to healthy individuals (57). The source of high IL6 protein levels in MM remains a debate. Some studies suggested that MM cells are able to produce IL6 themselves for autocrine stimulation. For example, two studies reported a high IL6 and IL6R mRNA expression levels in $CD38^{+}CD45^{-}$ MM cells isolated from patient samples as well as in a MM cell line, U266 (58,59). On the other hand, some other studies suggest that IL6 is primarily from the neighboring stromal cells by paracrine stimulation. For example, one study found that PMM cells and MM cell lines (RPMI8226 and U266) lost their ability to secrete IL6 if cultured in conventional culture for prolong period (2-3 weeks) (60). Another study demonstrated that IL6 mRNA is mainly expressed in $CD13^{+}CD15^{+}$ myeloid cells but not in MM cells by RT-PCR (57). In another study, increased IL6 secretion was detected when PMM cells were cocultured with stromal cells from MM patients or from healthy donors (53). It was also found that normal human mast cells and basophilic cells are capable of secreting IL6 upon activation by PMA and calcium ionophore (61). Direct cell-cell interaction between MM cells and stromal cells by β1, β2 integrins and fibronectin also contributed to high IL6 secretion in the culture (62). A mechanistic study found that the secretion of IL6 by stromal cells was induced by IL1-dependent synthesis of prostaglandin 2 by MM cells, and blockade of IL1/IL1R binding or PGE2 protein synthesis greatly reduced the IL6 level in BMMCs (63).

It was reported that IL6 secretion was positively correlated with the progression of MM. The relapsed MM shows high IL6 production compared to newly diagnosed MM, suggesting that the progression of MM is largely due to the expansion of IL6-secreting MM cells (64). IL6 is a

common stimulator of multiple intracellular signaling pathways in MM cells including JAK/STAT3, Ras/Raf/MAPK and PI3K/Akt (65–67). The mechanism of how IL6 triggers STAT3 in MM will be discussed below in section **1.3.3**.

1.2.7.2. IGF1/IGF1R

IGF1 is required for MM cell proliferation and survival. It stimulates MM cells by binding to its receptor IGF1R. Higher expression of IGF1R was found in MM cell lines and PMM cells compared to normal PCs and was correlated with shorter overall survival (68). It was found that IGF1 induced DNA synthesis, cell-cycle progression from G1 phase to S phase and cell growth in MM cell lines (69). Interestingly, IGF1 was found to have no effect on cell growth in normal B cells (69). Blockade of IGF1 binding to IGF1R using a monoclonal antibody resulted in decreased DNA synthesis and cell viability in MM cell lines (69,70). Additionally, blocking IGF1/IGF1R signaling did not affect the IL6 stimulation in MM cells and vice versa (71). In the same study, it was found that IGF1 resulted in phosphorylation of Erk but not STAT3 phosphorylation (71). This finding suggests that the signaling transductions triggered by IL6 and IGF1 are not completely overlapped. Another signaling pathway known to be activated by IGF1 is PI3K/Akt (65). While Erk activation increases cell proliferation, PI3K/Akt activation prevents MM cells from undergoing apoptosis. Akt is known to be able to phosphorylate a proapoptotic protein BAD, making it unable to bind to antiapoptotic proteins such as Bcl-xL (72). Without binding of BAD, anti-apoptotic proteins (e.g. Bcl-2, Bcl-xL and 14-3-3) can bind to mitochondria and prevent the release of cytochrome c, which is required to undergo intrinsic apoptosis (73). Overexpression of PTEN, but not other phosphatases such as SHP1 and SHP2, was able to block IGF/IGFR-induced PI3K/Akt activation in MM cell lines (74,75). Intriguingly, it was found that in MM cells that the

inhibition of IGF-induced PI3K signaling using LY294002 resulted in inactivation of both Akt and MAPK, whereas inhibition of IGF1-induced MAPK signaling using PD98059 did not affect PI3K activity, suggesting that PI3K is the manual upstream molecule of both PI3K/Akt and MAPK signaling pathways (76). IGF1 induced PI3K/Akt activity is also required for MM cells to attach to fibronectin in the bone marrow (77).

1.2.7.3. BAFF/APRIL signaling pathway

B cell activating factor (BAFF) and a proliferation-inducing ligand (APRIL) are the two tumor necrotic factor (TNF) family members which are known to activate NF-κB signaling pathway in malignant PCs (78). Binding of BAFF and APRIL to a membrane-bound type 1 tumor necrotic factor receptor (TNFR1) causes recruitment and phosphorylation of IκK, which triggers phosphorylation and proteasomal degradation of IKB, which is the inhibitory subunit of the NF-κB transcription factor complex (79). It was reported that the serum BAFF and APRIL concentrations in MM patients were significantly higher compared to those in healthy individuals (80). Moreover, MM patients with a level of BAFF or APRIL higher than the median showed a significantly shorter progression-free survival (80). The treatment of BAFF and APRIL resulted in dexamethasone-induced apoptosis in MM cell lines and PMM cells, and blockade of NF-κB signaling using an inhibitory peptide resulted in loss of dexamethasone resistance (81). Antibody against BRAF showed ability to reduce the degree of bone lytic lesion and improve survival in MM-bearing mice (82). In colorectal cancer cell lines, it was found that NF-κB can also bind to *APRIL* gene promoter to increased expression of APRIL (83), suggesting a positive feedback loop signaling between APRIL and NF-κB can exist in MM cells.

1.2.7.4. Notch

Notch is a transmembrane protein which cytosolic domain is cleaved by γ-secretase upon binding of ligands, Jagged or DLL (84). The cleaved Notch is able to translocate into the nucleus and regulate gene expression for biological processes such as differentiation and morphogenesis (85). Notch2 is overexpressed in MM patients with t(14;16) IgH-MAF translocation because Notch2 is a downstream target of MAF (86). Inhibition of Notch signaling pathway reduced the proliferation rate and induced apoptosis in MM cell lines (87). Moreover, Notch signaling pathway upregulate the expression level of CXCR4 in MM cells, which is responsible for bone marrow homing and is associated with poor prognosis (87). Importantly, Notch signaling pathway was reported to associate with resistance to melphalan and doxorubicin in both MM cell lines and PMM cells (88).

1.2.8. Tumor microenvironment and MM cells

Multiple cellular and non-cellular components within the bone marrow interact with MM cells and contribute to MM disease progression, as summarized in **Figure 1.3** (89). In this section, the relationship of each component with MM cells and how this relationship leads to MM pathogenesis will be discussed.

1.2.8.1. Bone marrow stromal cells

Bone marrow stromal cells (BMSCs) consist of multipotent progenitor cells which are responsible for formation of connective tissues such as bone, cartilage, adipocytes and stroma (90). Moreover, BMSCs provide mechanical support and residence to hematopoietic cells. The adhesion molecules on the surface of BMSCs, ICAM-1, VCAM-1 can interact with LFA-1 and VLA-4 expressed by MM cells, respectively. It was found that TNFα secreted by MM cells promoted the interaction between MM and BMSCs. Physical adhesion with MM cells and TNFα triggered the activation of

MAPK and NF-κB signaling pathways and the release of IL6 in BMSCs (91). BMSCs also contributes to drug resistance of MM cells by binding to their Notch1 receptor (92). Mesenchymal stem cells are the precursors of BMSCs (89). It was reported that mesenchymal stem cells from MM patients release more extracellular cytokines and growth factors such as IL6, VEGF and TNFα in exosomes which are important for MM oncogenesis compared to those from healthy donors (93).

1.2.8.2. Osteoclasts and osteoblasts

Bone lesions is a main feature of MM due to disturbed bone remodeling equilibrium between bone formation and bone breakdown or resorption in the bone marrow (94). There are two types of cells

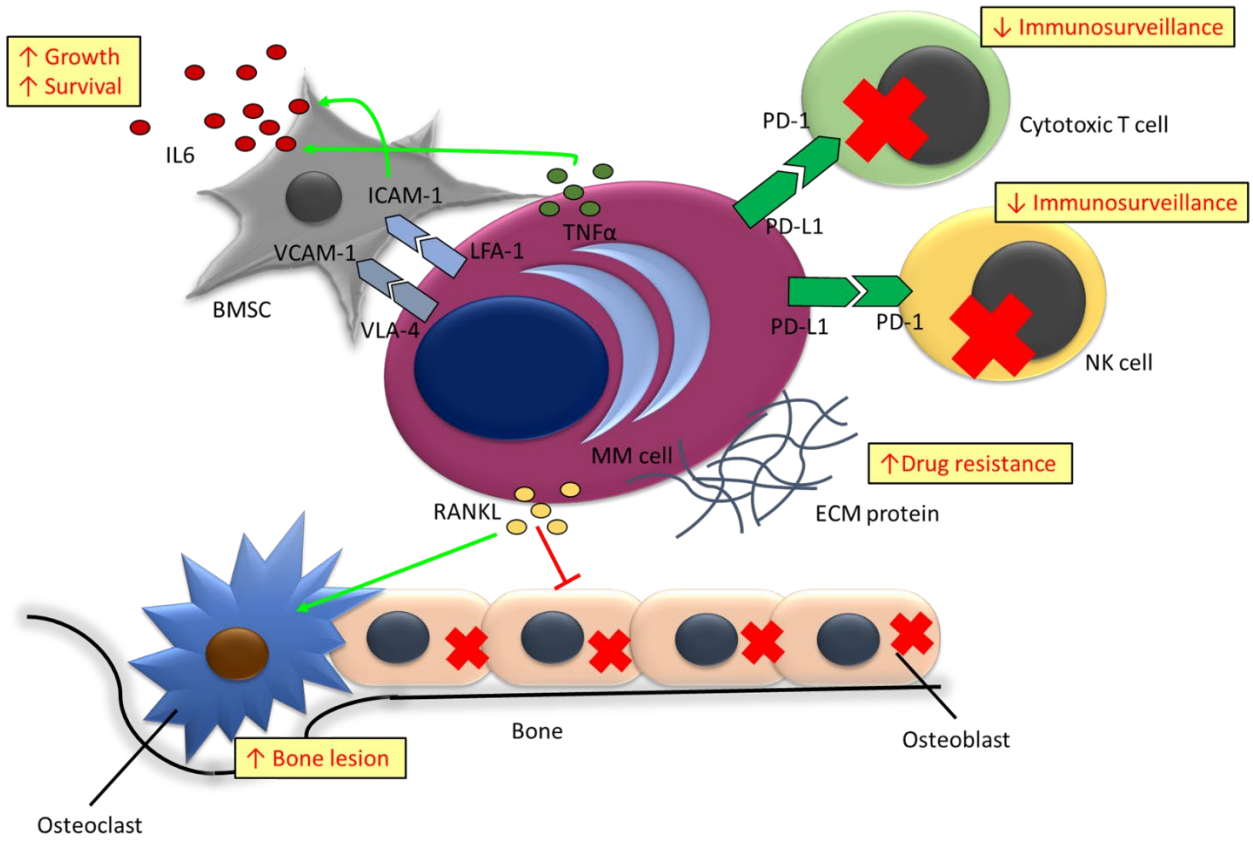

Figure 1.3. MM cells and the tumor microenvironment. MM cells promote the release of IL6 from BMSCs by VCAM-1-VLA-4 and ICAM-1-LFA-1 adhesions and TNFα, leading to increased MM cell growth and survival. Binding of PD-L1 on MM cells to PD-1 on cytotoxic T cells or NK cells suppresses the immune response to MM cells. MM cells release RANKL, which promotes osteoclast activity and suppresses osteoblast activity. Adhesion of MM cells to ECM proteins increases the drug resistance of MM cells.

in the bone which counteract each other: osteoblasts secrets matrix which is later mineralized to form new bones while osteoclasts digest bone materials (95). Both osteoblasts and osteoclasts surround osteocytes (i.e. bone cells) in a structure referred as "bone multicellular unit" within the bone marrow. It was found that MM cells promote the release of RANKL, a protein required for osteoclast differentiation and activation, in the preosteoblastic cells or BMSCs (96). It was found in other studies that PMM cells ($CD38^{++}CD138^{+}$) from patients can express RANKL themselves (97). On the other hand, the release of OPG from bone stromal cells, a protein inhibitor of osteoclasts, was downregulated by MM cells (96). Osteoclasts also promote proliferation and angiogenesis by secreting IL6 and osteopontin (98). The bone formation in MM is inhibited by suppressing osteoblastic differentiation and activity. It was known that Wnt/β-catenin pathway is essential for osteoblastic differentiation. In MM patients, the expression of an antagonist of Wnt pathway, Dkk-1, was positively correlated with severe bone lesions (97). Treatment of a neutralizing antibody against Dkk-1 was found to suppress tumor growth and bone disease in a MM animal model (99). It was also found that MM cells secrete another Wnt pathway antagonist, sFRP-2, which inhibits bone formation. Another mechanism by which MM cells downregulate osteoblastic differentiation is by inhibiting the transcriptional activity of Runx2 via physical interaction with osteoblasts (100).

1.2.8.3. Hematopoietic cells

The aberrant immunity is a contributing factor of MM progression. This is supported by the result that significantly higher progression-free survival and overall survival rates after allogeneic compared to autologous stem cell transplantation in 357 MM patients (101). An elevated level of IL6 and TGFβ in MM bone marrow promoted overexpression of CD39 and CD73 in T helper 17 (Th17) cells, which convert ATP to immunosuppressive ectonucleotide adenosine (102). Moreover, conversion of Th17 cells to regulatory T (Treg) cells was observed in MM bone marrow by elevated expression of *FOXP3* and *CTLA4*, the two signature genes of Treg cells (103). MM cells suppress the anti-tumor activity of cytotoxic T cells by direct cell-cell interaction. The interaction is mediated by PD-1 expressed by cytotoxic T cells and PD-L1 expressed by MM cells, both are overexpressed in MM patients (104). PD-1 and PD-L1 interaction inhibit the immune response triggered by the T cell receptor, leading to inability to eliminate MM cells. Similarly, in NK cells from MM patients, the PD-1 expression is upregulated while NKG2D (activating receptor of NK cells) expression is reduced (105). Tumor-associated macrophages are recruited to MM cells by chemoattractants like CCL2 as a source of pro-MM cytokines (IL6, TNFα, IL10, IL1β) and growth factors (VEGF-A) (89).

1.2.8.4. Extracellular matrix proteins

A comparative study revealed that the expression profile of ECM proteins in fibroblast-like cells isolated from MM patients is substantially different from that from MGUS or healthy individuals, and this difference favors the progression of MM (106). ECM proteins can mediate drug resistance of MM cells (107). For example, it was found that MM cell lines cultured in a plate coated with fibronectin exhibited significantly higher IC_{50} to mitoxantrone and doxorubicin compared to those

cultured in suspension (108). Similarly, in another study, it was found that combined treatment of soluble fibronectin and hyaluronan on MM cell lines significantly reduced dexamethasone-mediated apoptosis compared to MM cells with no or single treatment (109).

1.3. Signal transduction and activator of transcription (STAT3)

1.3.1 Discovery and characterization of STAT3

The discovery of Signal transducer and activator of transcription (STAT) family proteins was first published in 1992 (110). 3 proteins (91 kDa, 84 kDa and 113kDa) were purified out along with ISGF-3 (now known as interferon regulatory factor 9, IRF9) by affinity chromatography (111). These proteins are characterized to have transactivation ability and are able to be activated after stimulation of interferon-α (INFα) (112). The 91kDa and 84 kDa proteins were the first two STAT family members discovered due to different post-transcriptional mRNA splicing, hence named as STAT1α and STAT1β, respectively. The 113kDa protein was named as STAT2. Two more members, STAT3 and STAT4 were reported in 1994 by the same group (113). It was found that interleukin-6 (IL6) and epidermal growth factor (EGF), induced tyrosine phosphorylation, dimerization and DNA-binding ability of STAT3 (49,114). INFα, a stimulator of STAT1 and STAT2, is found to reduce STAT3 dimerization and DNA-binding ability and induce apoptosis (115). More STAT family members, STAT5a, STAT5b and STAT6 were later discovered. Among STAT family, STAT3 and STAT5 are thought to be related to tumor progression (116,117).

1.3.2 Structure of STAT3

Human *STAT3* gene is located on chromosome 17q. The predominant isoform of human STAT3, STAT3α, contains 770 amino acids (118) and has a molecular weight of 92kDa (113). STAT3

protein contains several major domains from N- to C-terminus: a N-terminal domain, a coiled-coil domain, a DNA-binding domain, a SH2 domain and a transactivation domain (only in STAT3α). The N terminal domain is essential for STAT3 tetramerization (2 dimerized STAT3 forming a complete DNA-binding complex) and nuclear translocation (119). The coiled-coil domain can be recognized by importin-α3, a carrier protein that transports STAT3 into the nucleus (120). The DNA-binding domain recognizes and binds to STAT3 target gene promoter (i.e. γ-activated sequence, GAS). The SH2 domain contains tyrosine residues that can be phosphorylated by receptor or non-receptor kinases. It is also responsible for the dimerization process. Finally, the transactivation domain exerts transcription factor activity. The transactivation domain in another alternatively spliced isoform STAT3β is absent and replaced with 7 acidic amino acid residues, which leads to a longer retention time in the nucleus compared to STAT3α (**Figure 1.4**) (121). A study compared the functions of STAT3α and STAT3β in cells showed that STAT3β is activated independently of the stimulation of cytokines and growth factors (122). Moreover, the same study indicated that the activity of both isoforms is dependent on Y705 phosphorylation. STAT3β was found to have a longer half-life in the nucleus and a stronger DNA-binding ability. On the other hand, STAT3α was found to have a better transcriptional activity compared to STAT3β. It is probably due to the highly acidic C-terminus sequence of STAT3α that disturb the DNA binding. Additionally, STAT3β is able to form a heterodimer with STAT3α to prevent STAT3α homodimerization, leading to downregulation of the transcriptional activity of STAT3α (123). A group studied the biological effect of STAT3β by genetically deleting the splicing site of STAT3 exon 23, leading to increased expression of only STAT3β (124). This increased STAT3β expression resulted in reduced tumor growth *in vivo*. Phosphorylation of S727 contributes to better transcriptional activity of STAT3α. The surrounding motif LPMSP is where the transcription co-

activator, CBP/p300 is recruited to. The presence of LPMSM is required for responding to IL-6 and OSM signaling (125).

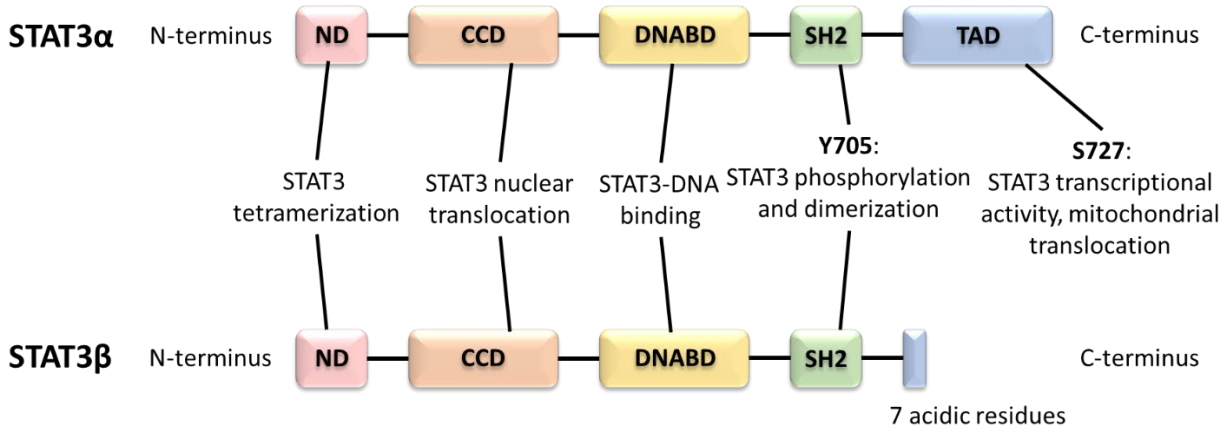

Figure 1.4. Structure of the two alternative splicing variants of STAT3. Both STAT3α and STAT3β contain N-terminal domain (ND), Coiled-coil domain (CCD), DNA-binding domain (DNABD) and Src homology 2 domain (SH2). STAT3α contains a C-terminal transactivation domain (TAD) which is replaced by 7 acidic amino acid residues in STAT3β.

1.3.3 STAT3 oncogenic signaling pathway

The canonical STAT3 activation pathway is triggered after stimulation of cytokines (e.g. IL-6) or growth factors (e.g. EGF) which bind to a receptor on cell membrane, leading to recruitment of intracellular protein kinases such as JAK and Src to phosphorylate STAT3 at the tyrosine residue Y705 (pSTAT3) within the Src homology 2 domain (SH2) (126–128). pSTAT3 forms homodimers and migrates into the nucleus to facilitate target gene transcription. In some cases, constitutively active protein tyrosine kinases are able to phosphorylate STAT3 independent of cytokine and growth factor stimulation. For example, in anaplastic lymphoma kinase-positive anaplastic large-cell lymphoma (ALK+ALCL), the constitutively active NPM-ALK resulted from t(2;5) translocation led to constantly phosphorylated and active STAT3 (129). Another common

phosphorylation site of STAT3 is a serine residue within the transactivation domain (S727) which is required to activate the transcription of STAT3 downstream target genes (130). It was reported that a different kinase, PKC-ϵ, catalyzed the S727 phosphorylation of STAT3 (131). STAT3 has been recognized as an oncoprotein that regulates the transcription of proteins related to survival (e.g. survivin, Bcl-2, Bcl-xL), proliferation (e.g. CCND), immune system suppression (e.g. TGFβ), metastasis (e.g. MMP), angiogenesis (e.g. VEGF-A) and drug resistance (e.g. c-Myc) (132,133). The STAT3 activation is tightly regulated in normal cells. The most common mechanism of STAT3 inhibition is by the intracellular protein tyrosine phosphatases (PTP) which bind and dephosphorylate STAT3 such as SHP-1, SHP-2, PIAS3 and SOCS3 (134). These PTPs have a SH2 domain which binds to STAT3 and a phosphatase domain.

STAT3 expression and activity are critical for early embryo development. Mice with *STAT3*$^{-/-}$ knockout are lethal to mouse embryos within 7 days (135). Several tools have been developed to study the biochemical and biological effects of STAT3. STAT3C is a biochemically engineered mutant of STAT3 carrying two residue changes, A661C and N663C (136). This mutant is found to increase STAT3 phosphorylation, STAT3 DNA binding activity, cell colony transformation, cell polarization, adhesion and migration in a human prostate cancer cell line (137). On the other hand, a dominant-negative construct of STAT3 with a Y705F mutation showed deficiency in DNA binding ability and phosphorylation by JAK (138).

It was recently discovered that STAT3 can exert its oncogenic effect by several non-canonical signaling pathways (139). First, unphosphorylated STAT3 was found to be able to enter into nucleus via interaction with importin-3 at the coiled-coil domain (120). It was shown that

unphosphorylated STAT3 can bind to GAS on DNA and trigger transcription as phosphorylated STAT3. Moreover, unphosphorylated STAT3 was found to incorporate with NF-κB and regulate the expression of NF-κB target genes (140). Second, STAT3 can translocate to mitochondria and shift the mode of cellular respiration from oxidative phosphorylation to aerobic glycolysis (aka. Warburg Effect), hence enhance cell survival and tumorigenesis (141). It was also reported that activated PKCε by EGF or TPA mediated mitochondrial translocation of monomeric pSTAT3 (S727) from the cytoplasm to mitochondria in mouse keratinocytes (142). Additionally, it was found that mitochondrial STAT3 regulate mitochondria-encoded genes. In a STAT3-knockout mouse model by Cre-lox recombination, a significant increase in mitochondrial genes such as cytochrome b, NADH dehydrogenase 5 and NADH dehydrogenase 6, all of which were related to cell senescence (143). In one study, an electron transport chain complex I subunit GRIM-19 was found to directly interact with STAT3, and this process was determined to be Ser 727 phosphorylation-dependent (144). Association of STAT3 on electron transport chain was found to reduce the release level of reactive oxygen species and suppress mitochondrial apoptosis (145). Additionally, mitochondrial pSTAT3 (S727) can directly bind to cyclophilin D, a protein responsible for the opening of mitochondrial permeability transition pore, to prevent the release of cytochrome c during intrinsic apoptosis (146). Third, STAT3 can regulate gene expression by chromatin remodeling. For example, it was found that SHP1 was hypermethylated by STAT3-DNA methyltransferase I (DNMT1) complex in T cell lymphoma cells (147). RNA interference of STAT3 or DNMT1 resulted in elevated SHP1 expression.

1.3.4 STAT3 in MM

STAT3 plays an essential role in MM tumorigenesis. Knockdown of STAT3 expression level in RPMI8226 cells by siRNA resulted in loss of malignant phenotypes including increased doubling time, increased G1 phase accumulation, reduced colony formation and increased apoptosis (148). STAT3 was found to be active in more than 50% of MM patients by four groups with different approaches. Bharti *et al.* found that purified $CD138^{+}$ cells from 14 of 22 (~63%) MM patients exhibited strong nuclear localization of STAT3 by immunofluorescence staining (5). Two other studies investigated STAT3 activity in PMM cells via detection of STAT3 phosphorylation states. One of them reported that more than 10% cells from 23 of 48 (~48%) MM patients showed pSTAT3 (Y705) nuclear staining (149). Another reported that 8 of 16 (50%) MM patient biopsies showed more than 66% cells with nuclear staining of pSTAT3 (S727) by immunohistochemistry (150). Since the whole BMMC population was examined in these two studies, it is expected that the actual proportion of pSTAT3-positive MM cells would be higher. Quantitative analysis of $CD38^{++}$ cells from 65 MM patients showed that the pSTAT3 (Y705) level was 3 times higher than healthy individuals (151). Clinically, it was found that MM patients with more than 30% $CD138^{+}$ cells with pSTAT3 (Y705) nuclear staining resulted in poorer progression-free survival and overall survival, with a hazard ratio of 3.3 and 3.7, respectively (152). Anti-STAT3 agents such as LLL12, SC09 and YM155 have shown ability to suppress the growth of STAT3-active MM tumor in animals (153–155). STAT3 activity is tightly associated with bortezomib, lenalidomide and dexamethasone resistance in MM cells. Zhang *et al.* discovered that the EGF/EGFR/JAK1/STAT3 signaling axis induced transcription of immunoproteasome subunit genes *LMP2* and *LMP7*, which counteract the anti-MM effect of bortezomib (156). Another group found that a dexamethasone-resistant 7TD1 cells showed a higher level of pJAK and pSTAT3 levels compared to dexamethasone-sensitive 7TD1 cells (157). It was reported that IL6-induced STAT3 activation

upregulated the expression level of heme oxygenase-1, which activated MAPK and resulted in lenalidomide resistance in MM cell lines and $CD138^+$ PMM cells (158).

The most common upstream activator of STAT3 in MM is IL6. It was found that treatment of MM cells with monoclonal IL6 antibody resulted in ablated STAT3 DNA binding ability and reduced expression of anti-apoptotic proteins such as Bcl-xL and Bcl-2 (159). Protein kinases that phosphorylate STAT3 including JAK1 and JAK2 are overexpressed in 27% and 57% in MM patients, respectively (160). Additionally, phosphatases such as SHP1, SHP2 and SOCS1 which inhibits STAT3 activity by dephosphorylation are found to be downregulated in MM cells (161,162).

The IL6/JAK/STAT3 signaling axis is always activated in MM. Some studies reported intracellular proteins which facilitate IL6/JAK/STAT3 signaling in MM cells. For example, A transmembrane phosphatase CD45 was found to associate with a Src family kinase Lyn, which in turn phosphorylates STAT3 (163). 90 kDa heat shock protein (Hsp90) also contributes to elevated STAT3 activity, but the mechanism remains unclear. Treatment of Hsp90 inhibitors resulted in a reduced level of both STAT3 and pSTAT3 (Y705), and addition of IL6 did not rescue this phenomenon (164). Interestingly, it was found that only $CD45^+$ MM cells are sensitive to Hsp90 inhibitors, which are found to be STAT3 active (165). RNA interference of GRK6, a kinase found to directly associate with Hsp90, resulted in dephosphorylation of STAT3 (166). A 14-3-3 family member, 14-3-3ζ was found necessary for phosphorylation of STAT3 at S727 in U266 cells, and inhibition of 14-3-3ζ resulted in ablation of STAT3 DNA-binding and transactivation ability (167). Interaction with ECM proteins can also induce STAT3 activation in MM cells. For instance, it was found that MM cells cultured on a fibronectin-coated plate rendered more pronounced IL6-induced

STAT3 activation compared to conventional culture (108). Another study found an ECM protein reelin is overexpressed in ~40% MM patients, and it activated STAT3 via FAK/Src/Syk signaling pathway (168). It was found that integrin β1 is responsible for binding with both fibronectin and reelin for STAT3 activation in MM cells.

Some proteins downregulate the activity of STAT3 by intervening its phosphorylation or DNA-binding ability in MM cells. For example, an extracellular chemokine, PF4 was a tumor suppressor which ablate STAT3 signaling by upregulating SOCS3 once bound to its receptor LRP1 (169). Upon binding of lipophilic ligands (from metabolism or nutrients), a nuclear receptor PPARγ translocates into the nucleus to the DNA-binding domain of STAT3 (170). Similarly, estrogen reporter upregulates the expression level of PIAS3, which in turn blocks STAT3-DNA interaction (171). A membrane-bound protein TJP1 was found to suppress the signaling of EGFR which activates JAK/STAT3 in MM cells (156). Overexpression of TJP1 resulted in a decreased level of pSTAT3 (Y705) and decreased STAT3-induced bortezomib resistance.

1.3.5 STAT3 SH2 domain inhibitors

Due to the oncogenic roles of STAT3 in various tumor types, inhibitors targeting upstream kinases, SH2 domain or DNA-binding ability of STAT3 have been developed. STAT3 SH2 domain inhibitors are the most commonly used and studied in the laboratory due to their direct binding to cytoplasmic STAT3. In 2001, Turkson *et al.* developed the first STAT3 inhibitor using the peptide sequence of Y705 phosphorylation site (P*YLKTK, * means phosphorylation) located within the SH2 domain of STAT3 (172). P*YLKTK substantially disrupts STAT1, STAT3 and STAT5 dimerization at 1 mM in transformed NIH3T3 cells with v-Src overexpression. Synthetic

peptidomimetic compounds were later developed to improve the high dose range and low stability and membrane penetrating ability of P*YLKTK. ISS-610 is structurally resembled P*YL, the three essential amino acids for SH2 domain binding except the P residue is replaced with a cyanobenzoate group (173). It was shown that ISS-610 preferentially bind to STAT3-STAT3 dimer compared to STAT3-STAT1, STAT1-STAT1 or STAT5-STAT5 dimer. However, high dosage of ISS-610 (~1 mM) is still required to substantially inhibit STAT3 dimerization. By screening the compound library, small molecule STAT3 inhibitors such as STA-21 and Stattic were developed with their high binding score inside the STAT3 Y705 phosphorylation site and improved IC_{50} against STAT3-active breast cancer cells (174,175). With the advanced technology in computational modeling, scientists were able to synthesize novel compounds that did not exist in any compound library such as S3I-M2001, S3I-201, S3I-201.1066 and S3I-1757 that specifically binds to STAT3 active sites (176–179). An orally bioavailable STAT3 inhibitor, BP-1-102 and OPB-31121 were synthesized for more convenient drug administration (180,181). Comparison between these STAT3 inhibitors are summarized in **Table 1.1**. Although these STAT3 inhibitors pose high specificity and efficacy in laboratory settings, very few of them have entered clinical trials, largely due to low response rate and adverse side effects. For example, a Phase I clinical trial of OPB-31121 on 18 patients with various solid cancers showed no complete response or partial response at all (182). Moreover, more than 65% of patients showed adverse side effects such as nausea, vomiting and diarrhea.

1.4 Three-dimensional (3D) cell culture

Given the importance of a variety of exogenous stimuli supporting the development of MM, it is indispensable to consider the microenvironment factors, which conventional cell culture does not

Table 1.1. STAT3 SH2 inhibitors tested in cancer cells.

Compound	Method	IC_{50} (*in vitro* cytotoxicity)	STAT Specificity	Cell lines	Reference
P*YLKTK	STAT3 Y705 phosphorylation site	Not determined	Can affect STAT1 and STAT5 as well	NIH3T3/v-Src	(172)
ISS-610	Modification of XY*L peptide at X residue	>1 mM, 48hr	Can affect STAT1 and STAT5 as well	NIH3T3/v-Src	(173)
STA-21	Structure-based screening using STAT3β crystal	≥ 20 μM	Does not affect STAT1 and STAT5	MDA-MB-231, MDA-MB-435, MDA-MB-453, MDA-MB-468, MCF-7	(174)
Stattic	Screening of chemical libraries consisting of a diverse collection of 17,298 substances	5-10 μM, but need 50-60 μM to bind to SH2 peptide	Does not affect STAT1 and STAT5	MDA-MB-231, MDA-MB-435	(175)
S3I-M2001	Computational modeling	50-100 μM	Dose not affect STAT1 but disrupts STAT1-STAT3 dimerization	NIH3T3/v-Src, MDA-MB-231, Panc-1	(176)
S3I-201	Computational modeling	30-100 μM	Can slightly affect STAT5, can kill STAT3-inactive cells	NIH3T3/v-Src, MDA-MB-435	(177)
S3I-201.1066	Modification from S3I-201	35-48 μM	Can affect STAT1	NIH3T3/v-Src, MDA-MB-231, Panc-1	(178)
BP-1-102	Modification form S3I-201.1066, orally bioavailable	<20 μM	Does not affect STAT1 and STAT5 dimerization	NIH3T3/v-Src, MDA-MB-231, Panc-1, DU145, A549	(180)
OPB-31121	Computational modeling	5-10 nM	Can affect STAT1 and STAT5	SNU 484, SNU 668	(181)
S3I-1757	Modification from S3I-201	50-100μM	Not determined	H358, A549, MDA-MB-231, MDA-MB-468	(179)

account for. There have been many animal models which better represent the behavior of disease in human body. However, a most cost-effective and time-saving model is required for large-scale gene expression analysis and therapeutic screening. Three-dimensional (3D) cell culture models have been postulated as a cost-effective but realistic approach to study tumor biology. In this section, the general classifications and advantages of 3D culture models, as well as their development specifically for studying MM, will be discussed.

1.4.1. Classification of 3D culture models

3D culture tumor models can be classified in three major forms: tumor explants, tumor-on-a-chip and tumor spheroid (183). Tumor explants refer as growing a freshly extracted tumor on a culture plate pre-coated with collagen and supplied with growth medium. Therapeutics can be injected intratumorally for efficacy assessment. This method recapitulates the architecture of a real tumor with the presence of tumor morphology, metastasis and vasculature. However, the experimental results from this method are hardly reproducible because of the heterogeneity nature of tumors. One study utilized breast cancer explants from three patients to test the therapeutic efficacy of caffeic acid, ursolic acid, and rosmarinic acid and found very different response patterns in the three explants (184). Tumor-on-a-chip is a method where crude tumor cells were cultured in a microplate with constant supplement of growth medium. For example, a tumor-on-chip model was designed to study the invasion of liver carcinoma cells into the stromal cells, which induced stromal cell apoptosis and increased level reactive oxidative species (185). Similar to tumor explants, the experimental data generated from tumor-on-chip technique has low reproducibility. The tumor spheroid 3D culture is the most widely employed method for cancer research. It uses single tumor cells to form a spheroid by suspending them to grow all directions. Tumor spheroid

3D culture can be classified into two groups: scaffold or scaffold-free (**Figure 1.5**). Scaffold 3D culture models have materials which form niches in which tumor cells can grow within (i.e. Matrigel, hydrogel, polymer etc). Tumor cells in the scaffold-free model are maintained in suspension by mechanical or magnetic forces (e.g. hanging drop, nanoplates, magnetic levitation etc.). The descriptions, advantages and disadvantages of all tumor spheroid 3D culture models are depicted in **Table 1.2**.

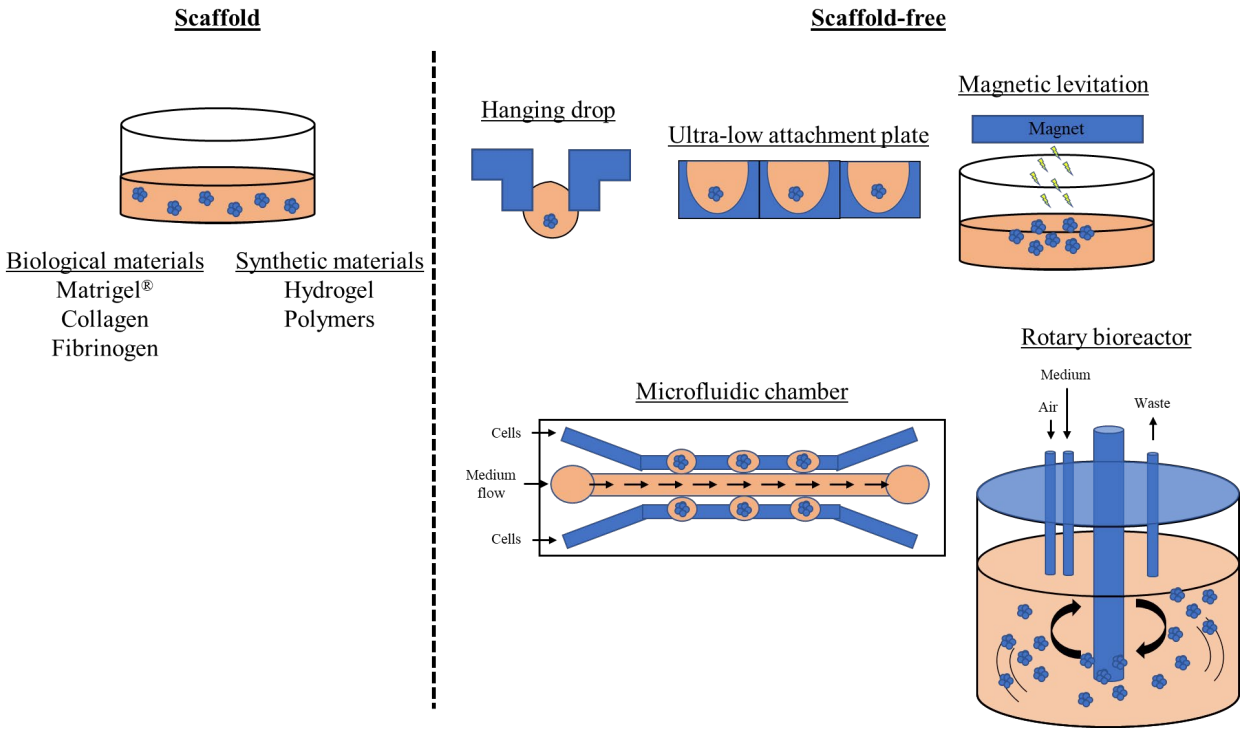

Figure 1.5. Scheme of different tumor spheroid 3D culture models. Tumor spheroid 3D culture models can be categorized based on the presence of scaffold or not. In scaffold 3D culture, cells are directly contacting with supportive materials which can be biological (e.g. collagen or fibrinogen) or synthetic (e.g. hydrogel or polymers). In scaffold-free 3D culture, cells are maintained suspended by mechanical forces for spheriod formations. Common examples are hanging drops, ultra-low attachment plates, magnetic levitation, microfluidic chambers and rotary bioreactors.

Table 1.2. Tumor spheroid 3D culture models.

Methods		Description	Advantages	Disadvantages
Scaffold	Biological materials (Matrigel, collagen, fibrinogen etc.)	Solidified biological materials used to create niches for tumor cells to grow within	More biologically relevant Materials are commercially available	Cell recovery from matrix is needed Variability between different batches of materials
	Synthetic materials (Hydrogel, PLGA)	Biocompatible polymers used to create niches for tumor cells to grow within	Capability to customize High stability and reproducibility	Cell recovery from matrix is needed. Complicated polymer synthesis process Immune response
Scaffold-free	Hanging drop	A droplet of growth medium with tumor cells is suspended in a specialized plate by surface tension	Easy preparation, no matrix is involved. Small cell number is needed Easy to harvest spheroid	Small spheroid size in culture. Not suitable for long-term culture Specialized plates are needed
	Ultra-low attachment plate	Culture plates coated with inert material which prevents attachment of cells to form a monolayer	Easy preparation, no matrix is involved Small cell number is needed Easy to harvest spheroid	Specialized plates are needed Small spheroid size in culture Expensive plates
	Magnetic levitation	Tumor cells are introduced with magnetic nanoparticles and suspended in a magnetic field	Easy to harvest spheroids	Laborious preparation procedure Nanoparticle may interfere with some biological processes
	Rotary bioreactor	Suspending tumor cells by rotation to create microgravity	Great spheroid size and numbers	Expensive equipment. Require constant supply of growth medium
	Microfluidic chamber	Flowing of growth medium and tumor cells into a fine-patterned plate which occasionally keeps tumor cells to form a spheroid	Good metastasis model	Great loss of cells Require constant supply of growth medium

1.4.2. Advantages of 3D culture in cancer research

3D culture provides a bridging role which connects the realistic perspective of *in vivo* tumor and feasibility to manipulate *in vitro*. The major advantage of 3D culture compared to conventional

culture is its higher similarity to *in vivo* growing conditions of a tumor. For instance, in a study, human oral cancer cells cultured in a 3D model showed indifferent growth rate and hypoxia at the core of tumor as compared to its corresponding xenograft *in vivo* (186). The efficacy of anti-cancer therapeutics was better reflected by 3D models than by conventional culture. It was found in three patient-derived glioblastoma cell lines that cells grown in a novel 3D culture model responded to both conventional and molecular therapeutics correspondingly to the patient clinical data (187). A transcriptomic comparison study found that both 3D cultured (ultra-low attachment plate) cells and xenografts, but not monolayer cultured cells, showed upregulation of genes related to hypoxia, TGF and Wnt signaling pathways and epithelial-mesenchymal transition in two non-small cell lung carcinoma cell lines (188). A proteomic and phosphoproteomic study revealed that colon cancer cells (HT29) cultured in 3D exhibited downregulation on cell growth pathway proteins compared to those in conventional culture (189). Consistent with this finding, another study found that the activity of Akt/mTOR/S6K gradually decreased from the surface to the core of a spheroid in 3D culture (190). Active S6K was found to inhibit the MAPK/ERK signaling pathway, hence preventing cell growth inside the spheroid. Importantly, a similar phenomenon was observed in the xenograft tumors but not in the monolayer culture.

3D culture often retains the ability of cancer cell to grow into a spheroid structure which consists of a quiescent core and a proliferative outer layer. Compared to the 2D monolayer, tumor cells in 3D spheroids show very different drug distribution and penetration patterns. In one study, it was found in 2 head and neck carcinoma cell lines that 4 different anti-cancer compounds are evenly distributed in 2D monolayer culture, but in 3D spheroid culture using an ultra-low attachment plate, the drug is mainly accumulated at the outer layer of spheroids (191). This finding suggested a

possible drug resistance mechanism of 3D cultured cells. Another study reported that culturing A549 and UTSCC15 cells in a Matrigel-based 3D culture resulted in spheroid formation and increased resistance to irradiation and cisplatin compared to conventional culture (192). In the same study, the genomic profile revealed that genes related to extracellular communication, cell adhesion and immune response were mostly altered between conventional and 3D culture. Another study reported that breast and glioblastoma cells cultured in a microfluidic 3D model exhibited a substantially higher reactive oxygen species level compared to those in conventional culture after 5 days (193). In addition, it was found that these 3D cultured cells became more cisplatin resistant compared to conventionally cultured cells on day 5, suggesting that reactive oxygen species may involve in the drug resistance mechanism in 3D cultured cancer cells. It was shown that three breast cancer cell lines cultured two 3D culture models, Matrigel and microfluidic chip exhibited a higher resistance to two anti-cancer agents, carnosic acid and doxorubicin (194). However, other studies suggested the responsiveness to chemotherapeutics in 3D cultured breast cancer cell lines was cell line-dependent and drug-specific (195,196). For instance, 3D cultured MDA-MB-231 and MCF-7 cells were shown to be more resistant to epirubicin than in conventional culture, but an opposite effect was seen in BT-474 cells(195). Another study showed that BT-474 and BT-549 cells but not MCF-7 cells were more resistant to paclitaxel in 3D spheroid culture compared to 2D monolayer culture (197). Studies have demonstrated that cells grown within 3D culture possess different gene expression profiles and phenotypes compared to the same cells grown in conventional culture. For example, in a study using a melanoma cell line, it was found that cells showed a slower proliferation rate and higher expression levels of chemokines and proangiogenic factors as a 3D multicellular tumor spheroid compared to those in monolayer culture (198). In another study, it was found that patient-derived glioblastoma cells in a spheroid-forming

3D culture model maintain similar genomic profile to the parental tumor as compared to those in conventional monolayer culture (199).

3D culture allows studies on the process of tumorigenesis of malignant cells *in vitro* compared to normal cells which cannot be achieved by conventional cells. Using a Matrigel-based 3D culture model, Peterson *et al* found that the breast cancer cell lines showed a higher cell proliferation rate compared to normal endothelial cell lines (200). Moreover, they found that malignant cells formed disorganized colonies, normal cells formed hollow and spherical acini (200). Interestingly, in another study, it was found that inhibition of β1 integrin by a monoclonal antibody resulted in reversion of malignant cell morphology to normal acini, suggesting the importance of β1 integrin in breast cancer oncogenesis (201). All in all, it is believed that 3D culture models are more representative of a tumor for oncogenesis studies and assessment of therapeutic efficacy.

1.4.3. 3D culture for studying MM

Based on the literature search, over 2000 studies have been published about 3D culture in various solid cancers, yet those for MM are very limited. Given the difficulty of maintaining cell viability in conventional culture (202), some 3D culture models have been postulated to prolong the survival of PMM cells *in vitro*. A Matrigel-based model was postulated by Kirshner *et al*., within which primary bone marrow cells are able to proliferate for up to 30 days (203,204). The model consists of two parts, a reconstructed endosteum consisting of fibronectin and collagen and a reconstructed bone marrow matrix containing Matrigel, fibronectin and collagen (**Figure 1.6**). With this model, it was found that the stromal cells supporting the growth of MM cells are well preserved. Moreover, it was found that treatment of bortezomib led to cell death in the $CD138^{+}CD56^{+}$ MM

cell population while the other cellular components remained unaffected, suggesting a precise representation of drug response as *in vivo*. This 3D model has also been used to assess the *in vitro* efficacy of novel therapeutics in MM cell lines (205,206). An animal-implanted polymeric 3D culture model (SCID-synth-hu) was proposed for expansion of PMM cells *in vivo* (207). Specifically, the polymeric scaffold was first inoculated with mouse BMSCs, and the scaffold was then implanted into the femur of SCID mice. Purified $CD138^{+}$ MM cells were injected into the mice for the development of MM. With 10 patient samples tested, all mice showed a time-dependent elevation of serum M protein concentration for up to 80 days, suggesting the growing

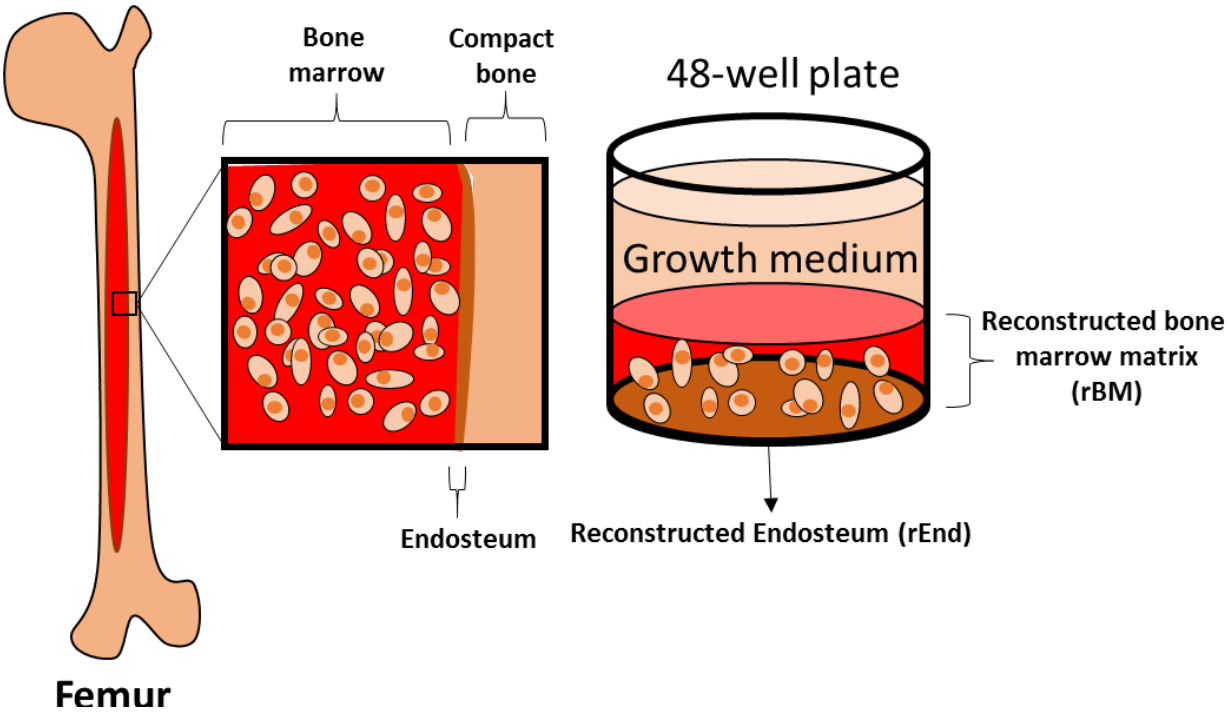

Figure 1.6. 3D culture model developed by Kirshner *et al.* The 3D culture system consists of a reconstructed endosteum (rEnd, brown) and a reconstructed bone marrow matrix (rBM, red), which recapitulates the real bone marrow cavity. For culture setup, a culture well plate is first coated with reconstructed endosteum solution. Reconstructed bone marrow matrix with MM cell lines or primary bone marrow mononuclear cells is applied to the coated well. After solidification of reconstructed bone marrow matrix, fresh growth medium will be applied on top of it.

of MM tumor *in vivo*. The drawback of this approach is the long tumor development time for follow up studies, which is approximately one month. A microfluidic 3D culture providing consistent supplement of fresh growth medium to primary BMMC cells was reported to enrich the percentage of MM cells (marked by $CD138^+$ and $CD38^+CD56^+$) to ~70% within 7 days (208). However, the dynamic flow led to rapid loss of total BMMCs, resulting in only ~1-2% viable cells left after 7 days. A bioreactor for culturing MM tumor explants was shown to reflect the clinical responsiveness to bortezomib (209). Specifically, it was found that after bortezomib treatment, the change in β2M level of the supernatant solution from the bioreactor is similar to that of the serum from the corresponding patients. The above 3D culture models possess different features of *in vivo* growing conditions, but their superiority compared to conventional culture has not been investigated. In 2015, a tissue-engineered bone marrow 3D culture model was reported to increase the proliferation rate of PMM cells up to 3 times within 10 days, as opposed to a decreased proliferation rate in conventional culture (210). However, PMM cells from patient biopsies showed a relatively steady cell proliferation rate *in vivo* (15). All in all, a 3D culture model which can preserve PMM cells without losing their biological behavior is required for long-term biological studies and therapeutic assessment. In addition, the biological and biochemical effects on MM cells cultured in 3D remains poorly understood.

1.5. Nanoparticle drug delivery systems

1.5.1. Enhanced permeability and retention effect

Nanoparticulated anti-cancer drug was first shown to increase drug utility *in vivo*, compared to the free form (211,212). Specifically, an anti-cancer protein neocarzinostatin was chemically

conjugated to polystyrene/polymaleic acid copolymers at alanine and lysine residues. Nanoparticular neocarzinostatin showed a 10-fold increase life-span in blood with 25% of toxicity compared to neocarzinostatin. Moreover, it doubled the lifespan of animals bearing an ascitic tumor compared to neocarzinostatin. The mechanism of how nanoparticular compounds improved therapeutic efficacy was further studied by the same group in 1986 (213). Specifically, proteins with different molecular weights were injected into tumor-bearing mice to monitor their clearance rate over time. It was found that large proteins (molecular weight greater than 69 kDa) were 10-fold more retained in the bloodstream compared to small proteins 60 minutes after injection. Moreover, higher concentrations of large proteins were detected at the tumor site compared to small proteins after 72 hours. These phenomena, referred as enhanced permeability and retention (EPR) effect, was thought to be due to that large proteins cannot leak out from normal capillary vessels (pore size ~6-12 nm) but from sparse vasculature (pore size <200 nm) of a tumor (**Figure 1.7**). This passively induces accumulation of large proteins at the tumor sites.

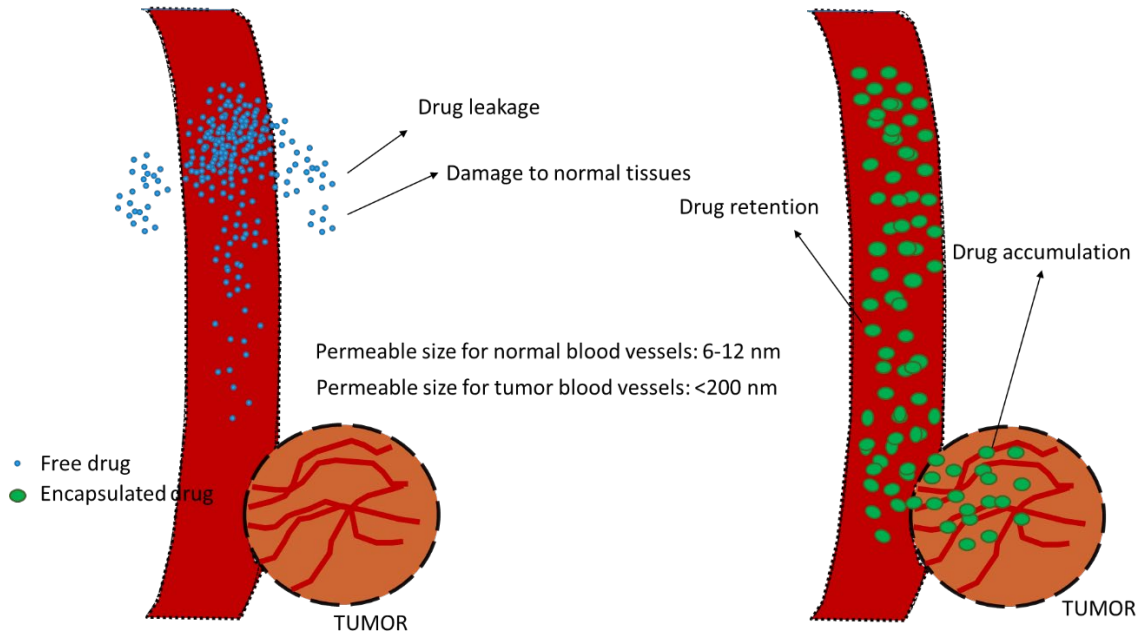

Figure 1.7. EPR effect on encapsulated drug delivery to a tumor. Most free drug (left panel) is small enough to leak out from the normal blood vessels with a permeable size of 6-12 nm. This leakage will cause less drug accumulation to tumor cells and cause damage to normal tissues. Encapsulation of drug in nanoparticles substantially increased the size, making them less permeable to normal blood vessels. As a result, more nanoparticles are able to reach the tumor.

1.5.2 Classification of nanoparticle delivery systems

To achieve EPR effect, many types of nanoparticles have been developed for encapsulation of anti-cancer therapeutics which can be classified as liposomes, polymeric micelles or nanoparticles, dendrimers and inorganic nanoparticles (**Figure 1.8**) (214). Liposomes are formed by a spherical lipid bilayer with an aquatic core at the center. Due to their similarity to the plasma membrane,

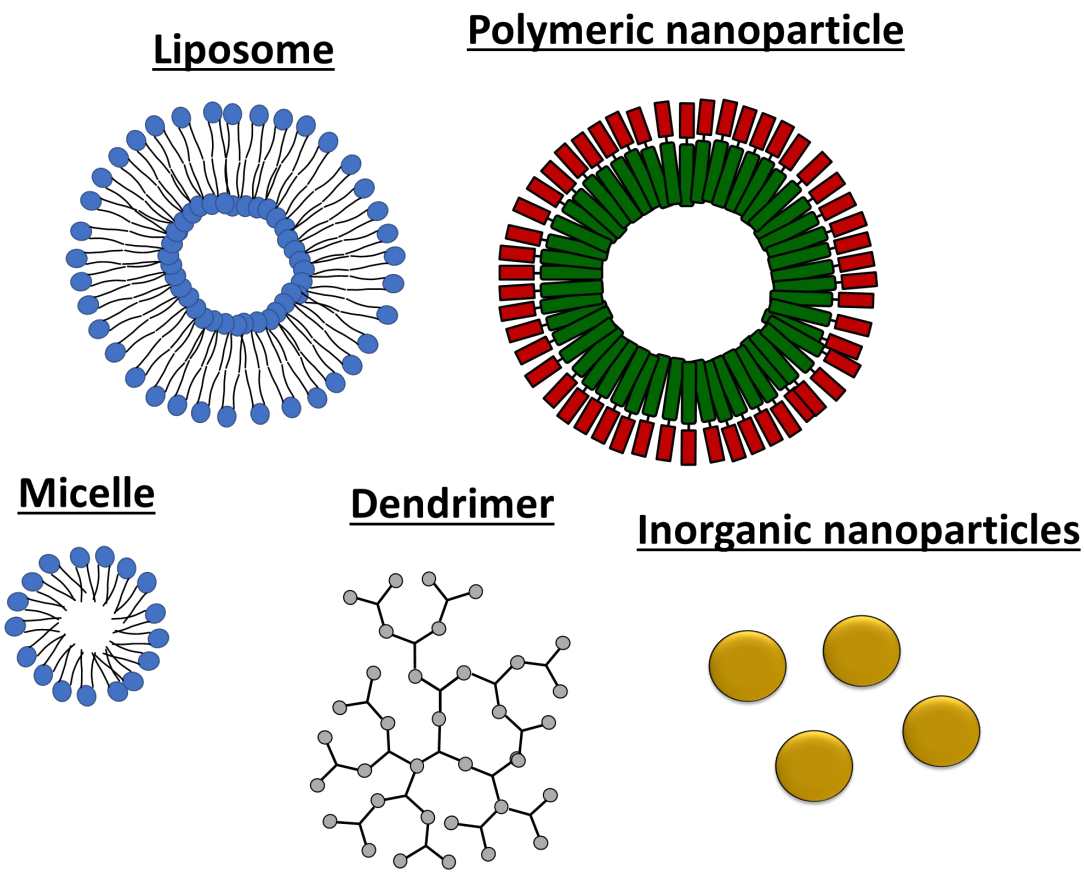

Figure 1.8. Major categories of nanoparticle drug delivery system. Liposomes are composed of a spherical lipid bilayer, creating a hydrophilic core. Micelles are assembly of free lipid acids to create a hydrophobic core. Similarly, polymeric nanoparticles consist of synthetic amphiphilic monomers which assemble into a spherical structure with a hydrophobic core. Dendrimers contain branchy molecules where drug can be carried within the branch network. Inorganic nanoparticles (e.g. gold, mesoporous silica, quantum dots, etc.) are made of inorganic materials and are able to carry drug by surface conjugation.

1.5.3. Antibody-conjugated nanoparticles

While drug-carrying nanoparticles are passively directed to the tumor site, more active targeting to tumor cells intratumorally is required for deeper drug response and lower toxicity to adjacent normal cells. Antibody-conjugated nanoparticles (ACNs) are proposed as a solution for active binding of nanoparticles to tumor cells overexpressing a surface antigen recognized by the conjugated antibody. The common methods used to conjugate antibodies on nanoparticles are 1) adsorption, 2) covalent linkage or 3) adaptor molecules. Adsorption relies on the ionic electrostatic interactions between the nanoparticles and the charged amino acid residues in the antibody. In one study, a ^{125}I radioactive antibody against osteogenic sarcoma cells was incubated with polymeric nanoparticles overnight (215). It was found that 36% of input antibody bound to the nanoparticles after adsorption by gel infiltration. The major drawbacks of adsorption include weak attachment and uncontrolled orientation of antibody attachment. Covalent attachment of antibodies can be achieved if a carboxyl, amine or carbonyl group is present on the nanoparticles with the aid of compounds such as EDC, NHS and maleimide (216,217). Alternatively, adapter molecules such as streptavidin and biotin can be used to modify nanoparticles and antibodies to facilitate their interaction (218).

The most common targeted antigen by ACNs is Human epidermal growth factor receptor 2 (HER2/EGFR), which is overexpressed in multiple solid cancers (219). Different nanoparticles conjugated with either commercial or purified HER-2/EGFR antibodies were used to encapsulate conventional chemotherapeutics such as paclitaxel, doxorubicin, tamoxifen and gemcitabine (220–227). These HER2 ACNs showed a significantly increased cell uptake in HER2-positive cells, which further led to significantly more cytotoxicity in HER2-positive cells and regression of HER2-positive tumors. For example, chitosan nanoparticle conjugated with a commercial HER2 antibody (Herceptin®) resulted in 5 times more cell uptake by HER2-positive SK-BR-3 cells compared to HER-2 negative MCF-7 cells after 24 hours (226). This led to significantly increased HER2-positive cell death from 70% to 90% *in vitro* and regression of HER-2 positive tumor volume by 50% *in vivo* compared to non-conjugated nanoparticles. Antibodies against other cancer cell-specific antigens such as p-glycoprotein, TRAIL receptor, Hsp70, mesothelin annexin A2, disialogangioside and VEGFR have also been reported for active nanoparticle delivery (228–235). Relatively few studies tested the efficacy of ACNs in a hematological cancer model. Our group reported that anti-CD30 conjugation on Doxil® (commercial doxorubicin-carrying liposomes) significantly increased the cell uptake from 5.3% to 27.0% in an anaplastic large-cell lymphoma cell line, SupM2, within 30 minutes (236). Moreover, conjugated Doxil® significantly reduced the IC_{50} of doxorubicin in SupM2 cells from ~30 to ~10 μg/ml. Conjugated Doxil® also resulted in a significantly smaller anaplastic large-cell lymphoma tumor volume (~100 mm^2) compared to non-conjugated Doxil® (~250 mm^2) 9 days after drug administration.

1.5.4. Nanoparticle delivery systems for MM

To improve the efficacy and biocompatibility of common anti-MM therapeutics, several nanoparticular formulations have been proposed. One group reported that bortezomib-loaded liposomes led to similar tumor inhibition effect with less loss of body weight (<10%) compared to free bortezomib (20%) on day 7 *in vivo*, suggesting their overall lower systematic toxicity (237). Another study used bortezomib-carrying chitosan nanoparticles to enhance ~40% more cytotoxicity to MM cells and ~50% more tumor suppression ability against MM tumor compared to bortezomib (238). In this study, the authors also conjugated CD38 antibody on the surface of the chitosan nanoparticles. Conjugated nanoparticles showed 2 to 3-fold more cell uptake by MM cells *in vitro* and 50% reduction of MM tumor progression compared to plain nanoparticles *in vivo*. A water-soluble chitosan-melphalan polymer formulation was proposed for specific drug delivery to MM cells to improve the water solubility and tumor specificity of melphalan (239). Specifically, it was found that melphalan was cleaved off from chitosan by cathepsin X, a cysteine protease which is highly expressed in many cancers. Encapsulation of carfilzomib in polymeric micelles resulted in comparable cytotoxicity compared to free carfilzomib in RPMI8226 cells (240). Moreover, another study found that co-encapsulation of carfilzomib and doxorubicin in liposomes resulted in twice more reduction of MM tumor volume compared to the combined free carfilzomib and free doxorubicin treatment (241). Besides therapeutic compounds, nanoparticles have been developed for oligonucleotide delivery as a MM therapy. In one study, chitosan/PLGA nanoparticles encapsulating miR34a was shown to induce 35-50% viability reduction in two MM cell lines (242). Compared to nanoparticles with scrambled miRNA, miR34a nanoparticles resulted in 50% reduction in tumor volume *in vivo* 19 days after treatment.

1.6. Thesis overview

1.6.1. Rationale

MM remains an incurable disease largely attributed to its high relapse rate. It is known that drug-resistant MM cells which survive after treatment of anti-MM regimens eventually expand and develop into relapsed and refractory MM. STAT3 plays an important role in resistance of multiple anti-MM agents including bortezomib, lenalidomide and dexamethasone (156–158). STAT3 is reported to be active in more than 50% of MM patients, and the high pSTAT3 level is associated with poor prognosis of MM patients (5,149,150). However, most MM cell lines grown in conventional cell culture are STAT3-inactive (243). It is known that STAT3 activation in MM cells is mostly achieved by exogenous stimulations from both soluble ligands or adhesion to BMSCs or ECM proteins as discussed in section **1.2.8.** Therefore, a cell culture system which preserves these exogenous stimulations is required to better understand the role of STAT3 in MM cells. Several 3D culture models for MM which contain some of the components in the bone marrow microenvironment have been proposed (section **1.4.3.**). Compared to other 3D culture models, which required expensive equipment (bioreactor and microfluidic device), complicated preparation procedures (3D tissue-engineered bone marrow) or animals (SCID-synth-hu), Kirshner's Matrigel®-based 3D culture model is relative cost- and effort-effective. Kirshner's 3D culture was shown to support the proliferation of PMM cells for up to 30 days (203). However, the biochemical and biological effects of this 3D culture model on both MM cell lines and PMM cells compared to conventional culture has not been investigated.

Although it has been shown that STAT3 inhibitors exhibited excellent anti-MM activity in pre-clinical studies, very few of them entered into clinical trials and none of them has been approved as a therapy for MM. This can be due to two reasons: first, most STAT3 inhibitors are hydrophobic

and cannot be effectively delivered in the blood circulation. Second, the severe adverse side effects such as nausea, vomiting and diarrhea in the clinical trial. These side effects can be due to the off-target toxicity of STAT3 inhibitors in normal cells, which greatly reduce their efficacy against tumor cells. Lavasanifar Lab has published a nanoparticle formulation as a solution for improved delivery of a STAT3 inhibitor, S3I-1757 (244). Nanoparticular S3I-1757 exhibited improved survival and tumor size suppression *in vivo* in melanoma-bearing mice compared to free S3I-1757. Because MM cells reside in the bone marrow environment with various normal hematopoietic cells and stromal cells, active targeting of nanoparticles specifically against MM cells is needed. Because CD38 is an antigen which is often overexpressed on the surface of MM cells, conjugation of anti-CD38 on the surface of nanoparticular S3I-1757 is expected to further improve the *in vitro* and *in vivo* efficacy.

1.6.2. Hypothesis

Based on the above rationale, I hypothesize that **STAT3 activity in MM cells is more pronounced in close-to-*in vivo* tumor microenvironment, hence improvement of STAT3 inhibitor by nanoparticle conjugation and anti-CD38 conjugation is a valid therapy for MM.**

1.6.3. Objectives

In **Chapter 2**, my primary objective is to investigate the biochemical and biological changes of MM cells in Kirshner's 3D culture compared to conventional cell culture. Biologically, I will examine the morphology and growth rate of MM cells in both culture systems. Biochemically, I will examine the activity of STAT3 and possibly other signaling pathways in 3D versus conventional culture. The importance of STAT3 activity in 3D and conventional culture will be

determined by the responsiveness of MM cells to STAT3 inhibition. The effect of STAT3 on drug resistance in MM cells cultured in both systems will be compared by combined treatment of STAT3 inhibitor and bortezomib. An oligonucleotide array will be conducted to compare the expression profile of cancer-related genes in both culture systems.

In **Chapter 3**, I will further study the impact of 3D culture environment on PMM cells from patients. Isolated BMMC will be cultured in either 3D or conventional culture. The cell viability and STAT3 activity of PMM cells will be monitored over time. To understand the effect of STAT3 activity on PMM cells, IL6 will be added to both culture systems to examine any effect on PMM cell growth. Lastly, STAT3 inhibitor treatment will further confirm of the importance of STAT3 on PMM cell growth in both culture systems.

In **Chapter 4**, my primary goal is to improve nanoparticular S3I-1757 (Null-S3I-NP) by anti-CD38 conjugation. The physical properties such as size, uniformity, S3I-1757 encapsulation efficiency and S3I-1757 release rate of anti-CD38 conjugated nanoparticles (CD38-S3I-NP) will be measured and compared with Null-S3I-NP. The MM cell-targeting ability of CD38-S3I-NP will be measured by cell uptake in MM cells and compared with Null-S3I-NP. Finally, *in vitro* cytotoxicity and *in vivo* tumor suppression ability of CD38-S3I-NP and Null-S3I-NP will be compared.

1.7. References

1. Palumbo A, Anderson K. Multiple Myeloma. N Engl J Med. 2011;364(11):1046–60.

2. Canadian Cancer Society. Canadian Cancer Statistics 2017. Can Cancer Soc. 2017;2017:1–

132.

3. Durie BGM, Salmon SE. A clinical staging system for multiple myeloma correlation of measured myeloma cell mass with presenting clinical features, response to treatment, and survival. Cancer. 1975;36(3):842–54.

4. Moreau P, Attal M, Facon T. Frontline therapy of multiple myeloma. Vol. 125, Blood. American Society of Hematology; 2015. p. 3076–84.

5. Bharti AC, Shishodia S, Reuben JM, Weber D, Alexanian R, Raj-Vadhan S, et al. Nuclear factor–κB and STAT3 are constitutively active in CD138 + cells derived from multiple myeloma patients, and suppression of these transcription factors leads to apoptosis. Blood. 2004;103(8):3175–84.

6. Kraskouskaya D, Duodu E, Arpin CC, Gunning PT, Sadowski I, Stone JC, et al. Progress towards the development of SH2 domain inhibitors. Chem Soc Rev. 2013;42(8):3337.

7. M. Cardoso M, N. Peca I, C. A. Roque A. Antibody-Conjugated Nanoparticles for Therapeutic Applications. Curr Med Chem. 2012;19(19):3103–27.

8. Terstappen LW, Johnsen S, Segers-Nolten IM, Loken MR. Identification and characterization of plasma cells in normal human bone marrow by high-resolution flow cytometry. Blood. 1990;76(9):1739–47.

9. Sanjuan Nandin I, Fong C, Deantonio C, Torreno-Pina JA, Pecetta S, Maldonado P, et al. Novel in vitro booster vaccination to rapidly generate antigen-specific human monoclonal antibodies. J Exp Med. 2017;214(8):2471–90.

10. Nera KP, Kohonen P, Narvi E, Peippo A, Mustonen L, Terho P, et al. Loss of Pax5 promotes

plasma cell differentiation. Immunity. 2006;24(3):283–93.

11. Edwards JCW, Cambridge G. B-cell targeting in rheumatoid arthritis and other autoimmune diseases. Vol. 6, Nature Reviews Immunology. Nature Publishing Group; 2006. p. 394–403.

12. Amanna IJ, Slifka MK. Mechanisms that determine plasma cell lifespan and the duration of humoral immunity. Vol. 236, Immunological Reviews. Wiley/Blackwell (10.1111); 2010. p. 125–38.

13. Becker N. Epidemiology of multiple myeloma. In: Moehler T, Goldschmidt H, editors. Recent Results in Cancer Research. New York: Springer; 2011. p. 25–35.

14. Kumar SK, Rajkumar SV, Dispenzieri A, Lacy MQ, Hayman SR, Buadi FK, et al. Improved survival in multiple myeloma and the impact of novel therapies. Blood. 2008;111(5):2516–20.

15. Gastinne T, Leleu X, Duhamel A, Moreau AS, Franck G, Andrieux J, et al. Plasma cell growth fraction using Ki-67 antigen expression identifies a subgroup of multiple myeloma patients displaying short survival within the ISS stage I. Eur J Haematol. 2007;79(4):297–304.

16. Gerecke C, Fuhrmann S, Strifler S, Schmidt-Hieber M, Einsele H, Knop S. The diagnosis and treatment of multiple myeloma. Dtsch Arztebl Int. 2016;113(27–28):470–6.

17. Kumar S, Kimlinger T, Morice W. Immunophenotyping in multiple myeloma and related plasma cell disorders. Vol. 23, Best Practice and Research: Clinical Haematology. Elsevier; 2010. p. 433–51.

18. Alberta Health System. Clinical Practice Guideline Multiple Myeloma. 2015;

19. Kyle RA, Therneau TM, Rajkumar SV, Offord JR, Larson DR, Plevak MF, et al. A Long-Term Study of Prognosis in Monoclonal Gammopathy of Undetermined Significance. N Engl J Med. 2002;346(8):564–9.

20. Sonneveld P, Broijl A. Treatment of relapsed and refractory multiple myeloma. Vol. 101, Haematologica. Haematologica; 2016. p. 396–406.

21. Greipp PR, Miguel JS, Dune BGM, Crowley JJ, Barlogie B, Bladé J, et al. International staging system for multiple myeloma. J Clin Oncol. 2005;23(15):3412–20.

22. Tandon N, Rajkumar S V, LaPlant B, Pettinger A, Lacy MQ, Dispenzieri A, et al. Clinical utility of the revised international staging system in unselected patients with newly diagnosed and relapsed multiple myeloma. Blood Cancer J. 2017;7(2):e528–e528.

23. Rosiñol L, Oriol A, Teruel AI, Hernández D, López-Jiménez J, de la Rubia J, et al. Superiority of bortezomib, thalidomide, and dexamethasone (VTD) as induction pretransplantation therapy in multiple myeloma: a randomized phase 3 PETHEMA/GEM study. Blood. 2012;120(8):1589–96.

24. Moreau P, Avet-Loiseau H, Facon T, Attal M, Tiab M, Hulin C, et al. Bortezomib plus dexamethasone versus reduced-dose bortezomib, thalidomide plus dexamethasone as induction treatment before autologous stem cell transplantation in newly diagnosed multiple myeloma. Blood. 2011;118(22):5752–8.

25. Cavo M, Tacchetti P, Patriarca F, Petrucci MT, Pantani L, Galli M, et al. Bortezomib with thalidomide plus dexamethasone compared with thalidomide plus dexamethasone as

induction therapy before, and consolidation therapy after, double autologous stem-cell transplantation in newly diagnosed multiple myeloma: a randomised phase 3. Lancet. 2010;376(9758):2075–85.

26. Harousseau J-L, Attal M, Avet-Loiseau H, Marit G, Caillot D, Mohty M, et al. Bortezomib plus dexamethasone is superior to vincristine plus doxorubicin plus dexamethasone as induction treatment prior to autologous stem-cell transplantation in newly diagnosed multiple myeloma: results of the IFM 2005-01 phase III trial. J Clin Oncol. 2010;28(30):4621–9.

27. Sonneveld P, Schmidt-Wolf IGH, Van Der Holt B, El Jarari L, Bertsch U, Salwender H, et al. Bortezomib induction and maintenance treatment in patients with newly diagnosed multiple myeloma: Results of the randomized phase III HOVON-65/ GMMG-HD4 trial. J Clin Oncol. 2012;30(24):2946–55.

28. Moreau P, Facon T, Attal M, Hulin C, Michallet M, Maloisel F, et al. Comparison of 200 mg/m2 melphalan and 8 Gy total body irradiation plus 140 mg/m2 melphalan as conditioning regimens for peripheral blood stem cell transplantation in patients with newly diagnosed multiple myeloma: Final analysis of the Intergroupe Francop. Blood. 2002;99(3):731–5.

29. Leleu X, Fouquet G, Hebraud B, Roussel M, Caillot D, Chrétien ML, et al. Consolidation with VTd significantly improves the complete remission rate and time to progression following VTd induction and single autologous stem cell transplantation in multiple myeloma. Vol. 27, Leukemia. 2013. p. 2242–67.

30. Khan ML, Reeder CB, Kumar SK, Lacy MQ, Reece DE, Dispenzieri A, et al. A comparison

of lenalidomide/dexamethasone versus cyclophosphamide/lenalidomide/dexamethasone versus cyclophosphamide/bortezomib/dexamethasone in newly diagnosed multiple myeloma. Br J Haematol. 2012;156(3):326–33.

31. Nijhof IS, Groen RWJ, Noort WA, Van Kessel B, De Jong-Korlaar R, Bakker J, et al. Preclinical evidence for the therapeutic potential of CD38-Targeted Immuno-chemotherapy in multiple Myeloma patients refractory to Lenalidomide and Bortezomib. Clin Cancer Res. 2015;21(12):2802–10.

32. Fonseca R, Debes-Marun CS, Picken EB, Dewald GW, Bryant SC, Winkler JM, et al. The recurrent IgH translocations are highly associated with nonhyperdiploid variant multiple myeloma. Blood. 2003;102(7):2562–7.

33. Leif Bergsagel P, Michael Kuehl W. Chromosome translocations in multiple myeloma. Vol. 20, Oncogene. Nature Publishing Group; 2001. p. 5611–22.

34. Neben K, Jauch A, Bertsch U, Heiss C, Hielscher T, Seckinger A, et al. Combining information regarding chromosomal aberrations t(4;14) and del(17p13) with the International Staging System classification allows stratification of myeloma patients undergoing autologous stem cell transplantation. Haematologica. 2010;95(7):1150–7.

35. Avet-Loiseau H, Attal M, Moreau P, Charbonnel C, Garban F, Hulin C, et al. Genetic abnormalities and survival in multiple myeloma: The experience of the Intergroupe Francophone du Myélome. Blood. 2007;109(8):3489–95.

36. Chiecchio L, Protheroe RKM, Ibrahim AH, Cheung KL, Rudduck C, Dagrada GP, et al. Deletion of chromosome 13 detected by conventional cytogenetics is a critical prognostic

factor in myeloma. Leukemia. 2006;20(9):1610–7.

37. Zhan F, Colla S, Wu X, Chen B, Stewart JP, Kuehl WM, et al. CKS1B, overexpressed in aggressive disease, regulates multiple myeloma growth and survival through SKP2- and p27Kip1-dependent and -independent mechanisms. Blood. 2007;109(11):4995–5001.

38. Shaughnessy JD, Qu P, Usmani S, Heuck CJ, Zhang Q, Zhou Y, et al. Pharmacogenomics of bortezomib test-dosing identifies hyperexpression of proteasome genes, especially PSMD4, as novel high-risk feature in myeloma treated with total therapy 3. Blood. 2011;118(13):3512–24.

39. Smadja N-V, Fruchart C, Isnard F, Louvet C, Dutel J-L, Cheron N, et al. Chromosomal analysis in multiple myeloma: cytogenetic evidence of two different diseases. Leukemia. 1998;12(6):960–9.

40. Magrangeas F, Lode L, Wuilleme S et al. Genetic heterogeneity in multiple myeloma. Leuk Off J Leuk Soc Am Leuk Res Fund, UK. 2005;19(2):191–4.

41. Cremer FW, Bila J, Buck I, Kartal M, Hose D, Ittrich C, et al. Delineation of distinct subgroups of multiple myeloma and a model for clonal evolution based on interphase cytogenetics. Genes Chromosom Cancer. 2005;44(2):194–203.

42. Hanamura I, Stewart JP, Huang Y, Zhan F, Santra M, Sawyer JR, et al. Frequent gain of chromosome band 1q21 in plasma-cell dyscrasias detected by fluorescence in situ hybridization: Incidence increases from MGUS to relapsed myeloma and is related to prognosis and disease progression following tandem stem-cell transplantatio. Blood. 2006;108(5):1724–32.

43. Klein U, Jauch A, Hielscher T, Hillengass J, Raab MS, Seckinger A, et al. Chromosomal aberrations +1q21 and del(17p13) predict survival in patients with recurrent multiple myeloma treated with lenalidomide and dexamethasone. Cancer. 2011;117(10):2136–44.

44. Quinn J, Glassford J, Percy L, Munson P, Marafioti T, Rodriguez-Justo M, et al. APRIL promotes cell-cycle progression in primary multiple myeloma cells: Influence of D-type cyclin group and translocation status. Blood. 2011;117(3):890–901.

45. Van Damme J. Identification of the human 26-kD protein, interferon beta 2 (IFN-beta 2), as a B cell hybridoma/plasmacytoma growth factor induced by interleukin 1 and tumor necrosis factor. J Exp Med. 1987;165(3):914–9.

46. Kishimoto T. Factors affecting B-cell growth and differentiation. Annu Rev Immunol. 1985;3(3):133–57.

47. Anderson KC, Jones RM, Morimoto C, Leavitt P, Barut BA. Response patterns of purified myeloma cells to hematopoietic growth factors. Blood. 1989;73(7):1915–24.

48. Levy JB, Schindler C, Raz R, Levy DE, Baron R, Horowitz MC. Activation of the JAK-STAT signal transduction pathway by oncostatin-M in cultured human and mouse osteoblastic cells. Endocrinology. 1996;137(4):1159–65.

49. Akira S, Nlshio Y, Lnoue M, Wang X-JJ, We&t S, Matsusaka TT, et al. Molecular cloning of APRF, a novel IFN-stimulated gene factor 3 p91-related transcription factor involved in the gp130-mediated signaling pathway. Cell. 1994;77(1):63–71.

50. Wegenka UM, Buschmann J, Lütticken C, Heinrich PC, Horn F, Lutticken C, et al. Acute-phase response factor, a nuclear factor binding to acute-phase response elements, is rapidly

activated by interleukin-6 at the posttranslational level. 1993;13(1).

51. Richards CD, Kerr C, Tanaka M, Hara T, Miyajima A, Pennica D, et al. Regulation of tissue inhibitor of metalloproteinase-1 in fibroblasts and acute phase proteins in hepatocytes in vitro by mouse oncostatin M, cardiotrophin-1, and IL-6. J Immunol. 1997;159(5):2431–7.

52. Campbell CL, Jiang Z, Savarese DMF, Savarese TM. Increased expression of the interleukin-11 receptor and evidence of STAT3 activation in prostate carcinoma. Am J Pathol. 2001;158(1):25–32.

53. Lokhorst HM, Lamme T, de Smet M, Klein S, de Weger RA, van Oers R, et al. Primary tumor cells of myeloma patients induce interleukin-6 secretion in long-term bone marrow cultures. Blood. 1994;84(7):2269–77.

54. Thabard W, Barillé S, Collette M, Harousseau JL, Rapp MJ, Bataille R, et al. Myeloma cells release soluble interleukin-6Ralpha in relation to disease progression by two distinct mechanisms: alternative splicing and proteolytic cleavage. Clin Cancer Res. 1999;5(10):2693–7.

55. Kallen KJ. The role of transsignalling via the agonistic soluble IL-6 receptor in human diseases. Vol. 1592, Biochimica et Biophysica Acta - Molecular Cell Research. Elsevier; 2002. p. 323–43.

56. Kamińska J, Koper OM, Dymicka-Piekarska V, Motybel E, Kłoczko J, Ke-Mona H. Angiogenic cytokines: IL-6, sIL-6R, TNF-α, sVCAM-1, and PDGF-AB in multiple myeloma patients depending on the stage of the disease. Edorium J Tumor Biol Edorium J Tumor Bio. 2015;22:11–9.

57. Portier M, Rajzbaum G, Zhang XG, Attal M, Rusalen C, Wijdenes J, et al. In vivo interleukin 6 gene expression in the tumoral environment in multiple myeloma. Eur J Immunol. 1991;21(7):1759–62.

58. Hata H, Xiao H, Petrucci MT, Woodliff J, Chang R, Epstein J. Interleukin-6 gene expression in multiple myeloma: a characteristic of immature tumor cells. Blood. 1993;81(12):3357–64.

59. Schwab G, Siegall CB, Aarden LA, Neckers LM, Nordan RP. Characterization of an interleukin-6-mediated autocrine growth loop in the human multiple myeloma cell line, U266. Blood. 1991;77(3):587–93.

60. B Klein, XG Zhang, M Jourdan, J Content, F Houssiau, L Aarden MP and RB. Paracrine rather than autocrine regulation of myeloma-cells growth and differentiation by interleukine-6. Blood. 1989;73(426):517–26.

61. Krüger-Krasagakes S, Möller A, Kolde G, Lippert U, Weber M, Henz BM. Production of interleukin-6 by human mast cells and basophilic cells. J Invest Dermatol. 1996;106(1):75–9.

62. Uchiyama H, Barut BA, Mohrbacher AF, Chauhan D, Anderson KC. Adhesion of human myeloma-derived cell lines to bone marrow stromal cells stimulates interleukin-6 secretion. Blood. 1993;82(12):3712–20.

63. Costes V, Portier M, Lu ZY, Rossi JF, Bataille R, Klein B. Interleukin-1 in multiple myeloma: Producer cells and their role in the control of IL-6 production. Br J Haematol. 1998;103(4):1152–60.

64. Hallek M, Bergsagel PL, Anderson KC, Taga T, Haleem A, Chen J. Multiple myeloma: increasing evidence for a multistep transformation process. Blood. 1998;91(1):3–21.

65. Tu Y, Gardner A, Lichtenstein A. The phosphatidylinositol 3-kinase/AKT kinase pathway in multiple myeloma plasma cells: roles in cytokine-dependent survival and proliferative responses. Cancer Res. 2000;60(23):6763–70.

66. Rowley M, Van Ness B. Activation of N-ras and K-ras induced by interleukin-6 in a myeloma cell line: Implications for disease progression and therapeutic response. Oncogene. 2002;21(57):8769–75.

67. Kolosenko I, Grandér D, Tamm KP. IL-6 activated JAK/STAT3 pathway and sensitivity to Hsp90 inhibitors in multiple myeloma. Curr Med Chem. 2014;46(8):3042–7.

68. Bataille R, Robillard N, Avet-Loiseau H, Hamusseau JL, Moreau P. CD221 (IGF-1R) is aberrantly expressed in multiple myeloma, in relation to disease severity. Haematologica. 2005;90(5):706–7.

69. Jelinek DF, Witzig TE, Arendt BK. A role for insulin-like growth factor in the regulation of IL-6-responsive human myeloma cell line growth. J Immunol. 1997;159(1):487–96.

70. Ge N-L, Rudikoff S. Insulin-like growth factor I is a growth and survival factor in human multiple myeloma cell lines. Blood. 2000;96(8):2856–61.

71. Ferlin M, Noraz N, Hertogh C, Brochier J, Taylor N, Klein B. Insulin-like growth factor induces the survival and proliferation of myeloma cells through an interleukin-6-independent transduction pathway. Br J Haematol. 2008;111(2):626–34.

72. Datta SR, Dudek H, Tao X, Masters S, Fu H, Gotoh Y, et al. Akt Phosphorylation of BAD

Couples Survival Signals to the Cell-Intrinsic Death Machinery. Cell. 1997;91(2):231–41.

73. Kennedy SG, Kandel ES, Cross TK, Hay N. Akt/Protein kinase B inhibits cell death by preventing the release of cytochrome c from mitochondria. Mol Cell Biol. 1999;19(8):5800–10.

74. Hyun T, Yam A, Pece S, Xie X, Zhang J, Miki T, et al. Loss of PTEN expression leading to high Akt activation in human multiple myelomas. Blood. 2000;96(10):3560–8.

75. Choi Y, Zhang J, Murga C, Yu H, Monia BP, Gutkind JS, et al. PTEN, but not SHIP and SHIP2, suppresses the PI3K/Akt pathway and induces growth inhibition and apoptosis of myeloma cells. Oncogene. 2002;21(34):5289–300.

76. Qiang YW, Kopantzev E, Rudikoff S. Insulinlike growth factor-I signaling in multiple myeloma: Downstream elements, functional correlates, and pathway cross-talk. Blood. 2002;99(11):4138–46.

77. Tai Y-T, Podar K, Catley L, Tseng Y-H, Akiyama M, Shringarpure R, et al. Insulin-like growth factor-1 induces adhesion and migration in human multiple myeloma cells via activation of beta1-integrin and phosphatidylinositol 3'-kinase/AKT signaling. Cancer Res. 2003;63(18):5850–8.

78. Demchenko YN, Kuehl WM. A critical role for the NFkB pathway in multiple myeloma. Oncotarget. 2010;1(1):59–68.

79. Ghosh S, Karin M. Missing pieces in the NF-κB puzzle. Vol. 109, Cell. Cell Press; 2002. p. S81–96.

80. Lemancewicz D, Bolkun L, Jablonska E, Kulczynska A, Bolkun-Skornicka U, Kloczko J,

et al. Evaluation of TNF superfamily molecules in multiple myeloma patients: Correlation with biological and clinical features. Leuk Res. 2013;37(9):1089–93.

81. Moreaux J, Legouffe E, Jourdan E, Quittet P, Rème T, Lugagne C, et al. BAFF and APRIL protect myeloma cells from apoptosis induced by interleukin 6 deprivation and dexamethasone. Blood. 2004;103(8):3148–57.

82. Neri P, Kumar S, Fulciniti MT, Vallet S, Chhetri S, Mukherjee S, et al. Neutralizing B-cell-activating factor antibody improves survival and inhibits osteoclastogenesis in a severe combined immunodeficient human multiple myeloma model. Clin Cancer Res. 2007;13(19):5903–9.

83. Xu J, Ding WF, Shao KK, Wang XD, Wang GH, Li HQ, et al. Transcription of promoter from the human APRIL gene regulated by Sp1 and NF-kB. Neoplasma. 2012;59(3):341–7.

84. Kopan R, Ilagan MXG. The canonical Notch signaling pathway: unfolding the activation mechanism. Vol. 137, Cell. Cell Press; 2009. p. 216–33.

85. Lai EC. Notch signaling: control of cell communication and cell fate. Development. 2004;131(5):965–73.

86. van Stralen E, van de Wetering M, Agnelli L, Neri A, Clevers HC, Bast BJEG. Identification of primary MAFB target genes in multiple myeloma. Exp Hematol. 2009;37(1):78–86.

87. Mirandola L, Apicella L, Colombo M, Yu Y, Berta DG, Platonova N, et al. Anti-Notch treatment prevents multiple myeloma cells localization to the bone marrow via the chemokine system CXCR4/SDF-1. Leukemia. 2013;27(7):1558–66.

88. Nefedova Y, Sullivan DM, Bolick SC, Dalton WS, Gabrilovich DI. Inhibition of notch

signaling induces apoptosis of myeloma cells and enhances sensitivity to chemotherapy. Blood. 2008;111(4):2220–9.

89. Bianchi G, Munshi N. Pathogenesis beyond the cancer clone (s) in multiple myeloma. Blood. 2015;125(20):3049–59.

90. Krebsbach PH, Kuznetsov SA, Bianco P, Gehron Robey P. Bone Marrow Stromal Cells: Characterization and Clinical Application. Crit Rev Oral Biol Med. 1999;10(2):165–81.

91. Hideshima T, Chauhan D, Schlossman R, Richardson P, Anderson KC. The role of tumor necrosis factor alpha in the pathophysiology of human multiple myeloma: therapeutic applications. Oncogene. 2001;20(33):4519–27.

92. Nefedova Y, Cheng P, Alsina M, Dalton WS, Gabrilovich DI. Involvement of Notch-1 signaling in bone marrow stroma-mediated de novo drug resistance of myeloma and other malignant lymphoid cell lines. Blood. 2004;103(9):3503–10.

93. Reagan MR, Ghobrial IM. Multiple myeloma mesenchymal stem cells: Characterization, origin, and tumor-promoting effects. Vol. 18, Clinical Cancer Research. 2012. p. 342–9.

94. Taube T, Beneton MNC, McCloskey E V., Rogers S, Greaves M, Kanis JA. Abnormal bone remodelling in patients with myelomatosis and normal biochemical indices of bone resorption. Eur J Haematol. 1992;49(4):192–8.

95. Sims NA, Martin TJ. Coupling the activities of bone formation and resorption: a multitude of signals within the basic multicellular unit. Bonekey Rep. 2014;3.

96. Giuliani N, Bataille R, Mancini C, Lazzaretti M, Barillé S. Myeloma cells induce imbalance in the osteoprotegerin/osteoprotegerin ligand system in the human bone marrow

environment. Blood. 2001;98(13):3527–33.

97. Sezer O, Heider U, Jakob C, Eucker J, Possinger K. Human bone marrow myeloma cells express RANKL. J Clin Oncol. 2002;20(1):353–4.

98. Abe M, Hiura K, Wilde J, Shioyasono A, Moriyama K, Hashimoto T, et al. Osteoclasts enhance myeloma cell growth and survival via cell-cell contact: A vicious cycle between bone destruction and myeloma expansion. Blood. 2004;104(8):2484–91.

99. Yaccoby S, Ling W, Zhan F, Walker R, Barlogie B, Shaughnessy JD. Antibody-based inhibition of DKK1 suppresses tumor-induced bone resorption and multiple myeloma growth in vivo. Blood. 2007;109(5):2106–11.

100. Giuliani N, Colla S, Morandi F, Lazzaretti M, Sala R, Bonomini S, et al. Myeloma cells block RUNX2/CBFA1 activity in human bone marrow osteoblast progenitors and inhibit osteoblast formation and differentiation. Blood. 2005;106(7):2472–83.

101. Stewart AK. Reduced-intensity allogeneic transplantation for myeloma: Reality bites. Vol. 113, Blood. American Society of Hematology; 2009. p. 3135–6.

102. Chalmin F, Mignot G, Bruchard M, Chevriaux A, Végran F, Hichami A, et al. Stat3 and Gfi-1 Transcription Factors Control Th17 Cell Immunosuppressive Activity via the Regulation of Ectonucleotidase Expression. Immunity. 2012;36(3):362–73.

103. Braga WMT, da Silva BR, de Carvalho AC, Maekawa YH, Bortoluzzo AB, Rizzatti EG, et al. FOXP3 and CTLA4 overexpression in multiple myeloma bone marrow as a sign of accumulation of CD4+ T regulatory cells. Cancer Immunol Immunother. 2014;63(11):1189–97.

104. Görgün G, Samur MK, Cowens KB, Paula S, Bianchi G, Anderson JE, et al. Lenalidomide enhances immune checkpoint blockade-induced immune response in multiple myeloma. Clin Cancer Res. 2015;21(20):4617–8.

105. Costello RT, Boehrer A, Sanchez C, Mercier D, Baier C, Le Treut T, et al. Differential expression of natural killer cell activating receptors in blood versus bone marrow in patients with monoclonal gammopathy. Immunology. 2013;139(3):338–41.

106. Slany A, Haudek-Prinz V, Meshcheryakova A, Bileck A, Lamm W, Zielinski C, et al. Extracellular matrix remodeling by bone marrow fibroblast-like cells correlates with disease progression in multiple myeloma. J Proteome Res. 2014;13(2):844–54.

107. Vincent T, Mechti N. Extracellular matrix in bone marrow can mediate drug resistance in myeloma. Vol. 46, Leukemia and Lymphoma. 2005. p. 803–11.

108. Shain KH, Yarde DN, Meads MB, Huang M, Jove R, Hazlehurst LA, et al. Beta-1 integrin adhesion enhances IL-6-mediated STAT3 signaling in myeloma cells: implications for microenvironment influence on tumor survival and proliferation. Cancer Res. 2009;69(3):1009–15.

109. Vincent T, Molina L, Espert L, Mechti N. Hyaluronan, a major non-protein glycosaminoglycan component of the extracellular matrix in human bone marrow, mediates dexamethasone resistance in multiple myeloma. Br J Haematol. 2003;121(2):259–69.

110. Fu X-Y, Schindler C, Improta T, Aebersoldt R, Darnell JE. The proteins of ISGF-3, the interferon a-induced transcriptional activator, define a gene family involved in signal transduction. Biochemistry. 1992;89(16):7840–3.

111. Schindler CC, Fu XYXY, Improta TT, Aebersold RR, Darnell JEJE. Proteins of transcription factor ISGF-3: one gene encodes the 91-and 84-kDa ISGF-3 proteins that are activated by interferon alpha. Proc Natl Acad Sci. 1992;89(16):7836–9.

112. Schindler C, Shuai K, Prezioso VR, Darnell JE. Interferon-dependent tyrosine phosphorylation of a latent cytoplasmic transcription factor. Science (80-). 1992;257(5071):809–13.

113. Zhong Z, Wen Z, Darnell Jr. JE. Stat3 and Stat4: members of the family of signal transducers and activators of transcription. Proc Natl Acad Sci U S A. 1994;91(11):4806–10.

114. Zhong Z, Wen Z, Darnell J. Stat3: a STAT family member activated by tyrosine phosphorylation in response to epidermal growth factor and interleukin-6. Science (80-). 1994;264(5155):95–8.

115. Thyrell L, Arulampalam V, Hjortsberg L, Farnebo M, Grandér D, Pokrovskaja Tamm K. Interferon alpha induces cell death through interference with interleukin 6 signaling and inhibition of STAT3 activity. Exp Cell Res. 2007;313(19):4015–24.

116. Rani A, Murphy JJ. STAT5 in Cancer and Immunity. J Interf Cytokine Res. 2016;36(4):226–37.

117. Levy DE, Lee C, Darnell J, Kerr I, Stark G, Levy D, et al. What does Stat3 do? J Clin Invest. 2002;109(9):1143–8.

118. Della Pietra L, Bressan A, Pezzotti AR, Serlupi-Crescenzi O. Highly conserved amino-acid sequence between murine STAT3 and a revised human STAT3 sequence. Gene.

1998;213(1–2):119–24.

119. Vogt M, Domoszlai T, Kleshchanok D, Lehmann S, Schmitt A, Poli V, et al. The role of the N-terminal domain in dimerization and nucleocytoplasmic shuttling of latent STAT3. J Cell Sci. 2011;124(6):900–9.

120. Liu L, McBride KM, Reich NC. STAT3 nuclear import is independent of tyrosine phosphorylation and mediated by importin- 3. Proc Natl Acad Sci. 2005;102(23):8150–5.

121. Huang Y, Qiu J, Dong S, Redell MS, Poli V, Mancini MA, et al. Stat3 isoforms, alpha and beta, demonstrate distinct intracellular dynamics with prolonged nuclear retention of Stat3beta mapping to its unique C-terminal end. J Biol Chem. 2007;282(48):34958–67.

122. Schaefer TS, Sanders LK, Park OK, Nathans D. Functional Differences between Stat3 and Stat3 . 1997;17(9):5307–16.

123. Zhang H-F, Chen Y, Wu C, Wu Z-Y, Tweardy DJ, Alshareef A, et al. The Opposing Function of STAT3 as an Oncoprotein and Tumor Suppressor Is Dictated by the Expression Status of STAT3b in Esophageal Squamous Cell Carcinoma. Clin Cancer Res. 22(3):691–703.

124. Zammarchi F, de Stanchina E, Bournazou E, Supakorndej T, Martires K, Riedel E, et al. Antitumorigenic potential of STAT3 alternative splicing modulation. Proc Natl Acad Sci. 2011;108(43):17779–84.

125. Sun W, Snyder M, Levy DE, Zhang JJ. Regulation of Stat3 transcriptional activity by the conserved LPMSP motif for OSM and IL-6 signaling. FEBS Lett. 2006;580(25):5880–4.

126. Song L, Turkson J, Karras JG, Jove R, Haura EB. Activation of Stat3 by receptor tyrosine kinases and cytokines regulates survival in human non-small cell carcinoma cells. Oncogene. 2003;22(27):4150–65.

127. Zong CS, Chan J, Levy DE, Horvath C, Sadowski HB, Wang LH. Mechanism of STAT3 activation by insulin-like growth factor I receptor. J Biol Chem. 2000;275(20):15099–105.

128. HEINRICH PC, BEHRMANN I, MÜLLER-NEWEN G, SCHAPER F, GRAEVE L. Interleukin-6-type cytokine signalling through the gp130/Jak/STAT pathway. Biochem J. 1998;334(2):297–314.

129. Zamo A, Chiarle R, Piva R, Howes J, Fan Y, Chilosi M, et al. Anaplastic lymphoma kinase (ALK) activates Stat3 and protects hematopoietic cells from cell death. Oncogene. 2002;21(7):1038–47.

130. Aggarwal BB, Kunnumakkara AB, Harikumar KB, Gupta SR, Tharakan ST, Koca C, et al. Signal transducer and activator of transcription-3, inflammation, and cancer: How intimate is the relationship? In: Annals of the New York Academy of Sciences. Wiley/Blackwell (10.1111); 2009. p. 59–76.

131. Aziz MH, Manoharan HT, Church DR, Dreckschmidt NE, Zhong W, Oberley TD, et al. Protein kinase Cε interacts with signal transducers and activators of transcription 3 (Stat3), phosphorylates Stat3Ser727, and regulates its constitutive activation in prostate cancer. Cancer Res. 2007;67(18):8828–38.

132. Zhang H-F, Lai R. STAT3 in Cancer—Friend or Foe? Cancers (Basel). 2014;6(3):1408–40.

133. Carpenter RL, Lo HW. STAT3 target genes relevant to human cancers. Vol. 6, Cancers.

Multidisciplinary Digital Publishing Institute (MDPI); 2014. p. 897–925.

134. Wormald S, Hilton DJ. Inhibitors of Cytokine Signal Transduction. Vol. 279, Journal of Biological Chemistry. American Society for Biochemistry and Molecular Biology; 2004. p. 821–4.

135. Takeda K, Noguchi K, Shi W, Tanaka T, Matsumoto M, Yoshida N, et al. Targeted disruption of the mouse Stat3 gene leads to early embryonic lethality. Dev Biol. 1997;94(8):3801–4.

136. Bromberg JF, Wrzeszczynska MH, Devgan G, Zhao Y, Pestell RG, Albanese C, et al. Stat3 as an oncogene. Cell. 1999;98(3):295–303.

137. Azare J, Leslie K, Al-Ahmadie H, Gerald W, Weinreb PH, Violette SM, et al. Constitutively activated Stat3 induces tumorigenesis and enhances cell motility of prostate epithelial cells through integrin beta 6. Mol Cell Biol. 2007;27(12):4444–53.

138. Kaptein A, Paillard V, Saunders M. Dominant negative Stat3 mutant inhibits interleukin-6-induced Jak-STAT signal transduction. J Biol Chem. 1996;271(11):5961–4.

139. Srivastava J, DiGiovanni J. Non-canonical Stat3 signaling in cancer. Mol Carcinog. 2016;55(12):1889–98.

140. Yang J, Liao X, Agarwal MK, Barnes L, Auron PE, Stark GR. Unphosphorylated STAT3 accumulates in response to IL-6 and activates transcription by binding to NF-kB. Genes Dev. 2007;21(11):1396–408.

141. Vander Heiden MG, Cantley LC, Thompson CB, Thompson3 CB. Understanding the Warburg Effect: The Metabolic Requirements of Cell Proliferation The Metabolic

Requirements of Cell Proliferation. Source Sci New Ser. 2009;324(5930):1029–33.

142. Macias E, Rao D, Carbajal S, Kiguchi K, Digiovanni J. Stat3 binds to mtDNA and regulates mitochondrial gene expression in keratinocytes. J Invest Dermatol. 2014;134(7):1971–80.

143. Kodama S, Yamada H, Annab L, Barrett JC. Elevated expression of mitochondrial cytochrome b and NADH dehydrogenase subunit 4/4L genes in senescent human cells. Exp Cell Res. 1995;219(1):82–6.

144. Tammineni P, Anugula C, Mohammed F, Anjaneyulu M, Larner AC, Sepuri NBV. The import of the transcription factor STAT3 into mitochondria depends on GRIM-19, a component of the electron transport chain. J Biol Chem. 2013;288(7):4723–32.

145. Szczepanek K, Chen Q, Larner AC, Lesnefsky EJ. Cytoprotection by the modulation of mitochondrial electron transport chain: The emerging role of mitochondrial STAT3. Mitochondrion. 2012;12(2):180–9.

146. Boengler K, Hilfiker-Kleiner D, Heusch G, Schulz R. Inhibition of permeability transition pore opening by mitochondrial STAT3 and its role in myocardial ischemia/reperfusion. Basic Res Cardiol. 2010;105(6):771–85.

147. Zhang Q, Wang HY, Marzec M, Raghunath PN, Nagasawa T, Wasik MA. STAT3- and DNA methyltransferase 1-mediated epigenetic silencing of SHP-1 tyrosine phosphatase tumor suppressor gene in malignant T lymphocytes. Proc Natl Acad Sci. 2005;102(19):6948–53.

148. Ge F, Zhang L, Tao S-C, Kitazato K, Zhang Z-P, Zhang X-E, et al. Quantitative Proteomic Analysis of Tumor Reversion in Multiple Myeloma Cells. J Proteome Res. 2011;10(2):845–

55.

149. Quintanilla-Martinez L, Kremer M, Specht K, Calzada-Wack J, Nathrath M, Schaich R, et al. Analysis of signal transducer and activator of transcription 3 (Stat 3) pathway in multiple myeloma: Stat 3 activation and cyclin D1 dysregulation are mutually exclusive events. Am J Pathol. 2003;162(5):1449–61.

150. Manni S, Brancalion A, Mandato E, Tubi LQ, Colpo A, Pizzi M, et al. Protein kinase CK2 inhibition down modulates the NF-κB and STAT3 survival pathways, enhances the cellular proteotoxic stress and synergistically boosts the cytotoxic effect of bortezomib on multiple myeloma and mantle cell Lymphoma Cells. Richards KL, editor. PLoS One. 2013;8(9):e75280.

151. Brown R, Yang S, Weatherburn C, Gibson J, Ho PJ, Suen H, et al. Phospho-flow detection of constitutive and cytokine-induced pSTAT3/5, pAKT and pERK expression highlights novel prognostic biomarkers for patients with multiple myeloma. Leukemia. 2015;29(2):483–90.

152. Jung S-H, Ahn S, Choi H-W, Shin M-G, Lee S, Yang D-H, et al. STAT3 expression is associated with poor survival in non-elderly adult patients with newly diagnosed multiple myeloma. Blood Res. 2017;52(4):293.

153. Lin L, Benson DM, Deangelis S, Bakan CE, Li PK, Li C, et al. A small molecule, LLL12 inhibits constitutive STAT3 and IL-6-induced STAT3 signaling and exhibits potent growth suppressive activity in human multiple myeloma cells. Int J Cancer. 2012;130(6):1459–69.

154. Wagner V, Hose D, Seckinger A, Weiz L, Meißner T, Rème T, et al. Preclinical efficacy of

sepantronium bromide (YM155) in multiple myeloma is conferred by down regulation of Mcl-1. Oncotarget. 2014;5(21):10237–50.

155. X X, Han K, Zhu J, Mao H, Lin X, Zhang Z, et al. An inhibitor of cholesterol absorption displays anti-myeloma activity by targeting the JAK2-STAT3 signaling pathway. Oncotarget. 2016;7(46):75539–50.

156. Zhang XD, Baladandayuthapani V, Lin H, Mulligan G, Li B-Z, Esseltine DLW, et al. Tight jnction protein 1 modulates proteasome capacity and proteasome inhibitor sensitivity in multiple myeloma via EGFR/JAK1/STAT3 signaling. Cancer Cell. 2016;29(5):639–52.

157. Liu T, Fei Z, Gangavarapu KJ, Agbenowu S, Bhushan A, Lai JCK, et al. Interleukin-6 and JAK2/STAT3 signaling mediate the reversion of dexamethasone resistance after dexamethasone withdrawal in 7TD1 multiple myeloma cells. Leuk Res. 2013;37(10):1322–8.

158. Wu W, Ma D, Wang P, Cao L, Lu T, Fang Q, et al. Potential crosstalk of the interleukin-6-heme oxygenase-1-dependent mechanism involved in resistance to lenalidomide in multiple myeloma cells. FEBS J. 2016;283(5):834–49.

159. Catlett-Falcone R, Landowski TH, Oshiro MM, Turkson J, Levitzki A, Savino R, et al. Constitutive activation of Stat3 signaling confers resistance to apoptosis in human U266 myeloma cells. Immunity. 1999;10(1):105–15.

160. de Oliveira MB, Fook-Alves VL, Eugenio AIP, Fernando RC, Sanson LFG, de Carvalho MF, et al. Anti-myeloma effects of ruxolitinib combined with bortezomib and lenalidomide: A rationale for JAK/STAT pathway inhibition in myeloma patients. Cancer Lett.

2017;403:206–15.

161. Galm O, Yoshikawa H, Esteller M, Osieka R, Herman JG. SOCS-1, a negative regulator of cytokine signaling, is frequently silenced by methylation in multiple myeloma. Blood. 2003;101(7):2784–8.

162. Beldi-Ferchiou A, Skouri N, Ben Ali C, Safra I, Abdelkefi A, Ladeb S, et al. Abnormal repression of SHP-1, SHP-2 and SOCS-1 transcription sustains the activation of the JAK/STAT3 pathway and the progression of the disease in multiple myeloma. Reddy S V., editor. PLoS One. 2017;12(4):e0174835.

163. Zhou Q, Yao Y, Ericson SG. The Protein Tyrosine Phosphatase CD45 Is Required for Interleukin 6 Signaling in U266 Myeloma Cells. Int J Hematol. 2004;79(1):63–73.

164. Khong T, Spencer A. Targeting HSP 90 Induces Apoptosis and Inhibits Critical Survival and Proliferation Pathways in Multiple Myeloma. Mol Cancer Ther. 2011;10(10):1909–17.

165. Lin H, Kolosenko I, Bj?rklund A-C, Protsyuk D, ?sterborg A, Grand?r D, et al. An activated JAK/STAT3 pathway and CD45 expression are associated with sensitivity to Hsp90 inhibitors in multiple myeloma. Exp Cell Res. 2013;319(5):600–11.

166. Tiedemann RE, Zhu YX, Schmidt J, Yin H, Shi CX, Que Q, et al. Kinome-wide RNAi studies in human multiple myeloma identify vulnerable kinase targets, including a lymphoid-restricted kinase, GRK6. Blood. 2010;115(8):1594–604.

167. Zhang J, Chen F, Li W, Xiong Q, Yang M, Zheng P, et al. 14-3-3ζ interacts with Stat3 and regulates its constitutive activation in multiple myeloma cells. Schneider-Stock R, editor. PLoS One. 2012;7(1):e29554.

168. Lin L, Yan F, Zhao D, Lv M, Liang X, Dai H, et al. Reelin promotes the adhesion and drug resistance of multiple myeloma cells via integrin β1 signaling and STAT3. Oncotarget. 2016;7(9):9844–58.

169. Liang P, Cheng SH, Cheng CK, Lau KM, Lin SY, Chow EYD, et al. Platelet factor 4 induces cell apoptosis by inhibition of STAT3 via up-regulation of SOCS3 expression in multiple myeloma. Haematologica. 2013;98(2):288–95.

170. Wang LH, Yang XY, Zhang X, Huang J, Hou J, Li J, et al. Transcriptional Inactivation of STAT3 by PPARγ Suppresses IL-6-Responsive Multiple Myeloma Cells. Immunity. 2004;20(2):205–18.

171. Wang LH, Yang XY, Mihalic K, Xiao W, Li D, Farrar WL. Activation of Estrogen Receptor Blocks Interleukin-6-inducible Cell Growth of Human Multiple Myeloma Involving Molecular Cross-talk between Estrogen Receptor and STAT3 Mediated by Co-regulator PIAS3. J Biol Chem. 2001;276(34):31839–44.

172. Turkson J, Ryan D, Kim JS, Zhang Y, Chen Z, Haura E, et al. Phosphotyrosyl peptides block Stat3-mediated DNA binding activity, gene regulation, and cell transformation. J Biol Chem. 2001;276(48):45443–55.

173. Turkson J, Kim JS, Zhang S, Yuan J, Huang M, Glenn M, et al. Novel peptidomimetic inhibitors of signal transducer and activator of transcription 3 dimerization and biological activity. Mol Cancer Ther. 2004;3(3):261–9.

174. Song H, Wang R, Wang S, Lin J. A low-molecular-weight compound discovered through virtual database screening inhibits Stat3 function in breast cancer cells. Proc Natl Acad Sci.

2005;102(13):4700–5.

175. Schust J, Sperl B, Hollis A, Mayer TU, Berg T. Stattic: a small-molecule inhibitor of STAT3 activation and dimerization. Chem Biol. 2006;13(11):1235–42.

176. Siddiquee KAZ, Gunning PT, Glen M, Katt WP, Zhang S, Schroeck C, et al. An oxazole-based small-molecule stat3 inhibitor modulates stat3 stability and processing and induces antitumor cell effects. ACS Chem Biol. 2007;2(12):787–98.

177. Siddiquee K, Zhang S, Guida WC, Blaskovich MA, Greedy B, Lawrence HR, et al. Selective chemical probe inhibitor of Stat3, identified through structure-based virtual screening, induces antitumor activity. Proc Natl Acad Sci U S A. 2007;104(18):7391–6.

178. Zhang X, Yue P, Fletcher S, Zhao W, Gunning PT, Turkson J. A novel small-molecule disrupts Stat3 SH2 domain–phosphotyrosine interactions and Stat3-dependent tumor processes. 2010;79(10).

179. Zhang X, Sun Y, Pireddu R, Yang H, Urlam MK, Lawrence HR, et al. A novel inhibitor of STAT3 homodimerization selectively suppresses STAT3 activity and malignant transformation. Cancer Res. 2013;73(6):1922–33.

180. Zhang X, Yue P, Page BDG, Li T, Zhao W, Namanja AT, et al. Orally bioavailable small-molecule inhibitor of transcription factor Stat3 regresses human breast and lung cancer xenografts. Proc Natl Acad Sci U S A. 2012;109(24):9623–8.

181. Kim MJ, Nam HJ, Kim HP, Han SW, Im SA, Kim TY, et al. OPB-31121, a novel small molecular inhibitor, disrupts the JAK2/STAT3 pathway and exhibits an antitumor activity in gastric cancer cells. Cancer Lett. 2013;335(1):154–152.

182. Oh D-Y, Lee S-H, Han S-W, Kim M-J, Kim T-M, Kim T-Y, et al. Phase I Study of OPB-31121, an Oral STAT3 Inhibitor, in Patients with Advanced Solid Tumors. Cancer Res Treat. 2015;47(4):607–15.

183. Nath S, Devi GR. Three-dimensional culture systems in cancer research: Focus on tumor spheroid model. Pharmacol Ther. 2016;163:94–108.

184. Carranza-Torres IE, Guzmán-Delgado NE, Coronado-Martínez C, Bañuelos-García JI, Viveros-Valdez E, Morán-Martínez J, et al. Organotypic culture of breast tumor explants as a multicellular system for the screening of natural compounds with antineoplastic potential. Biomed Res Int. 2015;2015:618021.

185. Menon N V, Chuah YJ, Cao B, Lim M, Kang Y. A microfluidic co-culture system to monitor tumor-stromal interactions on a chip. Biomicrofluidics. 2014;8(6).

186. Fischbach C, Chen R, Matsumoto T, Schmelzle T, Brugge JS, Polverini PJ, et al. Engineering tumors with 3D scaffolds. Nat Methods. 2007;4(10):855–60.

187. Gomez-Roman N, Stevenson K, Gilmour L, Hamilton G, Chalmers AJ. A novel 3D human glioblastoma cell culture system for modeling drug and radiation responses. Neuro Oncol. 2016;17(1):now164.

188. Boghaert ER, Lu X, Hessler PE, McGonigal TP, Oleksijew A, Mitten MJ, et al. The Volume of Three-Dimensional Cultures of Cancer Cells In Vitro Influences Transcriptional Profile Differences and Similarities with Monolayer Cultures and Xenografted Tumors. Neoplasia (United States). 2017;19(9):695–706.

189. Yue X, Lukowski JK, Weaver EM, Skube SB, Hummon AB. Quantitative Proteomic and

Phosphoproteomic Comparison of 2D and 3D Colon Cancer Cell Culture Models. J Proteome Res. 2016;15(12):4265–76.

190. Riedl A, Schlederer M, Pudelko K, Stadler M, Walter S, Unterleuthner D, et al. Comparison of cancer cells in 2D vs 3D culture reveals differences in AKT–mTOR–S6K signaling and drug responses. J Cell Sci. 2017;130(1):203–18.

191. Shan F, Close DA, Camarco DP, Johnston PA. High-Content Screening Comparison of Cancer Drug Accumulation and Distribution in Two-Dimensional and Three-Dimensional Culture Models of Head and Neck Cancer. Assay Drug Dev Technol. 2017;adt.2017.812.

192. Zschenker O, Streichert T, Hehlgans S, Cordes N. Genome-wide gene expression analysis in cancer cells reveals 3D growth to affect ECM and processes associated with cell adhesion but not DNA repair. PLoS One. 2012;7(4).

193. Liu Q, Zhang Z, Liu Y, Cui Z, Zhang T, Li Z, et al. Cancer cells growing on perfused 3D collagen model produced higher reactive oxygen species level and were more resistant to cisplatin compared to the 2D model. J Appl Biomater Funct Mater. 2018;2280800018764763.

194. Yildiz-Ozturk E, Gulce-Iz S, Anil M, Yesil-Celiktas O. Cytotoxic responses of carnosic acid and doxorubicin on breast cancer cells in butterfly-shaped microchips in comparison to 2D and 3D culture. Cytotechnology. 2017;69(2):337–47.

195. Lovitt CJ, Shelper TB, Avery VM. Evaluation of chemotherapeutics in a three-dimensional breast cancer model. J Cancer Res Clin Oncol. 2015;141(5):951–9.

196. Chitcholtan K, Sykes PH, Evans JJ. The resistance of intracellular mediators to doxorubicin

and cisplatin are distinct in 3D and 2D endometrial cancer. J Transl Med. 2012;10(1).

197. Imamura Y, Mukohara T, Shimono Y, Funakoshi Y, Chayahara N, Toyoda M, et al. Comparison of 2D and 3D culture models as drug-testing platforms in breast cancer. Vol. 30, Oncology Reports. [National Hellenic Research Foundation]; 2015. p. 1837–43.

198. Ghosh S, Spagnoli GC, Martin I, Ploegert S, Demougin P, Heberer M, et al. Three-dimensional culture of melanoma cells profoundly affects gene expression profile: A high density oligonucleotide array study. J Cell Physiol. 2005;204(2):522–31.

199. De Witt Hamer PC, Van Tilborg AAG, Eijk PP, Sminia P, Troost D, Van Noorden CJF, et al. The genomic profile of human malignant glioma is altered early in primary cell culture and preserved in spheroids. Oncogene. 2008;27(14):2091–6.

200. Petersen OW, Ronnov-Jessen L, Howlett AR, Bissell MJ. Interaction with basement membrane serves to rapidly distinguish growth and differentiation pattern of normal and malignant human breast epithelial cells. Proc Natl Acad Sci. 1992;89(19):9064–8.

201. Weaver VM, Petersen OW, Wang F, Larabell CA, Briand P, Damsky C, et al. Reversion of the malignant phenotype of human breast cells in three-dimensional culture and in vivo by integrin blocking antibodies. J Cell Biol. 1997;137(1):231–45.

202. Zlei M, Egert S, Wider D, Ihorst G, Wäsch R, Engelhardt M. Characterization of in vitro growth of multiple myeloma cells. Exp Hematol. 2007;35(10):1550–61.

203. Kirshner J, Thulien KJ, Martin LD, Debes Marun C, Reiman T, Belch AR, et al. A unique three-dimensional model for evaluating the impact of therapy on multiple myeloma. Blood. 2008;112(7):2935–45.

204. Parikh MR, Belch AR, Pilarski LM, Kirshner J. A Three-dimensional tissue culture model to study primary human bone marrow and its malignancies. J Vis Exp. 2014;(85):e50947–e50947.

205. Nierste BA, Gunn EJ, Whiteman KR, Lutz RJ, Kirshner J. Maytansinoid immunoconjugate IMGN901 is cytotoxic in a three-dimensional culture model of multiple myeloma. Am J Blood Res. 2016;6(1):6–18.

206. Gunn EJ, Williams JT, Huynh DT, Iannotti MJ, Han C, Barrios FJ, et al. The natural products parthenolide and andrographolide exhibit anti-cancer stem cell activity in multiple myeloma. Leuk Lymphoma. 2011;52(6):1085–97.

207. Calimeri T, Battista E, Conforti F, Neri P, Di Martino MT, Rossi M, et al. A unique three-dimensional SCID-polymeric scaffold (SCID-synth-hu) model for in vivo expansion of human primary multiple myeloma cells. Leukemia. 2011;25(4):707–11.

208. Zhang W, Lee WY, Siegel DS, Tolias P, Zilberberg J. Patient-specific 3D microfluidic tissue model for multiple myeloma. Tissue Eng Part C Methods. 2014;20(8):663–70.

209. Ferrarini M, Steimberg N, Ponzoni M, Belloni D, Berenzi A, Girlanda S, et al. Ex-Vivo dynamic 3-D culture of human tissues in the RCCS^{TM} bioreactor allows the study of multiple myeloma biology and response to therapy. Cheriyath V, editor. PLoS One. 2013;8(8):e71613.

210. de la Puente P, Muz B, Gilson RC, Azab F, Luderer M, King J, et al. 3D tissue-engineered bone marrow as a novel model to study pathophysiology and drug resistance in multiple myeloma. Biomaterials. 2015;73:70–84.

211. Maeda H, Ueda M, Morinaga T, Matsumoto T. Conjugation of Poly(styrene-co-maleic acid) Derivatives to the Antitumor Protein Neocarzinostatin: Pronounced Improvements in Pharmacological Properties. J Med Chem. 1985;28(4):455–61.

212. Maeda H, Takeshita J, Kanamaru R. A Lipophilic Derivative OF Neocarzinostatin a Polymer Conjugation of an Antitumor Protein Antibiotic. Int J Pept Protein Res. 1979;14(2):81–7.

213. Matsumura Y, Maeda H. A new concept for macromolecular therapeutics in cnacer chemotherapy: mechanism of tumoritropic accumulatio of proteins and the antitumor agents Smancs. Cancer Res. 1986;46(12 Pt 1):6387–92.

214. Richards DA, Maruani A, Chudasama V. Antibody fragments as nanoparticle targeting ligands: a step in the right direction. Chem Sci. 2017;8(1):63–77.

215. Illum L, Jones PDE, Kreuter J, Baldwin RW, Davis SS. Adsorption of monoclonal antibodies to polyhexylcyanoacrylate nanoparticles and subsequent immunospecific binding to tumour cells in vitro. Int J Pharm. 1983;17(1):65–76.

216. Akkapeddi P, Azizi S-A, Freedy AM, Cal PMSD, Gois PMP, Bernardes GJL. Construction of homogeneous antibody–drug conjugates using site-selective protein chemistry. Chem Sci. 2016;7(5):2954–63.

217. Jazayeri MH, Amani H, Pourfatollah AA, Pazoki-Toroudi H, Sedighimoghaddam B. Various methods of gold nanoparticles (GNPs) conjugation to antibodies. Vol. 9, Sensing and Bio-Sensing Research. Elsevier; 2016. p. 17–22.

218. Jain A, Cheng K. The principles and applications of avidin-based nanoparticles in drug

delivery and diagnosis. Vol. 245, Journal of Controlled Release. 2017. p. 27–40.

219. Yan M, Schwaederle M, Arguello D, Millis SZ, Gatalica Z, Kurzrock R. HER2 expression status in diverse cancers: review of results from 37,992 patients. Cancer Metastasis Rev. 2015;34(1):157–64.

220. Gao J, Xia Y, Chen H, Yu Y, Song J, Li W, et al. Polymer–lipid hybrid nanoparticles conjugated with anti-EGF receptor antibody for targeted drug delivery to hepatocellular carcinoma. Nanomedicine. 2014;9(2):279–93.

221. Karra N, Nassar T, Ripin AN, Schwob O, Borlak J, Benita S. Antibody conjugated PLGA nanoparticles for targeted delivery of paclitaxel palmitate: Efficacy and biofate in a lung cancer mouse model. Small. 2013;9(24):4221–36.

222. Mi Y, Liu X, Zhao J, Ding J, Feng SS. Multimodality treatment of cancer with herceptin conjugated, thermomagnetic iron oxides and docetaxel loaded nanoparticles of biodegradable polymers. Biomaterials. 2012;33(30):7519–29.

223. Vivek R, Thangam R, NipunBabu V, Rejeeth C, Sivasubramanian S, Gunasekaran P, et al. Multifunctional HER2-Antibody Conjugated Polymeric Nanocarrier-Based Drug Delivery System for Multi-Drug-Resistant Breast Cancer Therapy. ACS Appl Mater Interfaces. 2014;6(9):6469–80.

224. Arya G, Vandana M, Acharya S, Sahoo SK. Enhanced antiproliferative activity of Herceptin (HER2)-conjugated gemcitabine-loaded chitosan nanoparticle in pancreatic cancer therapy. Nanomedicine Nanotechnology, Biol Med. 2011;7(6):859–70.

225. Maya S, Sarmento B, Lakshmanan VK, Menon D, Jayakumar R. Actively targeted

cetuximab conjugated γ-poly(glutamic acid)-docetaxel nanomedicines for epidermal growth factor receptor over expressing colon cancer cells. J Biomed Nanotechnol. 2014;10(8):1416–28.

226. Choi W Il, Lee JH, Kim JY, Heo SU, Jeong YY, Kim YH, et al. Targeted antitumor efficacy and imaging via multifunctional nano-carrier conjugated with anti-HER2 trastuzumab. Nanomedicine Nanotechnology, Biol Med. 2015;11(2):359–68.

227. Sreeranganathan M, Uthaman S, Sarmento B, Mohan CG, Park IK, Jayakumar R. In vivo evaluation of cetuximab-conjugated poly(γ-glutamic acid)-docetaxel nanomedicines in EGFR-overexpressing gastric cancer xenografts. Int J Nanomedicine. 2017;12:7167–82.

228. Punfa W, Suzuki S, Pitchakarn P, Yodkeeree S, Naiki T, Takahashi S, et al. Curcumin-loaded PLGA nanoparticles conjugated with anti-P-glycoprotein antibody to overcome multidrug resistance. Asian Pacific J Cancer Prev. 2014;15(21):9249–58.

229. Punfa W, Yodkeeree S, Pitchakarn P, Ampasavate C, Limtrakul P. Enhancement of cellular uptake and cytotoxicity of curcumin-loaded PLGA nanoparticles by conjugation with anti-P-glycoprotein in drug resistance cancer cells. Acta Pharmacol Sin. 2012;33(6):823–31.

230. Ding B, Wu X, Fan W, Wu Z, Gao J, Zhang W, et al. Anti-DR5 monoclonal antibody-mediated DTIC-loaded nanoparticles combining chemotherapy and immunotherapy for malignant melanoma: target formulation development and in vitro anticancer activity. Int J Nanomedicine. 2011;6:1991–2005.

231. Gaca S, Reichert S, Multhoff G, Wacker M, Hehlgans S, Botzler C, et al. Targeting by cmHsp70.1-antibody coated and survivin miRNA plasmid loaded nanoparticles to

radiosensitize glioblastoma cells. J Control Release. 2013;172(1):201–6.

232. Jain NK, Tare MS, Mishra V, Tripathi PK. The development, characterization and in vivo anti-ovarian cancer activity of poly(propylene imine) (PPI)-antibody conjugates containing encapsulated paclitaxel. Nanomedicine Nanotechnology, Biol Med. 2015;11(1):207–18.

233. Mukerjee A, Ranjan AP, Vishwanatha JK. Targeted nanocurcumin therapy using annexin A2 antibody improves tumor accumulation and therapeutic efficacy against highly metastatic breast cancer. J Biomed Nanotechnol. 2016;12(7):1374–92.

234. Monterrubio C, Paco S, Olaciregui NG, Pascual-Pasto G, Vila-Ubach M, Cuadrado-Vilanova M, et al. Targeted drug distribution in tumor extracellular fluid of GD2-expressing neuroblastoma patient-derived xenografts using SN-38-loaded nanoparticles conjugated to the monoclonal antibody 3F8. J Control Release. 2017;255:108–19.

235. Öztürk K, Esendağlı G, Gürbüz MU, Tülü M, Çalış S. Effective targeting of gemcitabine to pancreatic cancer through PEG-cored Flt-1 antibody-conjugated dendrimers. Int J Pharm. 2017;517(1–2):157–67.

236. Molavi O, Xiong XB, Douglas D, Kneteman N, Nagata S, Pastan I, et al. Anti-CD30 antibody conjugated liposomal doxorubicin with significantly improved therapeutic efficacy against anaplastic large cell lymphoma. Biomaterials. 2013;34(34):8718–25.

237. Ashley JD, Stefanick JF, Schroeder VA, Suckow MA, Kiziltepe T, Bilgicer B. Liposomal bortezomib nanoparticles via boronic ester prodrug formulation for improved therapeutic efficacy in vivo. J Med Chem. 2014;57(12):5282–92.

238. de la Puente P, Luderer MJ, Federico C, Jin A, Gilson RC, Egbulefu C, et al. Enhancing

proteasome-inhibitory activity and specificity of bortezomib by CD38 targeted nanoparticles in multiple myeloma. J Control Release. 2018;270:158–76.

239. Li D, Lu B, Huang Z, Xu P, Zheng H, Yin Y, et al. A novel melphalan polymeric prodrug: Preparation and property study. Carbohydr Polym. 2014;111:928–35.

240. Ao L, Reichel D, Hu D, Jeong H, Kim KB, Bae Y, et al. Polymer Micelle Formulations of Proteasome Inhibitor Carfilzomib for Improved Metabolic Stability and Anticancer Efficacy in Human Multiple Myeloma and Lung Cancer Cell Lines. J Pharmacol Exp Ther. 2015;355(2):168–73.

241. Ashley JD, Quinlan CJ, Schroeder VA, Suckow MA, Pizzuti VJ, Kiziltepe T, et al. Dual Carfilzomib and Doxorubicin-Loaded Liposomal Nanoparticles for Synergistic Efficacy in Multiple Myeloma. Mol Cancer Ther. 2016;15(7):1452–9.

242. Cosco D, Cilurzo F, Maiuolo J, Federico C, Di Martino MT, Cristiano MC, et al. Delivery of miR-34a by chitosan/PLGA nanoplexes for the anticancer treatment of multiple myeloma. Sci Rep. 2015;5.

243. Wada A, Ito A, Iitsuka H, Tsuneyama K, Miyazono T, Murakami J, et al. Role of chemokine CX3CL1 in progression of multiple myeloma via CX3CR1 in bone microenvironments. Oncol Rep. 2015;33(6):2935–9.

244. Soleimani AH, Garg SM, Paiva IM, Vakili MR, Alshareef A, Huang Y-H, et al. Micellar nano-carriers for the delivery of STAT3 dimerization inhibitors to melanoma. Drug Deliv Transl Res. 2017;1–11.

CHAPTER 2

Role of STAT3 in MM cells cultured in a three-dimensional, reconstructed bone marrow model

A modified version of this chapter has been published as Huang et al." Constitutive activation of STAT3 in myeloma cells cultured in a three-dimensional, reconstructed bone marrow model" in Cancers 2018;10(6):206.

2.1. Introduction

Studies of malignant cells using three-dimensional (3D) culture systems are believed to provide information that is more representative of the 'real-life' *in vivo* conditions, as opposed to those using cells cultured conventionally in monolayer or cell suspension. In keeping with this concept, malignant cells cultured in 3D have been shown to display substantial differences in their growth characteristics, gene expression and drug resistance patterns when compared to cells cultured conventionally (1–3). Importantly, cells grown in biomimetic 3D systems are phenotypically similar to tumors formed *in vivo*. In one study, unlike their counterparts cultured in monolayer, glioblastoma cells cultured in 3D were found to phenotypically mimic xenografts formed in mice, with respect to their growth rate, levels of hypoxia and angiogenesis (4). Similarly, in another study, it was found that the drug resistance profile of glioblastoma cell lines derived from patient-derived xenografts correlates with the clinical outcome of these patients, and the correlations were better than that of cells cultured conventionally (5). From my literature search, I have identified a good number of studies employing various 3D models to study cancer biology, with the majority of these studies focusing on malignant epithelial cells and neurogenic cells. In comparison, studies of malignant hematopoietic cells using 3D culture models are relatively scarce, and the impact of 3D culture on these cancer cells is incompletely understood.

Multiple myeloma (MM), characterized by the accumulation of clonal malignant plasma cells in the three-dimensional bone marrow niches, represents 10% of all hematologic malignancies (6). Although the recent advances in various therapeutic modalities have improved the 5-year survival of MM patients to ~50%, MM remains to be an incurable disease (7,8). The tumor microenvironment within the bone marrow niche is believed to play an essential role in the

development and progression of MM. For example, it was found that vascular endothelial growth factor secreted by MM cells can induce the release of IL6 from bone marrow stromal cells, which in turn promotes the proliferation and survival of MM cells (9). In light of the importance of the microenvironment, several animal models have been developed to study the biology of MM and to evaluate various therapeutics designed to treat MM (10–12). Nonetheless, to my knowledge, studies of MM using 3D models are relatively few (13). For example, Ferrarini *et al.* employed a bioreactor system to create the 3D condition, although this bioreactor is relatively expensive and thus, not widely accessible (14). De la Puente *et al*. employed cross-linked fibrinogen matrix supplemented with patient-derived mononuclear cells and supernatants (15). Kirshner *et al.* described a 3D model in which Matrigel®, which is commercially available, was found to support the expansion of PMM cells for up to 30 days (16). This 3D model carries several important advantages over animal models, as it is relatively inexpensive and devoid of issues related to cross-species immune incompatibilities. I also believe that Kirshner's 3D model is more accessible to researchers, as it does not require the purchase of relatively expensive equipment or elaborative preparation of patient samples. Nonetheless, how exactly this 3D culture model impacts the biology of MM cells is largely unknown.

To evaluate the impact of the 3D culture on MM cells, I optimized a 3D reconstructed bone marrow model based on the method previously described by Kirshner *et al*. (16,17). The modifications to the system have generated several improvements, such as the fact that my system is highly amendable to histologic processing, immunocytochemical studies and possibly other morphologic studies (i.e. studies of cell-cell interactions). Importantly, my results have highlighted the importance of STAT3, which was found to be active in MM-3D cells but not those cultured

conventionally. my data supports the concept that STAT3 increases the expression of proteins which are responsible for enhanced cell survival, proliferation and drug resistance in MM (18–21). As STAT3 is often active in PMM cells (22), I believe that studies of MM in the 3D culture systems can generate results that are more representative of the disease.

2.2. Materials and methods

2.2.1. Cell lines, patient samples and materials

U266 cells were obtained from ATCC, and RPMI8226 cells were obtained from Dr. Linda Pilarski. Karpas 299 and SupM2 cells were purchased from ATCC. All cell lines were grown in RPMI1640 medium supplied with 10% FBS with 1% streptomycin and penicillin except U266 cells, which were grown in RPMI1640 medium supplied with 15% FBS. Same growth medium was applied to cells cultured in 3D culture and in conventional culture. Ficoll-Paque isolated bone marrow mononuclear cells from two MM patients and reconstituted bortezomib in sterile water (1 mg/ml) were obtained from Cross Cancer Institute, University of Alberta. Both patients #1 and #2 contained 10-20% monoclonal plasma cells according to their biopsy section. Stattic (Sigma) powder was dissolved in DMSO into 1 mg/ml solution. All procedures of patient sample handling were approved by Human Research Ethics Board, University of Alberta (HREBA.CC-16-0346 and HREBA.CC-17-0591). Animal procedures for this study were approved by Animal Care and Use Committee, University of Alberta (Pro00000282).

2.2.2. 3D culture

The method for 3D culture was adapted from a previous publication (17). In brief, 48-well plates were pre-coated with 100 µl of reconstructed endosteum (77 µg/ml fibronectin and 29 µg/ml

collagen I in PBS) before seeding of 3D cultures. U266 or RPMI8226 cell pellets were resuspended first with 20µl PBS. Matrigel® (Corning), 1 mg/ml fibronectin and 2 mg/ml collagen I were added to the resuspended cells in 4:2.5:1 ratio. 100 ul of cell matrix was loaded to each well and incubated at 37°C for 1 hour to allow polymerization. Finally, 1 ml of pre-warmed growth medium was added to the 3D culture. For recovery of 3D cells, 1 ml of cell recovery solution containing 5 mM EDTA, 1 mM sodium vanadate and 1.5 mM sodium fluoride was used.

2.2.3. Preparation of cells for immunocytochemistry

The procedure of preparing U266-3D cells for immunocytochemistry is outlined in **Figure 2.1**. Histogel wells for each sample were created by inserting an Eppendorf tube into a well (24- or 48-well plate) with 400 µl of liquid histogel (Thermo Scientific). Upon solidification of histogel, the Eppendorf tube was gently removed, leaving a concaved up and U-shaped well for 3D culture loading. The 3D cell culture was loaded into the well and allowed to solidify for 1 hour at 37°C. ~300 µl of growth medium was added to the 3D cell culture and incubated for two days. On the day of embedding, the growth medium was removed and 200 µl of liquid histogel was added on top to encapsulate the 3D cell culture within the histogel. The entire histogel was then fixed in 4% formaldehyde at 4°C overnight and processed for paraffin wax embedding. For U266 and Karpas 299 cells, $2x10^6$ cells were pelleted, resuspended in 100 µl histogel, transferred to a 7x7x5 mm plastic mold (Simport) and fixed in 4% paraformaldehyde for embedding. For U266 xenograft cells, 5 x 10^5 U266 cells stably transduced with luciferase gene were injected into a SCID mouse intravenously via tail vein. The mouse was euthanized when it became immobile and lost more than 20% body weight. The total bone marrow cells were isolated from the femur, resuspended in

100 µl histogel and transferred to a plastic mold for embedding. All of isolated bone marrow cells were confirmed to be U266 cells by bioluminescence imaging. After embedding, processing and

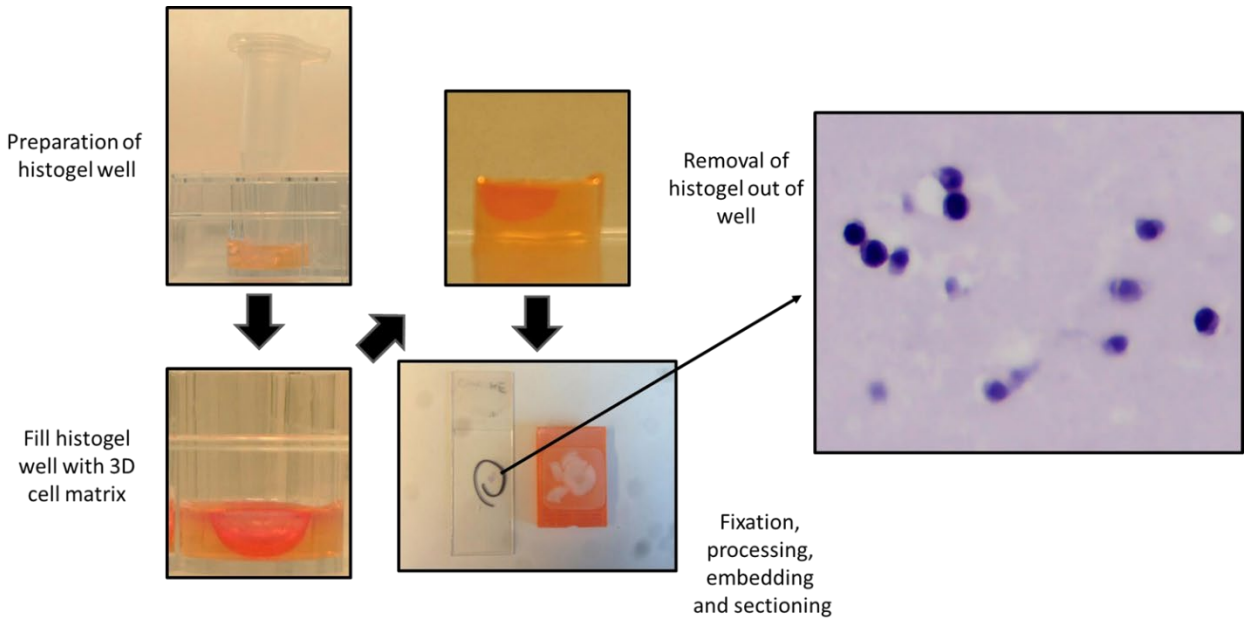

Figure 2.1. Schematic procedure of immunocytochemistry of MM-3D cells. A 1.5 ml Eppendorf was inserted into liquid histogel in a 48-well plate. Upon solidified, the "histogel well" was loaded with the 3D cell matrix containing Matrigel®, fibronectin, collagen I and MM cells. After solidification of 3D cell matrix, growth medium was applied on top of 3D cell matrix. On the day of harvest, the entire histogel well was scooped out of plate with a surgical knife and transferred to a tissue cassette for fixation, embedding, processing and sectioning. An image of H&E staining of MM-3D cells following this protocol was depicted on right side.

sectioning, the sample slides were rehydrated in xylene and decreasing concentrations of ethanol. The antigens were retrieved using 1X citrate buffer (Sigma) by microwaving in a pressure cooker for 20 minutes. The pSTAT3 antibody (Santa Cruz, clone B-7) was diluted as 1:50 in antibody diluent (DAKO). MACH2 mouse HRP polymer (Biocare Medical) was used as a secondary antibody. The chromogen and substrate were mixed and applied to each slide for 2 minutes for color development (DAKO).

2.2.4. DNA pulldown assay

Cell pellets from MM or MM-3D cells were lysed with CellLytic M (Sigma) with protease inhibitor and phosphatase inhibitor cocktails (Millipore) on ice for 30 minutes. 300 µg of total cell lysate was mixed with 3 pmol of STAT3 DNA probe (Biotin-5'-GATCTAGGAATTCCCAGAAGG-3') for 30 minutes on a rotator at room temperature. 75 µl of streptavadin agarose beads (Fisher Scientific) was added to the DNA-lysate mix. The whole solution was incubated on a rotator at 4oC overnight. The beads were washed three times with ice-cold PBS. SDS loading buffer was added to beads and boiled for 5 minutes to dissociate bound proteins. The beads were spun down and the supernatant was subject to SDS-PAGE.

2.2.5. Cellular thermal shift assay (CETSA)

The original protocol of CETSA was followed (23). In brief, both MM and MM-3D cells were cultured for 48 hours. Cells were harvested using cell recovery solution and incubated on ice for 1 hour with brief vortex every 15 minutes. Cells were pelleted and washed once with cold and sterile PBS. Cells were resuspended in PBS supplied with 5% protease inhibitor cocktail and 2.5% PMSF prior to heating. Resuspended cells were heated at 54^{o}C for U266 cells and 52^{o}C for RPMI8226 cells for 3 minutes using a thermal cycler. Cells were lysed by three freeze-thaw cycles in liquid nitrogen. Aggregated proteins were precipitated at 20,000 g for 20 minutes at 4^{o}C. The supernatant was collected, heated (70^{o}C for 10 minutes) and dissolved in 4X SDS loading buffer prior to SDS-PAGE.

2.2.6. Cell viability and apoptosis assays

Both MM and MM-3D cells on 48-well plates after drug treatment were recovered by cell recovery solution and resuspended in fresh growth medium. 100 µl resuspended cells were transferred to a 96-well plate. Cell viability was measured by CellTiter 96® AQueous One Solution Cell Proliferation Assay (i.e. MTS assay, Promega) or trypan blue exclusion assay (Amresco). The apoptosis was measured by following the instructions of FITC Annexin V Apoptosis Detection Kit I (BD Biosciences).

2.2.7. Oligonucleotide array

Total RNA of both U266 and U266-3D cells were prepared using RNeasy Mini Kit (Qiagen). First strand cDNA was synthesized using RT2 First Strand Kit (Qiagen). All PCR reactions were prepared by adding cDNA, RT2 SYBR Green ROX qPCR Mastermix (Qiagen) into the 96-well plates of RT2 Profiler Human Cancer PathwayFinder PCR Array (Qiagen). The array contains 84 representative genes which are responsible for 9 biological pathways which are complicated in human cancers. The cycle threshold (CT) values were obtained and standardized using the CT value of *GAPDH*. The logarithmic ratio of mRNA expression fold changes (3D to 2D) for each gene was calculated and ranked from highest to lowest.

2.2.8. Reverse transcriptase polymerase chain reaction (RT-PCR)

The total RNA of U266 cells in conventional culture for 2 days or in 3D culture for 1 to 4 days were extracted using RNeasy Plus Mini Kit (Qiagen). First strand cDNA was prepared using SuperScript® Reverse Transcriptase kit (Invitrogen). RT-PCR reactions were prepared using SYBR® Select Master Mix (Applied Biosystems). The sequence of all forward and reverse primers used in this study are summarized in **Table 2.1**. The fluorescence signal was detected and

measured by 7900HT Fast Real-Time PCR System and analyzed by SDS2.3. The gene expression was normalized to GAPDH.

Table 2.1. Forward and reverse primers used

Gene	Forward Primer	Reverse Primer
IL6	5'-TCCAGTTGCCTTCTTGGGAC-3'	5'-GTACTCCAGAAGACCAGAGG-3'
IL21	5'-TGTGAATGACTTGGTCCCTGAA-3'	5'-AACAGGAAAAAGCTGACCAC-3'
IL10	5'-GCCTAACATGCTTCGAGATC-3'	5'-TGATGTCTGGGTCTTGGTTC-3'
LPL	5'-ACAAGAGAGAACCAGACTCCAA-3'	5'-GCGGACACTGGGTAATGCT-3'
ANGPT2	5'-AACTTTCGGAAGAGCATGGAC-3'	5'-CGAGTCATCGTATTCGAGCGG-3'
DDIT3	5'-GGAAACAGAGTGGTCATTCCC-3'	5'-CTGCTTGAGCCGTTCATTCTC-3'
CA9	5'-GGATCTACCTACTGTTGAGGCT-3'	5'-CATAGCGCCAATGACTCTGGT-3'
GAPDH	5'-GGTCTCCTCTGACTTCAACAGCG-3'	5'-ACCACCCTGTTGCTGTAGCCAA-3'

2.2.9. Western blot analysis

Both MM and MM-3D cell pellets were lysed by 1X RIPA buffer (Millipore) with protease inhibitor and phosphatase inhibitor cocktails (Millipore) on ice for 30 minutes. Protein concentration of each lysate was measured using Pierce™ BCA protein assay kit (Thermo Scientific). Equal amount of protein was loaded on 10% homemade polyacrylamide gels for SDS-PAGE at 100 volts. Proteins in polyacrylamide gel were transferred to nitrocellulose membrane (Bio-Rad) at 100V for 2 hours. Primary antibodies used were anti-pSTAT3 (Y705) (1:2000, CST, #9145), anti-STAT3 (1:1000, CST#124H6), anti-pErk (T202/Y204) (1:2000, CST, #4377), anti-Erk (1:1000, Enzo, #ADI-KAP-MA001), anti-pAkt (S473) (1:1000, CST, #4060), anti-Akt (1:1000, CST, #9272), anti-cleaved (V1744) Notch1 (1:1000, CST, #4147), anti-Notch1 (1:1000, CST, #3439), anti-pIKBα (S32) (1:1000, CST, #9241), anti-IKBα (1:1000, CST, #4812), anti-β-actin (1:1000, CST, #58169), anti-PARP (1:1000, CST, #9532) and anti-Caspase3 (1:1000, CST,

#9665). Secondary antibodies used were HRP-conjugated anti-mouse (1:2000, CST, #7076) and anti-rabbit (1:2000, CST, #7074). Signals on the membrane were developed using Pierce™ ECL Western Blotting Substrate (Thermo Scientific) and exposed to X-ray films (Fuji).

2.2.10. Statistical analysis

All numerical data in this study was presented as the mean from experiment replicates or independent experiments as described in the figure legends. Statistical significance between groups were analyzed using Student's t-test with $\alpha=0.05$ except Figure 6, for which one-way ANOVA with Dunnett's multiple t-test ($\alpha=0.05$) were employed. The analysis was done using Microsoft Excel 365 except Figure 6, for which GraphPad Prism 7 was used for analysis.

2.3. Results

2.3.1. MM cells cultured in 3D form large clusters

I cultured two MM cell lines, U266 and RPMI8226. using the 3D model that had been optimized, as described in section **2.2.2.** (17). These cells were labeled MM-3D cells, and I compared their growth characteristics with cells cultured conventionally. As shown in **Figure 2.2A,** MM cells from both cell lines cultured conventionally settled in the bottom of the tissue culture flasks, and they were found to be present in small clusters composed of an average of 5-10 cells with a greatest dimension of 20-30 μm (i.e. U266) or predominantly in single cells (i.e. RPMI8226). In contrast, MM-3D cells from both cell lines were present predominantly as spherical, tight cell clusters that were composed of >20-30 cells with the greatest dimension of >50 μm ($p<0.05$, **Figure 2.2A**). I compared the cell growth in these two different culture conditions using the trypan blue exclusion assay. As shown in **Figure 2.2B**, I found that MM-3D cells grew significantly slower than those

cultured conventionally in the first few days of culture ($p<0.05$), although the differences were relatively small. These differences in cell growth became statistically insignificant on day 4 for RPMI8226 and on day 6 for U266.

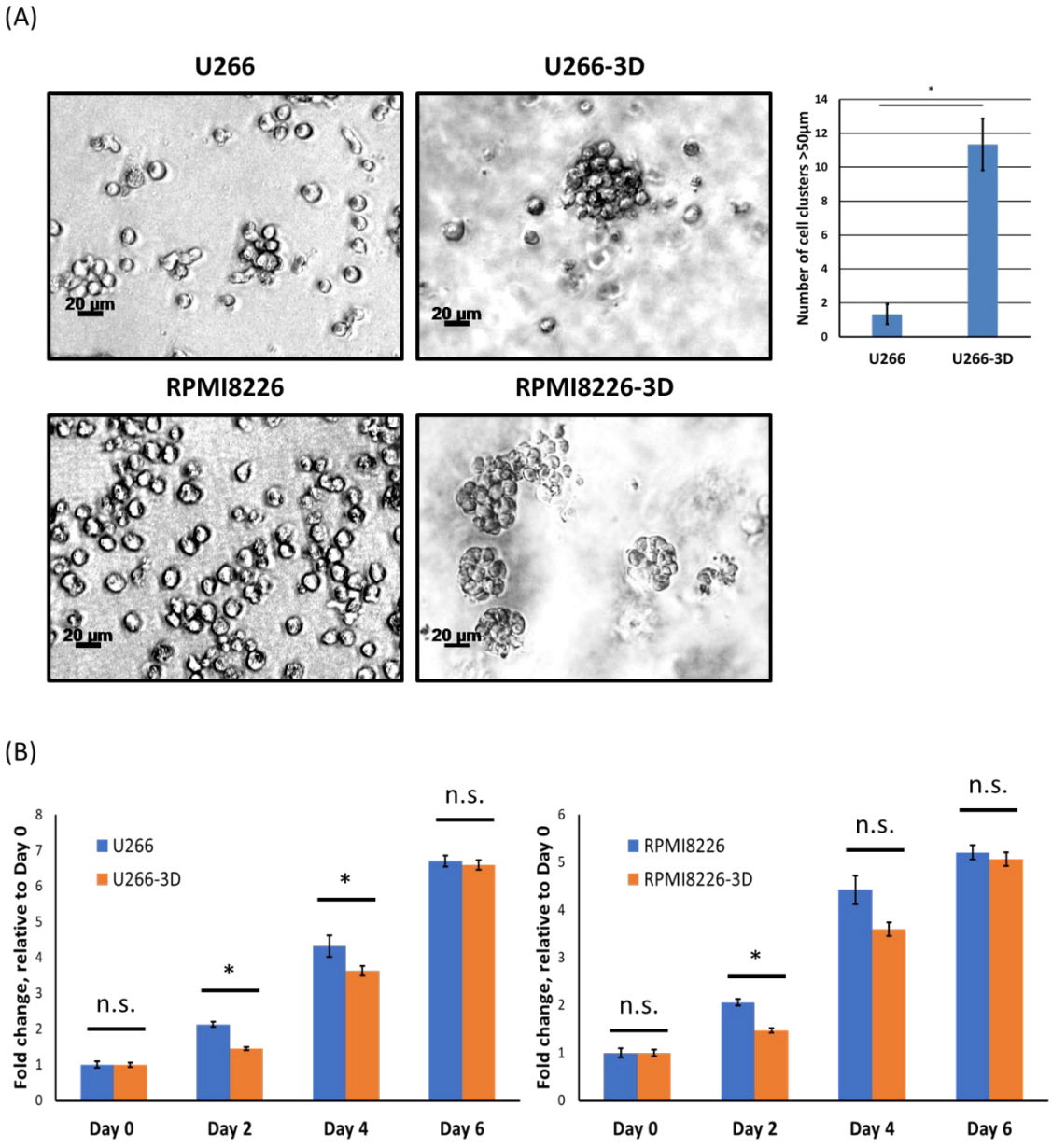

Figure 2.2. MM cells exhibit different appearances and growth patterns in conventional culture versus in 3D culture. (A) The morphology of U266 and RPMI8226 cells in conventional or 3D culture after 6 days was examined by phase contrast microscopy. Images were taken at 100X magnification. A scale bar equivalent to 20 µm is included in each graph. (B) The growth of U266

and RPMI8226 cells in conventional (blue bars) or 3D cultured (orange bars) was measured by the trypan blue exclusion assay at various time points. Fold changes of total viable cells were normalized to the cell number on day 0 (2.5x105 cells). The error bars represent standard deviation from a triplicate experiment, *$p<0.05$, n.s. not significant, Student's t-test.

2.3.2. STAT3 activity in MM cells is increased in 3D culture

Deregulations of several signaling pathways, including that of STAT3, Erk/MAPK, PI3K/Akt, NF-κB and Notch, are known to be important in the pathogenesis of MM (22,24–29). To determine if 3D culture has a significant impact on the cellular signaling in MM cells, I examined the status of these 5 pathways in U266 and RPMI8226 cells, cultured in 3D or conventionally. As shown in **Figure 2.3A**, using lysates prepared from cells harvested on day 2, I found that the active/phosphorylated form of STAT3 (pSTAT3) was expressed in MM-3D cells, whereas this band was not detectable in cells cultured conventionally. I did not observe consistent and/or obvious difference in the activation status of the other 4 signaling pathways (**Figure 2.3A**). This finding was confirmed by the quantification of the band intensity for pSTAT3.

In view of these findings, I focused my studies on STAT3. I then performed a time course experiment to study the kinetics of STAT3 activation in MM-3D cells. Cells from both MM cell lines were cultured in 3D for 4 days and the expression level of pSTAT3 was examined daily using Western blot analysis. Triplicate experiments were performed and results from a representative experiment are shown in **Figure 2.3B**. In U266 cells, the pSTAT3 band became detectable on day 1, and there was a time-dependent upregulation of pSTAT3 which peaked on day 4. In RPMI8226 cells, the pSTAT3 band also became detectable on day 1 and but it appeared to diminish gradually

thereafter. In comparison, no pSTAT3 band was detectable in cells cultured conventionally throughout the experiment (**Figure 2.3C**). Cell lysates from SupM2, an ALK-positive anaplastic

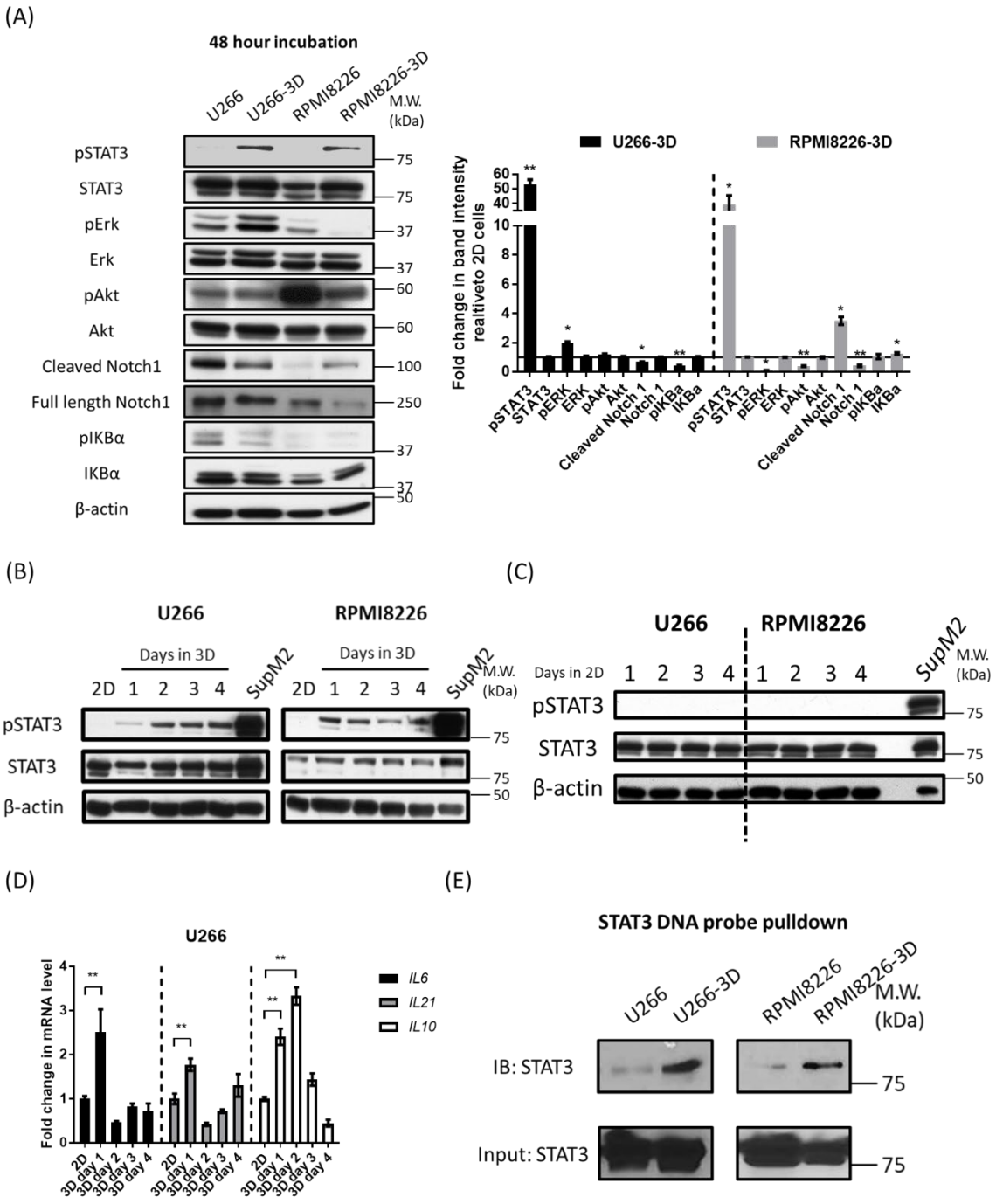

Figure 2.3. MM cells cultured in 3D acquire STAT3 activity. (A) The activity of various signaling pathways (STAT3, Erk/MAPK, PI3K/Akt, NF-κB and Notch) in U266 and RPMI8226

cells cultured conventionally (2D) or in 3D was examined by Western blot analysis after 48 hours. The relative band intensity compared to 2D (i.e. 1 fold) was quantified using ImageJ. The mean band intensity was obtained from three independent experiments. The black line represents 1-fold fold change in band intensity, *p<0.05, **p<0.001, Student's t-test. (B) The STAT3 activity of U266 and RPMI8226 cells in 2D or 3D culture from day 1 to day 4 were examined by Western blot analysis of pSTAT3 levels. SupM2 cells were included as a positive control for the pSTAT3 level. (C) The STAT3 activity of U266 and RPMI8226 cells in conventional (2D) culture from day 1 to day 4 were examined by Western blot analysis of pSTAT3 levels. (D) Quantitative RT-PCR of IL6 (black), IL21 (grey) and IL10 (white) mRNA levels in U266 cells in conventional culture (2D) or day 1 to 4 in 3D culture. 2.5x105 cells were seeded initially. The primers used for each gene are described in section 2.2.8 and Table 2.1. The error bars represent standard deviation from a triplicate experiment. **p<0.001 compared to 2D, one-way ANOVA with Dunnett's multiple t-test. (E) The DNA binding ability of STAT3 in U266 and RPMI8226 cells cultured in 2D or 3D was examined by DNA pulldown immunoblotting assay. The cells were harvested and lysed after 48 hours in culture. STAT3 in cell lysate was pulled down by a STAT3 DNA probe (described in section 2.2.4).

large cell lymphoma cell line known to have a high pSTAT3 expression (30), were used as the positive control. To explore the possible activators of STAT3 in 3D culture, I checked the expression level of several cytokines which are known to induce STAT3 phosphorylation in MM: IL6, IL21 and IL10 (31–33). As shown in **Figure 2.3D**, the expression of all three cytokines in U266 cells increased by 1.5-2.5 folds after 1 day of 3D culture compared to cells in conventional culture.

In support of the concept that the STAT3 transcriptional activity was indeed increased in MM-3D cells, I examined the DNA-binding ability of STAT3 using the protein-DNA pulldown assay. As shown in **Figure 2.3E**, a substantially high level of STAT3 protein in MM-3D cells was pulled

down with the biotinylated DNA probe containing the STAT3 consensus sequence; in comparison, no band was detectable when cells cultured conventionally were examined. To estimate the proportion of MM-3D cells showing pSTAT3 expression, I optimized the experimental protocol, as described in section **2.2.3.**, so that MM-3D cells and the surrounding matrix were readily fixed in formalin and processed for immunocytochemistry. As shown in **Figure 2.3F**, the vast majority of U266 cells cultured in 3D (overall 100 cells examined) showed definitive evidence of nuclear pSTAT3 staining, and this finding suggests that STAT3 activation in 3D culture was a generalized phenomenon and not restricted to a small cell subset. Additionally, a similar STAT3 activation pattern was also observed in the U266 cells xenografted in an animal, suggesting that the 3D culture reflected the *in vivo* MM condition better than the conventional culture. Lastly, I examined if the cell concentration affects the activation of STAT3 in MM-3D cells. Thus, I doubled the cell density from $2.5x10^5$/ml to $5.0x10^5$/ml at the beginning of the 3D culture. As shown in **Figure 2.3G**, while both cell lines acquired pSTAT3 on day 1, this signal decreased with time and became undetectable on day 3 or day 4. This time-dependent decrease in pSTAT3 was likely due to the depletion of nutrients in the tissue culture.

I also had collected evidence that the observed STAT3 activation in MM-3D is not a cell line-specific phenomenon. As shown in **Figure 2.3H**, I studied two primary patient bone marrow aspirate samples using western blot analysis, and I found that MM-3D cells, but not cells in conventional culture, showed a substantial level of pSTAT3 expression that peaked on day 2, similar to that seen in U266 cells cultured in 3D.

2.3.3. STAT3 activation in MM-3D cells is dependent on the 3D environment

To understand if the expression of pSTAT3 is truly dependent on the 3D culture environment, I extracted MM-3D cells from 3D culture matrix and transferred them to conventional cell culture. Specifically, the matrix was dissolved, and pelleted MM-3D cells were washed and re-suspended

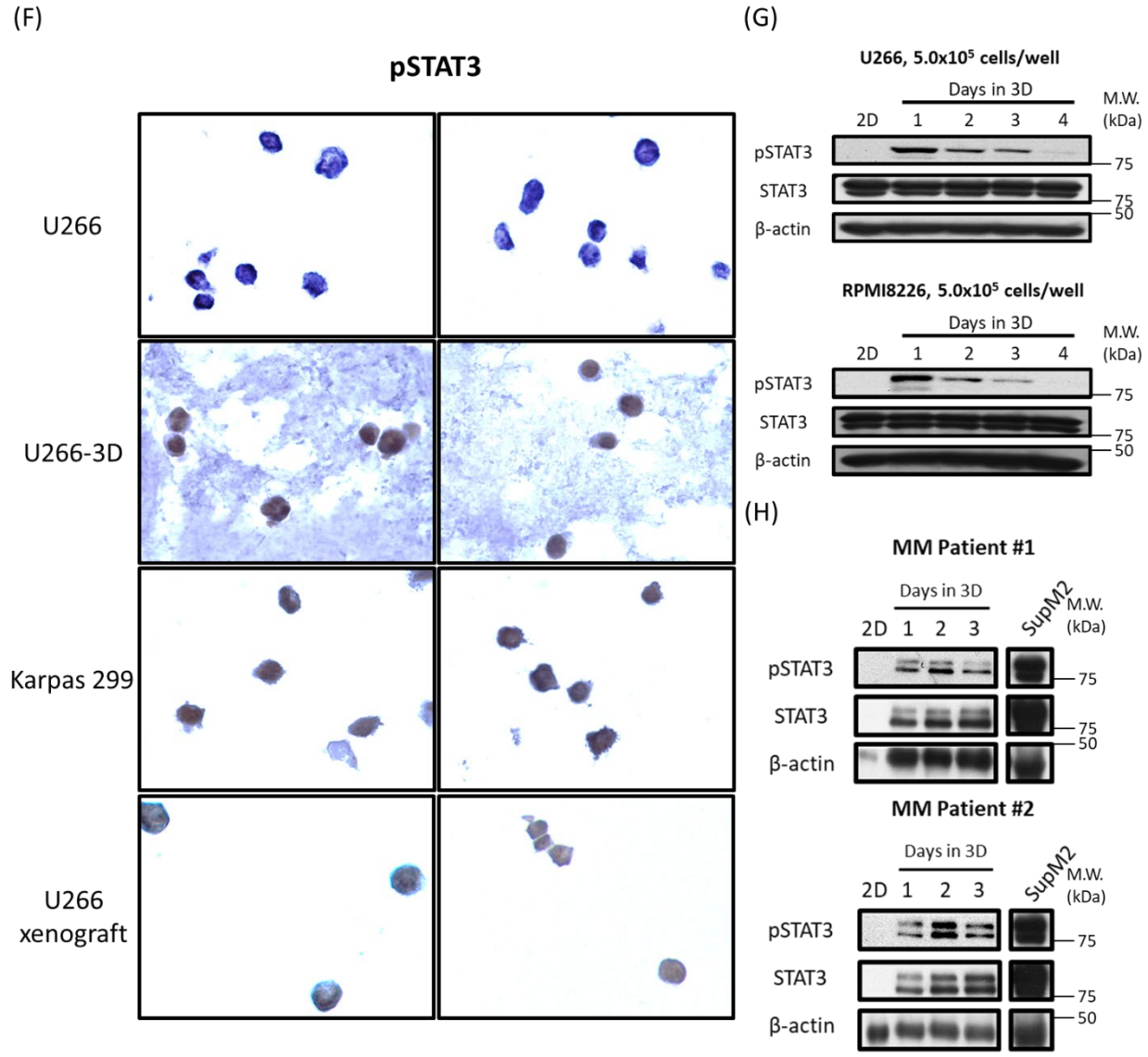

Figure 2.3 (cont'd). MM cells cultured in 3D acquire STAT3 activity. (F) Immunocytochemical analysis of pSTAT3 level in U266, U266-3D, Karpas 299 and U266 xenograft cells. The cells were fixed after 48 hours in culture. The procedure of processing, embedding and sectioning was described in section **2.2.3.** Two representative pictures were shown. Karpas 299 cells were included as a positive control for pSTAT3 staining. (G) Western blot analysis of pSTAT3 and STAT3 levels of U266 and RPMI8226 cells in 2D or 3D culture from

day 1 to day 4 with a higher cell concentration ($5.0x10^5$ cells). (H) Western blot analysis of pSTAT3 and STAT3 levels of PMM bone marrow cells in 2D or 3D culture from day 1 to day 3. SupM2 cells were included as a positive control for pSTAT3 level. β-actin was probed as a loading control in each blot. For all the above experiments except (F), $2.5x10^5$ cells were seeded initially. in growth medium at a cell density of $2.5x10^5$ cells/ml. The expression level of pSTAT3 was then evaluated at 24 hours and 48 hours using Western blot analysis. As shown in **Figure 2.4**, the pSTAT3 level substantially decreased on day 2 after transfer to conventional culture in both U266 and RPMI8226 cells.

2.3.4. STAT3 inhibition is effective in decreasing cell growth of MM-3D cells

To investigate the biological significance of 3D-induced STAT3 activation, I inhibited STAT3 using a STAT3 pharmacologic inhibitor, Stattic, which has been extensively described in the literature (34). Since I anticipated the intracellular drug level will be highly dependent on the types of tissue culture (e.g. cell suspension versus solid matrix), I employed cellular thermal shift assay

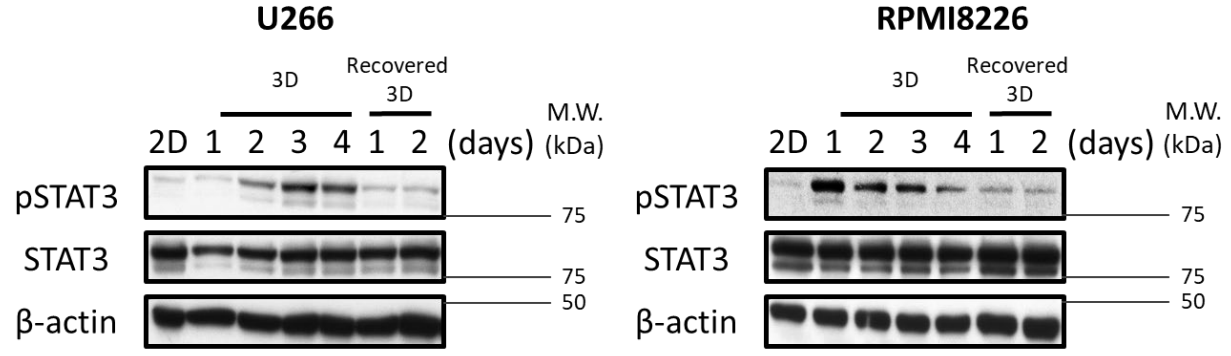

Figure 2.4. Acquired STAT3 activity in MM cells diminished upon recovery from 3D to conventional culture. The STAT3 activity in U266 and RPMI8226 cells before and after recovery from 3D culture by Western blot analysis of pSTAT3 level. U266 and RPMI8226 were pre-cultured in 3D culture for 2 days and 1 day prior to recovery to reach a substantial pSTAT3 level, respectively. β-actin was probed as a loading control. $2.5x10^5$ cells were seeded initially.

(CETSA) (23), to compare the extent of STAT3-Stattic binding in MM-3D cells and in cells cultured in suspension. As shown in **Figure 2.5A**, in U266-3D cells, Stattic was found to be substantially bound to STAT3 at a dose of 4 μM, which was found to induce more than 50%

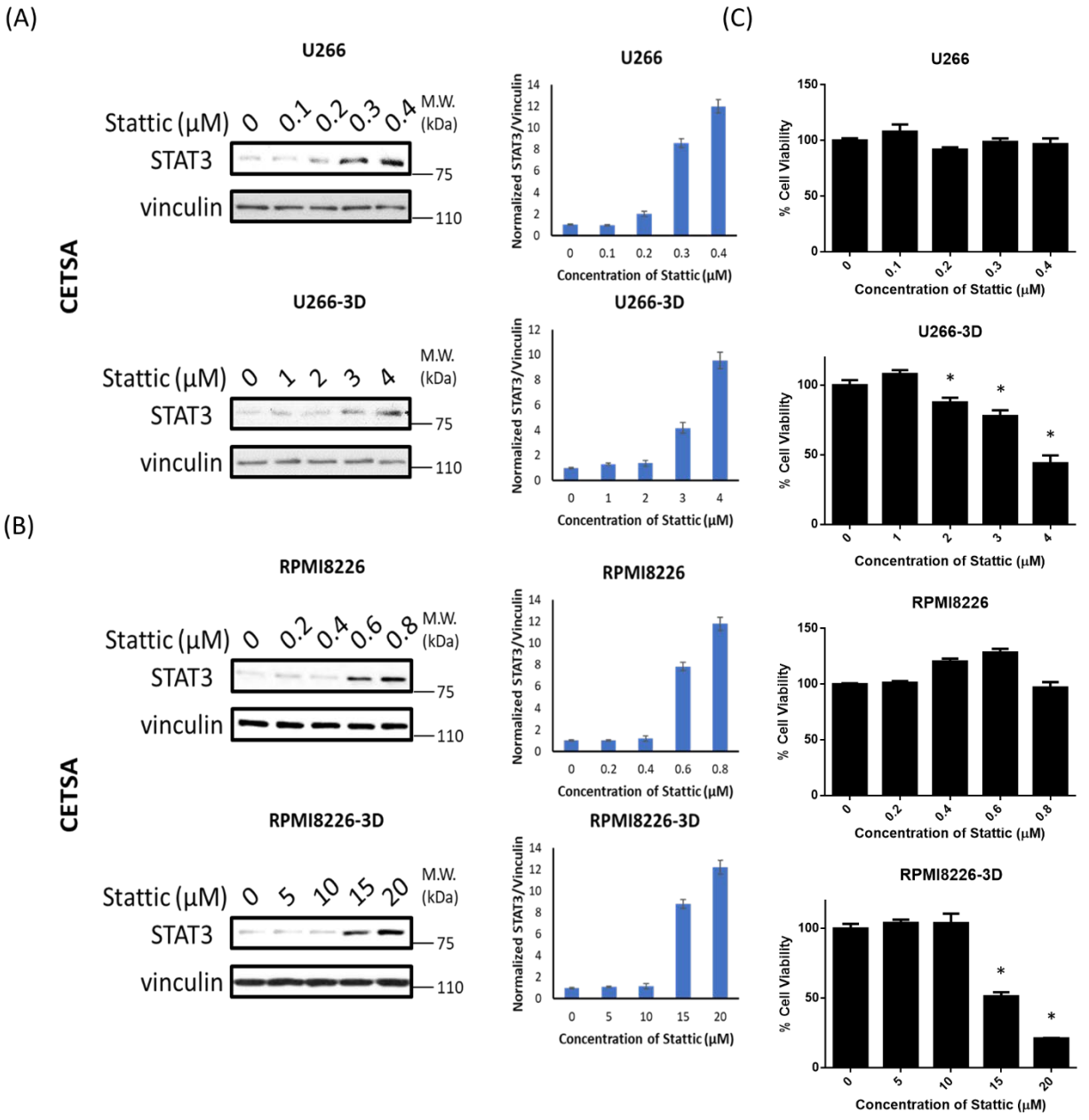

Figure 2.5. MM cells in 3D but not conventional culture undergoes apoptosis at equal drug accessibility. CETSA of (A) U266 and (B) RPMI8226 cells in conventional or 3D culture after 1 hour of Stattic treatment. Vinculin was blotted as a loading control. The STAT3/vinculin ratios

were quantified using ImageJ and shown on the right. Error bars represent the standard deviation from two independent experiments. (C) The effect of STAT3 inhibition on cell viability of U266 and RPMI8226 cells in conventional or 3D culture. The cells were treated with Stattic for 24 hours. Cell viability was measured by MTS assay and normalized to cells with no Stattic treatment. The error bars represent standard deviation from a triplicate experiment, *$p<0.05$, Student's t-test. For all the experiments above, U266 and RPMI8226 cells were cultured for 2 and 1 days before the Stattic treatment to reach a substantial pSTAT3 level, respectively. $2.5x10^5$ cells were seeded initially.

reduction in cell viability after 24 hours (**Figure 2.5C**). In comparison, in U266 cells grown conventionally, 0.3 μM of Stattic was the lowest dosage found to be effective in mediating a substantial physical binding between Stattic and STAT3, and this dosage of Stattic did not induce any significant loss of cell viability. Similarly, in RPMI8226-3D cells, a substantial Stattic-STAT3 binding was observed at 15 μM (**Figure 2.5B**), which induced more than 50% reduction in cell viability (**Figure 2.5C**). In comparison, only 0.6 μM of Stattic was required for a substantial Stattic-STAT3 binding in conventionally cultured cells, and no significant reduction in cell viability was seen at this dosage. In summary, with a comparable level of Stattic-STAT3 binding, MM-3D cells showed significant reduction in cell growth whereas cells in suspension did not show significant changes. These findings support the concept that STAT3 activation in MM-3D is biologically important. To investigate the mechanism underlying the Stattic-induced reduction in cell viability, I asked if apoptosis played a role. As shown in **Figure 2.5D**, Stattic was found to induce apoptosis in MM-3D cells, as shown by the level of Annexin V staining, cleaved PARP and caspase 3 (**Figure 2.5E**). Specifically, the expression of cleaved PARP and caspase 3 was detectable at the same dosages of Stattic at which a substantial binding between Stattic-STAT3 was found (i.e. 3-4 μM for U266 cells and 15-20 μM for RPMI8226 cells). In contrast, no sign of

apoptosis was observed in both cell lines cultured conventionally; specifically, no appreciable Annexin V staining, cleaved PARP and cleaved caspase 3 were found at the dose range where

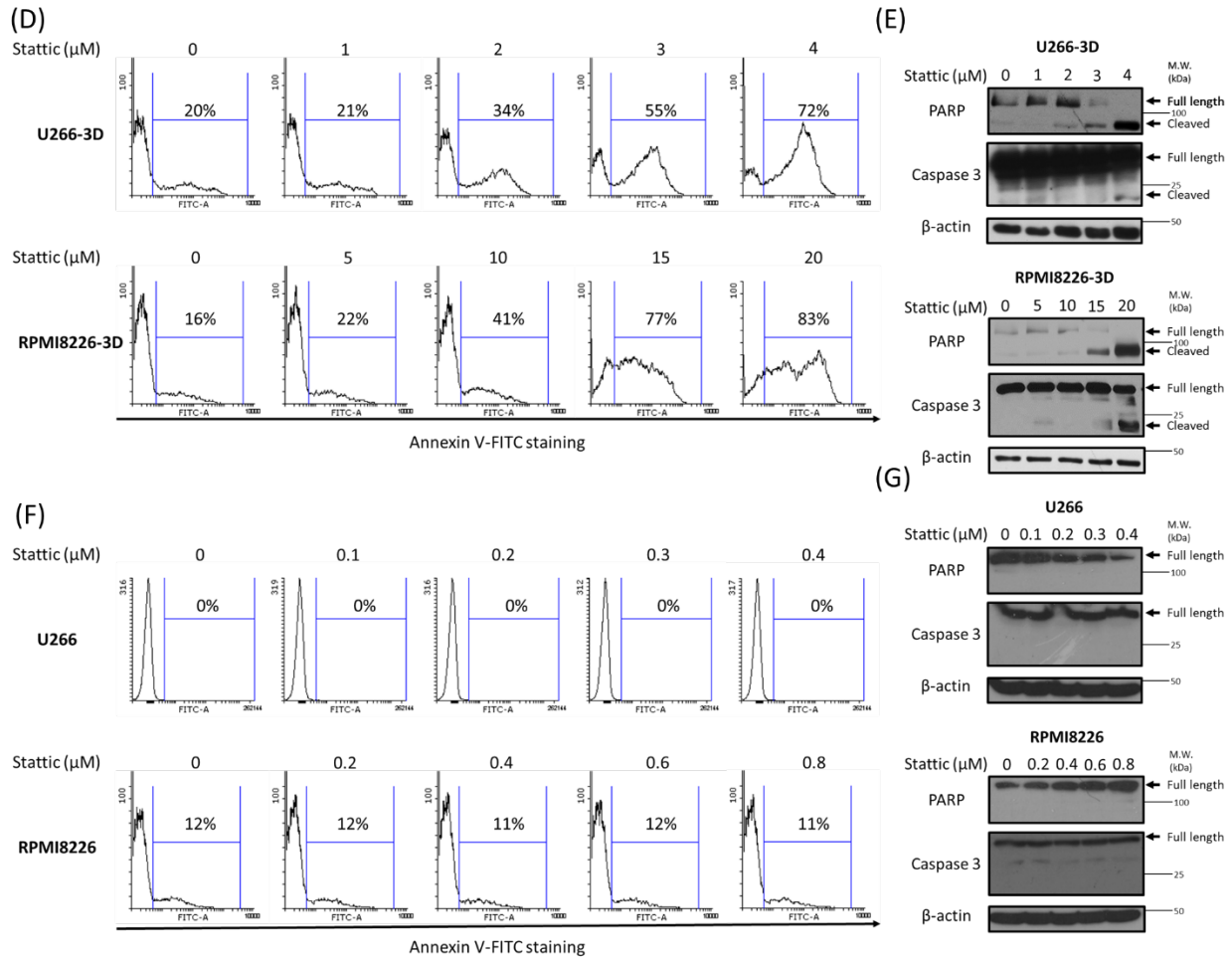

Figure 2.5 (Cont'd). MM cells in 3D but not conventional culture undergoes apoptosis at equal drug accessibility. (D) The effect of STAT3 inhibition on apoptosis in U266- and RPMI8226-3D cells. The cells were treated with Stattic for 24 hours and stained with an apoptotic marker Annexin V. The percentage of Annexin V-positive cells was analyzed by flow cytometry. (E) The expression levels of two apoptotic markers, cleaved PARP and cleaved caspase 3, in U266- and RPMI8226-3D cells after 24 hours of Stattic treatment were examined by Western blot analysis. β-actin was probed as a loading control. (F) The effect of STAT3 inhibition on apoptosis in U266 and RPMI8226 cells in conventional culture. The cells were treated with Stattic for 24 hours and stained with an apoptotic marker Annexin V. The percentage of Annexin V-positive cells was analyzed by flow cytometry. (G) The expression levels of two apoptotic markers, cleaved

PARP and cleaved caspase 3, in U266 and RPMI8226 cells cultured conventionally after 24 hours of Stattic treatment were examined by Western blot analysis. β-actin was probed as a loading control. For all the experiments above, U266 and RPMI8226 cells were cultured for 2 and 1 days before the Stattic treatment to reach a substantial pSTAT3 level, respectively. $2.5x10^5$ cells were seeded initially.

Stattic can effectively bind to STAT3 (i.e. 0.3-0.4 μM for U266 and 0.6-0.8 μM for RPMI8226) (**Figure 2.5F and 2.5G**).

2.3.5. STAT3 inhibition sensitizes MM-3D cells to bortezomib

Since EGFR-induced STAT3 activation has been shown to promote resistance to proteasome inhibitors in MM cells (21), I asked if the STAT3 activation in MM-3D cells contributes to resistance to bortezomib, a proteasome inhibitor commonly used in treating MM patients. To address this question, I tested if Stattic can sensitize the STAT3-active MM-3D cells to bortezomib-induced cytotoxicity. Thus, I cultured U266 cells in 3D for 48 hours, and this resulted in a relatively high expression level of pSTAT3 in these cells (**Figure 2.3**). I then treated these cells with bortezomib at dose (i.e. 7 nM) that I had already confirmed to be slightly lower than that of the inhibitory concentration at 50% (IC_{50}). For Stattic treatment, I used two doses where substantial Stattic can bind to STAT3, as illustrated in **Figure 2.5A and 2.5B**. As shown in **Figure 2.6A**, treatment with a combination of 7 nM of bortezomib and 3 or 4 μM of Stattic resulted in a significantly higher reduction in the number of viable U266-3D cells, as compared to cells treated with bortezomib or Stattic alone ($p<0.001$). Similar results were observed for RPMI8226-3D cells **(Figure 2.6A).** In contrast, Stattic treatment did not improve the cytotoxic effect to both MM cell lines cultured conventionally (**Figure 2.6B**).

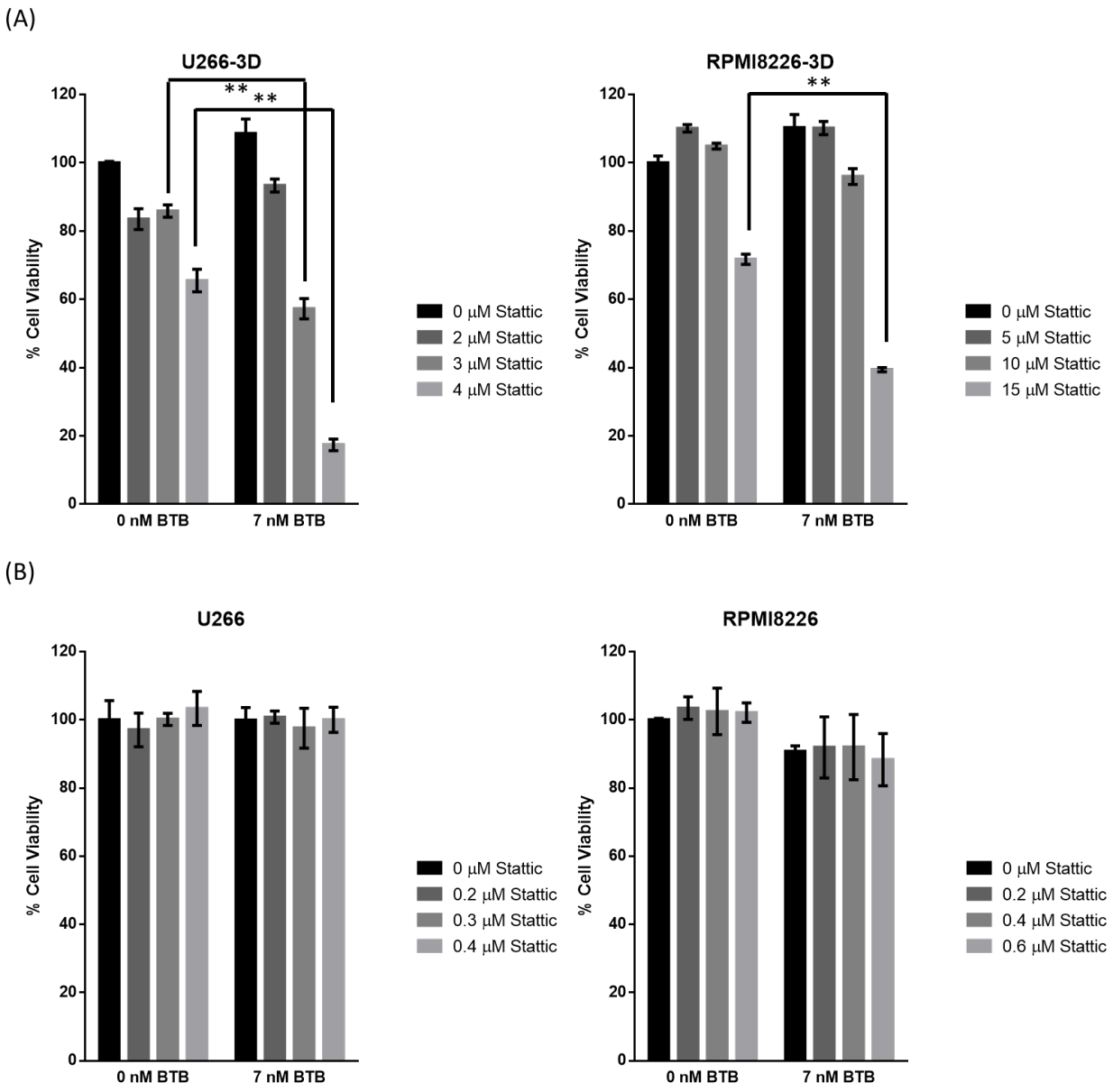

Figure 2.6. STAT3 inhibition in MM-3D cells sensitizes them to bortezomib. Cell viability of U266 and RPMI8226 cells in (A) 3D or (B) conventional culture was measured after treatment with Stattic, bortezomib (BTB) or both for 48 hours. U266 and RPMI8226 were pre-cultured in 3D for 2 days and 1 day before drug treatment to reach a substantial pSTAT3 level, respectively. Cell viability was measured by MTS assay and normalized to the cell viability of untreated cells. $2.5x10^5$ cells were seeded initially. The error bars represent standard deviation from a triplicate experiment, **p<0.001, Student's t-test.

2.3.6. Gene expression profiling in MM-3D cells

To better understand the biochemical changes induced by the 3D culture, I performed an oligonucleotide array comparing U266-3D and U266 cultured conventionally. The RT^2 Profiler Human Cancer PathwayFinder PCR Array containing 90 genes implicated in oncogenesis was used, as detailed in section **2.2.8**. Compared to U266 cells grown conventionally, U266-3D cells showed an increase in the expression of lipoprotein lipase (*LPL*, 14.1 folds), angiopoietin 2 (*ANGPT2*, 6.8 folds) and Snail homolog 3 (*SNAI3*, 3.5 folds), and a decrease in the expression of DNA-damage-inducible transcript 3 (*DDIT3*, -35.9 folds), carbonic anhydrase 9 (*CA9*, -22.3 folds) and ovalbumin (*SERPINB2*, -19.4 folds) (**Figure 2.7A**). By performing signaling pathway analysis using Pathway Common Network Visualizer (*www.pathwaycommons.org/pcviz*), I found that 4 out of these 6 most modulated genes (*LPL, ANGPT2, DDIT3 and CA9*) are directly or indirectly related to STAT3 (**Figure 2.7B**). The upregulation of *LPL* and *ANGPT2* and downregulation of

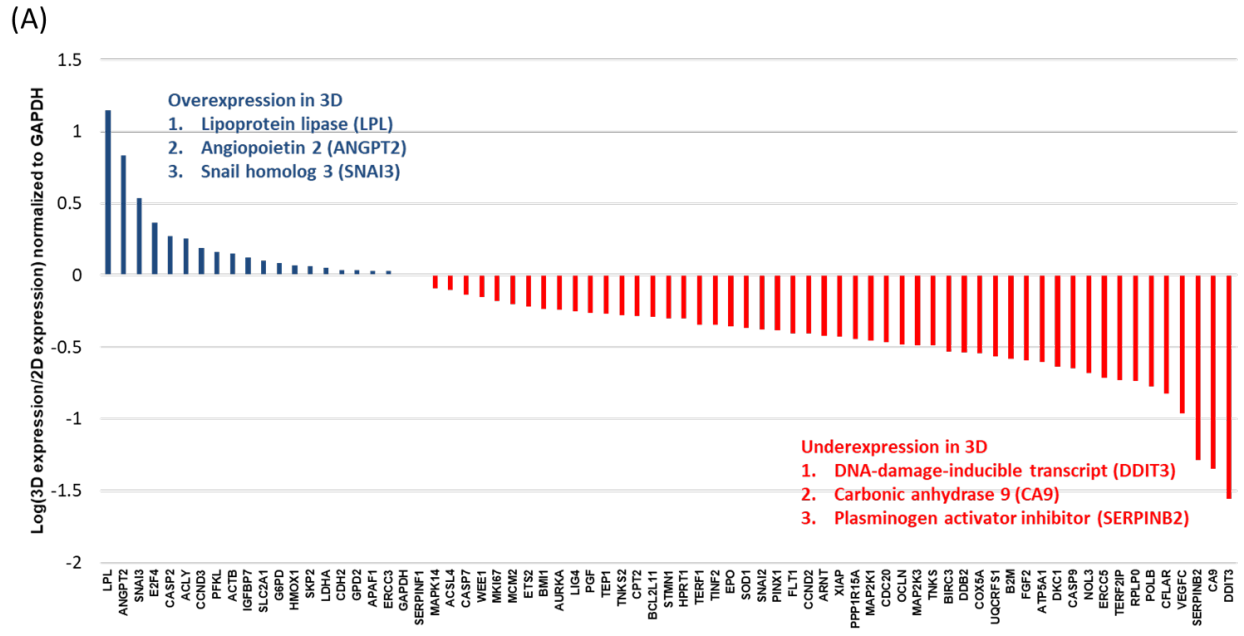

Figure 2.7. Gene expression changes in MM-3D cells are STAT3-relevant. (A) Oligonucleotide assay of human cancer-related genes using U266 or U266-3D cDNA. The cDNA

was extracted from U266 cells after 2 days in conventional (2D) or 3D culture. All 2D and 3D gene expressions were normalized to the corresponding *GAPDH* expressions. The logarithm of gene expression ratio (3D/2D) was computed for each gene and ranked from the highest (left) to the lowest (right). The top three most upregulated (blue) and downregulated (red) genes were indicated in the graph.

DDIT3 and *CA9* in 3D culture were confirmed by quantitative RT-PCR (**Figure 2.7C**). Specifically, the mRNA levels of *LPL* and *ANGPT2* increased by approximately 10 and 2.8 folds on day 2 in 3D culture compared to conventional culture on day 2, respectively ($p<0.001$). The mRNA levels of *DDIT3* and *CA9* decreased by approximately 10 folds in 3D culture compared to conventional culture on day 2 ($p<0.001$).

2.4. Discussion

The phenotype of cancer cells dedicating features such as chemoresistance, the rate of growth, morphology and mobility, is known to be greatly influenced by the microenvironment in which the cells exist. These findings suggest that it may be more biologically relevant to employ 3D culture models to study cancer biology (35). In support of this concept, many studies comparing malignant epithelial or neurogenic cells cultured in 3D and those cultured conventionally have revealed substantial phenotypic and biochemical differences (36). For instance, glioblastoma cells cultured in a 3D environment were found to have high levels of proliferation, invasiveness and IL-8 secretion when compared to the same cells grown in monolayer (4). Furthermore, several studies have shown that experimental manipulations of cancer cells can generate vastly different results, depending on whether cells were cultured in 3D or conventionally. For example, inhibition of β-integrin was found to ablate the spheroid architecture of breast cancer cells, but only when the

(B)

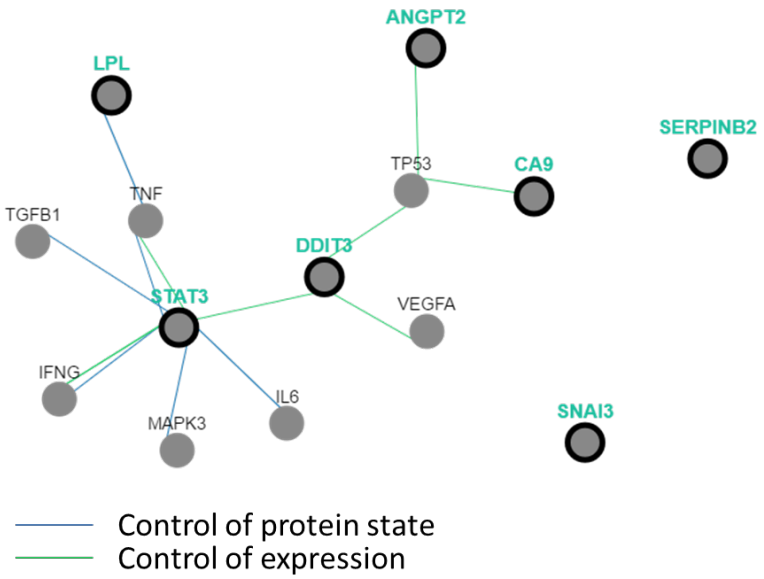

(C)

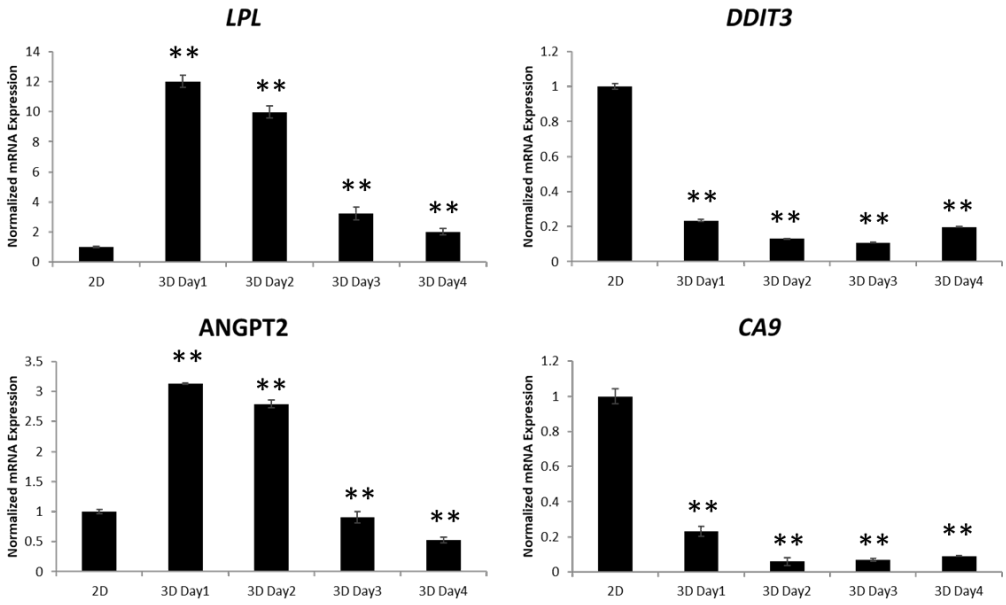

Figure 2.7 (Cont'd). Gene expression changes in MM-3D cells are STAT3-relevant. (B) Signaling pathway analysis of the top three most upregulated and downregulated genes from (A) and their relationship with STAT3 using *Pathway Common Network Visualizer*. A blue line connects two genes which one can affect the expression level of another. A green line connects two genes which one can affect the protein state of another. (C) Quantitative RT-PCR of *LPL*, *ANGPT2*, *DDIT3* and *CA9* mRNA levels in U266 cells in conventional culture (2D) or day 1 to 4

in 3D culture. $2.5x10^5$ cells were seeded initially. The primers used for each gene were described in **Table 2.1.** The error bars represent standard deviation from a triplicate experiment, **p<0.001 compared to 2D, Student's t-test.

cells were cultured in 3D but not in monolayer (37). There is direct evidence that results generated from using the 3D study models are more representative of the *in vivo* scenarios. As mentioned above, glioblastoma cell lines established from patient derived xenografts were found to have a drug resistant profile that correlated with the clinical outcome, but only if the cells were grown in a 3D environment (5). Overall, it appears that studying cancer biology using 3D models is biologically and clinically relevant.

To my knowledge, most of the published cancer studies using 3D models have focused on epithelial malignant cells (such as breast cancer) or neurogenic tumors (such as glioblastoma). In the field of MM research, I notice a relatively small number of studies on 3D culture. 3D dynamic devices such as bioreactor and microfluidic flow provide continuous nourishment to MM cells, but the equipment is expensive and does not allow high throughput drug screening (14,38). In another model, de la Puente *et al.* employed cross-linked fibrinogen-matrix supplemented by patient-derived bone marrow mononuclear cells and supernatants, and they successfully expanded fresh PMM cells derived from 3 different patients (15). However, the observation that there was a 2.5-fold increase in PMM cells within 7 days appears to be inconsistent with the fact that the proliferation index of MM is generally low (i.e. average 6.5% Ki-67 positivity in Stage III MM patients) (39). In my 3D culture system, which was adapted from Kirshner *et al.* (16,17), I employed a mixture of extracellular matrix proteins and Matrigel® designed to mimic the bone marrow matrix. This 'reconstructed' bone marrow matrix was previously shown to support the

proliferation of PMM cells for up to 30 days, a task that is difficult to achieve in conventional culture (16). The value of this 3D system was further demonstrated in the same study that a relatively high dose of bortezomib eliminated only a subset of MM cells growing in the 3D culture (16), and this finding contrasted with the observation in conventional culture in previous studies in which nano-molar doses of bortezomib were sufficient to induce substantial cytotoxicity (40,41). Importantly, as reported by Krishner *et al.*, the partial resistance to bortezomib seen in the 3D model was found to correlate with a poor clinical response to bortezomib monotherapy in MM patients (42,43). In light of these findings, two more recent studies have adapted the same 3D model for assessment of the efficacy of novel anti-MM agents. Specifically, one study reported that anti-CD56-conjugated maytansinoid is able to overcome drug resistance in a co-culture system including MM cells and stromal cells (44). In another study, two NF-κB inhibitors were found to induce cytotoxicity to putative MM cancer stem cells in the 3D model (45).

The biochemical effects of 3D culture on MM cells are not well understood. In this study, I have confirmed that the reconstructed bone marrow matrix can exert phenotypic and biochemical changes. Specifically, cells grown in this 3D culture system grew in large clusters instead of single cells or small clusters, as seen in the conventional culture system. In addition, the constitutive activation of STAT3 was observed in 3D cells but not in cells cultured conventionally. The upregulation of STAT3 was found to be rapid (i.e. within 24 hours), and I have evidence that this biochemical abnormality is dependent on the continuous 3D culture, as STAT3 became inactive when MM cells were brought back to conventional culture. The mechanism of STAT3 activation in 3D is likely multi-factorial. First, as shown in this study, there were increases in the expression of cytokines (i.e. IL6, IL21 and IL10) known to activate STAT3 in MM. Second, the physical

support of MM cells in 3D culture likely promotes whole-surface contact with extracellular matrix proteins, and this phenomenon leads to the 3D-induced spheriod formation and contributes to STAT3 activation. Similar observations were seen in 3D cultured breast cancer cells (46). I have found that the pSTAT3 nuclear staining was present in the vast majority of cells in the 3D culture, confirming that the elevated STAT3 activity is generalized phenomenon and not restricted to a small cell population. The 3D-induced upregulation of STAT3 activity may have contributed to the fact that the cell growth in the 3D environment caught up with that of conventional culture after a few days (i.e. **Figure 2.1**). In keeping with this concept, pharmacologic inhibition of STAT3 in MM-3D cells indeed resulted in a significant reduction in cell growth. The validity of these findings is also supported by the observation that MM cells in conventional culture were not sensitive to Stattic.

The oncogenic characteristics of STAT3 have been extensively reviewed (47–50). In MM, STAT3 is believed to upregulate various proteins which are responsible for enhancing cell survival, proliferation and drug resistance (51–53). STAT3 has been reported to be constitutively active in MM patients (22,54,55). Pharmacological agents such as curcumin, piperlongumine, icaritin and LLL12 which blocked STAT3 phosphorylation were reported to suppress PMM cell viability and/or MM tumor growth in animal models (22,56–58). Clinically, a high pSTAT3 level has been reported to correlate with poorer progress-free survival and overall survival in newly diagnosed MM patients (59). On the other hand, MM cell lines (e.g. RPMI8226) typically showed no evidence or a low level of STAT3 activity (60), except few of them with constitutive autocrine IL6 stimulation (e.g. U266 cells, (61)). In my hand, however, both U266 and RPMI8226 cells showed a low level of STAT3, possibly suggesting the emerging of STAT3-independent U266 cells in

conventional culture after many passages. The discrepancy of STAT3 activity in PMM cells and MM cell lines may result from the fact that various STAT3-activating cytokines and/or factors are abundant *in vivo* and in 3D culture models, but they are either absent or present in a low concentration in cell suspension. In this regard, extracellular matrix proteins, which are present *in vivo* and in 3D but not in cell suspension, have been found to be an important source of STAT3 activation in MM (62,63). In support of this concept, MM cells cultured on fibronectin-coated surface had more robust IL6-induced STAT3 activation than those cultured in cell suspension (62). In another study, it was found that MM cell lines showed STAT3 activation that could be enhanced by Reelin, an extracellular matrix protein (63). Overall, there is ample evidence that extracellular matrix proteins contribute to the aberrant STAT3 activity in MM, and this phenomenon is recapitulated in 3D culture systems but not in cell suspension.

My oligonucleotide array studies have revealed dramatic differences in the gene expression between MM-3D cells and cells cultured conventionally. Interestingly, *LPL* and *AGPNT2* (being significantly higher in MM-3D cells) as well as *DDIT3* (being significantly lower in MM-3D cells) are reported to associated with STAT3 signaling. LPL, known to hydrolyze triglycerides into free fatty acids and glycerol, has been shown to be upregulated by STAT3 in chronic lymphatic leukemia (CLL) (64). LPL is known to have oncogenic potential. As the result of the activity of LPL, it is believed that the generated free fatty acids binds to PPARα so as to promote the cell survival and proliferation of CLL cells (65). ANGPT2 concentrations in bone marrow have been found to be significantly higher in patients with active MM compared to those with smoldering MM, MGUS or healthy donors (66). ANGPT2 serum level is positively correlated with bone marrow microvascular vessel density in patients with active MM (66). Additionally, it was found

that bone marrow mononuclear cells from MM patients secreted substantially more ANGPT2 compared to those from healthy donors in a 3D bioreactor model (14). DDIT3 was found to be decreased in MM-3D cells and has been reported to have tumor suppressor effects. DDIT3 is a protein that induces apoptosis in various types of cancer cells upon endoplasmic reticulum stress (67). It is also reported that DDIT3 expression is supressed by STAT3, leading to enhanced survival in mesothelioma (68).

2.5. References

1. Wang K, Kievit FM, Erickson AE, Silber JR, Ellenbogen RG, Zhang M. Culture on 3D chitosan-hyaluronic acid scaffolds enhances stem cell marker expression and drug resistance in human glioblastoma cancer stem cells. Adv Healthc Mater. 2016;5(24):3173–81.
2. Yim EKF, Darling EM, Kulangara K, Guilak F, Leong KW. Nanotopography-induced changes in focal adhesions, cytoskeletal organization, and mechanical properties of human mesenchymal stem cells. Biomaterials. 2010;31(6):1299–306.
3. Ghosh S, Spagnoli GC, Martin I, Ploegert S, Demougin P, Heberer M, et al. Three-dimensional culture of melanoma cells profoundly affects gene expression profile: A high density oligonucleotide array study. J Cell Physiol. 2005;204(2):522–31.
4. Fischbach C, Chen R, Matsumoto T, Schmelzle T, Brugge JS, Polverini PJ, et al. Engineering tumors with 3D scaffolds. Nat Methods. 2007;4(10):855–60.
5. Gomez-Roman N, Stevenson K, Gilmour L, Hamilton G, Chalmers AJ. A novel 3D human glioblastoma cell culture system for modeling drug and radiation responses. Neuro Oncol. 2016;17(1):now164.

6. Gozzetti A, Candi V, Papini G, Bocchia M. Therapeutic advancements in multiple myeloma. Front Oncol. 2014;4:241.

7. Becker N. Epidemiology of multiple myeloma. In: Moehler T, Goldschmidt H, editors. Recent Results in Cancer Research. New York: Springer; 2011. p. 25–35.

8. Kumar SK, Rajkumar SV, Dispenzieri A, Lacy MQ, Hayman SR, Buadi FK, et al. Improved survival in multiple myeloma and the impact of novel therapies. Blood. 2008;111(5):2516–20.

9. Kyle RA, Rajkumar S V. Multiple myeloma. Blood. 2008;111(6):2962–72.

10. Menu E, Asosingh K, Van Riet I, Croucher P, Van Camp B, Vanderkerken K. Myeloma cells (5TMM) and their interactions with the marrow microenvironment. Blood Cells Mol Dis. 2004;33(2):111–9.

11. Tong AW, Huang YW, Zhang BQ, Netto G, Vitetta ES, Stone MJ. Heterotransplantation of human multiple myeloma cell lines in severe combined immunodeficiency (SCID) mice. Anticancer Res. 1993;13(3):593–7.

12. Calimeri T, Battista E, Conforti F, Neri P, Di Martino MT, Rossi M, et al. A unique three-dimensional SCID-polymeric scaffold (SCID-synth-hu) model for in vivo expansion of human primary multiple myeloma cells. Leukemia. 2011;25(4):707–11.

13. Ferrarini M, Mazzoleni G, Steimberg N, Belloni D, Ferrero E. Innovative models to assess multiple myeloma biology and the impact of drugs. InTech. 2013;(Mm):39–60.

14. Ferrarini M, Steimberg N, Ponzoni M, Belloni D, Berenzi A, Girlanda S, et al. Ex-Vivo dynamic 3-D culture of human tissues in the RCCS^{TM} bioreactor allows the study of multiple myeloma biology and response to therapy. Cheriyath V, editor. PLoS One. 2013;8(8):e71613.

15. de la Puente P, Muz B, Gilson RC, Azab F, Luderer M, King J, et al. 3D tissue-engineered bone marrow as a novel model to study pathophysiology and drug resistance in multiple myeloma. Biomaterials. 2015;73:70–84.

16. Kirshner J, Thulien KJ, Martin LD, Debes Marun C, Reiman T, Belch AR, et al. A unique three-dimensional model for evaluating the impact of therapy on multiple myeloma. Blood. 2008;112(7):2935–45.

17. Parikh MR, Belch AR, Pilarski LM, Kirshner J. A Three-dimensional tissue culture model to study primary human bone marrow and its malignancies. J Vis Exp. 2014;(85):e50947–e50947.

18. Veirman K De, Van Ginderachter JA, Lub S, Beule N De, Thielemans K, Bautmans I, et al. Multiple myeloma induces Mcl-1 expression and survival of myeloid-derived suppressor cells. Oncotarget. 2015;6(12):10532–47.

19. Romagnoli M, Séveno C, Wuillème-Toumi S, Amiot M, Bataille R, Minvielle S, et al. The imbalance between Survivin and Bim mediates tumour growth and correlates with poor survival in patients with multiple myeloma. Br J Haematol. 2009;145(2):180–9.

20. Spets H, Stromberg T, Georgii-Hemming P, Siljason J, Nilsson K, Jernberg-Wiklund H. Expression of the bcl-2 family of pro- and anti-apoptotic genes in multiple myeloma and normal plasma cells. Regulation during interleukin-6 (IL-6)-induced growth and survival. Eur J Haematol. 2002;69(2):76–89.

21. Zhang XD, Baladandayuthapani V, Lin H, Mulligan G, Li B-Z, Esseltine DLW, et al. Tight jnction protein 1 modulates proteasome capacity and proteasome inhibitor sensitivity in multiple myeloma via EGFR/JAK1/STAT3 signaling. Cancer Cell. 2016;29(5):639–52.

22. Bharti AC, Shishodia S, Reuben JM, Weber D, Alexanian R, Raj-Vadhan S, et al. Nuclear

factor–κB and STAT3 are constitutively active in CD138 + cells derived from multiple myeloma patients, and suppression of these transcription factors leads to apoptosis. Blood. 2004;103(8):3175–84.

23. Jafari R, Almqvist H, Axelsson H, Ignatushchenko M, Lundbäck T, Nordlund P, et al. The cellular thermal shift assay for evaluating drug target interactions in cells. Nat Protoc. 2014;9(9):2100–22.

24. Colombo M, Galletti S, Garavelli S, Platonova N, Paoli A, Basile A, et al. Notch signaling deregulation in multiple myeloma: A rational molecular target. Oncotarget. 2015;6(29):26826–40.

25. Bezieau S, Devilder M-C, Avet-Loiseau H, Mellerin M-P, Puthier D, Pennarun E, et al. High incidence of N and K-Ras activating mutations in multiple myeloma and primary plasma cell leukemia at diagnosis. Hum Mutat. 2001;18(3):212–24.

26. Liu P, Leong T, Quam L, Billadeau D, Kay NE, Greipp P, et al. Activating mutations of N- and K-ras in multiple myeloma show different clinical associations: analysis of the Eastern Cooperative Oncology Group Phase III Trial. Blood. 1996;88(7):2699–706.

27. Zhu J, Wang M, Cao B, Hou T, Mao X. Targeting the phosphatidylinositol 3-kinase/AKT pathway for the treatment of multiple myeloma. Curr Med Chem. 2014;21(27):3173–87.

28. Steinbrunn T, Stühmer T, Gattenlöhner S, Rosenwald A, Mottok A, Unzicker C, et al. Mutated RAS and constitutively activated Akt delineate distinct oncogenic pathways, which independently contribute to multiple myeloma cell survival. Blood. 2011;117(6):1998–2004.

29. Fuchs O. Targeting of NF-kappaB signaling pathway, other signaling pathways and epigenetics in therapy of multiple myeloma. Cardiovasc Hematol Disord Drug Targets.

2013;13(1):16–34.

30. Khoury JD, Medeiros LJ, Rassidakis GZ, Yared MA, Tsioli P, Leventaki V, et al. Differential expression and clinical significance of tyrosine-phosphorylated STAT3 in ALK+ and ALK- anaplastic large cell lymphoma. Clin Cancer Res. 2003;9(10 Pt 1):3692–9.

31. Kolosenko I, Grandér D, Tamm KP. IL-6 activated JAK/STAT3 pathway and sensitivity to Hsp90 inhibitors in multiple myeloma. Curr Med Chem. 2014;46(8):3042–7.

32. Yang T, Liu J, Yang M, Huang N, Zhong Y, Zeng T, et al. Cucurbitacin B exerts anti-cancer activities in human multiple myeloma cells in vitro and in vivo by modulating multiple cellular pathways. Oncotarget. 2017;8(4):5800–13.

33. Brenne A-T, Ro TB, Waage A, Sundan A, Borset M, Hjorth-Hansen H. Interleukin-21 is a growth and survival factor for human myeloma cells. Blood. 2002;99(10):3756–62.

34. Schust J, Sperl B, Hollis A, Mayer TU, Berg T. Stattic: a small-molecule inhibitor of STAT3 activation and dimerization. Chem Biol. 2006;13(11):1235–42.

35. Xu X, Farach-Carson MC, Jia X. Three-dimensional in vitro tumor models for cancer research and drug evaluation. Biotechnol Adv. 2014;32(7):1256–68.

36. Edmondson R, Broglie JJ, Adcock AF, Yang L. Three-dimensional cell culture systems and their applications in drug discovery and cell-based biosensors. Assay Drug Dev Technol. 2014;12(4):207–18.

37. Weaver VM, Petersen OW, Wang F, Larabell CA, Briand P, Damsky C, et al. Reversion of the malignant phenotype of human breast cells in three-dimensional culture and in vivo by integrin blocking antibodies. J Cell Biol. 1997;137(1):231–45.

38. Zhang W, Lee WY, Siegel DS, Tolias P, Zilberberg J. Patient-specific 3D microfluidic

tissue model for multiple myeloma. Tissue Eng Part C Methods. 2014;20(8):663–70.

39. Gastinne T, Leleu X, Duhamel A, Moreau AS, Franck G, Andrieux J, et al. Plasma cell growth fraction using Ki-67 antigen expression identifies a subgroup of multiple myeloma patients displaying short survival within the ISS stage I. Eur J Haematol. 2007;79(4):297–304.

40. Huang X, Di Liberto M, Jayabalan D, Liang J, Ely S, Bretz J, et al. Prolonged early G 1 arrest by selective CDK4/CDK6 inhibition sensitizes myeloma cells to cytotoxic killing through cell cycle-coupled loss of IRF4. Blood. 2012;120(5):1095–106.

41. Catley L, Weisberg E, Kiziltepe T, Tai YT, Hideshima T, Neri P, et al. Aggresome induction by proteasome inhibitor bortezomib and alpha-tubulin hyperacetylation by tubulin deacetylase (TDAC) inhibitor LBH589 are synergistic in myeloma cells. Blood. 2006;108(10):3441–9.

42. Richardson PG, Chanan-Khan A, Schlossman RL, Munshi NC, Wen P, Briemberg H, et al. Phase II trial of single agent bortezomib (VELCADE®) in patients with previously untreated multiple myeloma (MM). Blood. 2015;104(11).

43. Richardson PG, Barlogie B, Berenson J, Singhal S, Jagannath S, Irwin D, et al. A phase 2 study of bortezomib in relapsed, refractory myeloma. N Engl J Med. 2003;348(26):2609–17.

44. Nierste BA, Gunn EJ, Whiteman KR, Lutz RJ, Kirshner J. Maytansinoid immunoconjugate IMGN901 is cytotoxic in a three-dimensional culture model of multiple myeloma. Am J Blood Res. 2016;6(1):6–18.

45. Gunn EJ, Williams JT, Huynh DT, Iannotti MJ, Han C, Barrios FJ, et al. The natural products parthenolide and andrographolide exhibit anti-cancer stem cell activity in multiple

myeloma. Leuk Lymphoma. 2011;52(6):1085–97.

46. Park MC, Jeong H, Son SH, Kim YH, Han D, Goughnour PC, et al. Novel morphologic and genetic analysis of cancer cells in a 3D microenvironment identifies STAT3 as a regulator of tumor permeability barrier function. Cancer Res. 2016;76(5):1044–54.

47. Zhang H-FF, Lai R. STAT3 in cancer-friend or foe? Cancers (Basel). 2014;6(3):1408–40.

48. Yu H, Lee H, Herrmann A, Buettner R, Jove R. Revisiting STAT3 signalling in cancer: New and unexpected biological functions. Vol. 14, Nature Reviews Cancer. Nature Publishing Group; 2014. p. 736–46.

49. Levy DE, Lee C, Darnell J, Kerr I, Stark G, Levy D, et al. What does Stat3 do? J Clin Invest. 2002;109(9):1143–8.

50. Bromberg JF, Wrzeszczynska MH, Devgan G, Zhao Y, Pestell RG, Albanese C, et al. Stat3 as an oncogene. Cell. 1999;98(3):295–303.

51. Bommert K, Bargou RC, Stühmer T. Signalling and survival pathways in multiple myeloma. Eur J Cancer. 2006;42(11):1574–80.

52. Sikka S, Surana R, Dai X, Zhang J, Kumar AP, Tan BKH, et al. Targeting the STAT3 signaling pathway in cancer: Role of synthetic and natural inhibitors. Vol. 1845, Biochimica et Biophysica Acta - Reviews on Cancer. Elsevier; 2014. p. 136–54.

53. Hideshima T, Anderson KC. Molecular mechanisms of novel therapeutic approaches for multiple myeloma. Vol. 2, Nature Reviews Cancer. Nature Publishing Group; 2002. p. 927–37.

54. Manni S, Brancalion A, Mandato E, Tubi LQ, Colpo A, Pizzi M, et al. Protein kinase CK2 inhibition down modulates the NF-κB and STAT3 survival pathways, enhances the cellular proteotoxic stress and synergistically boosts the cytotoxic effect of bortezomib on multiple

myeloma and mantle cell Lymphoma Cells. Richards KL, editor. PLoS One. 2013;8(9):e75280.

55. Brown R, Yang S, Weatherburn C, Gibson J, Ho PJ, Suen H, et al. Phospho-flow detection of constitutive and cytokine-induced pSTAT3/5, pAKT and pERK expression highlights novel prognostic biomarkers for patients with multiple myeloma. Leukemia. 2015;29(2):483–90.

56. Yao Y, Sun Y, Shi M, Xia D, Zhao K, Zeng L, et al. Piperlongumine induces apoptosis and reduces bortezomib resistance by inhibiting STAT3 in multiple myeloma cells. Oncotarget. 2016;7(45):73497–508.

57. Zhu S, Wang Z, Li Z, Peng H, Luo Y, Deng M, et al. Icaritin suppresses multiple myeloma, by inhibiting IL-6/JAK2/STAT3. Oncotarget. 2015;6(12):10460–72.

58. Lin L, Benson DM, Deangelis S, Bakan CE, Li PK, Li C, et al. A small molecule, LLL12 inhibits constitutive STAT3 and IL-6-induced STAT3 signaling and exhibits potent growth suppressive activity in human multiple myeloma cells. Int J Cancer. 2012;130(6):1459–69.

59. Jung S-H, Ahn S, Choi H-W, Shin M-G, Lee S, Yang D-H, et al. STAT3 expression is associated with poor survival in non-elderly adult patients with newly diagnosed multiple myeloma. Blood Res. 2017;52(4):293.

60. Wada A, Ito A, Iitsuka H, Tsuneyama K, Miyazono T, Murakami J, et al. Role of chemokine CX3CL1 in progression of multiple myeloma via CX3CR1 in bone microenvironments. Oncol Rep. 2015;33(6):2935–9.

61. Catlett-Falcone R, Landowski TH, Oshiro MM, Turkson J, Levitzki A, Savino R, et al. Constitutive activation of Stat3 signaling confers resistance to apoptosis in human U266 myeloma cells. Immunity. 1999;10(1):105–15.

62. Shain KH, Yarde DN, Meads MB, Huang M, Jove R, Hazlehurst LA, et al. Beta-1 integrin adhesion enhances IL-6-mediated STAT3 signaling in myeloma cells: implications for microenvironment influence on tumor survival and proliferation. Cancer Res. 2009;69(3):1009–15.

63. Lin L, Yan F, Zhao D, Lv M, Liang X, Dai H, et al. Reelin promotes the adhesion and drug resistance of multiple myeloma cells via integrin β1 signaling and STAT3. Oncotarget. 2016;7(9):9844–58.

64. Rozovski U, Grgurevic S, Bueso-Ramos C, Harris DM, Li P, Liu Z, et al. Aberrant LPL expression, driven by STAT3, mediates free fatty acid metabolism in CLL cells. Mol Cancer Res. 2015;13(5).

65. Spaner DE, Lee E, Shi Y, Wen F, Li Y, Tung S, et al. PPAR-alpha is a therapeutic target for chronic lymphocytic leukemia. Leukemia. 2013;27(5):1090–9.

66. Belloni D, Marcatti M, Ponzoni M, Ciceri F, Veschini L, Corti A, et al. Angiopoietin-2 in bone marrow milieu promotes multiple myeloma-associated angiogenesis. Exp Cell Res. 2015;330(1):1–12.

67. Li Y, Guo Y, Tang J, Jiang J, Chen Z. New insights into the roles of CHOP-induced apoptosis in ER stress. Acta Biochim Biophys Sin (Shanghai). 2014;46(8):629–40.

68. Canino C, Luo Y, Marcato P, Blandino G, Pass HI, Cioce M. A STAT3-NFkB/DDIT3/CEBPβ axis modulates ALDH1A3 expression in chemoresistant cell subpopulations. Oncotarget. 2015;6(14):12637–53.

CHAPTER 3

The effect of STAT3 on primary multiple myeloma cells in 3D culture

A modified version of this chapter is in preparation for publication as "Huang, YH.; Almowaled, M.; Li, J.; Venner, C.P.; Sandhu, I.; Peters, A.; Lavasanifar, A.; Lai, R. The effect of STAT3 on primary multiple myeloma cells in 3D culture." I wrote the manuscript and conducted all the experiments. RL edited the manuscript. RL, AL and I designed experiments. CPV, IS and ACP provided patient bone marrow samples with patient consent. MA and JL provided assistance with bone marrow mononuclear cell extraction and flow cytometry analysis.

3.1. Introduction

Although immortalized human cancer cell lines have advanced cancer research since the 1950s, their suitability to represent real tumors was questioned recently. In fact, it was reported that 18 to 46% of human cancer cell lines are misidentified or cross-contaminated (1,2). Several comparative studies between primary cell lines and cell lines and found a remarkable difference at genomic profiles (3–5). Due to different growth conditions in artificial culture, it is expected that human cancer cell lines harbor gene mutations which are not seen in the natural disease. A comparative proteomic study between PMM cells and MM cell lines showed an upregulation of biosynthetic proteins including ribosomal subunits, chaperons and translational factors and a downregulation of immune response elements including complement receptors and MHC class I and II molecules (6). Most importantly, cancer cell lines do not retain the microenvironment elements which alter the behavior of cancer cells. MM is a hematological malignancy which known to heavily rely on extracellular interactions with the microenvironment (7). Preclinical evaluation of novel anti-myeloma agents such as daratumumab had been tested using PMM cells and are now approved to be used in the clinic (8,9). These reasons suggest primary cells as a better cell model for studying MM.

The major challenge of PMM cell culture is their rapid loss of cell viability in conventional culture even in the presence of stimulating cytokines and growth factors which are known to induce cell growth in MM cell lines (10). A three-dimensional (3D) reconstructed bone marrow matrix cell culture method was shown to maintain both the PMM cells and stromal cellular components for up to 30 days (11). However, the biochemical mechanism of how 3D culture maintains MM cell viability remained unknown. In **Chapter 2**, I showed that STAT3 signaling was activated in MM

cell lines in 3D cultured with 1-2 days, which is a phenomenon seen in >50% MM patients (12–14). Moreover, I found that 3D cultured MM cells underwent apoptosis after STAT3 inhibition, suggesting high dependence on STAT3 pathway in real MM. In contrast, no effect was seen in MM cells cultured conventionally. In this study, I question if STAT3 activity combined with 3D culture is essential for superior cell viability compared to conventional culture.

Here I employed the same 3D culture system to investigate its capability to maintain PMM cells freshly extracted from patients compared to conventional culture. To account for the interactions with the stromal cells, I did not purify the malignant MM cells and culture them alone. I used flow cytometry analysis to measure the cell viability ($CD38^+$) and STAT3 activity (pSTAT3 at Y705). Additionally, I modulated STAT3 activity to examine the effect on cell viability in both culture systems. This study provides understanding of the essential factors for long-term culturing of PMM cells.

3.2. Materials and Methods

3.2.1. PMM samples, 3D culture and Stattic/IL6 treatment

All procedures of patient sample handling were followed according to a protocol approved by HREBA (HREBA.CC-17-0591). MM Bone marrow aspirates with signed patient consent form were collected from Cross Cancer Institute at University of Alberta. Bone marrow mononuclear cells were extracted using Ficoll-Pague gradient solution (GE Health Care). The total viable cell number was estimated by trypan blue exclusion assay. The bone marrow mononuclear cells were subject to 3D culture as described previously (15). In brief, bone marrow mononuclear cells were resuspended in the reconstructed bone matrix containing 4 parts of Matrigel® (Corning), 2.5 parts

of 1 mg/ml fibronectin and 1 part of 2 mg/ml collagen I at a concentration of 1 million cells per 100 µl. 100 µl reconstructed bone matrix was loaded to each well on a 48-well plate pre-coated with reconstructed endosteum solution. After incubation at 37^{o}C for 1 hour, fresh bone marrow growth medium (BMGM, RPMI1460 medium supplied with 20% pooled human plasma from healthy donors) was added to the solidified reconstructed bone marrow matrix. Bone marrow mononuclear cells in 3D culture were harvested by dissolving in cell recovery solution (1xPBS with 5 mM EDTA, 1 mM Na3VO4 and 1.5 mM NaF solution. IL6 and Stattic lyophilized powder (Sigma) was dissolved in sterile water and DMSO, respectively, in a stock concentration of 10 µg/ml and 1 mg/ml, respectively. 3D cultured BMMCs were treated with 30 pg/ml IL6 every day for 3 days or with 0.4 µM and 4 µM Stattic once on day 2 for 24 hours.

3.2.2. Flow cytometry analysis

For CFSE staining, isolated bone marrow mononuclear cells were washed twice with DPBS (Gibco) and stained with 0.25 µM of CFSE in DPBS for 20 minutes in dark at room temperature prior to seeding in 3D culture. The cells at different time points were recovered from the 3D culture using cell recovery solution and washed with PBS twice before flow cytometry analysis using FACSCanto II (BD Biosciences). For CD38 staining, recovered 3D bone marrow mononuclear cells were washed in PBS twice and resuspended in 50 µl PBS containing 10 µl anti-CD38-PE (Santa Cruz) in dark at room temperature for 20 minutes. The cells were washed one time in PBS and subject to flow cytometry analysis using FACSCanto II. The same number of cells stained with isotype anti-mouse-PE were included as a reference control. For CD38-pSTAT3 double staining, recovered 3D bone marrow mononuclear cells were fixed in 2% paraformaldehyde at 37oC for 10 minutes. The cells were washed in PBS with 1% BSA once and permeabilized with

100% methanol on ice for 30 minutes. The cells were then washed twice in PBS with 1% BSA and resuspended in 50 µl PBS with 10 µl anti-CD38-PE and 5 µl anti-pSTAT3-FITC (Santa Cruz) in dark at room temperature for 20 minutes. The cells were washed one time in PBS with 1% BSA and subject to flow cytometry analysis using FACSCanto II. The data was analyzed by FlowJo program version 10 (Becton, Dickinson & Company).

3.3. Results

3.3.1. PMM cells are preserved significantly better in 3D culture

To address the question of whether PMM cells can be better preserved in 3D culture, I cultured BMMCs isolated from 13 consecutive myeloma patients in 3D and conventional culture simultaneously. Using flow cytometry, I assessed the number of PMM cells, as identified by the CD38 expression, in the sample on day 3, 7 and 10. The viability of the total cell population in the samples was assessed by performing the trypan blue exclusion assay. Thus, the absolute viable PMM cell counts were determined by multiplying the total viable cells (i.e. trypan blue) and the percentage of $CD38^+$ cells.

As shown in **Figure 3.1A**, the PMM cell numbers (after normalization to day 0) on day 3 were significantly higher in 3D than in conventional. Specifically, MM cases resulted in higher viability of $CD38^+$ MM cells 3 days in 3D culture compared to conventional culture (60% versus 27% of day 0, p=0.010, paired Student's t-test). Similarly, $CD38^+$ cell viability in 3D culture was significantly higher on day 7 (36% versus 21%, p=0.028, paired Student's t-test, **Figure 3.1B**) and day 10 (32% versus 14%, p=0.029, paired Student's-test, data not shown). Since the most

dramatic difference in CD38$^+$ cell viability between the two culture systems was seen on day 3, we used this time point for further experiments.

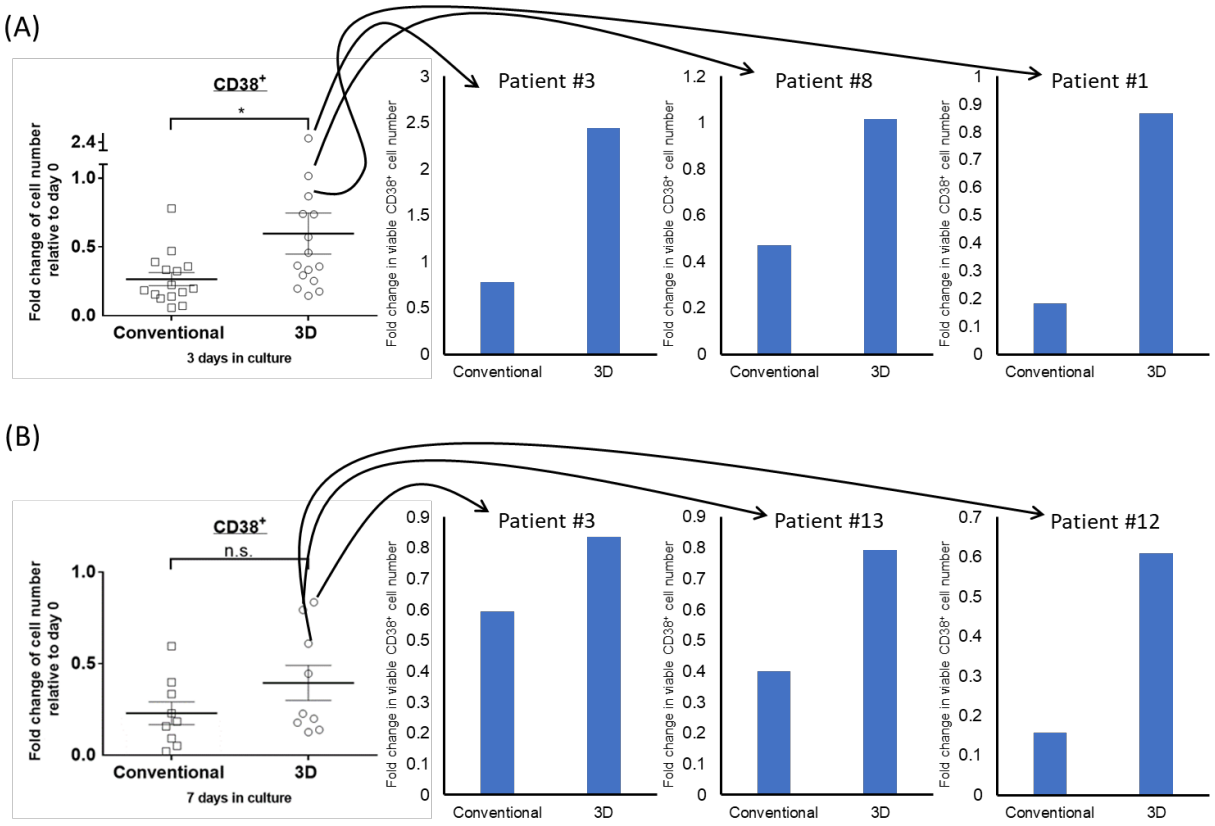

Figure 3.1. PMM cells are better preserved in 3D culture compared to conventional culture. Fold change of viable CD38$^+$ cell numbers from MM patients in conventional or 3D culture on (A) day 3 (n=15) and (B) day 7 (n=11) relative to day 0. The mean value was indicated with error bars representing standard error. *p<0.05, paired Student's t-test. Three representative cases for each day were shown.

3.3.2. PMM cell proliferation rate is similar between 3D and conventional culture

To determine if the superior cell viability in 3D is due to more rapid cell proliferation, I compared the proliferation rate of CD38$^+$ cells by CFSE staining in two culture methods. In principle, the number of CD38$^+$CFSE$^+$ cells is expected to decrease as the cells divide over time.

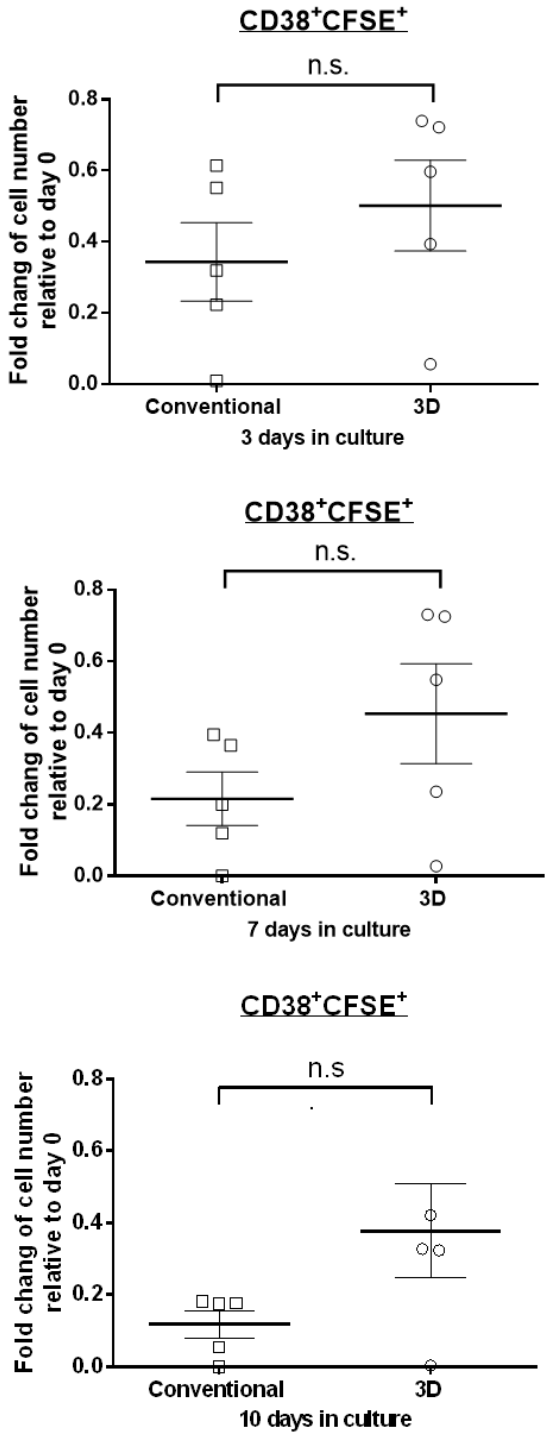

Figure 3.2. PMM cells in 3D did not proliferate more rapidly than those in conventional culture. Fold change of viable $CD38^{+}CFSE^{+}$ cell number from 5 MM patients in conventional or 3D culture on day 3, 7 and 10 relative to day 0. Cells were stained with 0.25 μM CFSE on day 0.

The mean value was indicated with error bars representing standard error. n.s. not significant, paired Student's t-test.

As shown in **Figure 3.2**, I found that in 5 of 5 MM cases, there is no significant difference in the fold change of $CD38^+CFSE^+$ cells between the two culture systems on day 3 (34% and 50% of day 0 for conventional and 3D culture, respectively, p=0.300, paired Student's t-test). A similar finding was observed on day 7 and day 10 (p=0.128 and p=0.076, respectively, paired Student's t-test). This finding suggests that the superior MM cell viability in 3D culture is not due to higher cell proliferation rate relative to conventional culture.

3.3.3. STAT3 is more active in PMM cells cultured in 3D culture

I previously reported that STAT3 is required for maintaining the cell viability of 2 MM cell lines (U266 and RPMI8226) in 3D culture but not in conventional culture (**Figure 2.3**). In light of this concept, I asked if STAT3 plays a role in maintaining a PMM cell viability in 3D culture. I assessed the STAT3 activity in PMM cells by double-staining the BMMCs from MM patients with CD38 and pSTAT3 (Y705) antibodies. As shown in **Figure 3.3A**, I found significantly more total viable $CD38^+pSTAT3^+$ cells remained in 3D culture after 3 days compared to conventional culture. Specifically, in 5 of 5 MM samples, the average fold change of $CD38^+pSTAT3^+$ cell number in 3D and conventional culture relative to day 0 was 0.66 and 0.10 fold, respectively (p=0.008, paired Student's t-test). Consistent with this finding, I observed a higher $CD38^+$ cell viability in 3D culture compared to conventional culture (0.17- and 0.36-fold of day 0, respectively, p=0.003, paired Student's t-test) as shown in **Figure 3.3B**. These findings suggest that $CD38^+$ MM cell viability is maintained in 3D culture due to the relatively higher STAT3 activity compared to conventional culture.

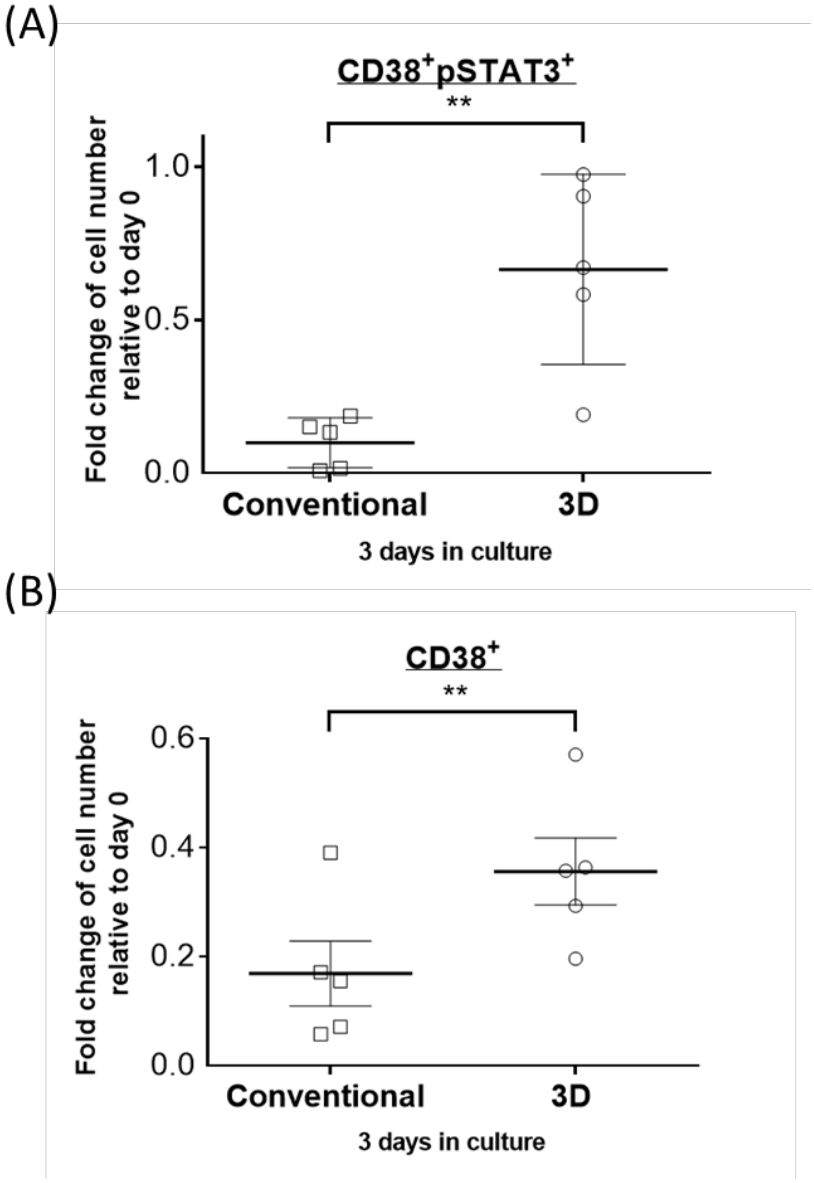

Figure 3.3. STAT3 activity is higher in PMM cells cultured in 3D. Fold change of viable $CD38^+pSTAT3^+$ (A) and $CD38^+$ (B) cell number from 5 MM patients in conventional or 3D culture on day 3 relative to day 0. The mean value was indicated with error bars representing standard error. **p<0.001, paired Student's t-test.

3.3.4. IL6 further improves PMM cell viability in 3D but not conventional culture

I next asked if the addition of IL6, the most well-known source of STAT3 activation in MM will help improve $CD38^+$ cells viability in both culture systems (16). I treated the BMMCs in the two

(A)

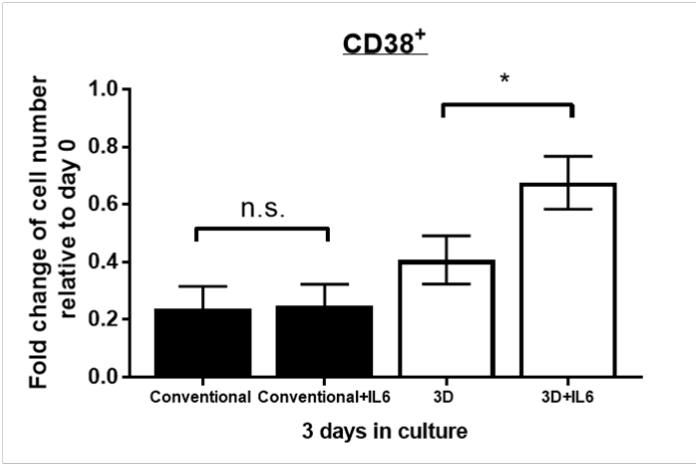

(B)

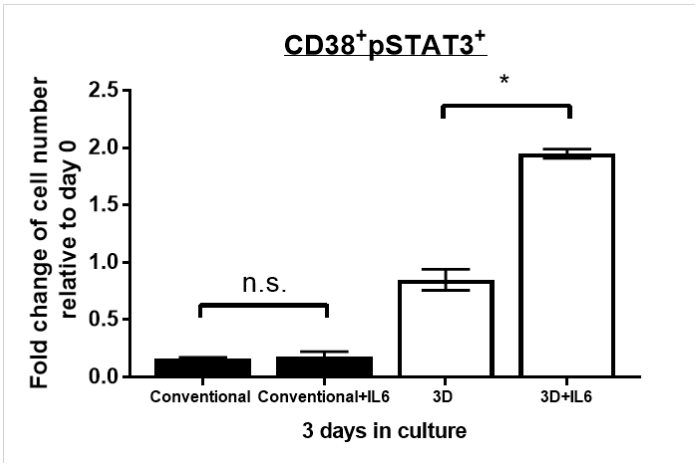

Figure 3.4. IL6 improved PMM cell viability in 3D but not in conventional culture. Fold change of viable $CD38^+$ (A) and $CD38^+pSTAT3^+$ (B) cell number from 3 MM patients in conventional or 3D culture on day 3 relative to day 0. 30 pg/ml IL6 was added to cells every 24 hours for 3 days. The mean value was indicated with error bars representing standard error. n.s. not significant, *$p<0.05$, paired Student's t-test.

culture systems with 30 pg/ml IL6, which is the average serum concentration measured in Stage III MM patients (17), every day for 3 days. As shown in **Figure 3.4A**, I found that IL6 led to a significant increase of the total viable $CD38^+$ cell numbers in 3D culture on day 3. Specifically, in 3 of 3 MM samples, treatment of IL6 led to a significant increase in viable $CD38^+$ cell number

from 0.41 fold to 0.68 fold relative to day 0 in 3D culture (p=0.021, paired Student's t-test). On the other hand, no significant difference was observed in conventional culture after treatment of IL6 (p=0.689, paired Student's t-test). Correlating with these findings, I observed a significant increase of $CD38^+pSTAT3^+$ cell number from 0.85 fold to 1.95 fold relative to day 0 in the presence of IL6 in 3D culture on day 3 (p=0.014, paired Student's t-test, **Figure 3.4B**). No increase in $CD38^+pSTAT3^+$ cell number was seen in conventional culture after IL6 treatment (p=0.737, paired Student's t-test, **Figure 3.4B**). This result suggests that MM cells in 3D culture are more prone to IL6-dependent STAT3 activation, which leads to further improved cell viability.

3.3.5 Stattic reduces PMM cell viability in 3D culture but not in conventional culture

Given the positive correlation between STAT3 activity and the survival of MM cells in 3D culture, I next asked if inhibition of STAT3 ablates MM cell viability. According to **Chapter 2**, compared to conventional culture, about 10-fold higher drug dose is required to achieve equivalent drug-protein binding in 3D culture. In keeping with this, I treated the BMMCs from MM patients in 3D culture with two different doses of Stattic (0.4 and 4 μM) required to substantially bind to STAT3 in U266 cells cultured conventionally and in 3D, respectively (**Figure 2.5A**). As shown in **Figure 3.5A**, in 3 of 3 MM cases, the total number of viable $CD38^+$ MM cells significantly decreased from 0.38 to 0.17 fold relative to day 0 in 3D culture after treated with 4 μM Stattic for 24 hours on day 3 (p=0.038, paired Student's t-test). On the other hand, the $CD38^+$ cell number was unchanged in 2D culture after the treatment of both 0.4 and 4 μM Stattic for 24 hours on day 3 (p=0.245 and p=0.478, respectively, paired Student's t-test). Consistent with these findings, the $CD38^+pSTAT3^+$ cell number in 3D significant decreased from 0.82 fold to 0.09 fold relative to day 0 in the presence of 4 μM Stattic (p=0.010, paired Student's t-test), and no significant change

(A)

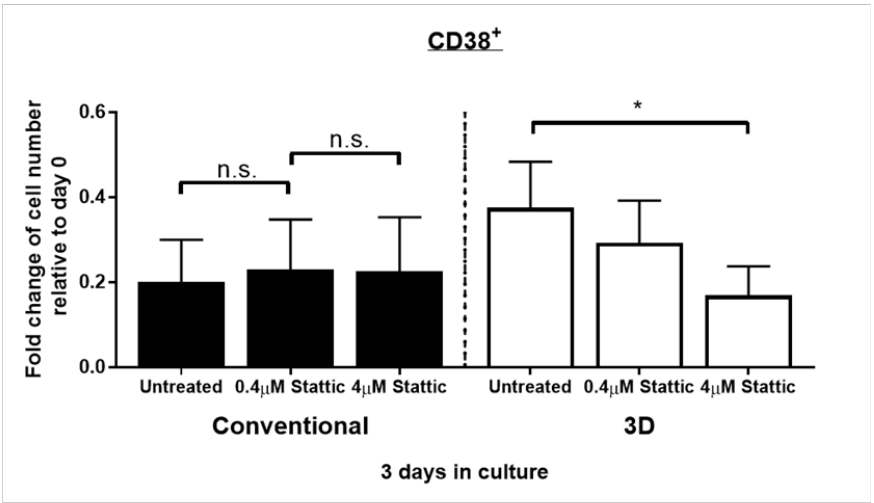

(B)

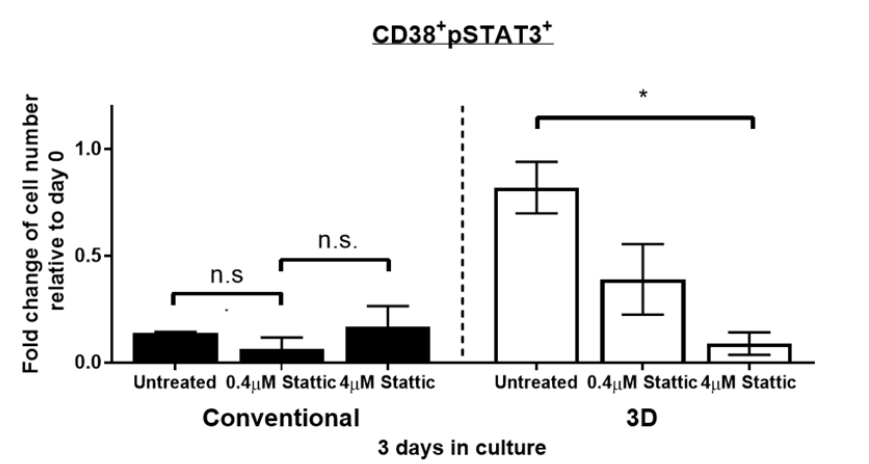

Figure 3.5. Stattic ablates PMM cell viability in 3D culture but not in conventional culture. Fold change of viable $CD38^+$ (A) and $CD38^+pSTAT3^+$ (B) cell number from 3 MM patients in conventional or 3D culture on day 3 relative to day 0. 0.4 or 4 μM Stattic was added to cells on day 2 for 24 hours. The mean value was indicated with error bars representing standard error. n.s. not significant, *$p<0.05$, paired Student's t-test.

was seen in conventional culture in the presence of both 0.4 and 4 μM Stattic ($p=0.278$ and $p=0.496$, respectively, paired Student's t-test) (**Figure 3.5B**). These results suggest that STAT3 activity contributes to superior MM cell viability in 3D culture but not in conventional culture.

3.4. Discussion

Primary cancer cells as a model provide a more realistic aspect of MM biology and a more precise evaluation of therapeutics for MM. For example, preclinical assessment of daratumumab on PMM cells showed that it improved the cell lysis induced by lenalidomide or bortezomib in refractory MM via activation of NK cells (8). Studies like these often applied treatment to cells immediately after extraction from patients. Additionally, the drug treatment usually did not exceed 48 hours because it is technically challenging to maintain primary cancer cells in conventional culture. A previous study profiled that the cell viability of purified $CD138^+$ PMM cells decreased to 20% within 3 days in conventional culture (10). This explains why most reported drug treatment experiments using PMM cells rarely exceed 48 hours after cell aspiration from patients.

Attempts have been made to increase the longevity of PMM cells in culture. In one study, it was shown in one MM case that the presence of IL6, VEGFR and IGF1, together with bone marrow stromal cells from healthy donor, resulted in increased viable PMM cell number from ~5% to ~40% of that on day 0 in conventional culture on day 7 (10). Another study reported that $CD138^+$ PMM cells from 4 MM patients cultured on a monolayer of human fetal bone marrow stromal cells stably expended from 30,000 cells to around 50,000 cells in 14 days (18). However, the fetal bone marrow stromal cells used in this study were collected from the femurs of 8-12 weeks old human fetuses after simultaneously abortion, which are technically infeasible to obtain. In another study, the authors used human pooled plasma (20%), instead of FCS, in a hope to increase the lifespan of PMM in conventional culture. It was found that the cell viability of $CD138^+$ PMM cells from 38 patients cultured with 20% pooled plasma patient sustained significantly more PMM cells on day 3 compared to those cultured with 10% FCS (60% vs. 40% of day 0) (19). A research group

suggested an animal model implanted with polymeric scaffold and human bone marrow stromal cells for *in vivo* enrichment of PMM cells (20). After injecting PMM cells from 10 patients into the scaffold, the serum paraprotein concentration in xenografted mice raised from 0 to at least 250 ng/ml after 80 days, suggesting the development of MM. However, it was also mentioned that this method will take at least a month for the tumor to develop. A microfluidic device was proposed to mimic the blood flow in the bone marrow to constantly nourish PMM cells with fresh growth medium (21). However, it was found that the PMM cell numbers (marked by $CD138^+$ or $CD38^+CD56^+$) significantly decreased from 4000 cells to 170 cells (4%) within 7 days in 3 MM patients. Moreover, this study did not include conventionally cultured PMM cells for comparison, hence it is hard to conclude if it is a better culture method compared to conventional culture. Another group has employed 3D tissue-engineered bone marrow culture to increase the viability of PMM cells (22). In this study, bone marrow mononuclear cells from 3 patients together with human endothelial cells were seeded into 3D culture. The cell proliferation was measured by the Ki67 staining and analyzed by flow cytometry. It was found that the $CD138^+$ PMM cells in 3D cultured showed a 2.5-fold increase in cell proliferation in 7 days, whereas those in conventional culture did not change their proliferation rate. However, this finding appears to contradict with the biology of myelomas, which are known to be slowly proliferative (<7% Ki-67 positivity in 35 MM patients) (23). Overall, I believe that more studies are needed to establish a more technically feasible method to keep PMM alive *in vitro* without substantially modifying their natural biological behavior.

While I adopted the method that is similar to that published by Kirshner *et al*. (11,24), I employed a different approach to estimate the number of viable PMM by combining both flow cytometric

analysis of $CD38^+$ percentage and trypan blue staining of viable BMMCs. Kirshner et al. demonstrated that 3D cultured PMM cells underwent cell proliferation via the disappearance of CFSE staining for up to 25 days in 4 patients. However, the change of PMM cell viability was not reported. Here I showed that 10% of PMM cell viability remained after 10 days in 3D culture with a relatively high number of patient samples (n=11). Importantly, I have included conventionally cultured PMM cells for comparison and found a significant higher PMM cell viability was maintained in 3D compared to conventional culture on day 3. I also reported that addition of IL6 can further improve the sustainability of PMM cells in 3D culture. Additionally, IL6 did not improve the cell viability of PMM cells, suggested the importance of 3D environment in inducing IL6-dependent STAT3 activation. This finding is different from what was found using human MM cell lines, where IL6 induces STAT3 activation and cell growth (25), suggesting that MM cell lines do not sufficiently reflect the true MM tumor *in vivo*.

I previously showed that STAT3 is activated in MM cell lines in 3D culture compared to conventional culture (**Chapter 2**). Moreover, blocking STAT3 induced apoptosis in 3D cultured MM cells but had no effect in conventionally cultured MM cells. In keeping with this concept, I asked if STAT3 activity is essential for maintaining the viability of PMM cells. STAT3 activity in PMM cells has been investigated with different parameters in three independent studies. Bharti *et al.* examined the activity of STAT3 using immunofluorescence staining of STAT3 and found that $CD138^+$ cells from >50% of 22 MM patients showed strong nuclear STAT3 staining which implicated high STAT3 transcriptional activity (12). In another study using flow cytometric analysis, it was shown that about 5-fold more $CD38^{++}$ cells were pSTAT3 (Y705)-positive in MM patients as compared to healthy donors (13). The third study reported that around 50% of 48 cases

showed pSTAT3 (Y705) positivity in $CD138^+$ MM cells by immunohistochemical analysis (14). The level of pSTAT3 (Y705) is positively correlated with poor progression-free survival and overall survival with hazard ratios of 3.7 and 3.5, respectively (26). These findings suggest the importance of STAT3 activity in PMM.

I demonstrated that STAT3 inhibition by Stattic induced significant cytotoxicity to PMM cells in 3D culture but not 2D culture. This finding is consistent to my previous finding that STAT3 is a much more important therapeutic target in MM cell lines cultured in 3D (**Figure 2.5C**). In support of this concept, some STAT3 inhibitors such as Icaritin and LLL12 have shown their ability to inhibit the cell growth of STAT3-active PMM cells in conventional culture (27,28). However, these studies did not account for the loss of cell viability and STAT3 activity during STAT3 inhibitor treatment, which may lead to underestimation of the potency of STAT3 inhibition *in vivo*. My study highlighted the dependence on STAT3 activity for PMM cells in the context of 3D environment, providing insight on targeting STAT3 and microenvironment as a promising strategy for treatment of MM.

In conclusion, this chapter provides an insight on the superiority of 3D culture in supporting the growth of PMM cells. In addition, I demonstrated that 3D cultured PMM cells are dependent on PMM STAT3 activity for superior cell viability compared to conventional culture. Prolonged longevity of PMM cells in 3D allowed long-termed gene manipulations and/or drug treatment for studying MM in a more realistic manner.

3.5. References

1. Huang Y, Liu Y, Zheng C, Shen C. Investigation of cross-contamination and misidentification of 278 widely used tumor cell lines. Talamas-Rohana P, editor. PLoS One. 2017;12(1):e0170384.
2. MacLeod RAF, Dirks WG, Matsuo Y, Kaufmann M, Milch H, Drexler HG. Widespread intraspecies cross-contamination of human tumor cell lines arising at source. Int J Cancer. 1999;83(4):555–63.
3. Sun Y, Liu Q. Deciphering the correlation between breast tumor samples and cell lines by integrating copy number changes and gene expression profiles. Biomed Res Int. 2015;2015:1–11.
4. Li A, Walling J, Kotliarov Y, Center A, Steed ME, Ahn SJ, et al. Genomic changes and gene expression profiles reveal that established glioma cell lines are poorly representative of primary human gliomas. Mol Cancer Res. 2008;6(1):21–30.
5. Gillet J-P, Varma S, Gottesman MM. The Clinical Relevance of Cancer Cell Lines. JNCI J Natl Cancer Inst. 2013;105(7):452–8.
6. Fernando RC, de Carvalho F, Mazzotti DR, Evangelista AF, Braga WMT, de Lourdes Chauffaille M, et al. Multiple myeloma cell lines and primary tumors proteoma: protein biosynthesis and immune system as potential therapeutic targets. Genes Cancer. 2015;6(11–12):462–71.
7. Bianchi G, Munshi N. Pathogenesis beyond the cancer clone (s) in multiple myeloma. Blood. 2015;125(20):3049–59.
8. Nijhof IS, Groen RWJ, Noort WA, Van Kessel B, De Jong-Korlaar R, Bakker J, et al. Preclinical evidence for the therapeutic potential of CD38-Targeted Immuno-chemotherapy in multiple Myeloma patients refractory to Lenalidomide and Bortezomib. Clin Cancer Res.

2015;21(12):2802–10.

9. van der Veer MS, de Weers M, van Kessel B, Bakker JM, Wittebol S, Parren PWHI, et al. Towards effective immunotherapy of myeloma enhanced elimination of myeloma cells by combination of lenalidomide with the human CD38 monoclonal antibody daratumumab. Haematologica. 2011;96(2):284–90.

10. Zlei M, Egert S, Wider D, Ihorst G, Wäsch R, Engelhardt M. Characterization of in vitro growth of multiple myeloma cells. Exp Hematol. 2007;35(10):1550–61.

11. Kirshner J, Thulien KJ, Martin LD, Debes Marun C, Reiman T, Belch AR, et al. A unique three-dimensional model for evaluating the impact of therapy on multiple myeloma. Blood. 2008;112(7):2935–45.

12. Bharti AC, Shishodia S, Reuben JM, Weber D, Alexanian R, Raj-Vadhan S, et al. Nuclear factor–κB and STAT3 are constitutively active in CD138 + cells derived from multiple myeloma patients, and suppression of these transcription factors leads to apoptosis. Blood. 2004;103(8):3175–84.

13. Brown R, Yang S, Weatherburn C, Gibson J, Ho PJ, Suen H, et al. Phospho-flow detection of constitutive and cytokine-induced pSTAT3/5, pAKT and pERK expression highlights novel prognostic biomarkers for patients with multiple myeloma. Leukemia. 2015;29(2):483–90.

14. Quintanilla-Martinez L, Kremer M, Specht K, Calzada-Wack J, Nathrath M, Schaich R, et al. Analysis of signal transducer and activator of transcription 3 (Stat 3) pathway in multiple myeloma: Stat 3 activation and cyclin D1 dysregulation are mutually exclusive events. Am J Pathol. 2003;162(5):1449–61.

15. Parikh MR, Belch AR, Pilarski LM, Kirshner J. A Three-dimensional tissue culture model

to study primary human bone marrow and its malignancies. J Vis Exp. 2014;(85):e50947–e50947.

16. Guo Y, Xu F, Lu T, Duan Z, Zhang Z. Interleukin-6 signaling pathway in targeted therapy for cancer. Vol. 38, Cancer Treatment Reviews. 2012. p. 904–10.

17. Kamińska J, Koper OM, Dymicka-Piekarska V, Motybel E, Kłoczko J, Ke-Mona H. Angiogenic cytokines: IL-6, sIL-6R, TNF-α, sVCAM-1, and PDGF-AB in multiple myeloma patients depending on the stage of the disease. Edorium J Tumor Biol Edorium J Tumor Bio. 2015;22:11–9.

18. Vincent L, Jin DK, Karajannis MA, Shido K, Hooper AT, Rashbaum WK, et al. Fetal Stromal − Dependent Paracrine and Intracrine Vascular Endothelial Growth Factor-A / Vascular Endothelial Growth Factor Receptor-1 Signaling Promotes Proliferation and Motility of Human Primary Myeloma Cells. 2005;(8):3185–92.

19. Quinn J, Glassford J, Percy L, Munson P, Marafioti T, Rodriguez-Justo M, et al. APRIL promotes cell-cycle progression in primary multiple myeloma cells: Influence of D-type cyclin group and translocation status. Blood. 2011;117(3):890–901.

20. Calimeri T, Battista E, Conforti F, Neri P, Di Martino MT, Rossi M, et al. A unique three-dimensional SCID-polymeric scaffold (SCID-synth-hu) model for in vivo expansion of human primary multiple myeloma cells. Leukemia. 2011;25(4):707–11.

21. Zhang W, Lee WY, Siegel DS, Tolias P, Zilberberg J. Patient-specific 3D microfluidic tissue model for multiple myeloma. Tissue Eng Part C Methods. 2014;20(8):663–70.

22. de la Puente P, Muz B, Gilson RC, Azab F, Luderer M, King J, et al. 3D tissue-engineered bone marrow as a novel model to study pathophysiology and drug resistance in multiple myeloma. Biomaterials. 2015;73:70–84.

23. Gastinne T, Leleu X, Duhamel A, Moreau AS, Franck G, Andrieux J, et al. Plasma cell growth fraction using Ki-67 antigen expression identifies a subgroup of multiple myeloma patients displaying short survival within the ISS stage I. Eur J Haematol. 2007;79(4):297–304.

24. Zhang W, Gu Y, Sun Q, Siegel DS, Tolias P, Yang Z, et al. Ex Vivo Maintenance of Primary Human Multiple Myeloma Cells through the Optimization of the Osteoblastic Niche. Wu M-H, editor. PLoS One. 2015;10(5):e0125995.

25. Catlett-Falcone R, Landowski TH, Oshiro MM, Turkson J, Levitzki A, Savino R, et al. Constitutive activation of Stat3 signaling confers resistance to apoptosis in human U266 myeloma cells. Immunity. 1999;10(1):105–15.

26. Jung S-H, Ahn S, Choi H-W, Shin M-G, Lee S, Yang D-H, et al. STAT3 expression is associated with poor survival in non-elderly adult patients with newly diagnosed multiple myeloma. Blood Res. 2017;52(4):293.

27. Zhu S, Wang Z, Li Z, Peng H, Luo Y, Deng M, et al. Icaritin suppresses multiple myeloma, by inhibiting IL-6/JAK2/STAT3. Oncotarget. 2015;6(12):10460–72.

28. Lin L, Benson DM, Deangelis S, Bakan CE, Li PK, Li C, et al. A small molecule, LLL12 inhibits constitutive STAT3 and IL-6-induced STAT3 signaling and exhibits potent growth suppressive activity in human multiple myeloma cells. Int J Cancer. 2012;130(6):1459–69.

CHAPTER 4

Conjugation of Anti-CD38 on polymers carrying STAT3 inhibitor as a therapy for multiple myeloma

A modified version of this chapter is in preparation for publication as "Huang, YH; Vakili, M.R.; Molavi, O.; Morrissey, Y.; Wu, CS.; Paiva, I.; Soleimani, A.H.; Lavasanifar, A.; Lai, R. Conjugation of Anti-CD38 on polymers carrying STAT3 inhibitor exhibited improved in vitro and in vivo anti-myeloma efficacy." I wrote the manuscript and conducted all the experiments. RL, OM and AL edited the manuscript. RL, AL, OM, MV and I designed experiments. MV synthesized the nanoparticles. OM, YM and I purified the CD38 antibody. IP and AS provided assistance with animal imaging. CW and MV provided assistance with in vitro experiments.

4.1. Introduction

Nanoparticles have been used as a drug delivery system which can encapsulate hydrophobic therapeutic compounds. In addition, nanoparticle-encapsulated drugs significantly increase the size, preventing leakage from capillary vessels into normal tissues and hence increasing accumulation at the tumor site. Nanoparticles conjugated with a tumor-specific antibody (ACNs) further increased their targeting ability and reduced toxicity to normal cells (1). For example, different forms of nanoparticles conjugated with anti-human epidermal receptor-2 (HER2) have been developed for HER2-positive breast cancer cells (2–5). It has been reported that ACNs resulted in superior cellular uptake and cytotoxicity *in vitro* as well as more tumor suppression *in vivo* compared to the unconjugated counterparts (5–10). ACNs can be used to target drug resistance cancer cells which overexpress drug efflux pumps (e.g. p-glycoprotein) on the cell membrane (6,11). ACNs are capable of targeting molecules which involve in the process of cancer development such as vascular endothelial growth factor receptor (VEGFR) for tumor angiogenesis (10) and matrix metalloproteinases (MMP) for tumor invasion (12). Moreover, ACNs can cross through the blood-brain barrier via receptor-mediated endocytosis to reach tumor cells in the brain (13). Due to these advantages, the studies on different formulations of ACNs have increased dramatically in the past decade.

Multiple myeloma (MM) is a hematological disease which is incurable because it always relapses and becomes refractory to chemotherapy. Signal transducer and activator of transcription 3 (STAT3) is found to be active in more than 50% of MM patients and is associated with resistance to bortezomib, thalidomide and dexamethasone (14–17). Due to the great oncogenic potential of STAT3 in MM, its inhibition was postulated as a therapeutic strategy. Many STAT3 inhibitors

have been reported to induce apoptosis in various STAT3-active cancer cells such as Stattic, S3I-201 and S3I-1757 (18–20). However, their non-specific distribution (in normal tissues and tumor) and high hydrophobicity result in off-target toxicity and poor therapeutic efficacy in patients. For example, a clinical trial of OPB-31121, an orally available STAT3 inhibitor reported more than 80% of patients experienced nausea or diarrhea and no partial response was seen in any patient (21). A previously published nanoparticular formulations by Lavasanifar Lab based on poly(ethylene oxide)-*block*-poly(α-benzyl carboxylate-ε-caprolactone) (PEO-*b*-PBCL) of a STAT3 inhibitor, S3I-1757 (denoted as Null-S3I-NP) have shown potential to address the shortcomings of free S3I-1757. Null-S3I-NP has been shown to substantially increase the size and water solubility of S3I-1757 (22). Moreover, Null-S3I-NP exhibited better tumor suppression and survival in animals with subcutaneously xenografted melanoma tumors (22).

ACNs have been evaluated in a variety of solid cancer models but are less explored in hematological cancer models. For diseases like MM with great cell heterogeneity and complex interactions with stromal cells, MM cell-specific targeting and drug delivery are highly demanding. In this study, my colleague Dr. Mohammad Vakili conjugated a monoclonal antibody against human CD38 (a surface marker highly expressed in MM cells) on the surface of Null-S3I-NP, namely CD38-S3I-NP, to enhance the MM-targeting ability. I hypothesized CD38-S3I-NP to show improved MM cellular uptake, *in vitro* cytotoxicity and *in vivo* efficacy compared to Null-S3I-NP due to its higher specificity against MM cells. The validity of this hypothesis was tested as reported in this manuscript in a series of *in vitro* and *in vivo* studies. For *in vitro* studies, I used two MM cell lines stimulated with interleukin-6 (IL6) to activate their STAT3. For *in vivo* study, I xenografted MM tumor in severe combined immunodeficient (SCID) mice by tail vein injection

of U266 cells stably expressing luciferase gene (U266-luc). This study also shed light on the possibility of customizing a nanoparticle formulation to improve the anti-cancer activity of encapsulated therapeutics in hematological cancer therapy.

4.2 Materials and Methods

4.2.1. Materials and cell culture

S3I-1757 (white powder with molecular weight of 521.6 g/mol, soluble in DMSO) was obtained from Glixx Laboratories (Southborough, MA, USA). Methoxy-PEO (average molecular weight of 5000 g/mol), diisopropylamine (99%), benzyl chloroformate (tech 95%), sodium (in kerosin), butyllithium (Bu-Li) in hexane (2.5 M solution), palladium-coated charcoal, pyrene and Cremophor® EL were purchased from Sigma Aldrich (St. Louis, MO, USA). α-benzyl carboxylate ε-caprolactone was prepared by Alberta Research Chemicals Inc (ARCI). Stannous octoate was purchased from MP Biomedicals Inc., Germany. All other chemicals were reagent grade. U266 and SupM2 cells were purchased from ATCC. RPMI8226 cells are a gift from Dr. Linda Pilarski. The cells were cultured in RPMI 1460 medium with L-glutamine (Life Technology), 10% FBS (Life technology) and, 100U/ml penicillin/streptomycin (Sigma Aldrich). All cells were incubated at 37^{o}C supplied with 5% atmospheric CO_2.

4.2.2. Purification of anti-CD38 antibody

The hybridoma cells (TBH-7) producing humanized anti-CD38 were cultured in RPMI1460 medium supplied with 10% fetal bovine serum. When the cells were confluent, they were transferred to RPMI1460 medium with 10% ultra low IgG fetal bovine serum (Gibco). The cell supernatant was collected after 48 hours. 150 ml of supernatant was concentrated to 5 ml using

Amicon Ultra-15 Centrifugal Filter Unit (Millipore). The concentrated supernatant was incubated in NAb™ Protein A/G Spin Column (ThermoFisher) for 10 minutes. The bound antibody was eluted out using the elution buffer (ThermoFisher). The concentration of purified anti-CD38 was measured by NanoDrop™ 1000 Spectrophotometer (ThermoFisher). The purified anti-CD38 was dialysed in sterile PBS overnight prior to nanoparticle conjugation.

4.2.3. Preparation of nanoparticles

Poly-(ethylene oxide)-*block*-poly-(α-benzyl carboxylate ε-caprolactone) (PEO-*b*-PBCL) was synthesized using the method previously described (23). In brief, α-benzyl carboxylate ε-caprolactone was mixed with methoxy-poly-(ethylene oxide) at 1:1.12 weight ratio with trace amount of stannous octoate. The reaction mixture was incubated for 4 hours at 140ºC in the vacuum oven and stopped by cooling the reaction at room temperature overnight. Null-NP was prepared from PEO-*b*-PBCL block copolymers as previously described (22). In brief, 20 mg of block copolymer was dissolved in tetrahydrofuran was mixed with 2 mg S3I-1757 dissolved in DMSO. The mixture was incubated at room temperature with stirring overnight. The excess S3I-1757 was removed by centrifugation. For anti-CD38 conjugation, anti-CD38 was mixed with 2-imidothiolane at room temperature, at pH 8.0 to synthesize thiolated anti-CD38. The maleimide PEO-*b*-PBCL was prepared by following a previously established protocol (24). Micellized maleimide PEO-*b*-PBCL was mixed with thiolated anti-CD38. The anti-CD38 conjugated nanoparticles were mixed with Null-S3I-NP in water to form CD38-S3I-NP through post-insertion method. The size and polydispersity index of Null-S3I-NP and CD38-S3I-NP were measured by Zetasizer Nano®. The S3I-1757 concentrations in CD38-S3I-NP and Null-S3I-NP were measured by high-performance liquid chromatography (HPLC) using a previously established protocol (22).

For the synthesis of Cy5.5-conugated nanoparticle, a previously described protocol was followed (25). Empty nanoparticles with and without anti-CD38 were synthesized as the no drug loading controls for the *in vitro* cell viability assay.

4.2.4. *In vitro* release assay

In vitro release assay was carried out as previously described (22). In brief, 1 ml of CD38-S3I-NP or Null-S3I-NP was put in a semi-permeable dialysis bag (molecular weight cutoff: 12,000-14,000 kDa). The bag was placed in sterile PBS and incubated in a shaking water bath at 37^{o}C. A 50 µl aliquot from the dialysis bag was collected at various time points for S3I-1757 concentration measurement by HPLC analysis. To maintain the total volume, 50 µl of PBS was added back to the dialysis bag after aliquot collection.

4.2.5. Cellular uptake assay

Nanoparticles conjugated with Cy5.5 (amount equivalent to 0.2 ng Cy5.5) was added to 1.0x10^{6} U266, RPMI8226 and SupM2 cells and cultured at 37^{o}C in dark for 4 hours. Cells were wash with sterile PBS twice and subject to flow cytometry (BD FACSCantoII) analysis using the Per-Cy5.5-APC fluorescence channel.

4.2.6. *In vitro* cell viability assay

Cell proliferation was assessed by CellTiter 96® AQueous one solution cell proliferation MTS assay (Promega). Approximately 2.5x10^{4} U266 or RPMI8226 cells were seeded in each well of a 96-well plate and treated for 24 or 48 hours. 20 µl 3-(4,5-dimethylthiazol-2-yl)-5-(3-carboxymethoxyphenyl)-2-(4-sulfophenyl)-2H-tetrazolium (MTS) was added to each well. The

absorbance of light at 490 nm was measured by FLUOstar OPTIMA microplate reader (BMG Labtech). The IC_{50} values were calculated by Graph Prism 7 from the cell viability versus logarithm of concentration curve.

4.2.7. Western blot analysis

Total cell lysates were prepared and lysed with 1X RIPA buffer (10X stock solution from Millipore) with protease inhibitor and phosphatase inhibitor cocktails (Millipore) on ice for 30 minutes. Protein concentrations were measured Pierce™ BCA Protein Assay Kit (Thermo Scientific). Cell lysates treated with SDS were subject to SDS-PAGE and transferred onto a nitrocellulose membrane. The membrane was probed with anti-pSTAT3 (Y705) (1:2000, CST, #9145), anti-STAT3 (1:1000, CST#124H6), and anti-β-actin (1:1000, CST, #58169) diluted in 5% BSA in TBS-Tween20 (0.05%, v/v). These antibodies were probed with HRP-conjugated anti-mouse (1:2000, CST, #7076) and anti-rabbit (1:2000, CST, #7074). The membrane was washed three times with TBST after secondary antibody treatment. The bands on membrane were developed with Pierce™ ECL western blotting substrate (Thermo Scientific) and exposed to X-ray films (Fuji).

4.2.8. *In vivo* studies using MM xenograft

The experimental protocols for all *in vivo* studies in this manuscript were approved by Animal Care and Use Committees, University of Alberta (#AUP00000282). Half of a million U266 cells stably expressing luciferase gene (U266-luc) was injected in SCID mice (Jackson, strain NOD.Cg-Prkdcscid Il2rgtm1Wjl/SzJ) intravenously. Twelve days after injection, 100 µl of Null-S3I-NP or CD38-S3I-NP colloidal dispersions in dextrose 5 % was injected to the mice intravenously via tail

vein for two consecutive days at a dose of 3 mg/kg per day. The tumor size was measured by quantifying the total flux of bioluminescence signals detectable (radiance ranged between 4.00 x 10^5 and 1.00 x 10^7 p/sec/cm^2/scr) on the ventral side of each animal at various time points using Living Image Software (PerkinElmer). At the endpoint defined by the score sheet (**Appendix**), the animals were euthanized and the bone marrow cells within the femur were collected and split into two portions. One portion was stored at -80^{o}C as cell pellets for Western blot analysis and another was stored in 4% paraformaldehyde at 4^{o}C for immunocytochemistry.

4.2.9. Immunocytochemistry

Mouse bone marrow cells in 4% paraformaldehyde (Sigma) was pelleted and resuspended in liquid histogel (Thermo Scientific) and transferred to a 15x15 mm^2 plastic mold (Leica). Upon solidified, the cell-histogel was subject to processing and embedding. The cell blocks were sectioned in 5-μm slides. Slides were rehydrated in xylene and decreasing concentrations of ethanol. The antigens were retrieved using 1X citrate buffer (Sigma) by microwaving in a pressure cooker for 20 minutes. The pSTAT3 antibody (Santa Cruz, clone B-7) was diluted as 1:50 in antibody diluent (DAKO). MACH2 mouse HRP polymer (Biocare Medical) was used as a secondary antibody. The chromogen and substrate were mixed and applied to each slide for 2 minutes for color development (DAKO).

4.3. Results

4.3.1. Synthesis and characterization of CD38-S3I-NP

To generate CD38-S3I-NP, monoclonal anti-CD38 antibodies were conjugated to the hydrophilic portion of PEO-*b*-PBCL. As illustrated in **Figure 4.1A**, anti-CD38 was first thiolated at the lysine

residues located on the constant portion of the heavy chain of the antibody. Thiolated anti-CD38 was then reacted with maleimide-functionalized PEO-*b*-PBCL, such that antibodies are attached to the surface of polymers. Lastly, CD38-conjugated polymers were mixed with NP loaded with S3I-1757 (i.e. Null-S3I-NP), to generate CD38-S3I-NP.

I then determined if the anti-CD38 conjugation had altered the physical and pharmacologic properties of Null-S3I-NP, as outlined in **Table 2.1**, the average size of CD38-S3I-NP was 91.4±9.4 nm, which is not significantly different from that of Null-S3I-NP (97.4±5.2 nm) ($p=0.39$). The polydispersity index was significantly higher in CD38-S3I-NP compared to that of Null-S3I-NP (0.367±0.016 versus 0.273±0.003, $p<0.001$). Thus, CD38-S3I-NP was significantly less uniform in size compared to Null-S3I-NP, suggesting that CD38-S3I-NP may be more prone to dissociation *in-vivo*. Similarly, there is no significant difference in drug encapsulation efficiency between CD38-S3I-NP and Null-S3I-NP (81.6±7.2% versus 87.0±9.2%, $p=0.469$) as well as drug loading (14.7±1.3% versus 15.7±1.7%, $p=0.469$). To assess the stability of CD38-S3I-NP in encapsulating S3I-1757 compared to Null-S3I-NP, I measured the amount of S3I-1757 released from CD38-S3I-NP or Null-S3I-NP over time. As shown in **Figure 4.1B,** significantly more S3I-1757 was released from CD38-S3I-NP than that from Null-S3I-NP after 1, 2 and 4 hours of incubation ($p<0.001$, $p<0.001$ and $p=0.002$, respectively). Nevertheless, both formulations reached a comparable amount of S3I-1757 release (~68%, $p=0.593$) at 24 hours.

Table 4.1. Physical properties of Null-S3I-NP and CD38-S3I-NP

Nanoparticle formulation	Average size (nm)	Polydispersity Index	Drug encapsulation efficiency (%)	Drug loading (weight %)
S3I-NP	97.4 ± 5.2	0.273 ± 0.003	87.0 ± 9.2%	15.7 ± 1.7%
CD38-S3I-NP	91.4 ± 9.4*	0.367 ± 0.016*	81.6 ± 7.2%	14.7 ± 1.3%

*$p<0.05$, compared to Null-S3I-NP

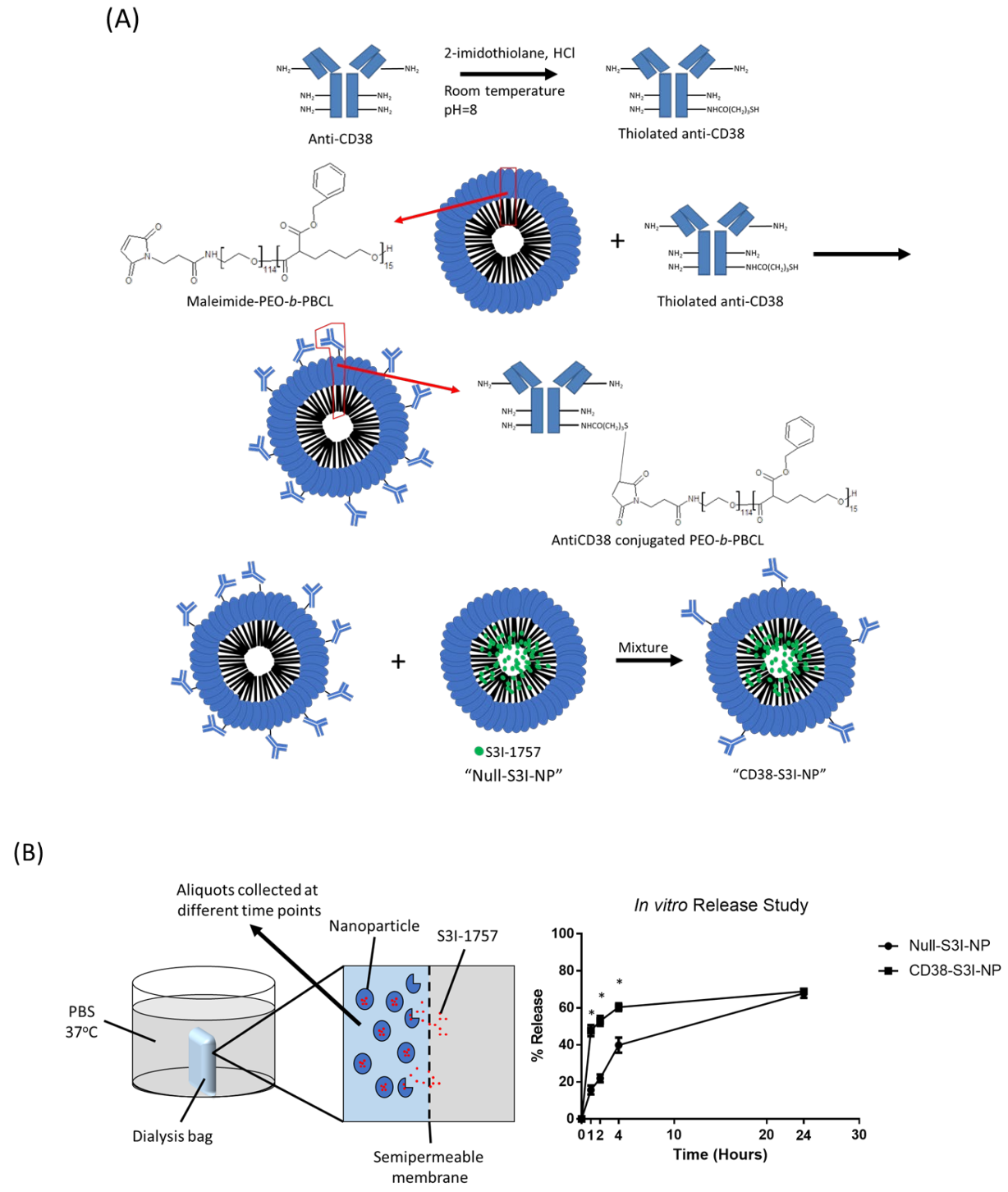

Figure 4.1. Synthesis and characterization of CD38-S3I-NP. (A) Chemical reactions of anti-CD38 conjugation to nanoparticular formulation PEO-*b*-PBCL. The final product was mixed with Null-S3I-NP to generate CD38-S3I-NP. (B) Release of S3I-1757 from Null-S3I-NP or CD38-S3I-NP *in vitro*. The percentage of S3I-1757 released was calculated by the lost amount of S3I-1757

compared to the initial total amount of S3I-1757. The error bar represents standard deviation from a triplicate experiment, *p<0.05, Student's t-test.

4.3.2. Anti-CD38 conjugation improves cellular uptake of nanoparticles by MM cells

I then determined if the conjugation of anti-CD38 to NP can significantly improve the uptake of NP by MM cells. To facilitate the detection and quantification of NP in vitro, Dr. Mohammad Vakili helped me synthesize Cy5.5 (a fluorophore)-conjugated NP with or without anti-CD38 coating (denoted as Cy5.5-CD38-NP and Cy5.5-Null-NP, respectively). NP used in these experiments was not loaded with the STAT3 inhibitor to avoid drug-induced cytotoxicity, which can potentially falsely elevate the level of NP uptake. Two MM cell lines (U266 and RPMI8226) were used. SupM2, an ALK-positive anaplastic large cell lymphoma cell line, was used as a negative control. The CD38 expression in the two MM cell lines and the absence of CD38 expression in SupM2 are illustrated in **Figure 4.2A and 4.2B**. As shown in **Figure 4.3**, both MM cell lines incubated with Cy5.5-CD38-NP for 4 hours exhibited a significantly higher level of intracellular Cy5.5 level compared to cells incubated with Cy5.5-Null-NP. Specifically, in U266 cells, Cy5.5-CD38-NP treatment yielded 43.2±0.1% Cy5.5-positive cells whereas Cy5.5-Null-NP treatment resulted in only 0.4±0.1% Cy5.5-positive cells ($p<0.001$). Similarly, in RMMI8226 cells, Cy5.5-CD38-NP yielded significantly higher Cy5.5-positive cells than Cy5.5-Null-NP treatment (76.7±1.1% versus 1.2±0.1%)($p<0.001$). Compared to the background (i.e. no treatment), Cy5.5-CD38-NP only minimally increased the proportion of Cy5.5-positive cells in SupM2 cells (9.2±0.3%).

4.3.3. CD38-S3I-NP is more cytotoxic to MM cells with STAT3-inhibiting ability compared to Null-S3I-NP

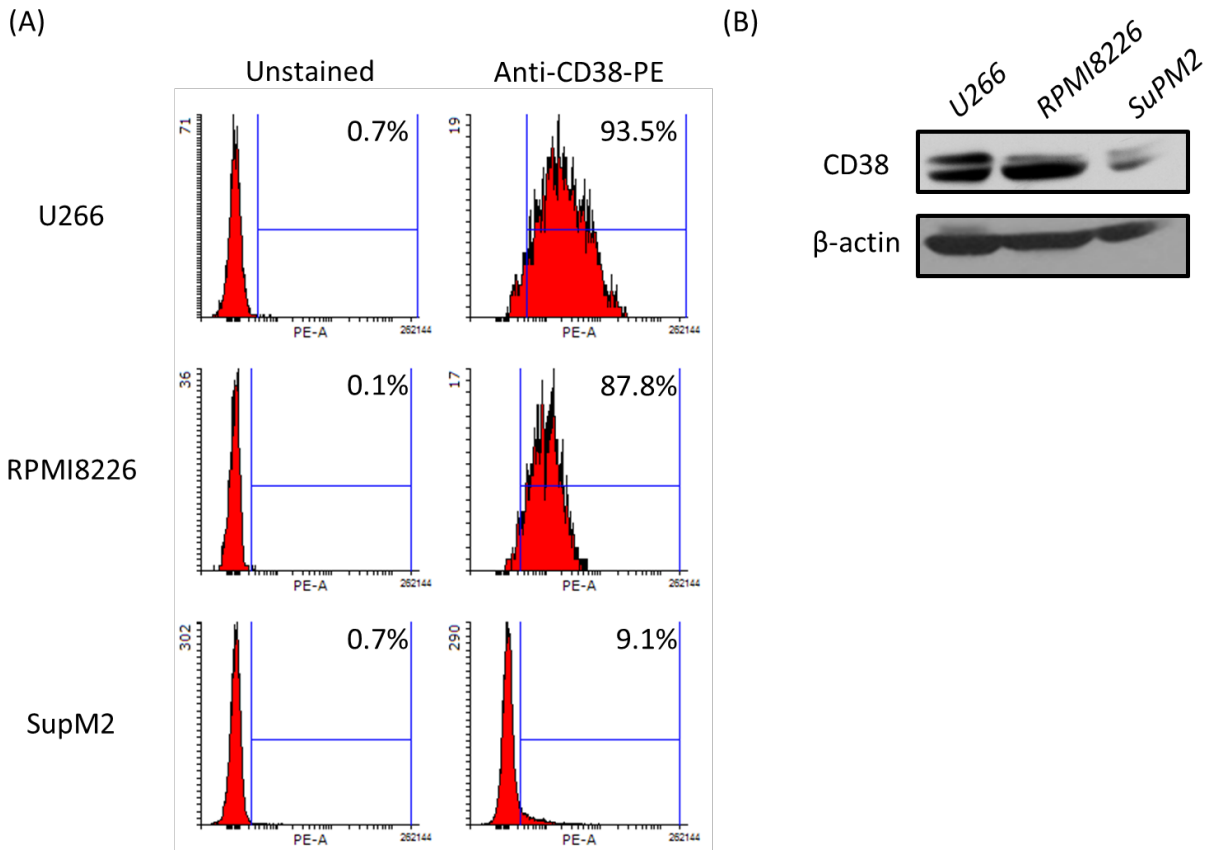

Figure 4.2. MM cell lines express high levels of CD38. Protein expression levels of CD38 measured by (A) Western blot analysis and (B) flow cytometry analysis in two MM cell lines (U266 and RPMI8226) and one non-MM cell line (SupM2). The gating of CD38 positivity in flow cytometry analysis was based on the unstained MM cells. β-actin was measured as a loading control for Western blot analysis.

I next assessed the cytotoxicity of CD38-S3I-NP compared to Null-S3I-NP in two MM cell lines (U266 and RPMI8226) using MTS assay. In these experiments, I added exogenous IL6 (2 ng/ml) to the cell culture to enhance STAT3 activity in the two MM cell lines. As shown in **Figure 4.4A**, in RPMI8226 cells, CD38-S3I-NP led to significantly lower cell viability compared to Null-S3I-NP at 50 μM at 48 hours (p=0.001). In U266 cells, significantly lower cell viability of CD38-S3I-NP was seen at 100 μM compared to Null-S3I-NP (p=0.007). In contrast, while there was a

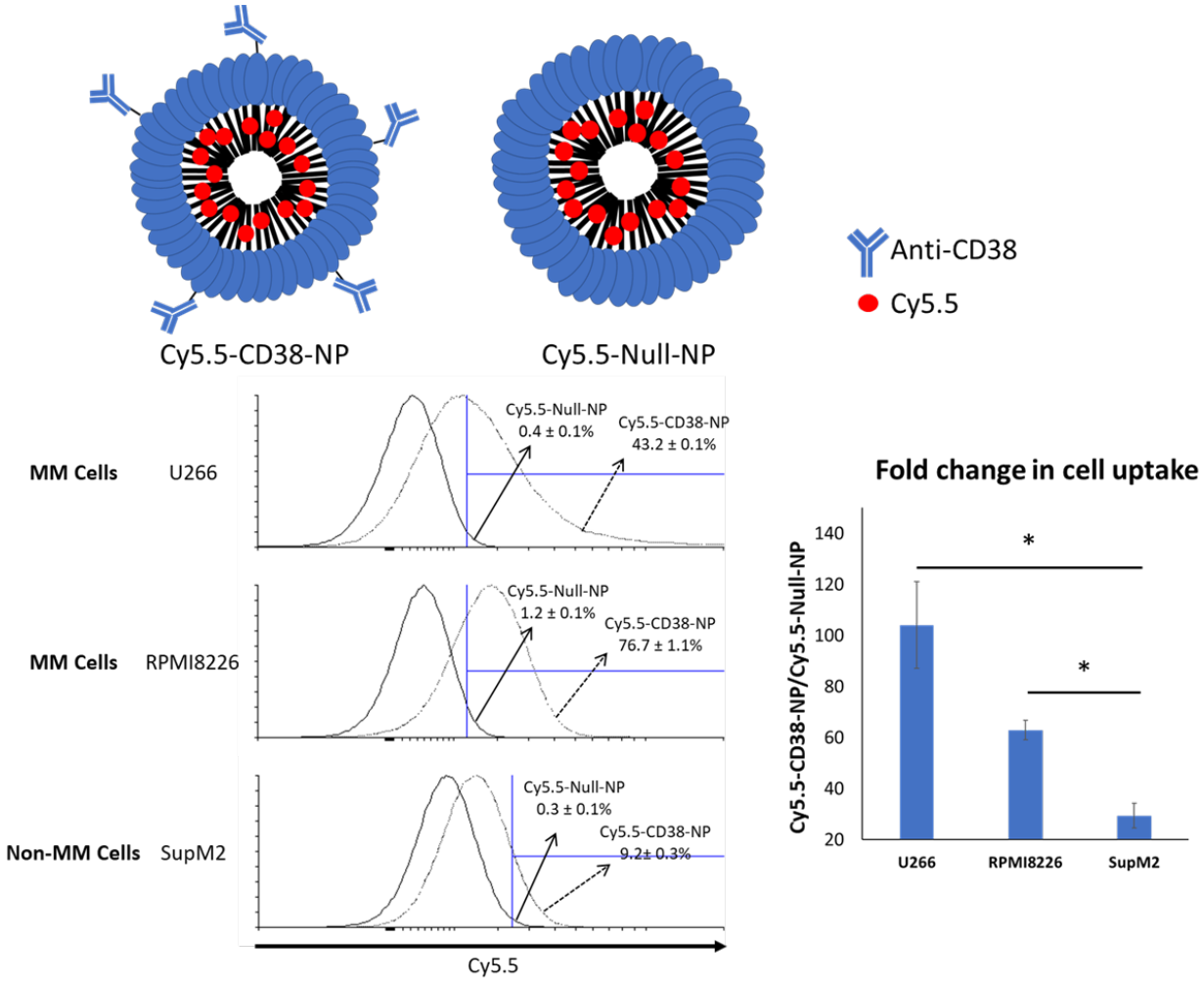

Figure 4.3. Anti-CD38-conjugated NP exhibits improved cellular uptake of S3I-1757 by MM cells. Flow cytometry analysis of Cy5.5-positive cell population 4 hours after treatment of Cy5.5-Null-NP or Cy5.5-CD38-NP. Cy5.5 was attached at the core of nanoparticles as illustrated in the top panel. The gated area was defined using the cells without any drug treatment. The representative dot plot from a triplicate experiment was shown. The error values represent standard deviation from the triplicate experiment. A non-MM cell line, SupM2 was included for comparison. The fold change in cell uptake was calculated by dividing the percentage of Cy5.5-positive cells with Cy5.5-CD38-NP treatment by that with Cy5.5-Null-NP treatment. The error bar represents standard deviation from a triplicate experiment, *$p<0.05$, Student's t-test.

significant reduction in the cell viability of SupM2 (approximately 50% at 100 μM, 48 hours) with either CD38-S3I-NP or Null-S3I-NP, there was no significant difference between the two formulations. As a comparison, we treated these cell lines with Null-NP and free CD38 antibodies. As shown in **Figure 4.4A**, this treatment resulted in a significant reduction in cell viability in all of these three cell lines, although the effect was not significantly different from Null-S3I-NP. The inhibitory concentration at 50% (IC_{50}) values generated from these experiments are summarized in **Table 4.2**.

In the same experiments, we also directly assessed the inhibitory effects of CD38-S3I-NP and Null-S3I-NP on STAT3 phosphorylation at residue Y705 (i.e. pSTAT3). Using Western blot analysis, we found that pSTAT3 induced by IL6 at 2 ng/ml was substantially decreased by Null-S3I-NP and CD38-S3I-NP at 24 hours (**Figure 4.4B**).

4.3.4. CD38-S3I-NP poses superior tumor-suppressive activity *in vivo*

To further elucidate if CD38-S3I-NP has therapeutic advantages over Null-S3I-NP, I employed a SCID mouse xenograft model. As detailed in section 4.2., I xenografted U266 cells stably expressing a luciferase expression construct (U266-luc) in SCID mice, such that the growth of tumors can be easily tracked ex-vivo using bioluminescence imaging. When the tumors became detectable, Null-S3I-NP or CD38-S3I-NP was injected intravenously. At 15 days after the injection of nanoparticular formulations, 4/4 animals in the Null-S3I-NP group reached the endpoints as defined in **Appendix**, while 1/4 animals in the CD38-S3I-NP group did not. Statistical analysis reveals a trend for a longer survival for the CD38-S3I-NP group, although the difference between the two groups does not reach statistical significance (p=0.079, Mantel-Cox test), most

likely due to the small sample size. As a control, both mice treated with PBS reached the endpoints on day 12.

(A)

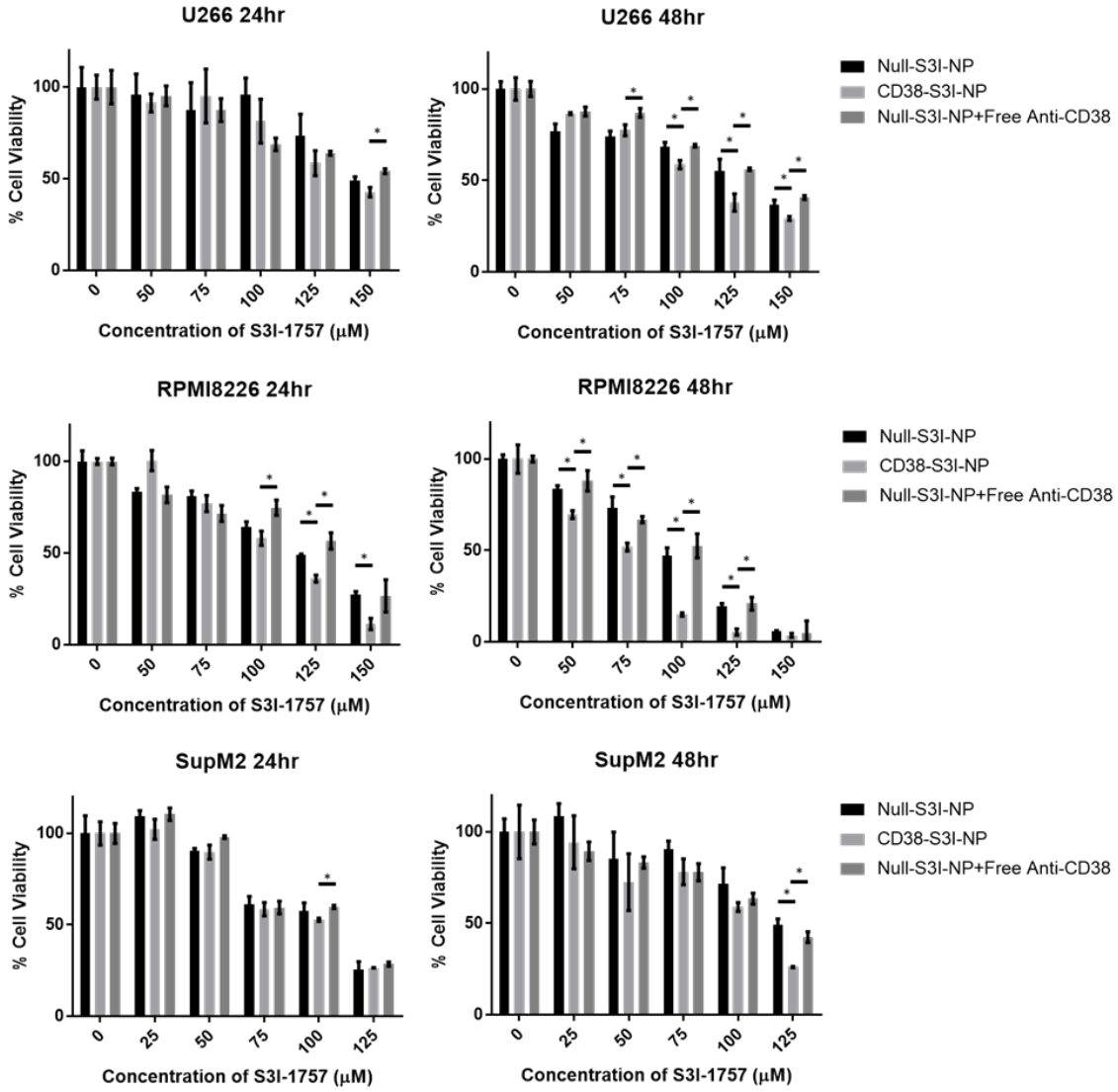

Figure 4.4. CD38-S3I-NP induces cytotoxicity and inhibits STAT3 activity in MM cells. (A) U266 and RPMI8226 cells were then treated with Null-S3I-NP or CD38-S3I-NP with the presence of IL6 (2 ng/ml) for 24 hours. Cell viability was measured using MTS cell viability assay in triplicate, *p<0.05, Student's t-test.

(B)

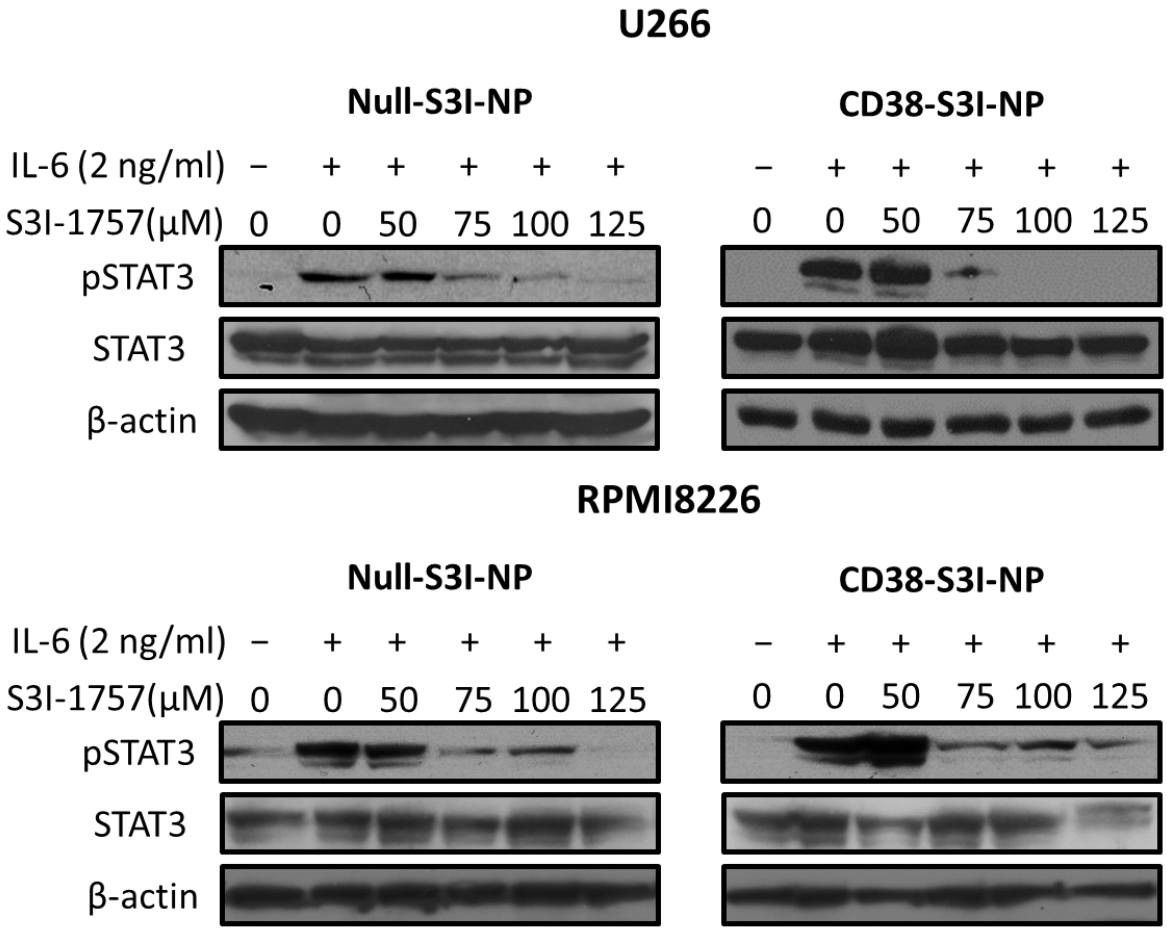

Figure 4.4 (cont'd). CD38-S3I-NP induces cytotoxicity and inhibits STAT3 activity in MM cells. (B) Western blot analysis of STAT3 and pSTAT3 levels in U266 and RPMI8226 cells treated with Null-S3I-NP or CD38-S3I-NP with the presence of IL6 (2 ng/ml) for 24 hours. β-actin was blotted as a loading control.

Other than the time needed to reach the endpoints, I also directly assessed tumor growth in the two study groups. Specifically, I summed up the levels of detectable bioluminescence (radiance ranged between 4.00 x 10^5 and 1.00 x 10^7 p/sec/cm^2/scr) by IVIS Spectrum *In Vivo* Imaging System. Images of a representative animal from each of the CD38-S3I-NP, Null-S3I-NP and PBS group are shown in **Figure 4.5A**. Animals in the CD38-S3I-NP group had a significantly lower tumor

Table 4.2. IC_{50} values of U266, RPMI8226 and SupM2 cells with different drug treatment

Cell line	Treatment	IC_{50} (μM)	
		24 hours	48 hours
U266	Null-S3I-NP	136.7-163.6	115.4-148.6 *
	CD38-S3I-NP	127.7-151.3	106.3-114.0 *
	Null-S3I-NP+Free Anti-CD38	143.5-172.4	128.6-139.4
RPMI8226	Null-S3I-NP	110.9-124.5 *	88.2-98.1 *
	CD38-S3I-NP	100.4-109.8	64.0-73.6 *
	Null-S3I-NP+Free Anti-CD38	108.9-142.2	87.2-99.5
SupM2	Null-S3I-NP	88.8-105.6	110.4-144.8
	CD38-S3I-NP	86.0-98.9	83.16-119.4
	Null-S3I-NP+Free Anti-CD38	90.1-110.0	106.9-134.9

*$p<0.05$
Range values represent 95% confidence intervals.

mass compared to the Null-S3I-NP group at 240 and 288 hours ($p=0.018$ and $p=0.006$, respectively) (**Figure 4.5A**). Since I had only two animals in the PBS group and the statistical significance cannot be determined, it is apparent that tumors grew substantially faster than those in the CD38-S3I-NP group, and perhaps, the Null-S3I-NP group.

I then assessed if the differences in tumor growth and survival between the CD38-S3I-NP and Null-S3I-NP groups correlates with a difference in STAT3 down-regulation. To achieve this goal, I extracted bone marrow cells from specific bone fragments in which the involvement by MM was confirmed by the expression of bioluminescence. The expression of pSTAT3 was then detected using Western blot analysis and immunocytochemistry. As shown in **Figure 4.5B**, pSTAT3 immunocytochemistry was performed and I found that MM cells from the CD38-S3I-NP group had no or barely detectable pSTAT3 signal, whereas MM cells from the Null-S3I-NP group had a

(A)

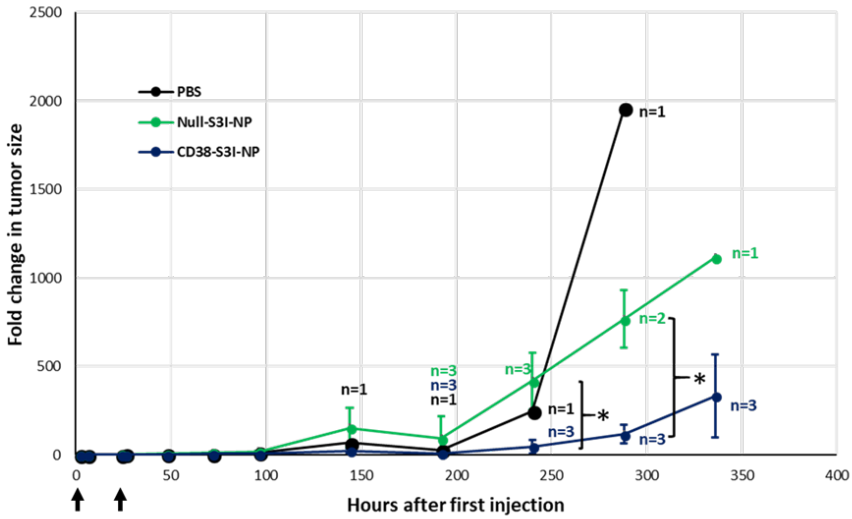
PBS
Null-S3I-NP
CD38-S3I-NP
Fold change in tumor size
Hours after first injection
n=1
n=3
n=2
*

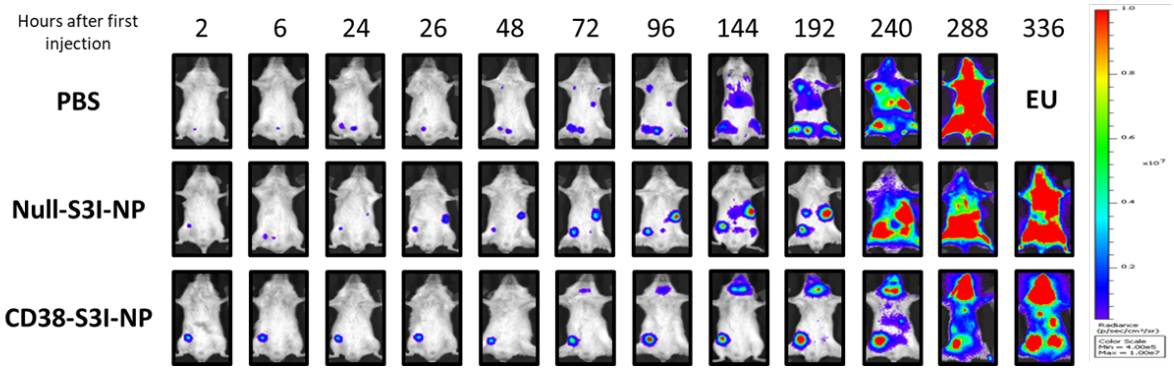
Hours after first injection
2
6
24
26
48
72
96
144
192
240
288
336
PBS
Null-S3I-NP
CD38-S3I-NP
EU

(B)

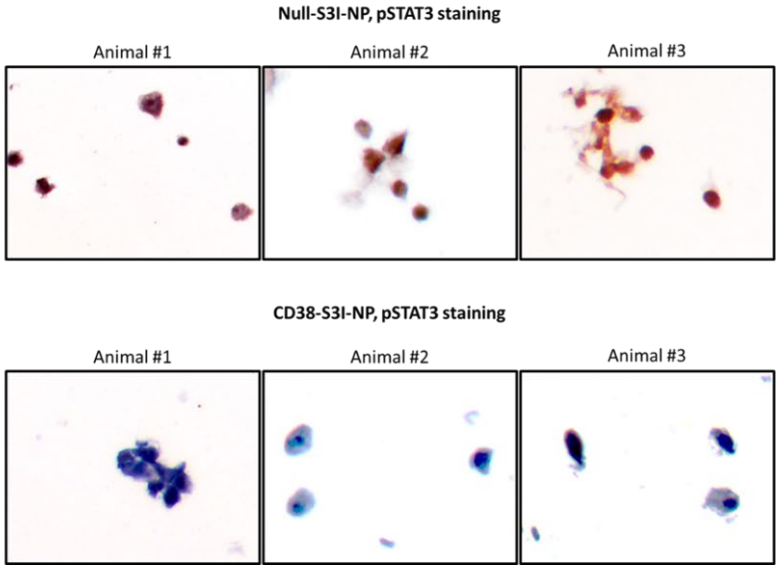
Null-S3I-NP, pSTAT3 staining
Animal #1
Animal #2
Animal #3
CD38-S3I-NP, pSTAT3 staining
Animal #1
Animal #2
Animal #3

(C)

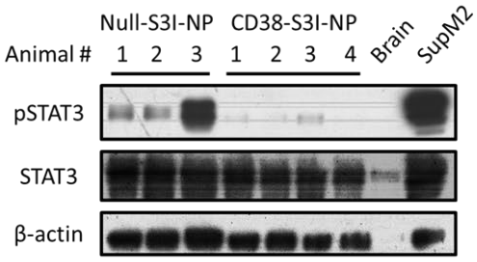
Null-S3I-NP
CD38-S3I-NP
Animal #
1 2 3 1 2 3 4
Brain
SupM2
pSTAT3
STAT3
β-actin

Figure 4.5. CD38-S3I-NP is more tumor suppressive than Null-S3I-NP in MM xenograft. (A) SCID mice intravenously injected with PBS (n=2), 3 mg/kg Null-S3I-NP (green line, n=4) or CD38-S3I-NP (blue line, n=4) everyday for two days. Animal numbers other than the initial numbers at different time points are indicated. The tumor size was quantified by the bioluminescence intensity and normalized to the initial bioluminescence signal (i.e. 2 hours post-injection). The representative bioluminescence images of animals treated with PBS, Null-S3I-NP or CD38-S3I-NP were shown. *$p<0.05$, Student's t-test. EU euthanized. (B) The pSTAT3 levels in bone marrow mononuclear cells extracted from the SCID mice in (A) at the endpoint. A non-tumorous brain tissue from a SCID mouse was used as a negative control. SupM2 cells were used as a positive control for pSTAT3. β-actin was blotted as a loading control. (C) Immunocytochemical staining of pSTAT3 and in bone marrow mononuclear cells from (B). Each image represents bone marrow cells from one animal. The images were taken at a magnification of 400X.

relatively strong pSTAT3 signal in most of the cells examined. This difference in pSTAT3 expression was confirmed by Western blot analysis (**Figure 4.5C**).

4.4. Discussion

Nanoparticle drug delivery systems are known to significantly improve the drug retention time in the bloodstream and lead to drug accumulation at the tumor sites, by a mechanism known as the enhanced retention and permeability effect (26). This is owed to the large size of nanoparticles compared to the free drug which prevents leakage from normal blood vessels but not from the relatively sparse vasculature within the tumor, resulting in passive accumulation of nanoparticles to the tumor. It is believed that ACNs help further target tumor cells with specific surface markers. Improved cell uptake of ACNs is believed to enhance the therapeutic efficacy *in vitro* and *in vivo*. One study reported that conjugation of trastuzumab (a HER2 antibody) on doxorubicin-carrying

iron oxide nanoparticles resulted in 5-fold more cellular uptake after 24 hours in HER2-positive SK-BR-3 cells compared to HER2-negative MCF-7 cells (5). Correlated with this, it was found that trastuzumab-conjugated nanoparticles induced three times more cell killing in SK-BR-3 cells compared to MCF-7 cells after 24 hours. Moreover, it was found that conjugated nanoparticles were substantially accumulated in the subcutaneous SK-BR-3 tumor after 24 hours, which led to 50% more tumor reduction compared to plain nanoparticles (5). Increased uptake of ACNs also prevents the uptake by normal cells and reduced immune response against nanoparticles, leading to less off-target effect and sequestering of nanoparticles by macrophage endocytosis *in vivo*. Specifically, in a study, nanoparticles conjugated with HER2 antibody resulted in 82% less macrophages cell uptake and 56% less tumor necrotic factor-alpha (TNFα), an inflammatory cytokine, release by macrophages (27).

CD38 is a transmembrane enzyme as well as an internalizing epitope that is highly expressed in a variety of hematological malignancies including MM and some subtypes of leukemia and non-Hodgkin lymphoma (28–36). CD38 catalyzes the production of cyclic ADP ribose from NAD+, an important stimulator for intracellular release of calcium from endoplasmic reticulum lumen into the cytoplasm (37). The activity of CD38 is tightly associated with B cell migration, proliferation and differentiation (38,39). Daratumumab is the first human CD38 antibody approved by Food and Drug Administration for treatment of MM which triggers complement-dependent cytotoxicity and antibody dependent cell-mediated cytotoxicity (40,41). Daratumumab can also induce programmed cell death of MM cells independent of the immune system (42). Finally, daratumumab blocks the enzymatic activity of CD38, resulting in the accumulation of toxic substrate NAD+ which may be lethal to MM cells (43). I choose to take advantage of targeting

ability of anti-CD38 for MM cells and conjugate it on the surface of Null-S3I-NP for enhanced delivery of a STAT3 inhibitor.

To my knowledge, ACN formulations were rarely studied in hematological malignancies compared to solid tumors. Lavasanifar Lab and Lai Lab have previously published a method where anti-CD30 is conjugated to a commercially available liposomal doxorubicin (Doxil®) for treatment of anaplastic large-cell lymphoma (44). The anti-CD30-conjugated Doxil® led to ~5-fold higher cellular uptake and ~2-fold more cytotoxicity compared to non-conjugated Doxil® in SupM2 cells. Moreover, anti-CD30-conjugated Doxil® resulted in significantly more reduction in tumor growth *in vivo* compared to Doxil®. Recently, a study reported that anti-CD38 conjugated chitosan nanoparticles carrying bortezomib exhibited a 2 to 3-fold increase in cell uptake by MM cells and a ~50% more reduction of MM tumor growth compared to non-targeted nanoparticles (45). However, this study reported that there was no significant difference in terms of *in vitro* cell cytotoxicity and apoptosis regardless of anti-CD38 conjugation. This suggests that anti-CD38 does improve the *in vivo* delivery of bortezomib to MM cells, but it does not resolve the bortezomib resistance in MM cells, which is partially mediated by STAT3 activity (16). The majority of previous studies on ACNs utilized conventional chemotherapeutics such as doxorubicin (5,44,46–48), paclitaxel (49–54) and gemcitabine (7,10,55,56). To the best of my knowledge, this is the first study that reports on the development of an anti-CD38 modified nanoparticle formulation for a specific inhibitor of a transcription factor (i.e. STAT3) as means for actively targeted delivery to MM cells. I demonstrated that conjugation of anti-CD38 resulted in increased cellular uptake and *in vitro* cytotoxicity in MM cells. Using an MM xenograft model, I demonstrated that the presence of CD38 antibody on nanoparticle was more effective in preventing the growth of MM tumor by

inhibiting the STAT3 activity *in vivo*. Additionally, I demonstrated that both Null-S3I-NP and CD38-S3I-NP were capable of inhibiting the phosphorylation of STAT3 *in vitro*, which has not been shown in the previous study (22).

Previous studies have reported the use of novel compounds like atovaquone, SC99 and LLL12 to induce cell cytotoxicity in MM cell lines and tumor growth suppression in MM xenograft models (57–59). However, these compounds are structurally hydrophobic and insoluble in the aquatic environment, which poses a major challenge in drug administration to humans. Moreover, these compounds were tested on subcutaneous MM tumors, where blood circulation and bone marrow microenvironment were not considered. In my study, I have adopted an MM xenograft model where MM cells are shown to be homing to the bone marrow cavity upon intravenous administration. Using this model, which represents the *in vivo* location of MM tumors in human more closely, I have demonstrated the better effect of CD38-S3I-NP containing a STAT3 inhibitor, S3I-1757, on suppressing the tumor growth *in vivo* compared to Null-S3I-NP.

I noticed some differences between Null-S3I-NP and CD38-S3I-NP regarding their physical properties including a higher PDI compared to Null-S3I-NP and a more rapid S3I-1757 release. Both of mentioned changes are expected following the post-insertion method of antibody modification. Using this method, antibody modified block copolymers insert themselves in the self-assembled nanoparticle structures resulting in nanoparticles with a broader size population. This may also reduce the compaction of nanoparticle structure leading to more rapid release of encapsulated drug from CD38-S3I-NP compared to Null-S3I-NPs. Hydrophobic interaction of S3I-1757 with anti-CD38 may partially be responsible for this observation as well. Despite CD38-

S3I-NP released S3I-1757 more rapidly compared to Null-S3I-NP, its more efficient cellular uptake by MM cells resulted in better *in vitro* cytotoxicity and *in vivo* tumor suppression.

In this chapter, I reported a method to conjugate anti-CD38 on a nanoparticle formulation carrying a STAT3 inhibitor for better MM cell-targeting. The anti-CD38 conjugation resulted in slight reduction of nanoparticle stability while substantially increased cellular uptake specifically by MM cells, which resulted in more cytotoxicity against MM cells and tumor-suppressive ability. This study provided insight on possible improvement of anti-STAT3 agents for the treatment of STAT3-dependent hematological cancers.

4.5. References

1. Arruebo M, Valladares M, González-Fernández Á. Antibody-conjugated nanoparticles for biomedical applications. J Nanomater. 2009;2009:1–24.

2. Mi Y, Liu X, Zhao J, Ding J, Feng SS. Multimodality treatment of cancer with herceptin conjugated, thermomagnetic iron oxides and docetaxel loaded nanoparticles of biodegradable polymers. Biomaterials. 2012;33(30):7519–29.

3. Parhi P, Sahoo SK. Trastuzumab guided nanotheranostics: A lipid based multifunctional nanoformulation for targeted drug delivery and imaging in breast cancer therapy. J Colloid Interface Sci. 2015;451:198–211.

4. Vivek R, Thangam R, NipunBabu V, Rejeeth C, Sivasubramanian S, Gunasekaran P, et al. Multifunctional HER2-Antibody Conjugated Polymeric Nanocarrier-Based Drug Delivery System for Multi-Drug-Resistant Breast Cancer Therapy. ACS Appl Mater Interfaces.

2014;6(9):6469–80.

5. Choi W Il, Lee JH, Kim JY, Heo SU, Jeong YY, Kim YH, et al. Targeted antitumor efficacy and imaging via multifunctional nano-carrier conjugated with anti-HER2 trastuzumab. Nanomedicine Nanotechnology, Biol Med. 2015;11(2):359–68.

6. Punfa W, Yodkeeree S, Pitchakarn P, Ampasavate C, Limtrakul P. Enhancement of cellular uptake and cytotoxicity of curcumin-loaded PLGA nanoparticles by conjugation with anti-P-glycoprotein in drug resistance cancer cells. Acta Pharmacol Sin. 2012;33(6):823–31.

7. Arya G, Vandana M, Acharya S, Sahoo SK. Enhanced antiproliferative activity of Herceptin (HER2)-conjugated gemcitabine-loaded chitosan nanoparticle in pancreatic cancer therapy. Nanomedicine Nanotechnology, Biol Med. 2011;7(6):859–70.

8. Sreeranganathan M, Uthaman S, Sarmento B, Mohan CG, Park IK, Jayakumar R. In vivo evaluation of cetuximab-conjugated poly(γ-glutamic acid)-docetaxel nanomedicines in EGFR-overexpressing gastric cancer xenografts. Int J Nanomedicine. 2017;12:7167–82.

9. Mukerjee A, Ranjan AP, Vishwanatha JK. Targeted nanocurcumin therapy using annexin A2 antibody improves tumor accumulation and therapeutic efficacy against highly metastatic breast cancer. J Biomed Nanotechnol. 2016;12(7):1374–92.

10. Öztürk K, Esendağlı G, Gürbüz MU, Tülü M, Çalış S. Effective targeting of gemcitabine to pancreatic cancer through PEG-cored Flt-1 antibody-conjugated dendrimers. Int J Pharm. 2017;517(1–2):157–67.

11. Punfa W, Suzuki S, Pitchakarn P, Yodkeeree S, Naiki T, Takahashi S, et al. Curcumin-loaded PLGA nanoparticles conjugated with anti-P-glycoprotein antibody to overcome

multidrug resistance. Asian Pacific J Cancer Prev. 2014;15(21):9249–58.

12. Hatakeyama H, Akita H, Ishida E, Hashimoto K, Kobayashi H, Aoki T, et al. Tumor targeting of doxorubicin by anti-MT1-MMP antibody-modified PEG liposomes. Int J Pharm. 2007;342(1–2):194–200.

13. Loureiro JA, Gomes B, Coelho MA, Do Carmo Pereira M, Rocha S. Targeting nanoparticles across the blood-brain barrier with monoclonal antibodies. Vol. 9, Nanomedicine. 2014. p. 709–22.

14. Bharti AC, Shishodia S, Reuben JM, Weber D, Alexanian R, Raj-Vadhan S, et al. Nuclear factor–κB and STAT3 are constitutively active in CD138 + cells derived from multiple myeloma patients, and suppression of these transcription factors leads to apoptosis. Blood. 2004;103(8):3175–84.

15. Liu T, Fei Z, Gangavarapu KJ, Agbenowu S, Bhushan A, Lai JCK, et al. Interleukin-6 and JAK2/STAT3 signaling mediate the reversion of dexamethasone resistance after dexamethasone withdrawal in 7TD1 multiple myeloma cells. Leuk Res. 2013;37(10):1322–8.

16. Zhang XD, Baladandayuthapani V, Lin H, Mulligan G, Li B-Z, Esseltine DLW, et al. Tight jnction protein 1 modulates proteasome capacity and proteasome inhibitor sensitivity in multiple myeloma via EGFR/JAK1/STAT3 signaling. Cancer Cell. 2016;29(5):639–52.

17. Wu W, Ma D, Wang P, Cao L, Lu T, Fang Q, et al. Potential crosstalk of the interleukin-6-heme oxygenase-1-dependent mechanism involved in resistance to lenalidomide in multiple myeloma cells. FEBS J. 2016;283(5):834–49.

18. Zhang X, Sun Y, Pireddu R, Yang H, Urlam MK, Lawrence HR, et al. A novel inhibitor of STAT3 homodimerization selectively suppresses STAT3 activity and malignant transformation. Cancer Res. 2013;73(6):1922–33.

19. Zhang X, Yue P, Fletcher S, Zhao W, Gunning PT, Turkson J. A novel small-molecule disrupts Stat3 SH2 domain–phosphotyrosine interactions and Stat3-dependent tumor processes. 2010;79(10).

20. Schust J, Sperl B, Hollis A, Mayer TU, Berg T. Stattic: a small-molecule inhibitor of STAT3 activation and dimerization. Chem Biol. 2006;13(11):1235–42.

21. Oh D-Y, Lee S-H, Han S-W, Kim M-J, Kim T-M, Kim T-Y, et al. Phase I Study of OPB-31121, an Oral STAT3 Inhibitor, in Patients with Advanced Solid Tumors. Cancer Res Treat. 2015;47(4):607–15.

22. Soleimani AH, Garg SM, Paiva IM, Vakili MR, Alshareef A, Huang Y-H, et al. Micellar nano-carriers for the delivery of STAT3 dimerization inhibitors to melanoma. Drug Deliv Transl Res. 2017;1–11.

23. Mahmud A, Xiong XB, Lavasanifar A. Novel self-associating POly(ethylene oxide)-block-poly(ε-caprolactone) block copolymers with functional side groups on the polyester block for drug delivery. Macromolecules. 2006;39(26):9419–28.

24. Kogan T. The synthesis of substituted methoxy-poly (ethyleneglycol) derivatives suitable for selective protein modification. Synth Commun. 1992;22(16):2417–24.

25. Garg SM, Paiva IM, Vakili MR, Soudy R, Agopsowicz K, Soleimani AH, et al. Traceable PEO-poly(ester) micelles for breast cancer targeting: The effect of core structure and

targeting peptide on micellar tumor accumulation. Biomaterials. 2017;144:17–29.

26. Nakamura Y, Mochida A, Choyke PL, Kobayashi H. Nanodrug Delivery: Is the Enhanced Permeability and Retention Effect Sufficient for Curing Cancer? Vol. 27, Bioconjugate Chemistry. 2016. p. 2225–38.

27. Badkas A, Frank E, Zhou Z, Jafari M, Chandra H, Sriram V, et al. Modulation of in vitro phagocytic uptake and immunogenicity potential of modified Herceptin®-conjugated PLGA-PEG nanoparticles for drug delivery. Colloids Surfaces B Biointerfaces. 2018;162:271–8.

28. van de Donk NWCJ, Lokhorst HM, Anderson KC, Richardson PG, Kyle R, Maldonado J, et al. How I treat plasma cell leukemia. Blood. 2012;120(12):2376–89.

29. Wang L, Wang H, Li PF, Lu Y, Xia ZJ, Huang HQ, et al. CD38 expression predicts poor prognosis and might be a potential therapy target in extranodal NK/T cell lymphoma, nasal type. Ann Hematol. 2015;94(8):1381–8.

30. Suzuki R, Suzumiya J, Nakamura S, Aoki S, Notoya A, Ozaki S, et al. Aggressive natural killer-cell leukemia revisited: Large granular lymphocyte leukemia of cytotoxic NK cells. Leukemia. 2004;18(4):763–70.

31. Marinov J, Koubek K, Stary J. Immunophenotypic significance of the “lymphoid” CD38 antigen in myeloid blood malignancies. Neoplasma. 1993;40(6):355–8.

32. Keyhani A, Huh YO, Jendiroba D, Pagliaro L, Cortez J, Pierce S, et al. Increased CD38 expression is associated with favorable prognosis in adult acute leukemia. Leuk Res. 2000;24(2):153–9.

33. Parry-Jones N, Matutes E, Morilla R, Brito-Babapulle V, Wotherspoon A, Swansbury GJ, et al. Cytogenetic abnormalities additional to t(11;14) correlate with clinical features in leukaemic presentation of mantle cell lymphoma, and may influence prognosis: A study of 60 cases by FISH. Br J Haematol. 2007;137(2):117–24.

34. Damle RN, Wasil T, Fais F, Ghiotto F, Valetto A, Allen SL, et al. Ig V gene mutation status and CD38 expression as novel prognostic indicators in chronic lymphocytic leukemia. Blood. 1999;94(6):1840–7.

35. Lin P, Owens R, Tricot G, Wilson CS. Flow Cytometric Immunophenotypic Analysis of 306 Cases of Multiple Myeloma. Am J Clin Pathol. 2004;121(4):482–8.

36. Zubiaur M, Izquierdo M, Terhorst C, Malavasi F, Sancho J. CD38 ligation results in activation of the Raf-1/mitogen-activated protein kinase and the CD3-z/z-associated protein-70 signaling pathways in jurkat T lymphocytes. JImmunol. 1997;159(1):193–205.

37. Aarhus R, Graeff RM, Dickey DM, Walseth TF, Lee HC. ADP-ribosyl cyclase and CD38 catalyze the synthesis of a calcium-mobilizing metabolite from NADP. J Biol Chem. 1995;270(51):30327–33.

38. Guse AH, Da Silva CP, Berg I, Skapenko AL, Weber K, Heyer P, et al. Regulation of calcium signalling in T lymphocytes by the second messenger cyclic ADP-ribose. Nature. 1999;398(6722):70–3.

39. Funaro A, Morra M, Calosso L, Zini MG, Ausiello CM, Malavasi F. Role of the human CD38 molecule in B cell activation and proliferation. Tissue Antigens. 1997;49(1):7–15.

40. de Weers M, Tai Y-T, van der Veer MS, Bakker JM, Vink T, Jacobs DCH, et al.

Daratumumab, a Novel Therapeutic Human CD38 Monoclonal Antibody, Induces Killing of Multiple Myeloma and Other Hematological Tumors. J Immunol. 2011;186(3):1840–8.

41. Beum P V, Lindorfer MA, Peek EM, Stukenberg PT, de Weers M, Beurskens FJ, et al. Penetration of antibody-opsonized cells by the membrane attack complex of complement promotes Ca2+ influx and induces streamers. Eur J Immunol. 2011;41(8):2436–46.

42. Overdijk MB, Jansen JHM, Nederend M, Lammerts van Bueren JJ, Groen RWJ, Parren PWHI, et al. The Therapeutic CD38 Monoclonal Antibody Daratumumab Induces Programmed Cell Death via Fcγ Receptor–Mediated Cross-Linking. J Immunol. 2016;197(3):807–13.

43. Preyat N, Leo O. Complex role of nicotinamide adenine dinucleotide in the regulation of programmed cell death pathways. Biochem Pharmacol. 2016;101:13–26.

44. Molavi O, Xiong XB, Douglas D, Kneteman N, Nagata S, Pastan I, et al. Anti-CD30 antibody conjugated liposomal doxorubicin with significantly improved therapeutic efficacy against anaplastic large cell lymphoma. Biomaterials. 2013;34(34):8718–25.

45. de la Puente P, Luderer MJ, Federico C, Jin A, Gilson RC, Egbulefu C, et al. Enhancing proteasome-inhibitory activity and specificity of bortezomib by CD38 targeted nanoparticles in multiple myeloma. J Control Release. 2018;270:158–76.

46. Son S, Shin S, Rao V, Um W, Jeon J, Ko H, et al. Trop2 antibody-conjugated bioreducible nanoparticles for targeted triple negative breast cancer therapy. Int J Biol Macromol. 2017;

47. Lee SM, Kim HJ, Kim SY, Kwon MK, Kim S, Cho A, et al. Drug-loaded gold plasmonic nanoparticles for treatment of multidrug resistance in cancer. Biomaterials.

2014;35(7):2272–82.

48. Al Faraj A, Shaik AP, Shaik AS. Magnetic single-walled carbon nanotubes as efficient drug delivery nanocarriers in breast cancer murine model: Noninvasive monitoring using diffusion-weighted magnetic resonance imaging as sensitive imaging biomarker. Int J Nanomedicine. 2014;10(1):157–68.

49. Debotton N, Zer H, Parnes M, Harush-Frenkel O, Kadouche J, Benita S. A quantitative evaluation of the molecular binding affinity between a monoclonal antibody conjugated to a nanoparticle and an antigen by surface plasmon resonance. Eur J Pharm Biopharm. 2010;74(2):148–56.

50. Dilnawaz F, Singh A, Mohanty C, Sahoo SK. Dual drug loaded superparamagnetic iron oxide nanoparticles for targeted cancer therapy. Biomaterials. 2010;31(13):3694–706.

51. Taylor RM, Sillerud LO. Paclitaxel-loaded iron platinum stealth immunomicelles are potent MRI imaging agents that prevent prostate cancer growth in a PSMA-dependent manner. Int J Nanomedicine. 2012;7:4341–52.

52. Karra N, Nassar T, Ripin AN, Schwob O, Borlak J, Benita S. Antibody conjugated PLGA nanoparticles for targeted delivery of paclitaxel palmitate: Efficacy and biofate in a lung cancer mouse model. Small. 2013;9(24):4221–36.

53. Jain NK, Tare MS, Mishra V, Tripathi PK. The development, characterization and in vivo anti-ovarian cancer activity of poly(propylene imine) (PPI)-antibody conjugates containing encapsulated paclitaxel. Nanomedicine Nanotechnology, Biol Med. 2015;11(1):207–18.

54. Mu Q, Kievit FM, Kant RJ, Lin G, Jeon M, Zhang M. Anti-HER2/neu peptide-conjugated

iron oxide nanoparticles for targeted delivery of paclitaxel to breast cancer cells. Nanoscale. 2015;7(43):18010–4.

55. Aggarwal S, Yadav S, Gupta S. EGFR targeted PLGA nanoparticles using gemcitabine for treatment of pancreatic cancer. J Biomed Nanotechnol. 2011;7(1):137–8.

56. Wang XB, Zhou HY. Molecularly targeted gemcitabine-loaded nanoparticulate system towards the treatment of EGFR overexpressing lung cancer. Biomed Pharmacother. 2015;70(C):123–8.

57. Lin L, Benson DM, Deangelis S, Bakan CE, Li PK, Li C, et al. A small molecule, LLL12 inhibits constitutive STAT3 and IL-6-induced STAT3 signaling and exhibits potent growth suppressive activity in human multiple myeloma cells. Int J Cancer. 2012;130(6):1459–69.

58. Zhang Z, Mao H, Du X, Zhu J, Xu Y, Wang S. A novel small molecule agent displays potent anti-myeloma activity by inhibiting the JAK2-STAT3 signaling pathway. Oncotarget. 2016;7(8):9296–308.

59. Xiang M, Kim H, Ho VT, Walker SR, Bar-Natan M, Anahtar M, et al. Gene expression-based discovery of atovaquone as a STAT3 inhibitor and anticancer agent. Blood. 2016;128(14):1845–53.

CHAPTER 5

General Discussion

5.1. Thesis summary

Despite the tremendous amount of MM research and significant therapeutic advances in MM, it is still an incurable disease in most of cases. The challenge is largely due to the high relapse rate of MM which are largely attributed to drug resistance. It has been shown that STAT3 transcriptional activity is associated with resistance to thalidomide, bortezomib and dexamethasone (1–3). In **Chapter 2**, I demonstrated that the STAT3 activity of 2 MM cell lines (U266 and RPMI8226) is more pronounced in a bone barrow-mimicking 3D culture model compared to conventional culture. Additionally, STAT3 inhibition induced apoptosis and sensitivity to bortezomib in MM cells in 3D culture but not in conventional culture. Consistent with these findings, I found that 3D culture preserved PMM cell viability compared to conventional culture with higher STAT3 activity (**Chapter 3**). To make STAT3 inhibitor more clinically available, S3I-1757-carrying nanoparticles with conjugation of anti-CD38, CD38-S3I-NP, was prepared (**Chapter 4**). I found that CD38-S3I-NP poses improved MM cell-targeting ability, *in vitro* cytotoxicity and *in vivo* tumor suppression compared to nanoparticles with no anti-CD38 conjugation. All these findings suggest that STAT3 is essential for MM cell survival under close-to-*in vivo* conditions, and STAT3 inhibitors in an active-targeting nanoparticle delivery system are a promising therapy for MM.

5.2. Scientific significance

The most important contribution of my work is that it redefines the importance of STAT3 activity in MM. According to previous analysis on MM patients, it was found that STAT3 is active in ~50% of cases based on nuclear pSTAT3 staining (4). However, I observed that if the 3D environment is present (i.e. in 3D culture or animal xenograft), even STAT3-inactive MM cells became STAT3 active (**Figure 2.3**). Moreover, I observed that the STAT3 activity acquired from

3D culture was lost if MM cells were transferred to conventional culture (**Figure 2.4**). This is consistent with my observation that the pSTAT3 level in primary $CD38^+$ MM cells rapidly decreased in conventional culture within 3 days (**Figure 3.3**). Collectively, this suggests that *in vivo* microenvironment contributes to STAT3 activation in MM cells. Moreover, it implicates that the importance of STAT3 activity in MM cells can be easily underestimated in conventional culture.

My work in **Chapter 2** explicitly compared the efficacy of Stattic in U266 and RPMI8226 cells using a recently developed technique, CETSA (**Figure 2.5A and 2.5B**). Comparison drug cytotoxicity between 3D and conventional cultures is technically challenging due to their completely environments leading to different drug accessibility. This observation is supported by the de la Puente *et al*'s finding that doxorubicin cell uptake is substantially lower in different scaffold 3D culture models compared to conventional culture (5). Different drug accessibility between 3D and conventional cultures was often overlooked when comparing the cytotoxicity of chemotherapeutics, which can lead to different interpretation of results. For example, in another study using Kirshner's 3D model to test the cytotoxicity of a anti-CD56 conjugated maysantinoid, it seemed that the IC_{50} value is ~10 folds higher in 3D cultured MM cells compared to conventionally cultured MM cells (6). However, if drug accessibility was considered (10~15 times higher in conventional culture compared to 3D culture in my hands, **Figure 2.5A and 2.5B**), the cytotoxicity effect will be comparable in the two culture systems.

In **Chapter 2**, I proposed a method by which the intact 3D matrix can be fixed and processed for immunocytochemistry with preservation of cell interactions, distribution and organization (section

2.2.3). Compared to the Matrigel®-based 3D culture used to study solid cancers, the Matrigel® used in my study was diluted with fibronectin and collagen IV solutions, thus more fragile and fluidic. Therefore, the immunohistochemical method proposed by which involves using histogel to sandwich the Matrigel for further processing is not applicable in my case (7). The value of my immunocytochemistry method is that it allows visualization of the interactions between MM cells and different other cell types and ECM proteins. Since it is well known that the tumor microenvironment significantly contributes to MM development, my method makes 3D culture an excellent tool for studying MM tumor microenvironment and identification of novel diagnostic markers or therapeutic targets in PMM cells.

My findings in **Chapter 3** suggest that STAT3 activity is a key factor for PMM cell survival in 3D culture. PMM cells is difficult to maintain in conventional cell culture, even with the presence of bone marrow stromal cells (BMSCs) and various cytokines and growth factors can only minimally improve PMM cell viability (8). Additionally, MM cells are known to have a naturally slow proliferation rate (9). As a result, many studies involved evaluating drug efficacy on PMM cells were in a time span of less than 3 days, and no study has been done to change gene expression in PMM cells, as summarized in **Table 5.1**. I found that STAT3 activity is correlated with PMM cell viability in 3D culture by treatment of IL6 or Stattic (**Figure 3.4 and 3.5**). This implies that the combining 3D culture with IL6 can make long-term culture of PMM possible, allowing long-term follow-up of drug treatment or gene manipulations (overexpression, knockout and knockdown).

Table 5.1. Therapeutic efficacy studies using PMM cells

Markers	Isolated MM cells?	Sample size	Treatment	Period	Reference
$CD138^+$	Yes	16	Daratumumab[1] + lenalidomide + complement	48hr	(10)
$CD138^+$	Yes	4	Bortezomib + SGK[2] inhibitor	48hr	(11)
$CD138^+$	No	21	Daratumumab + lenalidomide + IPH2102[3]	48hr	(12)
$CD38^+CD138^+$	No	7	NF-κB inhibitor	48hr	(13)
Not specified	No	6	CAR-T[4]	4hr	(14)
$CD138^+$	Yes	3	A1771726[5]	48hr	(15)
$CD138^+$	Yes	11	Daratumumab + lenalidomide or bortezomib	48hr	(16)
$CD38^+CD45^+$	No	13	Azacitidine[6]	72hr*	(17)
$CD38^+CD138^+$	No	7	SAR650984[7]	18hr	(18)
$CD138^+$	Yes	22	2D7-DB[8]	24hr	(19)
$CD138^+$	Yes	5	iNKT[9]	48hr	(20)
$CD138^+$	Yes	1	MV-Wue[10]	3.5 days¥	(21)
$CD138^+$	Yes	3	VPA[11]	48hr	(22)

1. CD38 monoclonal antibody
2. SGK – serum and glucocorticoid kinase
3. IPH2102 – An antibody against NK cell inhibitory receptor
4. Chimeric antigen receptor T cells engineered with B cell maturation antigen
5. Dihydroorotate dehydrogenase inhibitor
6. DNA methyltransferase inhibitor
7. CD38 monoclonal antibody
8. Single-chain diabody against HLA-A
9. Invariant NK T cells
10. Measles virus with anti-CD138 fragment
11. Valproic acid – a histone deacetylase inhibitor

* Overnight incubation + 48hr drug treatment

¥ Cultured in 20% FBS with 4ng/ml IL6

Another important feature in this thesis is that I proposed a nanoparticle formulation for better administration and delivery of STAT3 inhibitors with active MM cell-targeting ability, CD38-S3I-

NP (**Chapter 4**). Although it has been long known that STAT3 is an oncogenic protein in a variety of cancer models, there is very few STAT3 inhibitors which have been tested in cancer patients, and the clinical efficacy of them is very limited. For example, a completed Phase I clinical trial of OPB-31121 reported that 2 of 18 patients with various cancer types showed tumor shrinkage, and more than 70% of patients suffered from nausea, vomiting and diarrhea (23). I believe this low *in vivo* efficacy is due to excess off-target toxicity in normal cells/tissues due to the fact that STAT3 inhibitor is non-specifically distributed to normal tissues and to tumor. Encapsulation of S3I-1757 in my hand increased the size to ~90-100 nm (**Table 4.1**) to prevent leakage from capillary vessels. The anti-CD38 on CD38-S3I-NP further increased its targeting ability against MM cells. This concept was supported by the observations of improved cellular uptake and *in vitro/in vivo* efficacy compared to Null-NP.

Many technical difficulties have been overcome in my work. First, the differential of drug accessibility of MM cells cultured in conventional and 3D culture was overcome with CETSA. Second, the immunocytochemistry of 3D cultured MM cells became possible with my novel histogel-well method for embedding of fragile 3D matrix. This allows the visualization of detailed cell-stroma interactions, which plays an essential role on drug resistance in MM. Third, the protocol of double staining of CD38 and pSTAT3 for cytometry analysis of STAT3 activity in PMM cells was established. Fourth, the conjugation of CD38 antibody with the correct orientation (i.e. various region of anti-CD38 pointing out) on the surface of nanoparticles was achieved using specific thiolation at the constant region of antibody. Finally, the intravenous xenograft of MM was established using U266-luc, which allows a realistic evaluation of CD38-S3I-NP *in vivo*.

5.3. Future directions

The 3D culture study in **Chapter 2** could be more realistic if BMSCs were cultured together with U266 or RPMI8226 cells. It is well known that BMSCs release IL6 after stimulation of TNFα released by MM cells or direct cell-cell interaction with MM cells (reviewed in section **1.2.8.1.**). However, the BMSCs from MM patients have been shown to behave differently compared to those from healthy donors (e.g. HS-5, a bone marrow stromal cell lines available at ATCC (24)). For instance, it was found that BMSCs from MM patients showed a higher NF-κB transcriptional activity compared to those from healthy donors (25). Alternatively, if MM BMSCs are used, patient variability may result in low reproducibility of experimental data. In short, although studying MM cell lines in 3D culture is more representative compared to conventional culture, improvement is needed to mimic real MM microenvironment.

There two limitations regarding the choice of the two MM cell lines used in my study, U266 and RPMI8226. One was that the identity of the U266 and RPMI8226 cells used in my study was not confirmed using genotyping. Although highly unlikely, cross-contamination of these cells with other cell lines can lead to different cell behavior in 3D culture. Additionally, inclusion of more MM cell lines with variable chromosomal aberrations would further solidify my theory that STAT3 activation in 3D is not limited to a subgroup of MM cells. Also, inclusion of MM drug-resistant cell lines (e.g. MM1.R and RPMI8226.R) in this study will provide more insight on targeting STAT3 in patients with MM relapse.

Other than the known benefits of STAT3 on improving the survival, growth and drug resistance of MM cells, the function of STAT3 on lipid metabolism in MM is not well investigated. Based

on the oligonucleotide array result that I obtained (**Figure 2.7A**), the most upregulated gene in 3D culture, *LPL*, is responsible for lipid breakdown into glycerol and free fatty acids. It is likely that MM cells use lipid present in the 3D matrix as an additional energy source for cell survival and growth in 3D. This is advantageous to MM cells because cancer cells preferably generate energy via aerobic glycolysis (aka. Warburg effect), which is highly ineffective. It will be interesting to study how STAT3 contributes to the usage of lipid in 3D-cultured MM cells as a future direction.

Although I saw an overall STAT3 upregulation of PMM cells from patients, some variability of cell growth patterns was all observed as shown in **Figure 3.1B and 3.1C**. This is likely due to that the PMM cells were from consecutive MM patients with different clinical characteristics. Given sufficient number of sample sizes, it will be helpful to stratify patients based on their responsiveness to common MM therapeutics such as bortezomib, thalidomide or lenalidomide. Based on the importance of STAT3 on drug resistance (1–3), I believe that the refractory PMM cells better preserve STAT3 activity in 3D culture compared to drug sensitive PMM cells. Studying the role of STAT3 in relapse and refractory MM may provide a strategy to improve current anti-MM regimens.

Ultimately, the functionality of STAT3 inhibitor determines how well it blocks STAT3 and essentially eliminate MM cells. The two STAT3 inhibitors used in my study were both SH2 domain inhibitors which prevents STAT3 phosphorylation, but not necessarily DNA-binding ability and transcriptional activity. It has been shown that unphosphorylated STAT3 can be transcriptional active (26,27). Furthermore, it is recognized that there are two alternative splicing isoforms of STAT3, α and β, serving opposite functions in cancers (28). The oncogenic isoform

STAT3α contains a transactivation domain containing S727 residue, which distinguishes it from STAT3β. Therefore, I believe that using a STAT3 inhibitors which targets the transactivation domain of STAT3α, especially the LPMSP motif, will improve their anti-MM effect in 3D culture as well as MM xenograft.

5.4. References

1. Liu T, Fei Z, Gangavarapu KJ, Agbenowu S, Bhushan A, Lai JCK, et al. Interleukin-6 and JAK2/STAT3 signaling mediate the reversion of dexamethasone resistance after dexamethasone withdrawal in 7TD1 multiple myeloma cells. Leuk Res. 2013;37(10):1322–8.
2. Zhang XD, Baladandayuthapani V, Lin H, Mulligan G, Li B-Z, Esseltine DLW, et al. Tight jnction protein 1 modulates proteasome capacity and proteasome inhibitor sensitivity in multiple myeloma via EGFR/JAK1/STAT3 signaling. Cancer Cell. 2016;29(5):639–52.
3. Wu W, Ma D, Wang P, Cao L, Lu T, Fang Q, et al. Potential crosstalk of the interleukin-6-heme oxygenase-1-dependent mechanism involved in resistance to lenalidomide in multiple myeloma cells. FEBS J. 2016;283(5):834–49.
4. Bharti AC, Shishodia S, Reuben JM, Weber D, Alexanian R, Raj-Vadhan S, et al. Nuclear factor–κB and STAT3 are constitutively active in CD138 + cells derived from multiple myeloma patients, and suppression of these transcription factors leads to apoptosis. Blood. 2004;103(8):3175–84.
5. de la Puente P, Muz B, Gilson RC, Azab F, Luderer M, King J, et al. 3D tissue-engineered bone marrow as a novel model to study pathophysiology and drug resistance in multiple myeloma. Biomaterials. 2015;73:70–84.
6. Nierste BA, Gunn EJ, Whiteman KR, Lutz RJ, Kirshner J. Maytansinoid immunoconjugate

IMGN901 is cytotoxic in a three-dimensional culture model of multiple myeloma. Am J Blood Res. 2016;6(1):6–18.

7. Pinto MP, Jacobsen BM, Horwitz KB. An immunohistochemical method to study breast cancer cell subpopulations and their growth regulation by hormones in three-dimensional cultures. Front Endocrinol (Lausanne). 2011;2:15.

8. Zlei M, Egert S, Wider D, Ihorst G, Wäsch R, Engelhardt M. Characterization of in vitro growth of multiple myeloma cells. Exp Hematol. 2007;35(10):1550–61.

9. Gastinne T, Leleu X, Duhamel A, Moreau AS, Franck G, Andrieux J, et al. Plasma cell growth fraction using Ki-67 antigen expression identifies a subgroup of multiple myeloma patients displaying short survival within the ISS stage I. Eur J Haematol. 2007;79(4):297–304.

10. van der Veer MS, de Weers M, van Kessel B, Bakker JM, Wittebol S, Parren PWHI, et al. Towards effective immunotherapy of myeloma enhanced elimination of myeloma cells by combination of lenalidomide with the human CD38 monoclonal antibody daratumumab. Haematologica. 2011;96(2):284–90.

11. Hoang B, Shi Y, Frost PJ, Mysore V, Bardeleben C, Lichtenstein A. SGK kinase activity in multiple myeloma cells protects against ER stress apoptosis via a SEK-dependent mechanism. Mol Cancer Res. 2016;14(4):397–407.

12. Nijhof IS, Van Bueren JJL, Van Kessel B, Andre P, Morel Y, Lokhorst HM, et al. Daratumumab-Mediated lysis of primary multiple myeloma cells is enhanced in combination with the human Anti-KIR antibody IPH2102 and lenalidomide. Haematologica. 2015;100(2):263–8.

13. Walsby EJ, Pratt G, Hewamana S, Crooks PA, Burnett AK, Fegan C, et al. The NF-kappaB

inhibitor LC-1 has single agent activity in multiple myeloma cells and synergizes with bortezomib. Mol Cancer Ther. 2010;9(6):1574–82 ST–The NF–kappaB inhibitor LC–1 has sin.

14. Carpenter RO, Evbuomwan MO, Pittaluga S, Rose JJ, Raffeld M, Yang S, et al. B-cell maturation antigen is a promising target for adoptive T-cell therapy of multiple myeloma. Clin Cancer Res. 2013;19(8):2048–60.

15. Baumann P, Mandl-Weber S, Volkl A, Adam C, Bumeder I, Oduncu F, et al. Dihydroorotate dehydrogenase inhibitor A771726 (leflunomide) induces apoptosis and diminishes proliferation of multiple myeloma cells. Mol Cancer Ther. 2009;8(2):366–75.

16. Nijhof IS, Groen RWJ, Noort WA, Van Kessel B, De Jong-Korlaar R, Bakker J, et al. Preclinical evidence for the therapeutic potential of CD38-Targeted Immuno-chemotherapy in multiple Myeloma patients refractory to Lenalidomide and Bortezomib. Clin Cancer Res. 2015;21(12):2802–10.

17. Khong T, Sharkey J, Spencer A. The effect of azacitidine on interleukin-6 signaling and nuclear factor-kappaB activation and its in vitro and in vivo activity against multiple myeloma. Haematologica. 2008;93(6):860–9.

18. Deckert J, Wetzel MC, Bartle LM, Skaletskaya A, Goldmacher VS, Vallée F, et al. SAR650984, a novel humanized CD38-targeting antibody, demonstrates potent antitumor activity in models of multiple myeloma and other CD38+ hematologic malignancies. Clin Cancer Res. 2014;20(17):4574–83.

19. Sekimoto E, Ozaki S, Ohshima T, Shibata H, Hashimoto T, Abe M, et al. A single-chain Fv diabody against human leukocyte antigen-A molecules specifically induces myeloma cell death in the bone marrow environment. Cancer Res. 2007;67(3):1184–92.

20. Song W, Van Der Vliet HJJ, Tai YT, Prabhala R, Wang R, Podar K, et al. Generation of antitumor invariant natural killer T cell lines in multiple myeloma and promotion of their functions via lenalidomide: A strategy for immunotherapy. Clin Cancer Res. 2008;14(21):6955–62.

21. Hummel HD, Kuntz G, Russell SJ, Nakamura T, Greiner A, Einsele H, et al. Genetically engineered attenuated measles virus specifically infects and kills primary multiple myeloma cells. J Gen Virol. 2009;90(3):693–701.

22. Kaiser M, Zavrski I, Sterz J, Jakob C, Fleissner C, Kloetzel PM, et al. The effects of the histone deacetylase inhibitor valproic acid on cell cycle, growth suppression and apoptosis in multiple myeloma. Haematologica. 2006;91(2):248–51.

23. Oh D-Y, Lee S-H, Han S-W, Kim M-J, Kim T-M, Kim T-Y, et al. Phase I Study of OPB-31121, an Oral STAT3 Inhibitor, in Patients with Advanced Solid Tumors. Cancer Res Treat. 2015;47(4):607–15.

24. Roecklein BABA, Torok-storb B. Functionally Distinct Human Marrow Stromal Cell Lines Immortalized by Transduction With the Human Papilloma Virus. Blood. 1995;85(4):997–1006.

25. Markovina S, Callander NS, O'Connor SL, Xu G, Shi Y, Leith CP, et al. Bone marrow stromal cells from multiple myeloma patients uniquely induce bortezomib resistant NF-κB activity in myeloma cells. Mol Cancer. 2010;9.

26. Yang J, Liao X, Agarwal MK, Barnes L, Auron PE, Stark GR. Unphosphorylated STAT3 accumulates in response to IL-6 and activates transcription by binding to NF-kB. Genes Dev. 2007;21(11):1396–408.

27. Timofeeva OA, Chasovskikh S, Lonskaya I, Tarasova NI, Khavrutskii L, Tarasov SG, et al.

Mechanisms of unphosphorylated STAT3 transcription factor binding to DNA. J Biol Chem. 2012;287(17):14192–200.

28. Zhang H-F, Chen Y, Wu C, Wu Z-Y, Tweardy DJ, Alshareef A, et al. The Opposing Function of STAT3 as an Oncoprotein and Tumor Suppressor Is Dictated by the Expression Status of STAT3b in Esophageal Squamous Cell Carcinoma. Clin Cancer Res. 22(3):691–703.

BIBLIOGRAPHY

Aarhus, R., Graeff, R. M., Dickey, D. M., Walseth, T. F., & Lee, H. C. (1995). ADP-ribosyl cyclase and CD38 catalyze the synthesis of a calcium-mobilizing metabolite from NADP. *Journal of Biological Chemistry*, *270*(51), 30327–30333. https://doi.org/10.1074/jbc.270.51.30327

Abe, M., Hiura, K., Wilde, J., Shioyasono, A., Moriyama, K., Hashimoto, T., … Matsumoto, T. (2004). Osteoclasts enhance myeloma cell growth and survival via cell-cell contact: A vicious cycle between bone destruction and myeloma expansion. *Blood*, *104*(8), 2484–2491. https://doi.org/10.1182/blood-2003-11-3839

Aggarwal, B. B., Kunnumakkara, A. B., Harikumar, K. B., Gupta, S. R., Tharakan, S. T., Koca, C., … Sung, B. (2009). Signal transducer and activator of transcription-3, inflammation, and cancer: How intimate is the relationship? In *Annals of the New York Academy of Sciences* (Vol. 1171, pp. 59–76). Wiley/Blackwell (10.1111). https://doi.org/10.1111/j.1749-6632.2009.04911.x

Aggarwal, S., Yadav, S., & Gupta, S. (2011). EGFR targeted PLGA nanoparticles using gemcitabine for treatment of pancreatic cancer. *Journal of Biomedical Nanotechnology*, *7*(1), 137–138. https://doi.org/10.1166/jbn.2011.1238

Akira, S., Nlshio, Y., Lnoue, M., Wang, X.-J. J., We&t, S., Matsusaka, T. T., … Kishimoto, T. (1994). Molecular cloning of APRF, a novel IFN-stimulated gene factor 3 p91-related transcription factor involved in the gp130-mediated signaling pathway. *Cell*, *77*(1), 63–71. https://doi.org/10.1016/0092-8674(94)90235-6

Akkapeddi, P., Azizi, S.-A., Freedy, A. M., Cal, P. M. S. D., Gois, P. M. P., & Bernardes, G. J. L. (2016). Construction of homogeneous antibody–drug conjugates using site-selective protein

chemistry. *Chemical Science*, *7*(5), 2954–2963. https://doi.org/10.1039/C6SC00170J

Al Faraj, A., Shaik, A. P., & Shaik, A. S. (2014). Magnetic single-walled carbon nanotubes as efficient drug delivery nanocarriers in breast cancer murine model: Noninvasive monitoring using diffusion-weighted magnetic resonance imaging as sensitive imaging biomarker. *International Journal of Nanomedicine*, *10*(1), 157–168. https://doi.org/10.2147/IJN.S75074

Alberta Health System. (2015). Clinical Practice Guideline Multiple Myeloma.

Amanna, I. J., & Slifka, M. K. (2010, June 15). Mechanisms that determine plasma cell lifespan and the duration of humoral immunity. *Immunological Reviews*. Wiley/Blackwell (10.1111). https://doi.org/10.1111/j.1600-065X.2010.00912.x

Anderson, K. C., Jones, R. M., Morimoto, C., Leavitt, P., & Barut, B. A. (1989). Response patterns of purified myeloma cells to hematopoietic growth factors. *Blood*, *73*(7), 1915–1924.

Ao, L., Reichel, D., Hu, D., Jeong, H., Kim, K. B., Bae, Y., & Lee, W. (2015). Polymer Micelle Formulations of Proteasome Inhibitor Carfilzomib for Improved Metabolic Stability and Anticancer Efficacy in Human Multiple Myeloma and Lung Cancer Cell Lines. *Journal of Pharmacology and Experimental Therapeutics*, *355*(2), 168–173. https://doi.org/10.1124/jpet.115.226993

Arruebo, M., Valladares, M., & González-Fernández, Á. (2009). Antibody-conjugated nanoparticles for biomedical applications. *Journal of Nanomaterials*, *2009*, 1–24. https://doi.org/10.1155/2009/439389

Arya, G., Vandana, M., Acharya, S., & Sahoo, S. K. (2011). Enhanced antiproliferative activity of Herceptin (HER2)-conjugated gemcitabine-loaded chitosan nanoparticle in pancreatic cancer

therapy. *Nanomedicine: Nanotechnology, Biology, and Medicine*, *7*(6), 859–870. https://doi.org/10.1016/j.nano.2011.03.009

Ashley, J. D., Quinlan, C. J., Schroeder, V. A., Suckow, M. A., Pizzuti, V. J., Kiziltepe, T., & Bilgicer, B. (2016). Dual Carfilzomib and Doxorubicin-Loaded Liposomal Nanoparticles for Synergistic Efficacy in Multiple Myeloma. *Molecular Cancer Therapeutics*, *15*(7), 1452–1459. https://doi.org/10.1158/1535-7163.MCT-15-0867

Ashley, J. D., Stefanick, J. F., Schroeder, V. A., Suckow, M. A., Kiziltepe, T., & Bilgicer, B. (2014). Liposomal bortezomib nanoparticles via boronic ester prodrug formulation for improved therapeutic efficacy in vivo. *Journal of Medicinal Chemistry*, *57*(12), 5282–5292. https://doi.org/10.1021/jm500352v

Avet-Loiseau, H., Attal, M., Moreau, P., Charbonnel, C., Garban, F., Hulin, C., … Mathiot, C. (2007). Genetic abnormalities and survival in multiple myeloma: The experience of the Intergroupe Francophone du Myélome. *Blood*, *109*(8), 3489–3495. https://doi.org/10.1182/blood-2006-08-040410

Azare, J., Leslie, K., Al-Ahmadie, H., Gerald, W., Weinreb, P. H., Violette, S. M., & Bromberg, J. (2007). Constitutively activated Stat3 induces tumorigenesis and enhances cell motility of prostate epithelial cells through integrin beta 6. *Molecular & Cellular Biology*, *27*(12), 4444–4453. https://doi.org/10.1128/MCB.02404-06

Aziz, M. H., Manoharan, H. T., Church, D. R., Dreckschmidt, N. E., Zhong, W., Oberley, T. D., … Verma, A. K. (2007). Protein kinase Cε interacts with signal transducers and activators of transcription 3 (Stat3), phosphorylates Stat3Ser727, and regulates its constitutive activation in prostate cancer. *Cancer Research*, *67*(18), 8828–8838. https://doi.org/10.1158/0008-

5472.CAN-07-1604

B Klein, XG Zhang, M Jourdan, J Content, F Houssiau, L Aarden, M. P. and R. B. (1989). Paracrine rather than autocrine regulation of myeloma-cells growth and differentiation by interleukine-6. *Blood*, *73*(426), 517–526.

Badkas, A., Frank, E., Zhou, Z., Jafari, M., Chandra, H., Sriram, V., … Yadav, J. S. (2018). Modulation of in vitro phagocytic uptake and immunogenicity potential of modified Herceptin®-conjugated PLGA-PEG nanoparticles for drug delivery. *Colloids and Surfaces B: Biointerfaces*, *162*, 271–278. https://doi.org/10.1016/j.colsurfb.2017.12.001

Bataille, R., Robillard, N., Avet-Loiseau, H., Hamusseau, J. L., & Moreau, P. (2005). CD221 (IGF-1R) is aberrantly expressed in multiple myeloma, in relation to disease severity. *Haematologica*, *90*(5), 706–707.

Becker, N. (2011). Epidemiology of multiple myeloma. In T. Moehler & H. Goldschmidt (Eds.), *Recent Results in Cancer Research* (Vol. 183, pp. 25–35). New York: Springer. https://doi.org/10.1007/978-3-540-85772-3_2

Beldi-Ferchiou, A., Skouri, N., Ben Ali, C., Safra, I., Abdelkefi, A., Ladeb, S., … Ben Ahmed, M. (2017). Abnormal repression of SHP-1, SHP-2 and SOCS-1 transcription sustains the activation of the JAK/STAT3 pathway and the progression of the disease in multiple myeloma. *PLoS ONE*, *12*(4), e0174835. https://doi.org/10.1371/journal.pone.0174835

Belloni, D., Marcatti, M., Ponzoni, M., Ciceri, F., Veschini, L., Corti, A., … Ferrero, E. (2015). Angiopoietin-2 in bone marrow milieu promotes multiple myeloma-associated angiogenesis. *Experimental Cell Research*, *330*(1), 1–12. https://doi.org/10.1016/j.yexcr.2014.10.017

Beum, P. V, Lindorfer, M. A., Peek, E. M., Stukenberg, P. T., de Weers, M., Beurskens, F. J., … Taylor, R. P. (2011). Penetration of antibody-opsonized cells by the membrane attack complex of complement promotes Ca2+ influx and induces streamers. *European Journal of Immunology*, *41*(8), 2436–2446. https://doi.org/10.1002/eji.201041204

Bezieau, S., Devilder, M.-C., Avet-Loiseau, H., Mellerin, M.-P., Puthier, D., Pennarun, E., … Bataille, R. (2001). High incidence of N and K-Ras activating mutations in multiple myeloma and primary plasma cell leukemia at diagnosis. *Human Mutation*, *18*(3), 212–224. https://doi.org/10.1002/humu.1177

Bharti, A. C., Shishodia, S., Reuben, J. M., Weber, D., Alexanian, R., Raj-Vadhan, S., … Aggarwal, B. B. (2004). Nuclear factor–κB and STAT3 are constitutively active in CD138 + cells derived from multiple myeloma patients, and suppression of these transcription factors leads to apoptosis. *Blood*, *103*(8), 3175–3184. https://doi.org/10.1182/blood-2003-06-2151

Bianchi, G., & Munshi, N. (2015). Pathogenesis beyond the cancer clone (s) in multiple myeloma. *Blood*, *125*(20), 3049–3059. https://doi.org/10.1182/blood-2014-11-568881.BLOOD

Boengler, K., Hilfiker-Kleiner, D., Heusch, G., & Schulz, R. (2010). Inhibition of permeability transition pore opening by mitochondrial STAT3 and its role in myocardial ischemia/reperfusion. *Basic Research in Cardiology*, *105*(6), 771–785. https://doi.org/10.1007/s00395-010-0124-1

Boghaert, E. R., Lu, X., Hessler, P. E., McGonigal, T. P., Oleksijew, A., Mitten, M. J., … Vaidya, K. S. (2017). The Volume of Three-Dimensional Cultures of Cancer Cells In Vitro Influences Transcriptional Profile Differences and Similarities with Monolayer Cultures and Xenografted Tumors. *Neoplasia (United States)*, *19*(9), 695–706.

https://doi.org/10.1016/j.neo.2017.06.004

Bommert, K., Bargou, R. C., & Stühmer, T. (2006). Signalling and survival pathways in multiple myeloma. *European Journal of Cancer*, *42*(11), 1574–1580. https://doi.org/10.1016/j.ejca.2005.12.026

Braga, W. M. T., da Silva, B. R., de Carvalho, A. C., Maekawa, Y. H., Bortoluzzo, A. B., Rizzatti, E. G., … Colleoni, G. W. B. (2014). FOXP3 and CTLA4 overexpression in multiple myeloma bone marrow as a sign of accumulation of CD4+ T regulatory cells. *Cancer Immunology, Immunotherapy*, *63*(11), 1189–1197. https://doi.org/10.1007/s00262-014-1589-9

Brenne, A.-T., Ro, T. B., Waage, A., Sundan, A., Borset, M., & Hjorth-Hansen, H. (2002). Interleukin-21 is a growth and survival factor for human myeloma cells. *Blood*, *99*(10), 3756–3762. https://doi.org/10.1182/blood.V99.10.3756

Bromberg, J. F., Wrzeszczynska, M. H., Devgan, G., Zhao, Y., Pestell, R. G., Albanese, C., & Darnell, J. E. (1999). Stat3 as an oncogene. *Cell*, *98*(3), 295–303. https://doi.org/10.1016/S0092-8674(00)81959-5

Brown, R., Yang, S., Weatherburn, C., Gibson, J., Ho, P. J., Suen, H., … Joshua, D. (2015). Phospho-flow detection of constitutive and cytokine-induced pSTAT3/5, pAKT and pERK expression highlights novel prognostic biomarkers for patients with multiple myeloma. *Leukemia*, *29*(2), 483–490. https://doi.org/10.1038/leu.2014.204

Calimeri, T., Battista, E., Conforti, F., Neri, P., Di Martino, M. T., Rossi, M., … Tassone, P. (2011). A unique three-dimensional SCID-polymeric scaffold (SCID-synth-hu) model for in vivo expansion of human primary multiple myeloma cells. *Leukemia*, *25*(4), 707–711.

https://doi.org/10.1038/leu.2010.300

Campbell, C. L., Jiang, Z., Savarese, D. M. F., & Savarese, T. M. (2001). Increased expression of the interleukin-11 receptor and evidence of STAT3 activation in prostate carcinoma. *American Journal of Pathology*, *158*(1), 25–32. https://doi.org/10.1016/S0002-9440(10)63940-5

Canadian Cancer Society. (2017). Canadian Cancer Statistics 2017. *Canadian Cancer Society*, *2017*, 1–132. https://doi.org/0835-2976

Canino, C., Luo, Y., Marcato, P., Blandino, G., Pass, H. I., & Cioce, M. (2015). A STAT3-NFkB/DDIT3/CEBPβ axis modulates ALDH1A3 expression in chemoresistant cell subpopulations. *Oncotarget*, *6*(14), 12637–12653. https://doi.org/10.18632/oncotarget.3703

Carpenter, R. L., & Lo, H. W. (2014, April 16). STAT3 target genes relevant to human cancers. *Cancers*. Multidisciplinary Digital Publishing Institute (MDPI). https://doi.org/10.3390/cancers6020897

Carranza-Torres, I. E., Guzmán-Delgado, N. E., Coronado-Martínez, C., Bañuelos-García, J. I., Viveros-Valdez, E., Morán-Martínez, J., & Carranza-Rosales, P. (2015). Organotypic culture of breast tumor explants as a multicellular system for the screening of natural compounds with antineoplastic potential. *BioMed Research International*, *2015*, 618021. https://doi.org/10.1155/2015/618021

Catlett-Falcone, R., Landowski, T. H., Oshiro, M. M., Turkson, J., Levitzki, A., Savino, R., … Jove, R. (1999). Constitutive activation of Stat3 signaling confers resistance to apoptosis in human U266 myeloma cells. *Immunity*, *10*(1), 105–115. https://doi.org/10.1016/s1074-

7613(00)80011-4

Catley, L., Weisberg, E., Kiziltepe, T., Tai, Y. T., Hideshima, T., Neri, P., … Anderson, K. C. (2006). Aggresome induction by proteasome inhibitor bortezomib and alpha-tubulin hyperacetylation by tubulin deacetylase (TDAC) inhibitor LBH589 are synergistic in myeloma cells. *Blood*, *108*(10), 3441–3449. https://doi.org/10.1182/blood-2006-04-016055

Cavo, M., Tacchetti, P., Patriarca, F., Petrucci, M. T., Pantani, L., Galli, M., … Baccarani, M. (2010). Bortezomib with thalidomide plus dexamethasone compared with thalidomide plus dexamethasone as induction therapy before, and consolidation therapy after, double autologous stem-cell transplantation in newly diagnosed multiple myeloma: a randomised phase 3. *The Lancet*, *376*(9758), 2075–2085. https://doi.org/10.1016/S0140-6736(10)61424-9

Chalmin, F., Mignot, G., Bruchard, M., Chevriaux, A., Végran, F., Hichami, A., … Ghiringhelli, F. (2012). Stat3 and Gfi-1 Transcription Factors Control Th17 Cell Immunosuppressive Activity via the Regulation of Ectonucleotidase Expression. *Immunity*, *36*(3), 362–373. https://doi.org/10.1016/j.immuni.2011.12.019

Chiecchio, L., Protheroe, R. K. M., Ibrahim, A. H., Cheung, K. L., Rudduck, C., Dagrada, G. P., … Ross, F. M. (2006). Deletion of chromosome 13 detected by conventional cytogenetics is a critical prognostic factor in myeloma. *Leukemia*, *20*(9), 1610–1617. https://doi.org/10.1038/sj.leu.2404304

Chitcholtan, K., Sykes, P. H., & Evans, J. J. (2012). The resistance of intracellular mediators to doxorubicin and cisplatin are distinct in 3D and 2D endometrial cancer. *Journal of Translational Medicine*, *10*(1). https://doi.org/10.1186/1479-5876-10-38

Choi, W. Il, Lee, J. H., Kim, J. Y., Heo, S. U., Jeong, Y. Y., Kim, Y. H., & Tae, G. (2015). Targeted antitumor efficacy and imaging via multifunctional nano-carrier conjugated with anti-HER2 trastuzumab. *Nanomedicine: Nanotechnology, Biology, and Medicine*, *11*(2), 359–368. https://doi.org/10.1016/j.nano.2014.09.009

Choi, Y., Zhang, J., Murga, C., Yu, H., Monia, B. P., Gutkind, J. S., & Li, W. (2002). PTEN, but not SHIP and SHIP2, suppresses the PI3K/Akt pathway and induces growth inhibition and apoptosis of myeloma cells. *Oncogene*, *21*(34), 5289–5300. https://doi.org/10.1038/sj.onc.1205650

Colombo, M., Galletti, S., Garavelli, S., Platonova, N., Paoli, A., Basile, A., … Chiaramonte, R. (2015). Notch signaling deregulation in multiple myeloma: A rational molecular target. *Oncotarget*, *6*(29), 26826–26840. https://doi.org/10.18632/oncotarget.5025

Cosco, D., Cilurzo, F., Maiuolo, J., Federico, C., Di Martino, M. T., Cristiano, M. C., … Paolino, D. (2015). Delivery of miR-34a by chitosan/PLGA nanoplexes for the anticancer treatment of multiple myeloma. *Scientific Reports*, *5*. https://doi.org/10.1038/srep17579

Costello, R. T., Boehrer, A., Sanchez, C., Mercier, D., Baier, C., Le Treut, T., & Sébahoun, G. (2013). Differential expression of natural killer cell activating receptors in blood versus bone marrow in patients with monoclonal gammopathy. *Immunology*, *139*(3), 338–341. https://doi.org/10.1111/imm.12082

Costes, V., Portier, M., Lu, Z. Y., Rossi, J. F., Bataille, R., & Klein, B. (1998). Interleukin-1 in multiple myeloma: Producer cells and their role in the control of IL-6 production. *British Journal of Haematology*, *103*(4), 1152–1160. https://doi.org/10.1046/j.1365-2141.1998.01101.x

Cremer, F. W., Bila, J., Buck, I., Kartal, M., Hose, D., Ittrich, C., … Jauch, A. (2005). Delineation of distinct subgroups of multiple myeloma and a model for clonal evolution based on interphase cytogenetics. *Genes Chromosomes and Cancer*, *44*(2), 194–203. https://doi.org/10.1002/gcc.20231

Damle, R. N., Wasil, T., Fais, F., Ghiotto, F., Valetto, A., Allen, S. L., … Chiorazzi, N. (1999). Ig V gene mutation status and CD38 expression as novel prognostic indicators in chronic lymphocytic leukemia. *Blood*, *94*(6), 1840–1847. https://doi.org/10.1172/JCI118644

Datta, S. R., Dudek, H., Tao, X., Masters, S., Fu, H., Gotoh, Y., & Greenberg, M. E. (1997). Akt Phosphorylation of BAD Couples Survival Signals to the Cell-Intrinsic Death Machinery. *Cell*, *91*(2), 231–241. https://doi.org/10.1016/S0092-8674(00)80405-5

de la Puente, P., Luderer, M. J., Federico, C., Jin, A., Gilson, R. C., Egbulefu, C., … Azab, A. K. (2018). Enhancing proteasome-inhibitory activity and specificity of bortezomib by CD38 targeted nanoparticles in multiple myeloma. *Journal of Controlled Release*, *270*, 158–176. https://doi.org/10.1016/j.jconrel.2017.11.045

de la Puente, P., Muz, B., Gilson, R. C., Azab, F., Luderer, M., King, J., … Azab, A. K. (2015). 3D tissue-engineered bone marrow as a novel model to study pathophysiology and drug resistance in multiple myeloma. *Biomaterials*, *73*, 70–84. https://doi.org/10.1016/j.biomaterials.2015.09.017

de Oliveira, M. B., Fook-Alves, V. L., Eugenio, A. I. P., Fernando, R. C., Sanson, L. F. G., de Carvalho, M. F., … Colleoni, G. W. B. (2017). Anti-myeloma effects of ruxolitinib combined with bortezomib and lenalidomide: A rationale for JAK/STAT pathway inhibition in myeloma patients. *Cancer Letters*, *403*, 206–215.

https://doi.org/10.1016/j.canlet.2017.06.016

de Weers, M., Tai, Y.-T., van der Veer, M. S., Bakker, J. M., Vink, T., Jacobs, D. C. H., … Parren, P. W. H. I. (2011). Daratumumab, a Novel Therapeutic Human CD38 Monoclonal Antibody, Induces Killing of Multiple Myeloma and Other Hematological Tumors. *The Journal of Immunology*, *186*(3), 1840–1848. https://doi.org/10.4049/jimmunol.1003032

De Witt Hamer, P. C., Van Tilborg, A. A. G., Eijk, P. P., Sminia, P., Troost, D., Van Noorden, C. J. F., … Leenstra, S. (2008). The genomic profile of human malignant glioma is altered early in primary cell culture and preserved in spheroids. *Oncogene*, *27*(14), 2091–2096. https://doi.org/10.1038/sj.onc.1210850

Debotton, N., Zer, H., Parnes, M., Harush-Frenkel, O., Kadouche, J., & Benita, S. (2010). A quantitative evaluation of the molecular binding affinity between a monoclonal antibody conjugated to a nanoparticle and an antigen by surface plasmon resonance. *European Journal of Pharmaceutics and Biopharmaceutics*, *74*(2), 148–156. https://doi.org/10.1016/j.ejpb.2009.09.014

Della Pietra, L., Bressan, A., Pezzotti, A. R., & Serlupi-Crescenzi, O. (1998). Highly conserved amino-acid sequence between murine STAT3 and a revised human STAT3 sequence. *Gene*, *213*(1–2), 119–124. https://doi.org/10.1016/S0378-1119(98)00185-1

Demchenko, Y. N., & Kuehl, W. M. (2010). A critical role for the NFkB pathway in multiple myeloma. *Oncotarget*, *1*(1), 59–68. https://doi.org/10.18632/oncotarget.109

Dilnawaz, F., Singh, A., Mohanty, C., & Sahoo, S. K. (2010). Dual drug loaded superparamagnetic iron oxide nanoparticles for targeted cancer therapy. *Biomaterials*, *31*(13), 3694–3706.

https://doi.org/10.1016/j.biomaterials.2010.01.057

Ding, B., Wu, X., Fan, W., Wu, Z., Gao, J., Zhang, W., … Gao, S. (2011). Anti-DR5 monoclonal antibody-mediated DTIC-loaded nanoparticles combining chemotherapy and immunotherapy for malignant melanoma: target formulation development and in vitro anticancer activity. *International Journal of Nanomedicine*, *6*, 1991–2005. https://doi.org/10.2147/IJN.S24094

Durie, B. G. M., & Salmon, S. E. (1975). A clinical staging system for multiple myeloma correlation of measured myeloma cell mass with presenting clinical features, response to treatment, and survival. *Cancer*, *36*(3), 842–854. https://doi.org/10.1002/1097-0142(197509)36:3<842::AID-CNCR2820360303>3.0.CO;2-U

Edmondson, R., Broglie, J. J., Adcock, A. F., & Yang, L. (2014). Three-dimensional cell culture systems and their applications in drug discovery and cell-based biosensors. *ASSAY and Drug Development Technologies*, *12*(4), 207–218. https://doi.org/10.1089/adt.2014.573

Edwards, J. C. W., & Cambridge, G. (2006, May 7). B-cell targeting in rheumatoid arthritis and other autoimmune diseases. *Nature Reviews Immunology*. Nature Publishing Group. https://doi.org/10.1038/nri1838

Ferlin, M., Noraz, N., Hertogh, C., Brochier, J., Taylor, N., & Klein, B. (2008). Insulin-like growth factor induces the survival and proliferation of myeloma cells through an interleukin-6-independent transduction pathway. *British Journal of Haematology*, *111*(2), 626–634. https://doi.org/10.1111/j.1365-2141.2000.02364.x

Fernando, R. C., de Carvalho, F., Mazzotti, D. R., Evangelista, A. F., Braga, W. M. T., de Lourdes

Chauffaille, M., … Colleoni, G. W. B. (2015). Multiple myeloma cell lines and primary tumors proteoma: protein biosynthesis and immune system as potential therapeutic targets. *Genes & Cancer*, *6*(11–12), 462–471. https://doi.org/10.18632/GENESANDCANCER.88

Ferrarini, M., Mazzoleni, G., Steimberg, N., Belloni, D., & Ferrero, E. (2013). Innovative models to assess multiple myeloma biology and the impact of drugs. *InTech*, (Mm), 39–60. https://doi.org/10.5772/56515

Ferrarini, M., Steimberg, N., Ponzoni, M., Belloni, D., Berenzi, A., Girlanda, S., … Ferrero, E. (2013). Ex-Vivo dynamic 3-D culture of human tissues in the RCCS™ bioreactor allows the study of multiple myeloma biology and response to therapy. *PLoS ONE*, *8*(8), e71613. https://doi.org/10.1371/journal.pone.0071613

Fischbach, C., Chen, R., Matsumoto, T., Schmelzle, T., Brugge, J. S., Polverini, P. J., & Mooney, D. J. (2007). Engineering tumors with 3D scaffolds. *Nature Methods*, *4*(10), 855–860. https://doi.org/10.1038/nmeth1085

Fonseca, R., Debes-Marun, C. S., Picken, E. B., Dewald, G. W., Bryant, S. C., Winkler, J. M., … Greipp, P. R. (2003). The recurrent IgH translocations are highly associated with nonhyperdiploid variant multiple myeloma. *Blood*, *102*(7), 2562–2567. https://doi.org/10.1182/blood-2003-02-0493

Fu, X.-Y., Schindler, C., Improta, T., Aebersoldt, R., & Darnell, J. E. (1992). The proteins of ISGF-3, the interferon a-induced transcriptional activator, define a gene family involved in signal transduction. *Biochemistry*, *89*(16), 7840–7843. https://doi.org/10.1073/pnas.89.16.7840

Fuchs, O. (2013). Targeting of NF-kappaB signaling pathway, other signaling pathways and epigenetics in therapy of multiple myeloma. *Cardiovasc Hematol Disord Drug Targets*, *13*(1), 16–34. https://doi.org/10.2174/1871529X11313010003

Funaro, A., Morra, M., Calosso, L., Zini, M. G., Ausiello, C. M., & Malavasi, F. (1997). Role of the human CD38 molecule in B cell activation and proliferation. *Tissue Antigens*, *49*(1), 7–15. https://doi.org/10.1111/j.1399-0039.1997.tb02703.x

Gaca, S., Reichert, S., Multhoff, G., Wacker, M., Hehlgans, S., Botzler, C., … Rödel, F. (2013). Targeting by cmHsp70.1-antibody coated and survivin miRNA plasmid loaded nanoparticles to radiosensitize glioblastoma cells. *Journal of Controlled Release*, *172*(1), 201–206. https://doi.org/10.1016/J.JCONREL.2013.08.020

Galm, O., Yoshikawa, H., Esteller, M., Osieka, R., & Herman, J. G. (2003). SOCS-1, a negative regulator of cytokine signaling, is frequently silenced by methylation in multiple myeloma. *Blood*, *101*(7), 2784–2788. https://doi.org/10.1182/blood-2002-06-1735

Gao, J., Xia, Y., Chen, H., Yu, Y., Song, J., Li, W., … Guo, Y. (2014). Polymer–lipid hybrid nanoparticles conjugated with anti-EGF receptor antibody for targeted drug delivery to hepatocellular carcinoma. *Nanomedicine*, *9*(2), 279–293. https://doi.org/10.2217/nnm.13.20

Garg, S. M., Paiva, I. M., Vakili, M. R., Soudy, R., Agopsowicz, K., Soleimani, A. H., … Lavasanifar, A. (2017). Traceable PEO-poly(ester) micelles for breast cancer targeting: The effect of core structure and targeting peptide on micellar tumor accumulation. *Biomaterials*, *144*, 17–29. https://doi.org/10.1016/j.biomaterials.2017.08.001

Gastinne, T., Leleu, X., Duhamel, A., Moreau, A. S., Franck, G., Andrieux, J., … Facon, T. (2007).

Plasma cell growth fraction using Ki-67 antigen expression identifies a subgroup of multiple myeloma patients displaying short survival within the ISS stage I. *European Journal of Haematology*, *79*(4), 297–304. https://doi.org/10.1111/j.1600-0609.2007.00915.x

Ge, F., Zhang, L., Tao, S.-C., Kitazato, K., Zhang, Z.-P., Zhang, X.-E., & Bi, L.-J. (2011). Quantitative Proteomic Analysis of Tumor Reversion in Multiple Myeloma Cells. *Journal of Proteome Research*, *10*(2), 845–855. https://doi.org/10.1021/pr100992e

Ge, N.-L., & Rudikoff, S. (2000). Insulin-like growth factor I is a growth and survival factor in human multiple myeloma cell lines. *Blood*, *96*(8), 2856–2861.

Gerecke, C., Fuhrmann, S., Strifler, S., Schmidt-Hieber, M., Einsele, H., & Knop, S. (2016). The diagnosis and treatment of multiple myeloma. *Deutsches Arzteblatt International*, *113*(27–28), 470–476. https://doi.org/10.3238/arztebl.2016.0470

Ghosh, S., & Karin, M. (2002, April 19). Missing pieces in the NF-κB puzzle. *Cell*. Cell Press. https://doi.org/10.1016/S0092-8674(02)00703-1

Ghosh, S., Spagnoli, G. C., Martin, I., Ploegert, S., Demougin, P., Heberer, M., & Reschner, A. (2005). Three-dimensional culture of melanoma cells profoundly affects gene expression profile: A high density oligonucleotide array study. *Journal of Cellular Physiology*, *204*(2), 522–531. https://doi.org/10.1002/jcp.20320

Gillet, J.-P., Varma, S., & Gottesman, M. M. (2013). The Clinical Relevance of Cancer Cell Lines. *JNCI Journal of the National Cancer Institute*, *105*(7), 452–458. https://doi.org/10.1093/jnci/djt007

Giuliani, N., Bataille, R., Mancini, C., Lazzaretti, M., & Barillé, S. (2001). Myeloma cells induce

imbalance in the osteoprotegerin/osteoprotegerin ligand system in the human bone marrow environment. *Blood*, *98*(13), 3527–3533.

Giuliani, N., Colla, S., Morandi, F., Lazzaretti, M., Sala, R., Bonomini, S., … Rizzoli, V. (2005). Myeloma cells block RUNX2/CBFA1 activity in human bone marrow osteoblast progenitors and inhibit osteoblast formation and differentiation. *Blood*, *106*(7), 2472–2483. https://doi.org/10.1182/blood-2004-12-4986

Gomez-Roman, N., Stevenson, K., Gilmour, L., Hamilton, G., & Chalmers, A. J. (2016). A novel 3D human glioblastoma cell culture system for modeling drug and radiation responses. *Neuro-Oncology*, *17*(1), now164. https://doi.org/10.1093/neuonc/now164

Görgün, G., Samur, M. K., Cowens, K. B., Paula, S., Bianchi, G., Anderson, J. E., … Anderson, K. C. (2015). Lenalidomide enhances immune checkpoint blockade-induced immune response in multiple myeloma. *Clinical Cancer Research*, *21*(20), 4617–4618. https://doi.org/10.1158/1078-0432.CCR-15-0200

Gozzetti, A., Candi, V., Papini, G., & Bocchia, M. (2014). Therapeutic advancements in multiple myeloma. *Frontiers in Oncology*, *4*, 241. https://doi.org/10.3389/fonc.2014.00241

Greipp, P. R., Miguel, J. S., Dune, B. G. M., Crowley, J. J., Barlogie, B., Bladé, J., … Westin, J. (2005). International staging system for multiple myeloma. *Journal of Clinical Oncology*, *23*(15), 3412–3420. https://doi.org/10.1200/JCO.2005.04.242

Gunn, E. J., Williams, J. T., Huynh, D. T., Iannotti, M. J., Han, C., Barrios, F. J., … Kirshner, J. (2011). The natural products parthenolide and andrographolide exhibit anti-cancer stem cell activity in multiple myeloma. *Leukemia & Lymphoma*, *52*(6), 1085–1097.

https://doi.org/10.3109/10428194.2011.555891

Guo, Y., Xu, F., Lu, T., Duan, Z., & Zhang, Z. (2012). Interleukin-6 signaling pathway in targeted therapy for cancer. *Cancer Treatment Reviews*. https://doi.org/10.1016/j.ctrv.2012.04.007

Guse, A. H., Da Silva, C. P., Berg, I., Skapenko, A. L., Weber, K., Heyer, P., … Mayr, G. W. (1999). Regulation of calcium signalling in T lymphocytes by the second messenger cyclic ADP-ribose. *Nature*, *398*(6722), 70–73. https://doi.org/10.1038/18024

Hallek, M., Bergsagel, P. L., Anderson, K. C., Taga, T., Haleem, A., & Chen, J. (1998). Multiple myeloma: increasing evidence for a multistep transformation process. *Blood*, *91*(1), 3–21. https://doi.org/10.1182/blood.v97.2.483

Hanamura, I., Stewart, J. P., Huang, Y., Zhan, F., Santra, M., Sawyer, J. R., … Shaughnessy, J. D. (2006). Frequent gain of chromosome band 1q21 in plasma-cell dyscrasias detected by fluorescence in situ hybridization: Incidence increases from MGUS to relapsed myeloma and is related to prognosis and disease progression following tandem stem-cell transplantatio. *Blood*, *108*(5), 1724–1732. https://doi.org/10.1182/blood-2006-03-009910

Harousseau, J.-L., Attal, M., Avet-Loiseau, H., Marit, G., Caillot, D., Mohty, M., … Moreau, P. (2010). Bortezomib plus dexamethasone is superior to vincristine plus doxorubicin plus dexamethasone as induction treatment prior to autologous stem-cell transplantation in newly diagnosed multiple myeloma: results of the IFM 2005-01 phase III trial. *Journal of Clinical Oncology : Official Journal of the American Society of Clinical Oncology*, *28*(30), 4621–4629. https://doi.org/10.1200/JCO.2009.27.9158

Hata, H., Xiao, H., Petrucci, M. T., Woodliff, J., Chang, R., & Epstein, J. (1993). Interleukin-6

gene expression in multiple myeloma: a characteristic of immature tumor cells. *Blood*, *81*(12), 3357–3364.

Hatakeyama, H., Akita, H., Ishida, E., Hashimoto, K., Kobayashi, H., Aoki, T., … Harashima, H. (2007). Tumor targeting of doxorubicin by anti-MT1-MMP antibody-modified PEG liposomes. *International Journal of Pharmaceutics*, *342*(1–2), 194–200. https://doi.org/10.1016/j.ijpharm.2007.04.037

HEINRICH, P. C., BEHRMANN, I., MÜLLER-NEWEN, G., SCHAPER, F., & GRAEVE, L. (1998). Interleukin-6-type cytokine signalling through the gp130/Jak/STAT pathway. *Biochemical Journal*, *334*(2), 297–314. https://doi.org/10.1042/bj3340297

Hideshima, T., & Anderson, K. C. (2002, December 1). Molecular mechanisms of novel therapeutic approaches for multiple myeloma. *Nature Reviews Cancer*. Nature Publishing Group. https://doi.org/10.1038/nrc952

Hideshima, T., Chauhan, D., Schlossman, R., Richardson, P., & Anderson, K. C. (2001). The role of tumor necrosis factor alpha in the pathophysiology of human multiple myeloma: therapeutic applications. *Oncogene*, *20*(33), 4519–4527. https://doi.org/10.1038/sj.onc.1204623

Huang, X., Di Liberto, M., Jayabalan, D., Liang, J., Ely, S., Bretz, J., … Chen-Kiang, S. (2012). Prolonged early G 1 arrest by selective CDK4/CDK6 inhibition sensitizes myeloma cells to cytotoxic killing through cell cycle-coupled loss of IRF4. *Blood*, *120*(5), 1095–1106. https://doi.org/10.1182/blood-2012-03-415984

Huang, Y., Liu, Y., Zheng, C., & Shen, C. (2017). Investigation of cross-contamination and

misidentification of 278 widely used tumor cell lines. *PLoS ONE*, *12*(1), e0170384. https://doi.org/10.1371/journal.pone.0170384

Huang, Y., Qiu, J., Dong, S., Redell, M. S., Poli, V., Mancini, M. A., & Tweardy, D. J. (2007). Stat3 isoforms, alpha and beta, demonstrate distinct intracellular dynamics with prolonged nuclear retention of Stat3beta mapping to its unique C-terminal end. *The Journal of Biological Chemistry*, *282*(48), 34958–34967. https://doi.org/10.1074/jbc.M704548200

Hyun, T., Yam, A., Pece, S., Xie, X., Zhang, J., Miki, T., … Li, W. (2000). Loss of PTEN expression leading to high Akt activation in human multiple myelomas. *Blood*, *96*(10), 3560–3568.

Illum, L., Jones, P. D. E., Kreuter, J., Baldwin, R. W., & Davis, S. S. (1983). Adsorption of monoclonal antibodies to polyhexylcyanoacrylate nanoparticles and subsequent immunospecific binding to tumour cells in vitro. *International Journal of Pharmaceutics*, *17*(1), 65–76. https://doi.org/10.1016/0378-5173(83)90019-4

Imamura, Y., Mukohara, T., Shimono, Y., Funakoshi, Y., Chayahara, N., Toyoda, M., … Minami, H. (2015, April 1). Comparison of 2D and 3D culture models as drug-testing platforms in breast cancer. *Oncology Reports*. [National Hellenic Research Foundation]. https://doi.org/10.3892/or.2015.3767

Jafari, R., Almqvist, H., Axelsson, H., Ignatushchenko, M., Lundbäck, T., Nordlund, P., & Molina, D. M. (2014). The cellular thermal shift assay for evaluating drug target interactions in cells. *Nature Protocols*, *9*(9), 2100–2122. https://doi.org/10.1038/nprot.2014.138

Jain, A., & Cheng, K. (2017). The principles and applications of avidin-based nanoparticles in

drug delivery and diagnosis. *Journal of Controlled Release*. https://doi.org/10.1016/j.jconrel.2016.11.016

Jain, N. K., Tare, M. S., Mishra, V., & Tripathi, P. K. (2015). The development, characterization and in vivo anti-ovarian cancer activity of poly(propylene imine) (PPI)-antibody conjugates containing encapsulated paclitaxel. *Nanomedicine: Nanotechnology, Biology, and Medicine*, *11*(1), 207–218. https://doi.org/10.1016/j.nano.2014.09.006

Jazayeri, M. H., Amani, H., Pourfatollah, A. A., Pazoki-Toroudi, H., & Sedighimoghaddam, B. (2016, July 1). Various methods of gold nanoparticles (GNPs) conjugation to antibodies. *Sensing and Bio-Sensing Research*. Elsevier. https://doi.org/10.1016/j.sbsr.2016.04.002

Jelinek, D. F., Witzig, T. E., & Arendt, B. K. (1997). A role for insulin-like growth factor in the regulation of IL-6-responsive human myeloma cell line growth. *Journal of Immunology (Baltimore, Md. : 1950)*, *159*(1), 487–496.

Jung, S.-H., Ahn, S., Choi, H.-W., Shin, M.-G., Lee, S., Yang, D.-H., … Lee, J.-J. (2017). STAT3 expression is associated with poor survival in non-elderly adult patients with newly diagnosed multiple myeloma. *Blood Research*, *52*(4), 293. https://doi.org/10.5045/br.2017.52.4.293

Kallen, K. J. (2002, November 11). The role of transsignalling via the agonistic soluble IL-6 receptor in human diseases. *Biochimica et Biophysica Acta - Molecular Cell Research*. Elsevier. https://doi.org/10.1016/S0167-4889(02)00325-7

Kamińska, J., Koper, O. M., Dymicka-Piekarska, V., Motybel, E., Kłoczko, J., & Ke-Mona, H. (2015). Angiogenic cytokines: IL-6, sIL-6R, TNF-α, sVCAM-1, and PDGF-AB in multiple myeloma patients depending on the stage of the disease. *Edorium Journal of Tumor Biology*

Edorium J Tumor Bio, *22*, 11–19.

Kaptein, A., Paillard, V., & Saunders, M. (1996). Dominant negative Stat3 mutant inhibits interleukin-6-induced Jak-STAT signal transduction. *Journal of Biological Chemistry*, *271*(11), 5961–5964. https://doi.org/10.1074/jbc.271.11.5961

Karra, N., Nassar, T., Ripin, A. N., Schwob, O., Borlak, J., & Benita, S. (2013). Antibody conjugated PLGA nanoparticles for targeted delivery of paclitaxel palmitate: Efficacy and biofate in a lung cancer mouse model. *Small*, *9*(24), 4221–4236. https://doi.org/10.1002/smll.201301417

Kennedy, S. G., Kandel, E. S., Cross, T. K., & Hay, N. (1999). Akt/Protein kinase B inhibits cell death by preventing the release of cytochrome c from mitochondria. *Molecular and Cellular Biology*, *19*(8), 5800–5810. https://doi.org/10.1128/MCB.19.8.5800

Keyhani, A., Huh, Y. O., Jendiroba, D., Pagliaro, L., Cortez, J., Pierce, S., … Freireich, E. J. (2000). Increased CD38 expression is associated with favorable prognosis in adult acute leukemia. *Leukemia Research*, *24*(2), 153–159. https://doi.org/10.1016/S0145-2126(99)00147-2

Khan, M. L., Reeder, C. B., Kumar, S. K., Lacy, M. Q., Reece, D. E., Dispenzieri, A., … Keith Stewart, A. (2012). A comparison of lenalidomide/dexamethasone versus cyclophosphamide/lenalidomide/dexamethasone versus cyclophosphamide/bortezomib/dexamethasone in newly diagnosed multiple myeloma. *British Journal of Haematology*, *156*(3), 326–333. https://doi.org/10.1111/j.1365-2141.2011.08949.x

Khong, T., & Spencer, A. (2011). Targeting HSP 90 Induces Apoptosis and Inhibits Critical Survival and Proliferation Pathways in Multiple Myeloma. *Molecular Cancer Therapeutics*, *10*(10), 1909–1917. https://doi.org/10.1158/1535-7163.MCT-11-0174

Khoury, J. D., Medeiros, L. J., Rassidakis, G. Z., Yared, M. A., Tsioli, P., Leventaki, V., … Lai, R. (2003). Differential expression and clinical significance of tyrosine-phosphorylated STAT3 in ALK+ and ALK- anaplastic large cell lymphoma. *Clin Cancer Res*, *9*(10 Pt 1), 3692–3699.

Kim, M. J., Nam, H. J., Kim, H. P., Han, S. W., Im, S. A., Kim, T. Y., … Bang, Y. J. (2013). OPB-31121, a novel small molecular inhibitor, disrupts the JAK2/STAT3 pathway and exhibits an antitumor activity in gastric cancer cells. *Cancer Letters*, *335*(1), 154–152. https://doi.org/10.1016/j.canlet.2013.02.010

Kirshner, J., Thulien, K. J., Martin, L. D., Debes Marun, C., Reiman, T., Belch, A. R., & Pilarski, L. M. (2008). A unique three-dimensional model for evaluating the impact of therapy on multiple myeloma. *Blood*, *112*(7), 2935–2945. https://doi.org/10.1182/blood-2008-02-142430

Kishimoto, T. (1985). Factors affecting B-cell growth and differentiation. *Annual Review of Immunology*, *3*(3), 133–157. https://doi.org/10.1146/annurev.iy.03.040185.001025

Klein, U., Jauch, A., Hielscher, T., Hillengass, J., Raab, M. S., Seckinger, A., … Neben, K. (2011). Chromosomal aberrations +1q21 and del(17p13) predict survival in patients with recurrent multiple myeloma treated with lenalidomide and dexamethasone. *Cancer*, *117*(10), 2136–2144. https://doi.org/10.1002/cncr.25775

Kodama, S., Yamada, H., Annab, L., & Barrett, J. C. (1995). Elevated expression of mitochondrial cytochrome b and NADH dehydrogenase subunit 4/4L genes in senescent human cells. *Experimental Cell Research*, *219*(1), 82–86. https://doi.org/10.1006/excr.1995.1207

Kogan, T. (1992). The synthesis of substituted methoxy-poly (ethyleneglycol) derivatives suitable for selective protein modification. *Synthetic Communications*, *22*(16), 2417–2424. https://doi.org/10.1080/00397919208019100

Kolosenko, I., Grandér, D., & Tamm, K. P. (2014). IL-6 activated JAK/STAT3 pathway and sensitivity to Hsp90 inhibitors in multiple myeloma. *Current Medicinal Chemistry*, *46*(8), 3042–3047. https://doi.org/10.2174/09298673216661404141008 31

Kopan, R., & Ilagan, M. X. G. (2009, April 17). The canonical Notch signaling pathway: unfolding the activation mechanism. *Cell*. Cell Press. https://doi.org/10.1016/j.cell.2009.03.045

Kraskouskaya, D., Duodu, E., Arpin, C. C., Gunning, P. T., Sadowski, I., Stone, J. C., … Roller, P. P. (2013). Progress towards the development of SH2 domain inhibitors. *Chemical Society Reviews*, *42*(8), 3337. https://doi.org/10.1039/c3cs35449k

Krebsbach, P. H., Kuznetsov, S. A., Bianco, P., & Gehron Robey, P. (1999). Bone Marrow Stromal Cells: Characterization and Clinical Application. *Critical Reviews in Oral Biology & Medicine*, *10*(2), 165–181. https://doi.org/10.1177/10454411990100020401

Krüger-Krasagakes, S., Möller, A., Kolde, G., Lippert, U., Weber, M., & Henz, B. M. (1996). Production of interleukin-6 by human mast cells and basophilic cells. *Journal of Investigative Dermatology*, *106*(1), 75–79. https://doi.org/10.1111/1523-1747.ep12327815

Kumar, S. K., Rajkumar, S. V., Dispenzieri, A., Lacy, M. Q., Hayman, S. R., Buadi, F. K., …

Gertz, M. A. (2008). Improved survival in multiple myeloma and the impact of novel therapies. *Blood*, *111*(5), 2516–2520. https://doi.org/10.1182/blood-2007-10-116129

Kumar, S., Kimlinger, T., & Morice, W. (2010, September 1). Immunophenotyping in multiple myeloma and related plasma cell disorders. *Best Practice and Research: Clinical Haematology*. Elsevier. https://doi.org/10.1016/j.beha.2010.09.002

Kyle, R. A., & Rajkumar, S. V. (2008). Multiple myeloma. *Blood*, *111*(6), 2962–2972. https://doi.org/10.1182/blood-2007-10-078022

Kyle, R. A., Therneau, T. M., Rajkumar, S. V., Offord, J. R., Larson, D. R., Plevak, M. F., & Melton, L. J. (2002). A Long-Term Study of Prognosis in Monoclonal Gammopathy of Undetermined Significance. *New England Journal of Medicine*, *346*(8), 564–569. https://doi.org/10.1056/NEJMoa01133202

Lai, E. C. (2004). Notch signaling: control of cell communication and cell fate. *Development*, *131*(5), 965–973. https://doi.org/10.1242/dev.01074

Lee, S. M., Kim, H. J., Kim, S. Y., Kwon, M. K., Kim, S., Cho, A., … Yoo, K. H. (2014). Drug-loaded gold plasmonic nanoparticles for treatment of multidrug resistance in cancer. *Biomaterials*, *35*(7), 2272–2282. https://doi.org/10.1016/j.biomaterials.2013.11.068

Leif Bergsagel, P., & Michael Kuehl, W. (2001, September 8). Chromosome translocations in multiple myeloma. *Oncogene*. Nature Publishing Group. https://doi.org/10.1038/sj.onc.1204641

Leleu, X., Fouquet, G., Hebraud, B., Roussel, M., Caillot, D., Chrétien, M. L., … Moreau, P. (2013). Consolidation with VTd significantly improves the complete remission rate and time

to progression following VTd induction and single autologous stem cell transplantation in multiple myeloma. *Leukemia*. https://doi.org/10.1038/leu.2013.101

Lemancewicz, D., Bolkun, L., Jablonska, E., Kulczynska, A., Bolkun-Skornicka, U., Kloczko, J., & Dzieciol, J. (2013). Evaluation of TNF superfamily molecules in multiple myeloma patients: Correlation with biological and clinical features. *Leukemia Research*, *37*(9), 1089–1093. https://doi.org/10.1016/j.leukres.2013.05.014

Levy, D. E., Lee, C., Darnell, J., Kerr, I., Stark, G., Levy, D., … Desiderio, S. (2002). What does Stat3 do? *The Journal of Clinical Investigation*, *109*(9), 1143–1148. https://doi.org/10.1172/JCI15650

Levy, J. B., Schindler, C., Raz, R., Levy, D. E., Baron, R., & Horowitz, M. C. (1996). Activation of the JAK-STAT signal transduction pathway by oncostatin-M in cultured human and mouse osteoblastic cells. *Endocrinology*, *137*(4), 1159–1165. https://doi.org/10.1210/en.137.4.1159

Li, A., Walling, J., Kotliarov, Y., Center, A., Steed, M. E., Ahn, S. J., … Fine, H. A. (2008). Genomic changes and gene expression profiles reveal that established glioma cell lines are poorly representative of primary human gliomas. *Molecular Cancer Research*, *6*(1), 21–30. https://doi.org/10.1158/1541-7786.MCR-07-0280

Li, D., Lu, B., Huang, Z., Xu, P., Zheng, H., Yin, Y., … Xiong, F. (2014). A novel melphalan polymeric prodrug: Preparation and property study. *Carbohydrate Polymers*, *111*, 928–935. https://doi.org/10.1016/j.carbpol.2014.04.062

Li, Y., Guo, Y., Tang, J., Jiang, J., & Chen, Z. (2014). New insights into the roles of CHOP-induced apoptosis in ER stress. *Acta Biochimica et Biophysica Sinica*, *46*(8), 629–640.

https://doi.org/10.1093/abbs/gmu048

Liang, P., Cheng, S. H., Cheng, C. K., Lau, K. M., Lin, S. Y., Chow, E. Y. D., … Ng, M. H. L. (2013). Platelet factor 4 induces cell apoptosis by inhibition of STAT3 via up-regulation of SOCS3 expression in multiple myeloma. *Haematologica*, *98*(2), 288–295. https://doi.org/10.3324/haematol.2012.065607

Lin, H., Kolosenko, I., Bj?rklund, A.-C., Protsyuk, D., ?sterborg, A., Grand?r, D., … Tamm, K. P. (2013). An activated JAK/STAT3 pathway and CD45 expression are associated with sensitivity to Hsp90 inhibitors in multiple myeloma. *Experimental Cell Research*, *319*(5), 600–611. https://doi.org/10.1016/j.yexcr.2012.12.006

Lin, L., Benson, D. M., Deangelis, S., Bakan, C. E., Li, P. K., Li, C., & Lin, J. (2012). A small molecule, LLL12 inhibits constitutive STAT3 and IL-6-induced STAT3 signaling and exhibits potent growth suppressive activity in human multiple myeloma cells. *International Journal of Cancer*, *130*(6), 1459–1469. https://doi.org/10.1002/ijc.26152

Lin, L., Yan, F., Zhao, D., Lv, M., Liang, X., Dai, H., … Ge, Q. (2016). Reelin promotes the adhesion and drug resistance of multiple myeloma cells via integrin β1 signaling and STAT3. *Oncotarget*, *7*(9), 9844–9858. https://doi.org/10.18632/oncotarget.7151

Lin, P., Owens, R., Tricot, G., & Wilson, C. S. (2004). Flow Cytometric Immunophenotypic Analysis of 306 Cases of Multiple Myeloma. *American Journal of Clinical Pathology*, *121*(4), 482–488. https://doi.org/10.1309/74R4-TB90-BUWH-27JX

Liu, L., McBride, K. M., & Reich, N. C. (2005). STAT3 nuclear import is independent of tyrosine phosphorylation and mediated by importin- 3. *Proceedings of the National Academy of*

Sciences, *102*(23), 8150–8155. https://doi.org/10.1073/pnas.0501643102

Liu, P., Leong, T., Quam, L., Billadeau, D., Kay, N. E., Greipp, P., … Van Ness, B. (1996). Activating mutations of N- and K-ras in multiple myeloma show different clinical associations: analysis of the Eastern Cooperative Oncology Group Phase III Trial. *Blood*, *88*(7), 2699–2706. https://doi.org/10.1002/humu.1177

Liu, Q., Zhang, Z., Liu, Y., Cui, Z., Zhang, T., Li, Z., & Ma, W. (2018). Cancer cells growing on perfused 3D collagen model produced higher reactive oxygen species level and were more resistant to cisplatin compared to the 2D model. *Journal of Applied Biomaterials & Functional Materials*, 2280800018764763. https://doi.org/10.1177/2280800018764763

Liu, T., Fei, Z., Gangavarapu, K. J., Agbenowu, S., Bhushan, A., Lai, J. C. K., … Cao, S. (2013). Interleukin-6 and JAK2/STAT3 signaling mediate the reversion of dexamethasone resistance after dexamethasone withdrawal in 7TD1 multiple myeloma cells. *Leukemia Research*, *37*(10), 1322–1328. https://doi.org/10.1016/j.leukres.2013.06.026

Lokhorst, H. M., Lamme, T., de Smet, M., Klein, S., de Weger, R. A., van Oers, R., & Bloem, A. C. (1994). Primary tumor cells of myeloma patients induce interleukin-6 secretion in long-term bone marrow cultures. *Blood*, *84*(7), 2269–2277.

Loureiro, J. A., Gomes, B., Coelho, M. A., Do Carmo Pereira, M., & Rocha, S. (2014, April). Targeting nanoparticles across the blood-brain barrier with monoclonal antibodies. *Nanomedicine*. https://doi.org/10.2217/nnm.14.27

Lovitt, C. J., Shelper, T. B., & Avery, V. M. (2015). Evaluation of chemotherapeutics in a three-dimensional breast cancer model. *Journal of Cancer Research and Clinical Oncology*,

141(5), 951–959. https://doi.org/10.1007/s00432-015-1950-1

M. Cardoso, M., N. Peca, I., & C. A. Roque, A. (2012). Antibody-Conjugated Nanoparticles for Therapeutic Applications. *Current Medicinal Chemistry*, *19*(19), 3103–3127. https://doi.org/10.2174/092986712800784667

Macias, E., Rao, D., Carbajal, S., Kiguchi, K., & Digiovanni, J. (2014). Stat3 binds to mtDNA and regulates mitochondrial gene expression in keratinocytes. *Journal of Investigative Dermatology*, *134*(7), 1971–1980. https://doi.org/10.1038/jid.2014.68

MacLeod, R. A. F., Dirks, W. G., Matsuo, Y., Kaufmann, M., Milch, H., & Drexler, H. G. (1999). Widespread intraspecies cross-contamination of human tumor cell lines arising at source. *International Journal of Cancer*, *83*(4), 555–563. https://doi.org/10.1002/(SICI)1097-0215(19991112)83:4<555::AID-IJC19>3.0.CO;2-2

Maeda, H., Takeshita, J., & Kanamaru, R. (1979). A Lipophilic Derivative OF Neocarzinostatin a Polymer Conjugation of an Antitumor Protein Antibiotic. *International Journal of Peptide and Protein Research*, *14*(2), 81–87. https://doi.org/10.1111/j.1399-3011.1979.tb01730.x

Maeda, H., Ueda, M., Morinaga, T., & Matsumoto, T. (1985). Conjugation of Poly(styrene-co-maleic acid) Derivatives to the Antitumor Protein Neocarzinostatin: Pronounced Improvements in Pharmacological Properties. *Journal of Medicinal Chemistry*, *28*(4), 455–461. https://doi.org/10.1021/jm00382a012

Magrangeas F, Lode L, Wuilleme S, et al. (2005). Genetic heterogeneity in multiple myeloma. *Leukemia : Official Journal of the Leukemia Society of America, Leukemia Research Fund, U.K*, *19*(2), 191–194. https://doi.org/10.1038/sj.leu.2403555

Mahmud, A., Xiong, X. B., & Lavasanifar, A. (2006). Novel self-associating POly(ethylene oxide)-block-poly(ε-caprolactone) block copolymers with functional side groups on the polyester block for drug delivery. *Macromolecules*, *39*(26), 9419–9428. https://doi.org/10.1021/ma0613786

Manni, S., Brancalion, A., Mandato, E., Tubi, L. Q., Colpo, A., Pizzi, M., … Piazza, F. (2013). Protein kinase CK2 inhibition down modulates the NF-κB and STAT3 survival pathways, enhances the cellular proteotoxic stress and synergistically boosts the cytotoxic effect of bortezomib on multiple myeloma and mantle cell Lymphoma Cells. *PLoS ONE*, *8*(9), e75280. https://doi.org/10.1371/journal.pone.0075280

Marinov, J., Koubek, K., & Stary, J. (1993). Immunophenotypic significance of the "lymphoid" CD38 antigen in myeloid blood malignancies. *Neoplasma*, *40*(6), 355–358.

Matsumura, Y., & Maeda, H. (1986). A new concept for macromolecular therapeutics in cnacer chemotherapy: mechanism of tumoritropic accumulatio of proteins and the antitumor agents Smancs. *Cancer Research*, *46*(12 Pt 1), 6387–6392. https://doi.org/10.1021/bc100070g

Maya, S., Sarmento, B., Lakshmanan, V. K., Menon, D., & Jayakumar, R. (2014). Actively targeted cetuximab conjugated γ-poly(glutamic acid)-docetaxel nanomedicines for epidermal growth factor receptor over expressing colon cancer cells. *Journal of Biomedical Nanotechnology*, *10*(8), 1416–1428. https://doi.org/10.1166/jbn.2014.1841

Menon, N. V, Chuah, Y. J., Cao, B., Lim, M., & Kang, Y. (2014). A microfluidic co-culture system to monitor tumor-stromal interactions on a chip. *Biomicrofluidics*, *8*(6). https://doi.org/10.1063/1.4903762

Menu, E., Asosingh, K., Van Riet, I., Croucher, P., Van Camp, B., & Vanderkerken, K. (2004). Myeloma cells (5TMM) and their interactions with the marrow microenvironment. *Blood Cells, Molecules & Diseases*, *33*(2), 111–119. https://doi.org/10.1016/j.bcmd.2004.04.012

Mi, Y., Liu, X., Zhao, J., Ding, J., & Feng, S. S. (2012). Multimodality treatment of cancer with herceptin conjugated, thermomagnetic iron oxides and docetaxel loaded nanoparticles of biodegradable polymers. *Biomaterials*, *33*(30), 7519–7529. https://doi.org/10.1016/j.biomaterials.2012.06.100

Mirandola, L., Apicella, L., Colombo, M., Yu, Y., Berta, D. G., Platonova, N., … Chiaramonte, R. (2013). Anti-Notch treatment prevents multiple myeloma cells localization to the bone marrow via the chemokine system CXCR4/SDF-1. *Leukemia*, *27*(7), 1558–1566. https://doi.org/10.1038/leu.2013.27

Molavi, O., Xiong, X. B., Douglas, D., Kneteman, N., Nagata, S., Pastan, I., … Lai, R. (2013). Anti-CD30 antibody conjugated liposomal doxorubicin with significantly improved therapeutic efficacy against anaplastic large cell lymphoma. *Biomaterials*, *34*(34), 8718–8725. https://doi.org/10.1016/j.biomaterials.2013.07.068

Monterrubio, C., Paco, S., Olaciregui, N. G., Pascual-Pasto, G., Vila-Ubach, M., Cuadrado-Vilanova, M., … Carcaboso, A. M. (2017). Targeted drug distribution in tumor extracellular fluid of GD2-expressing neuroblastoma patient-derived xenografts using SN-38-loaded nanoparticles conjugated to the monoclonal antibody 3F8. *Journal of Controlled Release*, *255*, 108–119. https://doi.org/10.1016/J.JCONREL.2017.04.016

Moreau, P., Attal, M., & Facon, T. (2015, May 14). Frontline therapy of multiple myeloma. *Blood*. American Society of Hematology. https://doi.org/10.1182/blood-2014-09-568915

Moreau, P., Avet-Loiseau, H., Facon, T., Attal, M., Tiab, M., Hulin, C., … Harousseau, J. L. (2011). Bortezomib plus dexamethasone versus reduced-dose bortezomib, thalidomide plus dexamethasone as induction treatment before autologous stem cell transplantation in newly diagnosed multiple myeloma. *Blood*, *118*(22), 5752–5758. https://doi.org/10.1182/blood-2011-05-355081

Moreau, P., Facon, T., Attal, M., Hulin, C., Michallet, M., Maloisel, F., … Harousseau, J. L. (2002). Comparison of 200 mg/m2 melphalan and 8 Gy total body irradiation plus 140 mg/m2 melphalan as conditioning regimens for peripheral blood stem cell transplantation in patients with newly diagnosed multiple myeloma: Final analysis of the Intergroupe Francop. *Blood*, *99*(3), 731–735. https://doi.org/10.1182/blood.V99.3.731

Moreaux, J., Legouffe, E., Jourdan, E., Quittet, P., Rème, T., Lugagne, C., … Tarte, K. (2004). BAFF and APRIL protect myeloma cells from apoptosis induced by interleukin 6 deprivation and dexamethasone. *Blood*, *103*(8), 3148–3157. https://doi.org/10.1182/blood-2003-06-1984

Mu, Q., Kievit, F. M., Kant, R. J., Lin, G., Jeon, M., & Zhang, M. (2015). Anti-HER2/neu peptide-conjugated iron oxide nanoparticles for targeted delivery of paclitaxel to breast cancer cells. *Nanoscale*, *7*(43), 18010–18014. https://doi.org/10.1039/C5NR04867B

Mukerjee, A., Ranjan, A. P., & Vishwanatha, J. K. (2016). Targeted nanocurcumin therapy using annexin A2 antibody improves tumor accumulation and therapeutic efficacy against highly metastatic breast cancer. *Journal of Biomedical Nanotechnology*, *12*(7), 1374–1392. https://doi.org/10.1166/jbn.2016.2240

Nakamura, Y., Mochida, A., Choyke, P. L., & Kobayashi, H. (2016). Nanodrug Delivery: Is the Enhanced Permeability and Retention Effect Sufficient for Curing Cancer? *Bioconjugate*

Chemistry. https://doi.org/10.1021/acs.bioconjchem.6b00437

Nath, S., & Devi, G. R. (2016). Three-dimensional culture systems in cancer research: Focus on tumor spheroid model. *Pharmacology & Therapeutics*, *163*, 94–108. https://doi.org/10.1016/j.pharmthera.2016.03.013

Neben, K., Jauch, A., Bertsch, U., Heiss, C., Hielscher, T., Seckinger, A., … Goldschmidt, H. (2010). Combining information regarding chromosomal aberrations t(4;14) and del(17p13) with the International Staging System classification allows stratification of myeloma patients undergoing autologous stem cell transplantation. *Haematologica*, *95*(7), 1150–1157. https://doi.org/10.3324/haematol.2009.016436

Nefedova, Y., Cheng, P., Alsina, M., Dalton, W. S., & Gabrilovich, D. I. (2004). Involvement of Notch-1 signaling in bone marrow stroma-mediated de novo drug resistance of myeloma and other malignant lymphoid cell lines. *Blood*, *103*(9), 3503–3510. https://doi.org/10.1182/blood-2003-07-2340

Nefedova, Y., Sullivan, D. M., Bolick, S. C., Dalton, W. S., & Gabrilovich, D. I. (2008). Inhibition of notch signaling induces apoptosis of myeloma cells and enhances sensitivity to chemotherapy. *Blood*, *111*(4), 2220–2229. https://doi.org/10.1182/blood-2007-07-102632

Nera, K. P., Kohonen, P., Narvi, E., Peippo, A., Mustonen, L., Terho, P., … Lassila, O. (2006). Loss of Pax5 promotes plasma cell differentiation. *Immunity*, *24*(3), 283–293. https://doi.org/10.1016/j.immuni.2006.02.003

Neri, P., Kumar, S., Fulciniti, M. T., Vallet, S., Chhetri, S., Mukherjee, S., … Raje, N. (2007). Neutralizing B-cell-activating factor antibody improves survival and inhibits

osteoclastogenesis in a severe combined immunodeficient human multiple myeloma model. *Clinical Cancer Research*, *13*(19), 5903–5909. https://doi.org/10.1158/1078-0432.CCR-07-0753

Nierste, B. A., Gunn, E. J., Whiteman, K. R., Lutz, R. J., & Kirshner, J. (2016). Maytansinoid immunoconjugate IMGN901 is cytotoxic in a three-dimensional culture model of multiple myeloma. *American Journal of Blood Research*, *6*(1), 6–18.

Nijhof, I. S., Groen, R. W. J., Noort, W. A., Van Kessel, B., De Jong-Korlaar, R., Bakker, J., … Mutis, T. (2015). Preclinical evidence for the therapeutic potential of CD38-Targeted Immuno-chemotherapy in multiple Myeloma patients refractory to Lenalidomide and Bortezomib. *Clinical Cancer Research*, *21*(12), 2802–2810. https://doi.org/10.1158/1078-0432.CCR-14-1813

Oh, D.-Y., Lee, S.-H., Han, S.-W., Kim, M.-J., Kim, T.-M., Kim, T.-Y., … Bang, Y.-J. (2015). Phase I Study of OPB-31121, an Oral STAT3 Inhibitor, in Patients with Advanced Solid Tumors. *Cancer Research and Treatment*, *47*(4), 607–615. https://doi.org/10.4143/crt.2014.249

Overdijk, M. B., Jansen, J. H. M., Nederend, M., Lammerts van Bueren, J. J., Groen, R. W. J., Parren, P. W. H. I., … Boross, P. (2016). The Therapeutic CD38 Monoclonal Antibody Daratumumab Induces Programmed Cell Death via Fcγ Receptor–Mediated Cross-Linking. *The Journal of Immunology*, *197*(3), 807–813. https://doi.org/10.4049/jimmunol.1501351

Öztürk, K., Esendağlı, G., Gürbüz, M. U., Tülü, M., & Çalış, S. (2017). Effective targeting of gemcitabine to pancreatic cancer through PEG-cored Flt-1 antibody-conjugated dendrimers. *International Journal of Pharmaceutics*, *517*(1–2), 157–167.

https://doi.org/10.1016/j.ijpharm.2016.12.009

Palumbo, A., & Anderson, K. (2011). Multiple Myeloma. *New England Journal of Medicine*, *364*(11), 1046–1060. https://doi.org/10.1056/NEJMra1011442

Parhi, P., & Sahoo, S. K. (2015). Trastuzumab guided nanotheranostics: A lipid based multifunctional nanoformulation for targeted drug delivery and imaging in breast cancer therapy. *Journal of Colloid and Interface Science*, *451*, 198–211. https://doi.org/10.1016/J.JCIS.2015.03.049

Parikh, M. R., Belch, A. R., Pilarski, L. M., & Kirshner, J. (2014). A Three-dimensional tissue culture model to study primary human bone marrow and its malignancies. *Journal of Visualized Experiments*, (85), e50947–e50947. https://doi.org/10.3791/50947

Park, M. C., Jeong, H., Son, S. H., Kim, Y. H., Han, D., Goughnour, P. C., … Kim, S. (2016). Novel morphologic and genetic analysis of cancer cells in a 3D microenvironment identifies STAT3 as a regulator of tumor permeability barrier function. *Cancer Research*, *76*(5), 1044–1054. https://doi.org/10.1158/0008-5472.CAN-14-2611

Parry-Jones, N., Matutes, E., Morilla, R., Brito-Babapulle, V., Wotherspoon, A., Swansbury, G. J., & Catovsky, D. (2007). Cytogenetic abnormalities additional to t(11;14) correlate with clinical features in leukaemic presentation of mantle cell lymphoma, and may influence prognosis: A study of 60 cases by FISH. *British Journal of Haematology*, *137*(2), 117–124. https://doi.org/10.1111/j.1365-2141.2007.06526.x

Petersen, O. W., Ronnov-Jessen, L., Howlett, A. R., & Bissell, M. J. (1992). Interaction with basement membrane serves to rapidly distinguish growth and differentiation pattern of normal

and malignant human breast epithelial cells. *Proceedings of the National Academy of Sciences*, *89*(19), 9064–9068. https://doi.org/10.1073/pnas.89.19.9064

Portier, M., Rajzbaum, G., Zhang, X. G., Attal, M., Rusalen, C., Wijdenes, J., … Klein, B. (1991). In vivo interleukin 6 gene expression in the tumoral environment in multiple myeloma. *European Journal of Immunology*, *21*(7), 1759–1762. https://doi.org/10.1002/eji.1830210727

Preyat, N., & Leo, O. (2016). Complex role of nicotinamide adenine dinucleotide in the regulation of programmed cell death pathways. *Biochemical Pharmacology*, *101*, 13–26. https://doi.org/10.1016/j.bcp.2015.08.110

Punfa, W., Suzuki, S., Pitchakarn, P., Yodkeeree, S., Naiki, T., Takahashi, S., & Limtrakul, P. (2014). Curcumin-loaded PLGA nanoparticles conjugated with anti-P-glycoprotein antibody to overcome multidrug resistance. *Asian Pacific Journal of Cancer Prevention*, *15*(21), 9249–9258. https://doi.org/10.7314/APJCP.2014.15.21.9249

Punfa, W., Yodkeeree, S., Pitchakarn, P., Ampasavate, C., & Limtrakul, P. (2012). Enhancement of cellular uptake and cytotoxicity of curcumin-loaded PLGA nanoparticles by conjugation with anti-P-glycoprotein in drug resistance cancer cells. *Acta Pharmacologica Sinica*, *33*(6), 823–831. https://doi.org/10.1038/aps.2012.34

Qiang, Y. W., Kopantzev, E., & Rudikoff, S. (2002). Insulinlike growth factor-I signaling in multiple myeloma: Downstream elements, functional correlates, and pathway cross-talk. *Blood*, *99*(11), 4138–4146. https://doi.org/10.1182/blood.V99.11.4138

Quinn, J., Glassford, J., Percy, L., Munson, P., Marafioti, T., Rodriguez-Justo, M., & Yong, K.

(2011). APRIL promotes cell-cycle progression in primary multiple myeloma cells: Influence of D-type cyclin group and translocation status. *Blood*, *117*(3), 890–901. https://doi.org/10.1182/blood-2010-01-264424

Quintanilla-Martinez, L., Kremer, M., Specht, K., Calzada-Wack, J., Nathrath, M., Schaich, R., … Fend, F. (2003). Analysis of signal transducer and activator of transcription 3 (Stat 3) pathway in multiple myeloma: Stat 3 activation and cyclin D1 dysregulation are mutually exclusive events. *The American Journal of Pathology*, *162*(5), 1449–1461. https://doi.org/10.1016/S0002-9440(10)64278-2

Rani, A., & Murphy, J. J. (2016). STAT5 in Cancer and Immunity. *Journal of Interferon & Cytokine Research*, *36*(4), 226–237. https://doi.org/10.1089/jir.2015.0054

Reagan, M. R., & Ghobrial, I. M. (2012). Multiple myeloma mesenchymal stem cells: Characterization, origin, and tumor-promoting effects. *Clinical Cancer Research*. https://doi.org/10.1158/1078-0432.CCR-11-2212

Richards, C. D., Kerr, C., Tanaka, M., Hara, T., Miyajima, A., Pennica, D., … Langdon, C. M. (1997). Regulation of tissue inhibitor of metalloproteinase-1 in fibroblasts and acute phase proteins in hepatocytes in vitro by mouse oncostatin M, cardiotrophin-1, and IL-6. *Journal of Immunology (Baltimore, Md. : 1950)*, *159*(5), 2431–2437.

Richards, D. A., Maruani, A., & Chudasama, V. (2017). Antibody fragments as nanoparticle targeting ligands: a step in the right direction. *Chem. Sci.*, *8*(1), 63–77. https://doi.org/10.1039/C6SC02403C

Richardson, P. G., Barlogie, B., Berenson, J., Singhal, S., Jagannath, S., Irwin, D., … Anderson,

K. C. (2003). A phase 2 study of bortezomib in relapsed, refractory myeloma. *New England Journal of Medicine*, *348*(26), 2609–2617. https://doi.org/10.1056/NEJMoa030288

Richardson, P. G., Chanan-Khan, A., Schlossman, R. L., Munshi, N. C., Wen, P., Briemberg, H., … Anderson, K. C. (2015). Phase II trial of single agent bortezomib (VELCADE®) in patients with previously untreated multiple myeloma (MM). *Blood*, *104*(11).

Riedl, A., Schlederer, M., Pudelko, K., Stadler, M., Walter, S., Unterleuthner, D., … Dolznig, H. (2017). Comparison of cancer cells in 2D vs 3D culture reveals differences in AKT–mTOR–S6K signaling and drug responses. *Journal of Cell Science*, *130*(1), 203–218. https://doi.org/10.1242/jcs.188102

Romagnoli, M., Séveno, C., Wuillème-Toumi, S., Amiot, M., Bataille, R., Minvielle, S., & Barillé-Nion, S. (2009). The imbalance between Survivin and Bim mediates tumour growth and correlates with poor survival in patients with multiple myeloma. *British Journal of Haematology*, *145*(2), 180–189. https://doi.org/10.1111/j.1365-2141.2009.07608.x

Rosiñol, L., Oriol, A., Teruel, A. I., Hernández, D., López-Jiménez, J., de la Rubia, J., … Programa para el Estudio y la Terapéutica de las Hemopatías Malignas/Grupo Español de Mieloma (PETHEMA/GEM) group. (2012). Superiority of bortezomib, thalidomide, and dexamethasone (VTD) as induction pretransplantation therapy in multiple myeloma: a randomized phase 3 PETHEMA/GEM study. *Blood*, *120*(8), 1589–1596. https://doi.org/10.1182/blood-2012-02-408922

Rowley, M., & Van Ness, B. (2002). Activation of N-ras and K-ras induced by interleukin-6 in a myeloma cell line: Implications for disease progression and therapeutic response. *Oncogene*, *21*(57), 8769–8775. https://doi.org/10.1038/sj.onc.1205387

Rozovski, U., Grgurevic, S., Bueso-Ramos, C., Harris, D. M., Li, P., Liu, Z., … Estrov, Z. (2015). Aberrant LPL expression, driven by STAT3, mediates free fatty acid metabolism in CLL cells. *Molecular Cancer Research*, *13*(5).

Sanjuan Nandin, I., Fong, C., Deantonio, C., Torreno-Pina, J. A., Pecetta, S., Maldonado, P., … Batista, F. D. (2017). Novel in vitro booster vaccination to rapidly generate antigen-specific human monoclonal antibodies. *The Journal of Experimental Medicine*, *214*(8), 2471–2490. https://doi.org/10.1084/jem.20170633

Schaefer, T. S., Sanders, L. K., Park, O. K., & Nathans, D. (1997). Functional Differences between Stat3$_{\beta}$ and Stat3$_{NL}$, *17*(9), 5307–5316.

Schindler, C. C., Fu, X. Y. X. Y., Improta, T. T., Aebersold, R. R., & Darnell, J. E. J. E. (1992). Proteins of transcription factor ISGF-3: one gene encodes the 91-and 84-kDa ISGF-3 proteins that are activated by interferon alpha. *Proceedings of the National Academy of Sciences*, *89*(16), 7836–7839. https://doi.org/10.1073/pnas.89.16.7836

Schindler, C., Shuai, K., Prezioso, V. R., & Darnell, J. E. (1992). Interferon-dependent tyrosine phosphorylation of a latent cytoplasmic transcription factor. *Science*, *257*(5071), 809–813. https://doi.org/10.1126/SCIENCE.1496401

Schust, J., Sperl, B., Hollis, A., Mayer, T. U., & Berg, T. (2006). Stattic: a small-molecule inhibitor of STAT3 activation and dimerization. *Chemistry and Biology*, *13*(11), 1235–1242. https://doi.org/10.1016/j.chembiol.2006.09.018

Schwab, G., Siegall, C. B., Aarden, L. A., Neckers, L. M., & Nordan, R. P. (1991). Characterization of an interleukin-6-mediated autocrine growth loop in the human multiple

myeloma cell line, U266. *Blood*, *77*(3), 587–593.

Sezer, O., Heider, U., Jakob, C., Eucker, J., & Possinger, K. (2002). Human bone marrow myeloma cells express RANKL. *J Clin Oncol*, *20*(1), 353–354. https://doi.org/10.1200/JCO.2002.20.1.353

Shain, K. H., Yarde, D. N., Meads, M. B., Huang, M., Jove, R., Hazlehurst, L. A., & Dalton, W. S. (2009). Beta-1 integrin adhesion enhances IL-6-mediated STAT3 signaling in myeloma cells: implications for microenvironment influence on tumor survival and proliferation. *Cancer Research*, *69*(3), 1009–1015. https://doi.org/10.1158/0008-5472.CAN-08-2419

Shan, F., Close, D. A., Camarco, D. P., & Johnston, P. A. (2017). High-Content Screening Comparison of Cancer Drug Accumulation and Distribution in Two-Dimensional and Three-Dimensional Culture Models of Head and Neck Cancer. *ASSAY and Drug Development Technologies*, adt.2017.812. https://doi.org/10.1089/adt.2017.812

Shaughnessy, J. D., Qu, P., Usmani, S., Heuck, C. J., Zhang, Q., Zhou, Y., … Barlogie, B. (2011). Pharmacogenomics of bortezomib test-dosing identifies hyperexpression of proteasome genes, especially PSMD4, as novel high-risk feature in myeloma treated with total therapy 3. *Blood*, *118*(13), 3512–3524. https://doi.org/10.1182/blood-2010-12-328252

Siddiquee, K. A. Z., Gunning, P. T., Glen, M., Katt, W. P., Zhang, S., Schroeck, C., … Turkson, J. (2007). An oxazole-based small-molecule stat3 inhibitor modulates stat3 stability and processing and induces antitumor cell effects. *ACS Chemical Biology*, *2*(12), 787–798. https://doi.org/10.1021/cb7001973

Siddiquee, K., Zhang, S., Guida, W. C., Blaskovich, M. A., Greedy, B., Lawrence, H. R., …

Turkson, J. (2007). Selective chemical probe inhibitor of Stat3, identified through structure-based virtual screening, induces antitumor activity. *Proceedings of the National Academy of Sciences of the United States of America*, *104*(18), 7391–7396. https://doi.org/10.1073/pnas.0609757104

Sikka, S., Surana, R., Dai, X., Zhang, J., Kumar, A. P., Tan, B. K. H., … Bishayee, A. (2014, April 1). Targeting the STAT3 signaling pathway in cancer: Role of synthetic and natural inhibitors. *Biochimica et Biophysica Acta - Reviews on Cancer*. Elsevier. https://doi.org/10.1016/j.bbcan.2013.12.005

Sims, N. A., & Martin, T. J. (2014). Coupling the activities of bone formation and resorption: a multitude of signals within the basic multicellular unit. *BoneKEy Reports*, *3*. https://doi.org/10.1038/bonekey.2013.215

Slany, A., Haudek-Prinz, V., Meshcheryakova, A., Bileck, A., Lamm, W., Zielinski, C., … Drach, J. (2014). Extracellular matrix remodeling by bone marrow fibroblast-like cells correlates with disease progression in multiple myeloma. *Journal of Proteome Research*, *13*(2), 844–854. https://doi.org/10.1021/pr400881p

Smadja, N.-V., Fruchart, C., Isnard, F., Louvet, C., Dutel, J.-L., Cheron, N., … Bastard, C. (1998). Chromosomal analysis in multiple myeloma: cytogenetic evidence of two different diseases. *Leukemia*, *12*(6), 960–969. https://doi.org/10.1038/sj.leu.2401041

Soleimani, A. H., Garg, S. M., Paiva, I. M., Vakili, M. R., Alshareef, A., Huang, Y.-H., … Lavasanifar, A. (2017). Micellar nano-carriers for the delivery of STAT3 dimerization inhibitors to melanoma. *Drug Delivery and Translational Research*, 1–11. https://doi.org/10.1007/s13346-017-0369-4

Son, S., Shin, S., Rao, V., Um, W., Jeon, J., Ko, H., … Park, J. H. (2017). Trop2 antibody-conjugated bioreducible nanoparticles for targeted triple negative breast cancer therapy. *International Journal of Biological Macromolecules*. https://doi.org/10.1016/j.ijbiomac.2017.10.113

Song, H., Wang, R., Wang, S., & Lin, J. (2005). A low-molecular-weight compound discovered through virtual database screening inhibits Stat3 function in breast cancer cells. *Proceedings of the National Academy of Sciences*, *102*(13), 4700–4705. https://doi.org/10.1073/pnas.0409894102

Song, L., Turkson, J., Karras, J. G., Jove, R., & Haura, E. B. (2003). Activation of Stat3 by receptor tyrosine kinases and cytokines regulates survival in human non-small cell carcinoma cells. *Oncogene*, *22*(27), 4150–4165. https://doi.org/10.1038/sj.onc.1206479

Sonneveld, P., & Broijl, A. (2016, April 1). Treatment of relapsed and refractory multiple myeloma. *Haematologica*. Haematologica. https://doi.org/10.3324/haematol.2015.129189

Sonneveld, P., Schmidt-Wolf, I. G. H., Van Der Holt, B., El Jarari, L., Bertsch, U., Salwender, H., … Goldschmidt, H. M. (2012). Bortezomib induction and maintenance treatment in patients with newly diagnosed multiple myeloma: Results of the randomized phase III HOVON-65/ GMMG-HD4 trial. *Journal of Clinical Oncology*, *30*(24), 2946–2955. https://doi.org/10.1200/JCO.2011.39.6820

Spaner, D. E., Lee, E., Shi, Y., Wen, F., Li, Y., Tung, S., … Gorzcynski, R. (2013). PPAR-alpha is a therapeutic target for chronic lymphocytic leukemia. *Leukemia*, *27*(5), 1090–1099. https://doi.org/10.1038/leu.2012.329

Spets, H., Stromberg, T., Georgii-Hemming, P., Siljason, J., Nilsson, K., & Jernberg-Wiklund, H. (2002). Expression of the bcl-2 family of pro- and anti-apoptotic genes in multiple myeloma and normal plasma cells. Regulation during interleukin-6 (IL-6)-induced growth and survival. *European Journal of Haematology*, *69*(2), 76–89. https://doi.org/10.1034/j.1600-0609.2002.01549.x

Sreeranganathan, M., Uthaman, S., Sarmento, B., Mohan, C. G., Park, I. K., & Jayakumar, R. (2017). In vivo evaluation of cetuximab-conjugated poly(γ-glutamic acid)-docetaxel nanomedicines in EGFR-overexpressing gastric cancer xenografts. *International Journal of Nanomedicine*, *12*, 7167–7182. https://doi.org/10.2147/IJN.S143529

Srivastava, J., & DiGiovanni, J. (2016). Non-canonical Stat3 signaling in cancer. *Molecular Carcinogenesis*, *55*(12), 1889–1898. https://doi.org/10.1002/mc.22438

Steinbrunn, T., Stühmer, T., Gattenlöhner, S., Rosenwald, A., Mottok, A., Unzicker, C., … Bargou, R. C. (2011). Mutated RAS and constitutively activated Akt delineate distinct oncogenic pathways, which independently contribute to multiple myeloma cell survival. *Blood*, *117*(6), 1998–2004. https://doi.org/10.1182/blood-2010-05-284422

Stewart, A. K. (2009, April 2). Reduced-intensity allogeneic transplantation for myeloma: Reality bites. *Blood*. American Society of Hematology. https://doi.org/10.1182/blood-2008-12-173526

Sun, W., Snyder, M., Levy, D. E., & Zhang, J. J. (2006). Regulation of Stat3 transcriptional activity by the conserved LPMSP motif for OSM and IL-6 signaling. *FEBS Letters*, *580*(25), 5880–5884. https://doi.org/10.1016/j.febslet.2006.09.054

Sun, Y., & Liu, Q. (2015). Deciphering the correlation between breast tumor samples and cell lines by integrating copy number changes and gene expression profiles. *BioMed Research International*, *2015*, 1–11. https://doi.org/10.1155/2015/901303

Suzuki, R., Suzumiya, J., Nakamura, S., Aoki, S., Notoya, A., Ozaki, S., … Oshimi, K. (2004). Aggressive natural killer-cell leukemia revisited: Large granular lymphocyte leukemia of cytotoxic NK cells. *Leukemia*, *18*(4), 763–770. https://doi.org/10.1038/sj.leu.2403262

Szczepanek, K., Chen, Q., Larner, A. C., & Lesnefsky, E. J. (2012). Cytoprotection by the modulation of mitochondrial electron transport chain: The emerging role of mitochondrial STAT3. *Mitochondrion*, *12*(2), 180–189. https://doi.org/10.1016/j.mito.2011.08.011

Tai, Y.-T., Podar, K., Catley, L., Tseng, Y.-H., Akiyama, M., Shringarpure, R., … Anderson, K. C. (2003). Insulin-like growth factor-1 induces adhesion and migration in human multiple myeloma cells via activation of beta1-integrin and phosphatidylinositol 3'-kinase/AKT signaling. *Cancer Research*, *63*(18), 5850–5858. https://doi.org/10.1158/0008-5472.can-06-0190

Takeda, K., Noguchi, K., Shi, W., Tanaka, T., Matsumoto, M., Yoshida, N., … Akira, S. (1997). Targeted disruption of the mouse Stat3 gene leads to early embryonic lethality. *Developmental Biology*, *94*(8), 3801–3804.

Tammineni, P., Anugula, C., Mohammed, F., Anjaneyulu, M., Larner, A. C., & Sepuri, N. B. V. (2013). The import of the transcription factor STAT3 into mitochondria depends on GRIM-19, a component of the electron transport chain. *Journal of Biological Chemistry*, *288*(7), 4723–4732. https://doi.org/10.1074/jbc.M112.378984

Tandon, N., Rajkumar, S. V, LaPlant, B., Pettinger, A., Lacy, M. Q., Dispenzieri, A., … Kumar, S. K. (2017). Clinical utility of the revised international staging system in unselected patients with newly diagnosed and relapsed multiple myeloma. *Blood Cancer Journal*, *7*(2), e528–e528. https://doi.org/10.1038/bcj.2017.13

Taube, T., Beneton, M. N. C., McCloskey, E. V., Rogers, S., Greaves, M., & Kanis, J. A. (1992). Abnormal bone remodelling in patients with myelomatosis and normal biochemical indices of bone resorption. *European Journal of Haematology*, *49*(4), 192–198. https://doi.org/10.1111/j.1600-0609.1992.tb00046.x

Taylor, R. M., & Sillerud, L. O. (2012). Paclitaxel-loaded iron platinum stealth immunomicelles are potent MRI imaging agents that prevent prostate cancer growth in a PSMA-dependent manner. *International Journal of Nanomedicine*, *7*, 4341–4352. https://doi.org/10.2147/IJN.S34381

Terstappen, L. W., Johnsen, S., Segers-Nolten, I. M., & Loken, M. R. (1990). Identification and characterization of plasma cells in normal human bone marrow by high-resolution flow cytometry. *Blood*, *76*(9), 1739–1747.

Thabard, W., Barillé, S., Collette, M., Harousseau, J. L., Rapp, M. J., Bataille, R., … Barille, S. (1999). Myeloma cells release soluble interleukin-6Ralpha in relation to disease progression by two distinct mechanisms: alternative splicing and proteolytic cleavage. *Clinical Cancer Research*, *5*(10), 2693–2697.

Thyrell, L., Arulampalam, V., Hjortsberg, L., Farnebo, M., Grandér, D., & Pokrovskaja Tamm, K. (2007). Interferon alpha induces cell death through interference with interleukin 6 signaling and inhibition of STAT3 activity. *Experimental Cell Research*, *313*(19), 4015–4024.

https://doi.org/10.1016/j.yexcr.2007.08.007

Tiedemann, R. E., Zhu, Y. X., Schmidt, J., Yin, H., Shi, C. X., Que, Q., … Stewart, A. K. (2010). Kinome-wide RNAi studies in human multiple myeloma identify vulnerable kinase targets, including a lymphoid-restricted kinase, GRK6. *Blood*, *115*(8), 1594–1604. https://doi.org/10.1182/blood-2009-09-243980

Tong, A. W., Huang, Y. W., Zhang, B. Q., Netto, G., Vitetta, E. S., & Stone, M. J. (1993). Heterotransplantation of human multiple myeloma cell lines in severe combined immunodeficiency (SCID) mice. *Anticancer Research*, *13*(3), 593–597.

Tu, Y., Gardner, A., & Lichtenstein, A. (2000). The phosphatidylinositol 3-kinase/AKT kinase pathway in multiple myeloma plasma cells: roles in cytokine-dependent survival and proliferative responses. *Cancer Research*, *60*(23), 6763–6770.

Turkson, J., Kim, J. S., Zhang, S., Yuan, J., Huang, M., Glenn, M., … Jove, R. (2004). Novel peptidomimetic inhibitors of signal transducer and activator of transcription 3 dimerization and biological activity. *Molecular Cancer Therapeutics*, *3*(3), 261–269.

Turkson, J., Ryan, D., Kim, J. S., Zhang, Y., Chen, Z., Haura, E., … Jove, R. (2001). Phosphotyrosyl peptides block Stat3-mediated DNA binding activity, gene regulation, and cell transformation. *Journal of Biological Chemistry*, *276*(48), 45443–45455. https://doi.org/10.1074/jbc.M107527200

Uchiyama, H., Barut, B. A., Mohrbacher, A. F., Chauhan, D., & Anderson, K. C. (1993). Adhesion of human myeloma-derived cell lines to bone marrow stromal cells stimulates interleukin-6 secretion. *Blood*, *82*(12), 3712–3720.

Van Damme, J. (1987). Identification of the human 26-kD protein, interferon beta 2 (IFN-beta 2), as a B cell hybridoma/plasmacytoma growth factor induced by interleukin 1 and tumor necrosis factor. *Journal of Experimental Medicine*, *165*(3), 914–919. https://doi.org/10.1084/jem.165.3.914

van de Donk, N. W. C. J., Lokhorst, H. M., Anderson, K. C., Richardson, P. G., Kyle, R., Maldonado, J., … Kucharz, E. (2012). How I treat plasma cell leukemia. *Blood*, *120*(12), 2376–2389. https://doi.org/10.1182/blood-2012-05-408682

van der Veer, M. S., de Weers, M., van Kessel, B., Bakker, J. M., Wittebol, S., Parren, P. W. H. I., … Mutis, T. (2011). Towards effective immunotherapy of myeloma enhanced elimination of myeloma cells by combination of lenalidomide with the human CD38 monoclonal antibody daratumumab. *Haematologica*, *96*(2), 284–290. https://doi.org/10.3324/haematol.2010.030759

van Stralen, E., van de Wetering, M., Agnelli, L., Neri, A., Clevers, H. C., & Bast, B. J. E. G. (2009). Identification of primary MAFB target genes in multiple myeloma. *Experimental Hematology*, *37*(1), 78–86. https://doi.org/10.1016/j.exphem.2008.08.006

Vander Heiden, M. G., Cantley, L. C., Thompson, C. B., & Thompson3, C. B. (2009). Understanding the Warburg Effect: The Metabolic Requirements of Cell Proliferation The Metabolic Requirements of Cell Proliferation. *Source: Science, New Series*, *324*(5930), 1029–1033. https://doi.org/10.1126/science.1160809.Understanding

Veirman, K. De, Van Ginderachter, J. A., Lub, S., Beule, N. De, Thielemans, K., Bautmans, I., … Valckenborgh, E. Van. (2015). Multiple myeloma induces Mcl-1 expression and survival of myeloid-derived suppressor cells. *Oncotarget*, *6*(12), 10532–10547.

https://doi.org/10.18632/oncotarget.3300

Vincent, L., Jin, D. K., Karajannis, M. A., Shido, K., Hooper, A. T., Rashbaum, W. K., … Hicklin, D. J. (2005). Fetal Stromal − Dependent Paracrine and Intracrine Vascular Endothelial Growth Factor-A / Vascular Endothelial Growth Factor Receptor-1 Signaling Promotes Proliferation and Motility of Human Primary Myeloma Cells, (8), 3185–3192. https://doi.org/10.1158/0008-5472.CAN-04-3598

Vincent, T., & Mechti, N. (2005). Extracellular matrix in bone marrow can mediate drug resistance in myeloma. *Leukemia and Lymphoma*. https://doi.org/10.1080/10428190500051448

Vincent, T., Molina, L., Espert, L., & Mechti, N. (2003). Hyaluronan, a major non-protein glycosaminoglycan component of the extracellular matrix in human bone marrow, mediates dexamethasone resistance in multiple myeloma. *British Journal of Haematology*, *121*(2), 259–269. https://doi.org/10.1046/j.1365-2141.2003.04282.x

Vivek, R., Thangam, R., NipunBabu, V., Rejeeth, C., Sivasubramanian, S., Gunasekaran, P., … Kannan, S. (2014). Multifunctional HER2-Antibody Conjugated Polymeric Nanocarrier-Based Drug Delivery System for Multi-Drug-Resistant Breast Cancer Therapy. *ACS Applied Materials & Interfaces*, *6*(9), 6469–6480. https://doi.org/10.1021/am406012g

Vogt, M., Domoszlai, T., Kleshchanok, D., Lehmann, S., Schmitt, A., Poli, V., … Muller-Newen, G. (2011). The role of the N-terminal domain in dimerization and nucleocytoplasmic shuttling of latent STAT3. *Journal of Cell Science*, *124*(6), 900–909. https://doi.org/10.1242/jcs.072520

Wada, A., Ito, A., Iitsuka, H., Tsuneyama, K., Miyazono, T., Murakami, J., … Sugiyama, T.

(2015). Role of chemokine CX3CL1 in progression of multiple myeloma via CX3CR1 in bone microenvironments. *Oncology Reports*, *33*(6), 2935–2939. https://doi.org/10.3892/or.2015.3941

Wagner, V., Hose, D., Seckinger, A., Weiz, L., Meißner, T., Rème, T., … Raab, M. S. (2014). Preclinical efficacy of sepantronium bromide (YM155) in multiple myeloma is conferred by down regulation of Mcl-1. *Oncotarget*, *5*(21), 10237–10250. https://doi.org/10.18632/oncotarget.2529

Wang, K., Kievit, F. M., Erickson, A. E., Silber, J. R., Ellenbogen, R. G., & Zhang, M. (2016). Culture on 3D chitosan-hyaluronic acid scaffolds enhances stem cell marker expression and drug resistance in human glioblastoma cancer stem cells. *Advanced Healthcare Materials*, *5*(24), 3173–3181. https://doi.org/10.1002/adhm.201600684

Wang, L. H., Yang, X. Y., Mihalic, K., Xiao, W., Li, D., & Farrar, W. L. (2001). Activation of Estrogen Receptor Blocks Interleukin-6-inducible Cell Growth of Human Multiple Myeloma Involving Molecular Cross-talk between Estrogen Receptor and STAT3 Mediated by Co-regulator PIAS3. *Journal of Biological Chemistry*, *276*(34), 31839–31844. https://doi.org/10.1074/jbc.M105185200

Wang, L. H., Yang, X. Y., Zhang, X., Huang, J., Hou, J., Li, J., … Farrar, W. L. (2004). Transcriptional Inactivation of STAT3 by PPARγ Suppresses IL-6-Responsive Multiple Myeloma Cells. *Immunity*, *20*(2), 205–218. https://doi.org/10.1016/S1074-7613(04)00030-5

Wang, L., Wang, H., Li, P. F., Lu, Y., Xia, Z. J., Huang, H. Q., & Zhang, Y. J. (2015). CD38 expression predicts poor prognosis and might be a potential therapy target in extranodal NK/T cell lymphoma, nasal type. *Annals of Hematology*, *94*(8), 1381–1388.

https://doi.org/10.1007/s00277-015-2359-2

Wang, X. B., & Zhou, H. Y. (2015). Molecularly targeted gemcitabine-loaded nanoparticulate system towards the treatment of EGFR overexpressing lung cancer. *Biomedicine and Pharmacotherapy*, *70*(C), 123–128. https://doi.org/10.1016/j.biopha.2015.01.008

Weaver, V. M., Petersen, O. W., Wang, F., Larabell, C. A., Briand, P., Damsky, C., & Bissell, M. J. (1997). Reversion of the malignant phenotype of human breast cells in three-dimensional culture and in vivo by integrin blocking antibodies. *The Journal of Cell Biology*, *137*(1), 231–245. https://doi.org/10.1083/jcb.137.1.231

Wegenka, U. M., Buschmann, J., Lütticken, C., Heinrich, P. C., Horn, F., Lutticken, C., & Heinrich, P. C. (1993). Acute-phase response factor, a nuclear factor binding to acute-phase response elements, is rapidly activated by interleukin-6 at the posttranslational level, *13*(1). https://doi.org/10.1128/MCB.13.1.276

Wormald, S., & Hilton, D. J. (2004, January 9). Inhibitors of Cytokine Signal Transduction. *Journal of Biological Chemistry*. American Society for Biochemistry and Molecular Biology. https://doi.org/10.1074/jbc.R300030200

Wu, W., Ma, D., Wang, P., Cao, L., Lu, T., Fang, Q., … Wang, J. (2016). Potential crosstalk of the interleukin-6-heme oxygenase-1-dependent mechanism involved in resistance to lenalidomide in multiple myeloma cells. *The FEBS Journal*, *283*(5), 834–849. https://doi.org/10.1111/febs.13633

X, X., Han, K., Zhu, J., Mao, H., Lin, X., Zhang, Z., … Mao, X. (2016). An inhibitor of cholesterol absorption displays anti-myeloma activity by targeting the JAK2-STAT3 signaling pathway.

Oncotarget, *7*(46), 75539–75550. https://doi.org/10.18632/oncotarget.12265

Xiang, M., Kim, H., Ho, V. T., Walker, S. R., Bar-Natan, M., Anahtar, M., … Frank, D. A. (2016). Gene expression-based discovery of atovaquone as a STAT3 inhibitor and anticancer agent. *Blood*, *128*(14), 1845–1853. https://doi.org/10.1182/blood-2015-07-660506

Xu, J., Ding, W. F., Shao, K. K., Wang, X. D., Wang, G. H., Li, H. Q., & Wang, H. M. (2012). Transcription of promoter from the human APRIL gene regulated by Sp1 and NF-kB. *Neoplasma*, *59*(3), 341–347. https://doi.org/10.4149/neo_2012_044

Xu, X., Farach-Carson, M. C., & Jia, X. (2014). Three-dimensional in vitro tumor models for cancer research and drug evaluation. *Biotechnology Advances*, *32*(7), 1256–1268. https://doi.org/10.1016/j.biotechadv.2014.07.009

Yaccoby, S., Ling, W., Zhan, F., Walker, R., Barlogie, B., & Shaughnessy, J. D. (2007). Antibody-based inhibition of DKK1 suppresses tumor-induced bone resorption and multiple myeloma growth in vivo. *Blood*, *109*(5), 2106–2111. https://doi.org/10.1182/blood-2006-09-047712

Yan, M., Schwaederle, M., Arguello, D., Millis, S. Z., Gatalica, Z., & Kurzrock, R. (2015). HER2 expression status in diverse cancers: review of results from 37,992 patients. *Cancer and Metastasis Reviews*, *34*(1), 157–164. https://doi.org/10.1007/s10555-015-9552-6

Yang, J., Liao, X., Agarwal, M. K., Barnes, L., Auron, P. E., & Stark, G. R. (2007). Unphosphorylated STAT3 accumulates in response to IL-6 and activates transcription by binding to NF-kB. *Genes and Development*, *21*(11), 1396–1408. https://doi.org/10.1101/gad.1553707

Yang, T., Liu, J., Yang, M., Huang, N., Zhong, Y., Zeng, T., … Zou, Q. (2017). Cucurbitacin B

exerts anti-cancer activities in human multiple myeloma cells in vitro and in vivo by modulating multiple cellular pathways. *Oncotarget*, *8*(4), 5800–5813. https://doi.org/10.18632/oncotarget.10584

Yao, Y., Sun, Y., Shi, M., Xia, D., Zhao, K., Zeng, L., … Xu, K. (2016). Piperlongumine induces apoptosis and reduces bortezomib resistance by inhibiting STAT3 in multiple myeloma cells. *Oncotarget*, *7*(45), 73497–73508. https://doi.org/10.18632/oncotarget.11988

Yildiz-Ozturk, E., Gulce-Iz, S., Anil, M., & Yesil-Celiktas, O. (2017). Cytotoxic responses of carnosic acid and doxorubicin on breast cancer cells in butterfly-shaped microchips in comparison to 2D and 3D culture. *Cytotechnology*, *69*(2), 337–347. https://doi.org/10.1007/s10616-016-0062-3

Yim, E. K. F., Darling, E. M., Kulangara, K., Guilak, F., & Leong, K. W. (2010). Nanotopography-induced changes in focal adhesions, cytoskeletal organization, and mechanical properties of human mesenchymal stem cells. *Biomaterials*, *31*(6), 1299–1306. https://doi.org/10.1016/j.biomaterials.2009.10.037

Yu, H., Lee, H., Herrmann, A., Buettner, R., & Jove, R. (2014, November 1). Revisiting STAT3 signalling in cancer: New and unexpected biological functions. *Nature Reviews Cancer*. Nature Publishing Group. https://doi.org/10.1038/nrc3818

Yue, X., Lukowski, J. K., Weaver, E. M., Skube, S. B., & Hummon, A. B. (2016). Quantitative Proteomic and Phosphoproteomic Comparison of 2D and 3D Colon Cancer Cell Culture Models. *Journal of Proteome Research*, *15*(12), 4265–4276. https://doi.org/10.1021/acs.jproteome.6b00342

Zammarchi, F., de Stanchina, E., Bournazou, E., Supakorndej, T., Martires, K., Riedel, E., … Cartegni, L. (2011). Antitumorigenic potential of STAT3 alternative splicing modulation. *Proceedings of the National Academy of Sciences*, *108*(43), 17779–17784. https://doi.org/10.1073/pnas.1108482108

Zamo, A., Chiarle, R., Piva, R., Howes, J., Fan, Y., Chilosi, M., … Inghirami, G. (2002). Anaplastic lymphoma kinase (ALK) activates Stat3 and protects hematopoietic cells from cell death. *Oncogene*, *21*(7), 1038–1047. https://doi.org/10.1038/sj/onc/1205152

Zhan, F., Colla, S., Wu, X., Chen, B., Stewart, J. P., Kuehl, W. M., … Shaughnessy, J. D. (2007). CKS1B, overexpressed in aggressive disease, regulates multiple myeloma growth and survival through SKP2- and p27Kip1-dependent and -independent mechanisms. *Blood*, *109*(11), 4995–5001. https://doi.org/10.1182/blood-2006-07-038703

Zhang, H.-F., Chen, Y., Wu, C., Wu, Z.-Y., Tweardy, D. J., Alshareef, A., … Lai, R. (n.d.). The Opposing Function of STAT3 as an Oncoprotein and Tumor Suppressor Is Dictated by the Expression Status of STAT3b in Esophageal Squamous Cell Carcinoma. *Clin Cancer Res*, *22*(3), 691–703. https://doi.org/10.1158/1078-0432.CCR-15-1253

Zhang, H.-F. F., & Lai, R. (2014). STAT3 in cancer-friend or foe? *Cancers*, *6*(3), 1408–1440. https://doi.org/10.3390/cancers6031408

Zhang, H.-F., & Lai, R. (2014). STAT3 in Cancer—Friend or Foe? *Cancers*, *6*(3), 1408–1440. https://doi.org/10.3390/cancers6031408

Zhang, J., Chen, F., Li, W., Xiong, Q., Yang, M., Zheng, P., … Ge, F. (2012). 14-3-3ζ interacts with Stat3 and regulates its constitutive activation in multiple myeloma cells. *PLoS ONE*,

7(1), e29554. https://doi.org/10.1371/journal.pone.0029554

Zhang, Q., Wang, H. Y., Marzec, M., Raghunath, P. N., Nagasawa, T., & Wasik, M. A. (2005). STAT3- and DNA methyltransferase 1-mediated epigenetic silencing of SHP-1 tyrosine phosphatase tumor suppressor gene in malignant T lymphocytes. *Proceedings of the National Academy of Sciences*, *102*(19), 6948–6953. https://doi.org/10.1073/pnas.0501959102

Zhang, W., Gu, Y., Sun, Q., Siegel, D. S., Tolias, P., Yang, Z., … Vogl, T. (2015). Ex Vivo Maintenance of Primary Human Multiple Myeloma Cells through the Optimization of the Osteoblastic Niche. *PLOS ONE*, *10*(5), e0125995. https://doi.org/10.1371/journal.pone.0125995

Zhang, W., Lee, W. Y., Siegel, D. S., Tolias, P., & Zilberberg, J. (2014). Patient-specific 3D microfluidic tissue model for multiple myeloma. *Tissue Engineering. Part C, Methods*, *20*(8), 663–670. https://doi.org/10.1089/ten.TEC.2013.0490

Zhang, X. D., Baladandayuthapani, V., Lin, H., Mulligan, G., Li, B.-Z., Esseltine, D. L. W., … Orlowski, R. Z. (2016). Tight jnction protein 1 modulates proteasome capacity and proteasome inhibitor sensitivity in multiple myeloma via EGFR/JAK1/STAT3 signaling. *Cancer Cell*, *29*(5), 639–652. https://doi.org/10.1016/j.ccell.2016.03.026

Zhang, X., Sun, Y., Pireddu, R., Yang, H., Urlam, M. K., Lawrence, H. R., … Sebti, S. M. (2013). A novel inhibitor of STAT3 homodimerization selectively suppresses STAT3 activity and malignant transformation. *Cancer Research*, *73*(6), 1922–1933. https://doi.org/10.1158/0008-5472.CAN-12-3175

Zhang, X., Yue, P., Fletcher, S., Zhao, W., Gunning, P. T., & Turkson, J. (2010). A novel small-

molecule disrupts Stat3 SH2 domain–phosphotyrosine interactions and Stat3-dependent tumor processes, *79*(10). https://doi.org/10.1016/j.bcp.2010.01.001

Zhang, X., Yue, P., Page, B. D. G., Li, T., Zhao, W., Namanja, A. T., … Turkson, J. (2012). Orally bioavailable small-molecule inhibitor of transcription factor Stat3 regresses human breast and lung cancer xenografts. *Proceedings of the National Academy of Sciences of the United States of America*, *109*(24), 9623–9628. https://doi.org/10.1073/pnas.1121606109

Zhang, Z., Mao, H., Du, X., Zhu, J., Xu, Y., & Wang, S. (2016). A novel small molecule agent displays potent anti-myeloma activity by inhibiting the JAK2-STAT3 signaling pathway. *Oncotarget*, *7*(8), 9296–9308. https://doi.org/10.18632/oncotarget.6974

Zhong, Z., Wen, Z., & Darnell, J. (1994). Stat3: a STAT family member activated by tyrosine phosphorylation in response to epidermal growth factor and interleukin-6. *Science*, *264*(5155), 95–98. https://doi.org/10.1126/science.8140422

Zhong, Z., Wen, Z., & Darnell Jr., J. E. (1994). Stat3 and Stat4: members of the family of signal transducers and activators of transcription. *Proc Natl Acad Sci U S A*, *91*(11), 4806–4810.

Zhou, Q., Yao, Y., & Ericson, S. G. (2004). The Protein Tyrosine Phosphatase CD45 Is Required for Interleukin 6 Signaling in U266 Myeloma Cells. *International Journal of Hematology*, *79*(1), 63–73. https://doi.org/10.1007/BF02983536

Zhu, J., Wang, M., Cao, B., Hou, T., & Mao, X. (2014). Targeting the phosphatidylinositol 3-kinase/AKT pathway for the treatment of multiple myeloma. *Current Medicinal Chemistry*, *21*(27), 3173–3187. https://doi.org/10.2174/09298673216661406012045l3

Zhu, S., Wang, Z., Li, Z., Peng, H., Luo, Y., Deng, M., … Zhang, G. (2015). Icaritin suppresses

multiple myeloma, by inhibiting IL-6/JAK2/STAT3. *Oncotarget*, *6*(12), 10460–10472. https://doi.org/10.18632/oncotarget.3399

Zlei, M., Egert, S., Wider, D., Ihorst, G., Wäsch, R., & Engelhardt, M. (2007). Characterization of in vitro growth of multiple myeloma cells. *Experimental Hematology*, *35*(10), 1550–1561. https://doi.org/10.1016/j.exphem.2007.06.016

Zong, C. S., Chan, J., Levy, D. E., Horvath, C., Sadowski, H. B., & Wang, L. H. (2000). Mechanism of STAT3 activation by insulin-like growth factor I receptor. *Journal of Biological Chemistry*, *275*(20), 15099–15105. https://doi.org/10.1074/jbc.M000089200

Zschenker, O., Streichert, T., Hehlgans, S., & Cordes, N. (2012). Genome-wide gene expression analysis in cancer cells reveals 3D growth to affect ECM and processes associated with cell adhesion but not DNA repair. *PLoS ONE*, *7*(4). https://doi.org/10.1371/journal.pone.0034279

Zubiaur, M., Izquierdo, M., Terhorst, C., Malavasi, F., & Sancho, J. (1997). CD38 ligation results in activation of the Raf-1/mitogen-activated protein kinase and the CD3-z/z-associated protein-70 signaling pathways in jurkat T lymphocytes. *J.Immunol.*, *159*(1), 193–205.

HEALTH SCIENCES LABORATORY ANIMAL SERVICES
SOP: MONITORING HEALTH STATUS IN THE MOUSE
Effective Date: January 2014

I. Purpose

1. Establish the mouse cage environment and visual health indicators that when observed require staff to undock a cage and then evaluate and measure additional health indicators.
2. Establish the health indicators that are evaluated and measured in the mouse to objectively determine the intervention points and the humane endpoints.

II. Observation Procedures

1. Observe the mouse cage environment

a. Food and water consumption is normal for the number of animals in the cage; abnormal is lack of or excessive consumption of food or water.
b. Cage bottom and bedding is normal dryness; normal is less than 1/3 of the cage bottom is wet when viewed from underneath and no condensation is visible on the sides of the cage; abnormal is either greater than 1/3 of the cage bottom is wet or any condensation present on the sides of the cage.
c. Cages normally do not contain blood, pus, diarrhea or other exudate; abnormal is if any of these are present.

If the cage environment is normal, proceed to step II. 2.
If an abnormality in the cage environment is observed, proceed to step III.

2. Observe the visual health indicators for mice

a. Responsiveness: normal is bright, alert and responsive; abnormal is lethargic or moribund/nonresponsive.
b. Mouse posture: normal is with back extended and moves freely; abnormal posture is a hunched or arched back.
c. Hair coat appearance: normal is smooth, groomed and glossy hair coat; abnormal hair coat is rough, un-groomed and dull appearing, and can appear dry or with pilo-erection present.
d. Respiration rate and effort: normal rate of <170 breaths/minute and only able to detect minor chest movement.

If the visual health indicators are normal, proceed to observe the next cage of mice.
If an abnormal visual health indicator is present, proceed to step III.

III. Evaluation and Measurement Procedure

1. For mouse cage environment abnormalities, visually evaluate each mouse to determine which animals demonstrate abnormal health indicators and then proceed to the step III. 2. for these mice only. If it cannot be determined which animal(s) demonstrate an abnormal health indicators, each mouse in the cage should be individually evaluated and measured for steps III. 2., III. 3., III. 4.

2. Evaluate responsiveness of the mouse—follow scoring sheet for recording and intervention points and endpoints.

3. Evaluate body condition or measure body weight—follow scoring sheet for recording and intervention points and endpoints.

4. Evaluate respiration rate and effort—follow scoring sheet for recording and intervention points and endpoints.

Score Sheet for Monitoring Health Status in the Mouse *Use one sheet per animal*

Animal #_____**Date** _____

Researcher_____

Score Sheet

Date							
Initial Body Weight [1.]							
Current Body Weight							
% Body Weight Change							
A. Body Weight Score							
B. Responsiveness Score							
C. Respiration Score							
D. Tumor Score							
E. Mobility Score							
TOTAL SCORE (add A to E)							

Use the score sheet guide to determine intervention points and endpoints. Animals are euthanized if the total score is 3 or more. For animals with a total score of 1 or 2, they are scored daily with interventions as per the Animal Use Protocol.

1. For initial body weight—if the initial body weight for an animal is not available, the average of normal cage mates can be used, or the average for the strain can be used.

Score Sheet: Assigning Scores A-E

A. Body Weight Score

0-5% body weight loss = score of 0
6-12% body weight loss = score of 1
13-19% body weight loss = score of 2
20% or more body weight loss = score of 3 (requires euthanasia)

B. Responsiveness Score

Bright, alert and responsive = score of 0
Quiet and responds to movement = score of 1
Lethargic, does not respond to movement, responds to touch = score of 2
Moribund and nonresponsive = score of 3 (requires euthanasia)

C. Respiration Score

Normal rate (less than 170 breaths/minute) and effort = score of 0
Mild increase (170-200 breaths/minute) or increased effort visible on the chest = score of 1
Moderate elevation in rate (200-240/minute) or increased effort obvious on chest = score of 2
Severe; open mouth breathing or holding elbows out from chest = score of 3 (requires euthanasia)

D. Tumor Score

Noticeable size <0.5 cm, skin overlying growth is normal = score of 0
Small size 0.5 to 1.0 cm, or skin red/inflamed only over tumor = score of 1
Mid-size 1.0-1.4 cm size, or skin red/inflamed over and around tumor = score of 2
Large size 1.5 cm or larger, or skin opened/ulcerated over tumor = score of 3 (requires euthanasia)

E. Mobility Score

Normal movement and mobility = score of 0
Reduced and slow mobility, not visibly lame = score of 1
Lameness on 1 limb, weight bearing = score of 2
Non weight bearing or unable to use a limb = score of 3 (requires euthanasia)